

**NEW POLYMER ARCHITECTURES:
SYNTHESIS AND CHARACTERIZATION OF
POLYURETHANE-CROWN ETHER BASED
POLYROTAXANES**

By

Ya Xi Shen

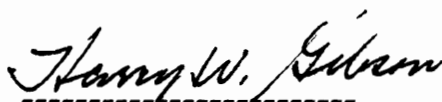
Dissertation presented to the faculty of the Virginia Polytechnic Institute
and State University in partial fulfillment of the requirements for the
degree of

DOCTOR OF PHILOSOPHY

IN

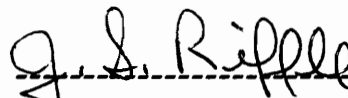
MATERIALS ENGINEERING SCIENCE

APPROVED:

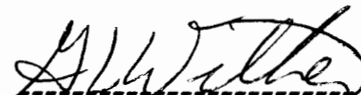


H. W. Gibson, Chair



J. E. McGrath

J. S. Riffle

T. C. Ward

G. L. Wilkes

February, 1992
Blacksburg, Virginia

ABSTRACT

NEW POLYMER ARCHITECTURES: SYNTHESIS AND CHARACTERIZATION OF POLYURETHANE-CROWN ETHER BASED POLYROTAXANES

By

Ya Xi Shen

Committee Chairman: Professor Harry W. Gibson

Department of Chemistry

Rotaxane chemistry provides a new direction of research in polymer architectures. Unlike conventional polymers, polyrotaxanes are molecular composites comprised of macrocycles threaded by linear polymer backbones with no covalent bonds between the two components. This novel class of materials displays unusual chemical and physical properties due to their unique architectures.

The studies include crown ether and blocking group syntheses, synthetic methodologies leading to rotaxanes and polyrotaxanes and structure-property relationships of polyrotaxanes.

Crown ethers (30-crown-10, 36-crown-12, 42-crown-14, 48-crown-16 and 60-crown-20) were systematically synthesized from low molecular weight glycols with 30 - 60% yields. Bis(*p*-phenylene)-32-crown-4 and bis(*p*-phenylene)-34-crown-10 (BPP34C10) were also synthesized in 8 - 13% yields; the latter was synthesized with four different synthetic

routes. All crown ethers were prepared in large quantities. A series of monofunctionalized triaryl derivatives were also synthesized as rotaxane blocking groups.

A series of polyrotaxanes comprised of a polyurethane backbone and crown ethers with ring size ranging from 36 - 60 membered were synthesized via the statistical threading method. The polyrotaxane formation was proven by multiple reprecipitations, $^1\text{H-NMR}$ and GPC analyses. The threading efficiency (rings per repeat unit) increases from 0.16 to 0.87 with an increase in ring size of crown ethers from 36 to 60 membered at 1.5 molar ratio of crown ether to linear glycol.

Host-guest complexation of paraquat dication and BPP34C10 has been studied. A series of difunctionalized paraquat dication derivatives was synthesized and used to prepare host-guest complexes (pseudorotaxanes) with BPP34C10. X-Ray crystal structures of the complexes were determined. Furthermore, a class of viologen-containing polyurethane elastomeric polyrotaxanes was synthesized via this host-guest complexation. The threading efficiencies from this method were quantitative.

Through rotaxane formation, polymer solubilities increase and glass transition temperatures decrease. Evidenced by DSC and WAXS analyses, the crown ether forms crystalline domains without dethreading from the amorphous polyurethane backbone. This process is kinetically "retarded". It is time and temperature dependent and reversible. It can only be observed for polyrotaxanes with large rings and high ring contents, which provide high mobilities of rings along the backbone and also wide $T_m - T_g$ windows. The study of recrystallization kinetics has also shown that 60-crown-20 recrystallizes much slower in a polyrotaxane than in its physical blend with the model polymer.

ACKNOWLEDGEMENTS

My deepest and most sincere thanks go to Dr. Harry W. Gibson for his advise and patience. Under his guidance, I have become a synthetic polymer chemist from a physical chemist. I also wish to thank him for his concern about me in life in general.

I would like to thank Dr. J. E. McGrath, Dr. J. S. Riffle, Dr. G. L. Wilkes and Dr. T. C. Ward for being on my committee and their advice, suggestions and encouragement throughout the course of my research.

I would like to thank Dr. G. L. Wilkes and his group, especially D. Loveday, for characterization of viologen-containing polyurethane elastomeric polyrotaxanes.

I would like to thank Dr. H. Marand and his group, especially Dr. A. Prasad, for characterization of polyurethane-crown ether based polyrotaxanes and so many valuable suggestions and help from Dr. H. Marand.

I would like to thank Dr. J. E. McGrath and Dr. T. C. Ward and their groups, especially Dr. M. Netopilik, for solution characterization of all my polymers.

I would like to thank Dr. J. S. Merola, M. Berg and P. Engen for X-ray crystal analyses.

I would like to thank everyone in Dr. Gibson's group, especially Dr. C. Wu, Dr. J-P Leblanc, Dr. Y. Delaviz, J. Sze and P. Engen for their friendship and also comments and help.

I would like to thank Materials Engineering Science program and Department of Chemistry for providing such a good program which has broadened my scope of understanding of polymer materials.

Finally, I would like to thank NSF and the NSF Science and Technology Center for financial support.

DEDICATION

to my mother Fuhui Gao and father Jingshui Shen,

to Miss Yuanting Lin,

they are the most important persons in my life

and

to Professor Thomas T. -S. Huang,

who brought me to America, the land of freedom.

TABLE OF CONTENTS

ABSTRACT	ii
ACKNOWLEDGEMENTS	iv
DEDICATION	vi
CHAPTER	
I. INTRODUCTION TO NEW POLYMER ARCHITECTURES: POLYROTAXANES	1
I-1: CONVENTIONAL POLYMER ARCHITECTURES	2
I-1-1: LINEAR POLYMERS (FLEXIBLE THREAD, RIGID ROD, LADDER)	2
I-1-2: BRANCHED POLYMERS (COMB, STAR, TREE)	4
I-1-3: NETWORK POLYMERS	7
I-1-4: BLOCK COPOLYMERS	8
I-2: NEW POLYMER ARCHITECTURES: POLYROTAXANES	11
I-3: HISTORY OF ROTAXANE CHEMISTRY	14
I-3-1: ROTAXANES	14
I-3-2: POLYROTAXANES	20
I-3-3: RAPID DEVELOPMENT IN CATENANE SYNTHESIS	25
I-3-4: OTHER WORK ON ROTAXANE CHEMISTRY DONE IN OUR LABORATORY	28
I-4: SYNTHETIC METHODOLOGIES	30
I-4-1: CHEMICAL CONVERSION	30

I-4-2: STATISTICAL THREADING	31
I-4-3: TEMPLATE SYNTHESIS	32
I-4-4: DRIVING FORCES FOR THREADING	33
REFERENCES	35
LIST OF SCHEMES	42
II. CROWN ETHER MACROCYCLES	46
II-1: CONCEPTS OF DESIGNING MACROCYCLES FOR ROTAXANES AND POLYROTAXANES	46
II-1-1: EFFECTIVE CAVITY SIZE	46
II-1-2: ABILITY TO COMPLEX A GUEST MOLECULE	48
II-1-3: FUNCTIONALIZED MACROCYCLES	48
II-1-4: MELTING POINT, SOLUBILITY AND STABILITY	49
II-2: SYNTHETIC APPROACHES	50
II-2-1: SYNTHETIC METHODS	50
II-2-2: TEMPLATE EFFECT	52
II-3: RESULTS AND DISCUSSION	53
II-3-1: PREPARATION OF PRECURSORS FOR CROWN ETHERS	53
II-3-2: SYSTEMATIC SYNTHESSES OF <i>m</i> -CROWN- <i>n</i>	56
II-3-3: BIS(<i>p</i> -PHENYLENE) BASED CROWN ETHERS	59
II-4: CONCLUSIONS	64
II-5: EXPERIMENTAL	65
II-5-1: HEXA(ETHYLENE GLYCOL)	66
II-5-2: OLIGO(ETHYLENE GLYCOL) DITOSYLATES	68

II-5-3: PENTA(ETHYLENE GLYCOL) DIIODIDE	70
II-5-4: 60C20 AND 30C10	72
II-5-5: 36C12	73
II-5-6: 42C14	74
II-5-7: 48C16	74
II-5-8: SYNTHESIS OF BPP34C10	75
II-5-8-1: Four-Step Route	75
II-5-8-2: Two-Step Route	79
II-5-8-3: One-Step Route	81
II-5-8-4: Template One-Step Route	82
II-5-9: SYNTHESIS OF BPP32C4	83
REFERENCES	85
LIST OF SCHEMES	88
LIST OF TABLES	101
LIST OF FIGURES	105
III. MONOFUNCTIONALIZED TRIARYL DERIVATIVES (BLOCKING GROUPS)	117
III-1: DESIGN AND USE OF BLOCKING GROUPS	117
III-1-1: DESIGN CONCEPTS	117
III-1-2: USE OF BLOCKING GROUPS	119
III-2: RESULTS AND DISCUSSION	120
III-2-1: GRIGNARD REACTIONS	122
III-2-2: MODIFICATION METHOD 1	123
III-2-3: MODIFICATION METHOD 2	126

III-3: EXPERIMENTAL	130
III-3-1: GRIGNARD REACTIONS	131
III-3-2: MODIFICATION METHOD 1	133
III-3-3: MODIFICATION METHOD 2	140
REFERENCES	146
LIST OF SCHEMES	148
LIST OF FIGURES	156
IV. POLY(URETHANE-CROWN ETHER) ROTAXANES VIA THE STATISTICAL THREADING APPROACH	163
IV-1: POLYURETHANES	164
IV-1-1: STARTING MATERIALS	164
IV-1-2: CHEMICAL REACTIONS OF POLYFUNCTIONAL ISOCYANATES	167
IV-1-3: POLYURETHANE PRODUCTS AND THEIR APPLICATIONS	170
IV-2: RESULTS AND DISCUSSION	171
IV-2-1: SYNTHESSES OF POLYROTAXANES	171
IV-2-1-1: Threading Equilibrium	172
IV-2-1-2: Polymerizations	173
IV-2-1-3: Purification	174
IV-2-1-4: Threading Efficiencies	175
IV-2-2: SYNTHESIS OF MODEL POLYURETHANE	181
IV-2-3: CHARACTERIZATION OF THE POLYMERS	182
IV-2-3-1: The Physical Behaviors of the Polymers	182
IV-2-3-2: ¹ H-NMR Analyses	183

IV-2-3-3: Solubilities	185
IV-2-3-4: Intrinsic Viscosity Measurements	189
IV-2-3-5: GPC Analyses and Molecular Weights	189
IV-2-3-6: FTIR Analysis	194
IV-2-3-7: DSC Analyses and Glass Transition Temperatures	196
IV-2-3-8: Crystallization Behaviors	198
IV-2-3-8-1: Evidenced by DSC Analyses	198
IV-2-3-8-2: Evidenced by X-Ray Analyses	200
IV-2-3-8-3: Crystallization Kinetics	201
IV-3: CONCLUSIONS	202
IV-3-1: SYNTHESIS	202
IV-3-2: CHARACTERIZATION	203
IV-4: EXPERIMENTAL	204
IV-4-1: POLYURETHANE-ROTAXA-36-CROWN-12	205
IV-4-2: POLYURETHANE-ROTAXA-42-CROWN-14	206
IV-4-3: POLYURETHANE-ROTAXA-48-CROWN-16	206
IV-4-4: POLYURETHANE-ROTAXA-60-CROWN-20	207
IV-4-5: POLYURETHANE-UREA-ROTAXA-60-CROWN-20	208
IV-4-6: MODEL POLYURETHANE	208
REFERENCES	210
LIST OF SCHEMES	211
LIST OF TABLES	220

LIST OF FIGURES	234
V. HOST-GUEST COMPLEXATION OF PARAQUAT DICATION DERIVATIVES AND BPP34C10. PART 1: ROTAXANE MODEL STUDIES	254
V-1: PARAQUAT DICATION DERIVATIVES	255
V-1-1: SYNTHESIS	255
V-1-2: GENERAL PROPERTIES	256
V-2: HOST-GUEST COMPLEXATION OF BPP34C10 AND PARAQUAT DICATION DERIVATIVES	259
V-2-1: X-RAY STRUCTURES AND CAVITY SIZE OF BPP34C10	259
V-2-2: THE HOST-GUEST COMPLEXATION	260
V-3: RESULTS AND DISCUSSION	262
V-3-1: SYNTHESSES OF DIFUNCTIONALIZED PARAQUAT DICATION DERIVATIVES	262
V-3-2: COMPLEXATION OF DIFUNCTIONALIZED PARAQUAT DICATION DERIVATIVES AND BPP34C10: PSEUDOROTAXANES	265
V-3-2-1: Solution Complexation and Preparation of Complex Crystals	265
V-3-2-2: ¹ H-NMR Study of Solution Complexation	266
V-3-2-3: X-Ray Crystal Analysis	269
V-4: EXPERIMENTAL	271
V-4-1: N,N'-BIS(2-HYDROXYETHYL)-4,4'-BIPYRIDINIUM HEXAFLUOROPHOSPHATE	272
V-4-2: N,N'-BIS(CARBOMETHOXYETHYL)-4,4'- BIPYRIDINIUM HEXAFLUOROPHOSPHATE	274

V-4-3: N,N'-BIS(CARBOXYETHYL)-4,4'-BIPYRIDINIUM HEXAFLUOROPHOSPHATE	275
V-4-4: A TYPICAL PROCEDURE TO PREPARE HOST- GUEST COMPLEXES	276
REFERENCES	278
LIST OF SCHEMES	284
LIST OF TABLES	287
LIST OF FIGURES	294
VI. HOST-GUEST COMPLEXATION OF PARAQUAT DICATION DERIVATIVES AND BPP34C10. PART 2: SYNTHESIS OF VIOLOGEN-CONTAINING POLYURETHANE ELASTOMERIC ROTAXANES	317
VI-1: LINEAR THERMOPLASTIC POLYURETHANE ELASTOMERS	318
VI-1-1: THERMOPLASTIC ELASTOMERS	318
VI-1-2: SYNTHESIS OF THERMOPLASTIC POLYURETHANE ELASTOMERS	320
VI-1-3: STARTING MATERIALS	322
VI-1-4: MORPHOLOGY WITHIN THE HARD SEGMENT DOMAIN	324
VI-2: VIOLOGEN-CONTAINING POLYMERS	325
VI-2-1: CONVENTIONAL VIOLOGEN-CONTAINING POLYMERS	325
VI-2-2: VIOLOGEN CONTAINING THERMOPLASTIC ELASTOMERS	327
VI-3: RESULTS AND DISCUSSION	328
V-3-1: SYNTHESSES OF LINEAR THERMOPLASTIC POLY(URETHANE-VIOLOGEN-PTMO)-ROTAXA- BPP34C10 AND THEIR CORRESPONDING	

MODEL POLYMERS	328
VI-3-1-1: Polymerization	328
VI-3-1-2: Purification	330
VI-3-1-3: ¹ H-NMR Analyses and Polymer Compositions	331
VI-3-1-4: Viscosity Measurements	332
VI-3-1-5: Counter Anion Exchanges	334
VI-3-1-6: Polymer Films	334
VI-4: EXPERIMENTAL	336
VI-4-1: SYNTHESIS OF POLY(URETHANE-VIOLOGEN- PTMO-650)	337
VI-4-2: SYNTHESIS OF POLY(URETHANE-VIOLOGEN- PTMO-650)-ROTAXA-BPP34C10	337
VI-4-3: SYNTHESIS OF POLY(URETHANE-VIOLOGEN- PTMO-1000)	338
VI-4-4: SYNTHESIS OF POLY(URETHANE-VIOLOGEN- PTMO-1000)-ROTAXA-BPP34C10	339
VI-4-5: SYNTHESIS OF POLY(URETHANE-VIOLOGEN- PTMO-2000)	339
VI-4-6: SYNTHESIS OF POLY(URETHANE-VIOLOGEN- PTMO-2000)-ROTAXA-BPP34C10	340
VI-4-7: ISOLATION	340
VI-4-8: PURIFICATION	341
VI-4-9: FILM CASTING	341
REFERENCES	342
LIST OF SCHEMES	346

LIST OF TABLES	351
LIST OF FIGURES	356
VII.SUMMARIZATION, GENERAL CONCLUSIONS, POLYROTAXANE POTENTIAL APPLICATIONS AND SUGGESTIONS FOR FUTURE WORK	363
VII-1: SUMMARIZATION AND GENERAL CONCLUSIONS	363
VII-1-1: MACROCYCLES	363
VII-1-2: BLOCKING GROUPS	365
VII-1-3: POLYROTAXANES VIA THE STATISTICAL THREADING METHOD	366
VII-1-4: POLYROTAXANES VIA HOST-GUEST COMPLEXATION	368
VII-2: POTENTIAL APPLICATIONS OF POLYROTAXANES	370
VII-3: SUGGESTIONS FOR FUTURE WORK	371
VII-3-1: DIFUNCTIONAL BLOCKING GROUPS AND POLYROTAXANES WITH BULKY SPACERS	371
VII-3-2: POLYMERIC "MOLECULAR SHUTTLES"	373
VII-3-3: SLIP-LINKED POLYMERS	374
VII-3-4: POLYROTAXANES BASED ON REDOX- SWITCHED CROWN ETHERS	375
REFERENCES	377
LIST OF SCHEMES	378
VITA	383

CHAPTER I:

INTRODUCTION TO NEW POLYMER ARCHITECTURES: POLYROTAXANES

Since Carothers began synthesizing polymers in the 1930's using well-established organic reactions with the knowledge of the chain-like structure of giant molecules proposed by H. Staudinger in 1920, polymer synthesis has rapidly developed and indeed has changed our life. Today, from our home to our vehicle, from industrial to commercial, from ground to outer space, synthetic polymers are everywhere.

The term "polymer" is derived from the Greek words "poly" and "meros", meaning many and parts, respectively. How are those parts put together to form a polymer? Staudinger proposed that they are held together by covalent bonds like those in low molecular weight organic compounds, which we accept today. However, this concept now has to be modified since the birth of a new class of polymer materials: polyrotaxanes and polycatenanes whose components are not covalently bonded.

I-1: CONVENTIONAL POLYMER ARCHITECTURES¹

The art of designing polymers in terms of polymer architecture generally applies to the macromolecules having special topological structures. Macromolecules can be linear, branched or cyclic. The linear polymer chains have two ends, the branched ones have more than two ends, but the cyclic polymers have no end. On the other hand, macromolecules can also be designed as three dimensional networks or shaped like stars, combs, ladders, and so on.

I-1-1: LINEAR POLYMERS (FLEXIBLE THREAD, RIGID ROD, LADDER)

Linear polymers can be thread-like or rope-like chains (**I-1a**) or rigid rods (**I-1b**) with two ends.



I-1a



I-1b

When the individual repeat units are all the same, the polymer is a homopolymer and its structure may be most simply represented as $-(A)_n-$, where A is the repeat unit and n is the number of the repeat units or degree of polymerization (DP). When the repeat units are of more than one type, the polymer is a copolymer. However, copolymers

could be random copolymers or block copolymers (see section I-1-3). For example, the structure of an alternating copolymer formed from A and B monomers can be represented as $-(AB)_n-$. The bonds linking the units are generally covalent bonds formed during the polymerization.

There are different polymerization processes by which linear polymers can be obtained. The step-growth polymerization (condensation polymerization) process produces step-growth polymers or condensation polymers such as polyesters, polyethers, polyamides, polyimides, polyurethanes, polyureas, polysulfides, polysulfones, etc. To form high molecular weight linear polymers, it is required that the monomers possess difunctionality, high purity and high reactivity. The chain-growth polymerization (addition polymerization) process produces chain-growth polymers or addition polymers, of which the most common type is the family of vinyl polymers. The chain-growth polymerization can be subclassified as free-radical polymerization, anionic polymerization and cationic polymerization depending on the initiator which in turn is related to the characteristics of the monomer used, generally the polarity of functional groups of the monomer.

Linear polymers show properties distinct from low molecular weight compounds in both solution and the solid state. Those properties are due to chain entanglement, molecular interactions (inter- and intra-molecular), crystallinity, and so on. When we talk about the crystalline polymers, we often refer to semicrystalline polymers. Such polymers, however, are only even partially crystalline and hence contain both

crystalline and amorphous regions. Linear polymer chains are arrayed regularly in the crystalline phase (usually chain folded lamellar) but adopt a random coil conformation in the amorphous phase. Such a conformation is also usually found for the polymers in solution. Also stereoisomerization of linear polymer chains (for example, tacticity) can lead to different polymer properties, especially the crystallinity of linear polymers.

Ladder polymers (**I-1c**) are double-stranded linear polymers. The structures comprise two parallel strands with regular cross-links such as polyquinoxaline, polyimidazopyrrolone, etc. The permanence properties of ladder polymers are superior even to those of conventional network polymers. This type of polymers is usually used as high temperature resistant polymers.

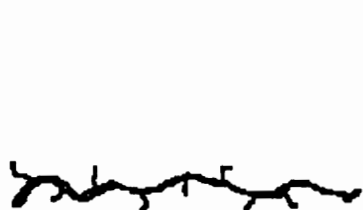


I-1c

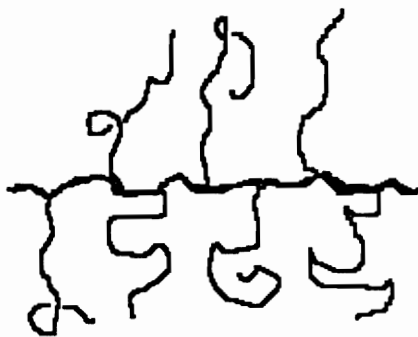
I-1-2: BRANCHED POLYMERS² (COMB, STAR, TREE)

Branched polymers can be short-chain branched (**I-2**) or long-chain-branched (**I-3**, **I-4** and **I-5**) according to the length of side chains. Short-chain branched polymers behave more like linear polymers. However, long-chain branched polymers form a class of polymers between the strictly linear polymers and polymer networks. Branched polymers are characterized by the presence of branch points, i.e., atoms

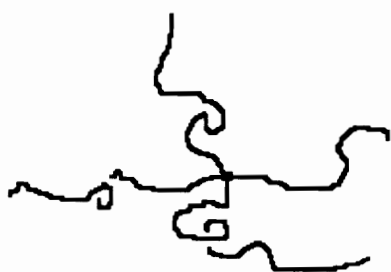
or small groups from which more than two long chains emanate, or by the presence of more than two end groups. There are several types of branchings which classify branched polymers into several categories: comb-like (I-3), star-like (I-4), and random (or tree-like) (I-5) branches.



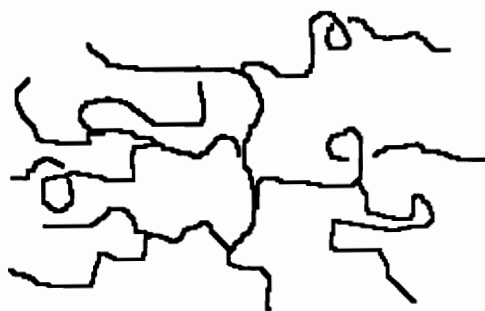
I-2



I-3



I-4



I-5

Comb-like polymers have a backbone from which branches emanate at various positions. Star-like polymers have a single branch point from which emanate a number of arms. Randomly branched (tree-like) polymers have no main chain and branches carry branches. For comb-like polymers, besides the branch point, the ratio of the molecular weight of the backbone to that of single branch, M_{bb}/M_{br} , is also an

important factor in the characterization. If M_{bb}/M_{br} approaches to zero, the comb-like polymers revert to star-like polymers.

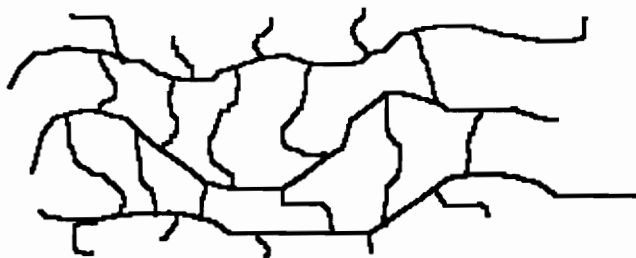
There are several ways to prepare branched polymers by controlled branching. The most straightforward method is to carry out the polymerization of difunctional monomers in the presence of a small amounts of multifunctional comonomer. The formation of random branching is statistical. This method can be applied to both step-growth polymerization³ and free-radical polymerization.⁴⁻⁶ Of course, attention must be paid to possible gelation when this method is used. In the preparation of star-like polymers, multifunctional initiators can be used to control branch point and number of arms.⁷⁻¹⁰ The dendritic hyperbranched polymers can be prepared via "divergent-growth" and "convergent-growth" approaches.¹¹ Another approach is to prepare linear macromonomers first; then the macromonomers are connected to the main chain by graft-copolymerization techniques, either "graft-from" or "graft-to".¹² The structure of polymer can be precisely controlled with this method.

The branched polymers show different properties reflecting the characteristics of the polymer architectures. For example, the intrinsic viscosity $[\eta]$ and intrinsic translational friction coefficient $[f]$ of branched polymers are smaller than those of linear analogies because of the smaller radii of gyration. However, compared with the linear homologue, long-chain branching has little influence on bulk properties of polymers

such as glass transition temperature and crystallinity, since the branching chain could behave as the main chain.

I-1-3: NETWORK POLYMERS¹³

As represented by I-6, a network polymer is an interconnected branched polymer. This type of polymers can also be called thermoset polymers.



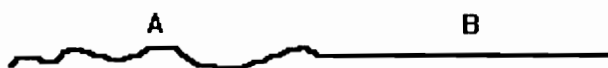
I-6

Generally network polymers are synthesized by polymerization of monomers with average functionality greater than 2 and reaction to sufficiently high conversion. Chemically crosslinking linear or branched polymers, such as "vulcanization" or "curing", is another way to produce network polymers.

The molecular weights of network polymers are infinite (relatively). Due to the network formation, the polymers exhibit properties different from linear and branched polymers, e.g., rubber elasticity, gel-formation, etc. However, network polymers are insoluble and thus possess poor processibility.

I-1-4: BLOCK COPOLYMERS¹⁴

Different from homopolymers, random and alternating copolymers, block copolymers have a linear arrangement of blocks of varying monomer composition. Also different from polymer blends, a block copolymer contains two or more polymers but they are connected end-on-end. Structure **I-7** represents a diblock segmented copolymer containing A and B blocks, where the A segment is flexible and the B segment is rigid.



I-7

The synthetic techniques leading to block copolymers have been well established^{14(a)}. Generally there are two different approaches. The first one is condensation. In this approach, blocks (polymers or oligomers) are interconnected via the reaction of functional groups present at the ends of different blocks. Segmented polyurethanes (thermoplastic elastomers) are prepared via interconnecting prepolymers with chain extender, a difunctional monomer which reacts with prepolymers. The second approach is called living polymerization. Active sites on a block (polymer or oligomer) are created which then initiate the free radical, anionic or cationic polymerization of another monomer to build the second block. For example, poly(styrene-block-butadiene) can be synthesized via anionic living polymerization.

Block copolymers exhibit interesting properties owing to their special molecular structures both in solution and in the solid state. Especially in the solid state, due to the microdomain formation, block copolymers with incompatible sequences show characteristic morphological behavior. They could be thermoplastic elastomers showing the same elastomeric properties as a crosslinked rubber due to the fact that so-called physical crosslinking forms in the crystalline or glassy phase which is separate from the amorphous, viscous or rubbery phase. However, these thermoplastic elastomers are soluble in common solvents whereas crosslinked elastomers are insoluble. The thermoplastic elastomers will be discussed in detail in Chapter VI.

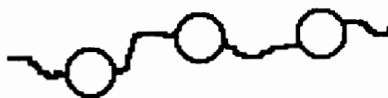
So far we have discussed some basic polymer architectures. There are some other systems that have recently become subjects of interest such as cyclic polymers¹⁵ and polymacrocycles.¹⁶ Cyclic polymers have no end (**I-8**). Polymacrocycles are the polymers containing macrocycles, either incorporated into the polymer backbone (**I-9a**) or as pendant groups (**I-9b**). Compared with its linear analogs, a cyclic polymer has smaller hydrodynamic volume and hence different solution properties.¹⁵ In the solid state, the cyclic polymers may possess different shear rate dependence.¹⁵ Different mechanical properties resulting from the reduced number of entanglements should also be expected.

However, polymer chemists have not been satisfied. With the rapid development of synthetic organic chemistry, polymers with more

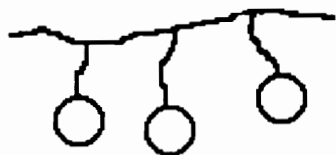
complicated architectures such as polymer chains incorporating knots (I-10),¹⁷ bulk complexes, etc. have also been focused on. Not only do they play with sophisticated chemistry to build unusual molecular architectures, but also polymer scientists have synthesized polymers with unusual morphological architectures using other more routine techniques. For example, the sol-gel process has been used to combine inorganic glass with organic polymers to form inorganic-organic hybrid network materials.¹⁸



I-8



I-9a



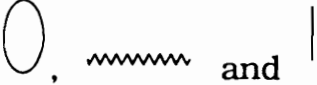
I-9b



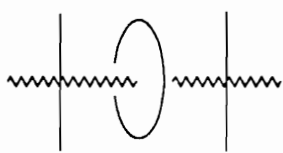
I-10

I-2: NEW POLYMER ARCHITECTURES: POLYROTAXANES

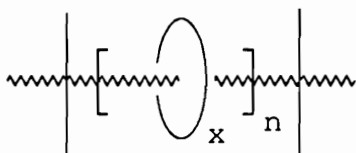
Polymers with different architectures show different properties as a consequence of their structure characteristics. However, the conventional architectures are generated by changing atom connections and groups or species are held together at fixed positions with covalent bonds.

Rotaxane chemistry, on the other hand, provides a new direction of research in polymer architectures. Rotaxanes (Latin: *rota* = the wheel, *axis* = the axle) are a class of compounds with a special topological structure; a cyclic species is threaded by a linear species with no covalent bond between the two components and the ends of the linear species are blocked by bulky groups called blocking group. The structure of rotaxanes may be systematically represented by **I-11**, where  represent macrocycle, linear molecule and blocking group, respectively. The polymers derived from rotaxanes, polyrotaxanes, can be envisaged as molecular composites. By different synthetic routes, polyrotaxanes with different structures can be obtained. For examples, linear polymerization in the presence of a macrocycle and a monofunctional blocking group produces polyrotaxane **I-12a**; linear polymerization in the presence of a macrocycle and a difunctional blocking group or polymerization of a difunctional rotaxane with functional groups at the ends of the linear component produce

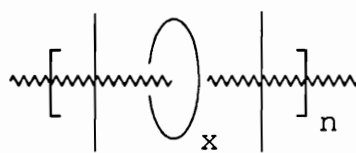
polyrotaxanes **I-12b**; polymerization of a difunctional rotaxane with functional groups on the ring produces polyrotaxane **I-12c**; or a monofunctional rotaxane can be attached to a polymer backbone as pendant groups (**I-12d**) via chemical reactions. Of course, there are more complicated structures such as slip-linked polyrotaxane **I-12e** which can be built up via more complicated routes (see section VII-3-3).



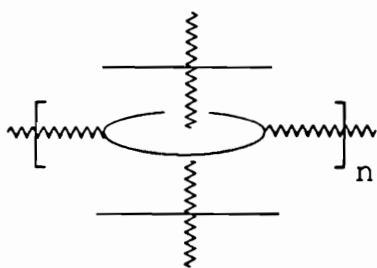
I-11



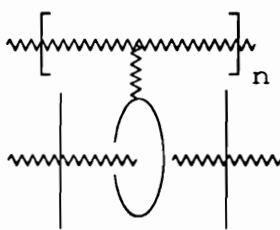
I-12a



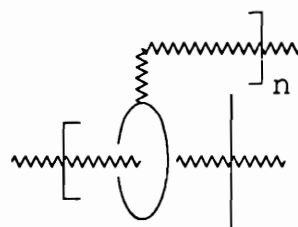
I-12b



I-12c



I-12d



I-12e

Polyrotaxanes are expected to exhibit novel physical and chemical properties such as glass transition, solubility, viscosity, mechanical behavior, and so on, which are derived not directly from covalent bonding

of the repeat units but from physical interactions of the cyclic and linear components. The interactions between these two components could be van der Waal interactions and hydrogen bonding under the restriction of limiting space. In the presence of rings, the polymer chains tend to be loose packed and interchain interactions are largely reduced. Hence polyrotaxanes are expected to possess large free volumes. Due to the mobility of rings along the chain (in the case that there is no blocking group among macrocycles like **I-12a**), the morphology of polyrotaxanes could be very interesting. For example, macrocycles may stay in the amorphous region if the backbone of the polyrotaxane is semicrystalline, or they may form other crystalline phases different from that of the backbone. Generally, the two species, macrocycle and polymer backbone tend to exhibit their own characteristics and also associated ones. The final properties of a polyrotaxane are determined by the degree of independence of the two species, which depends on the properties of the two species such as polarity, rigidity, ring size, chain length, chain diameter, and so on. Polyrotaxanes can be considered as physical analogs of copolymers and true "molecular composites" or molecular interpenetrating networks. As a class of novel materials with unusual properties, polyrotaxanes are expected to offer wide and special applications in the areas such as blend compatibilization, adhesion, novel tough physically crosslinked systems, controlled release, electronically conductive polymers, molecular-scale information processors, engineering materials, etc.

This dissertation focuses on the synthesis and characterization of polyurethane-based polyrotaxanes having schematic structure **I-12a**.

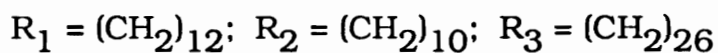
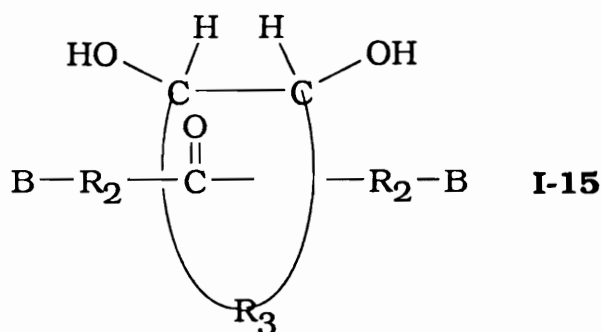
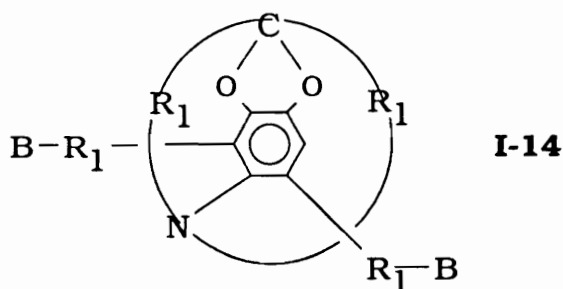
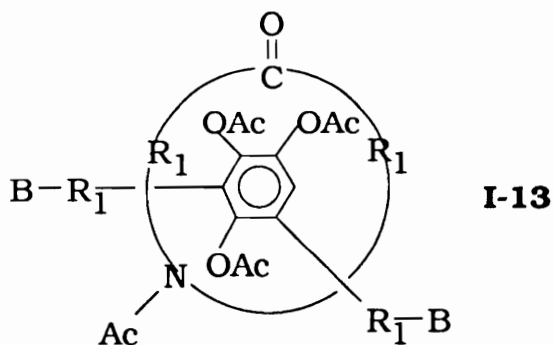
I-3: HISTORY OF ROTAXANE CHEMISTRY¹⁹

I-3-1: ROTAXANES

The first mention in print of the idea of a stable union of a linear molecule threaded through a cyclic one appeared in 1961.²⁰ The synthesis of rotaxanes has been worked out cursorily by Stetter and Lihotzky in 1962;²¹ however, the results were not published. In 1967, the first experimental report was made by Schill and coworkers and the name rotaxane was given.²²

Using an aromatic ring as a construction base from which to build the linear and cyclic species as a so-called prerotaxane, the compound with a linear species set inside and covalently bonded into a cyclic species, and then chemically releasing the ring, Schill *et al.* reported the synthesis of **I-13** from **I-14**.^{23,24} They also synthesized **I-15** in only 0.12% yield starting from the 28-membered macrocyclic diol and the long-chain α,ω -bifunctional ketone.^{25,26} There was a bond formation and cleavage process between the diol and ketone in the synthesis. Two possible intermediates formed when the diol bonded to ketone; one was the prerotaxane and the other was a topological isomer formed when the

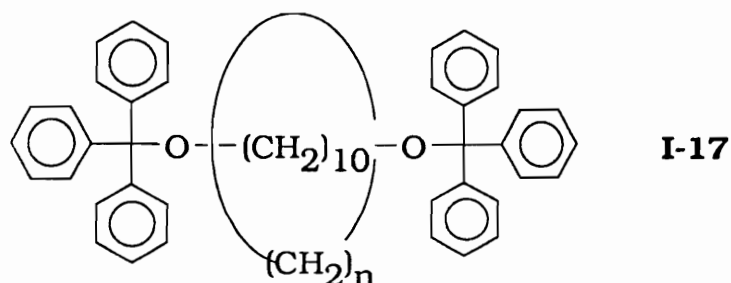
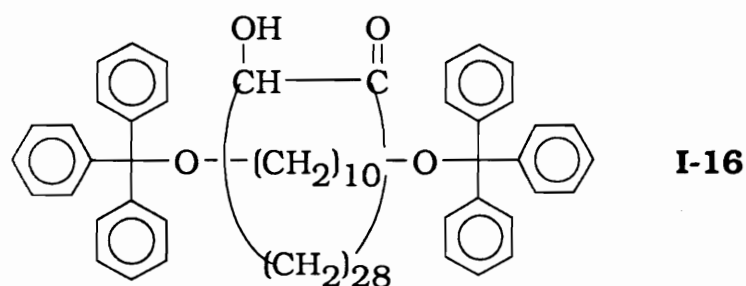
linear segment bonded from outside the cavity of the macrocycle, which reverted back to the starting materials when the bonds were cleaved.



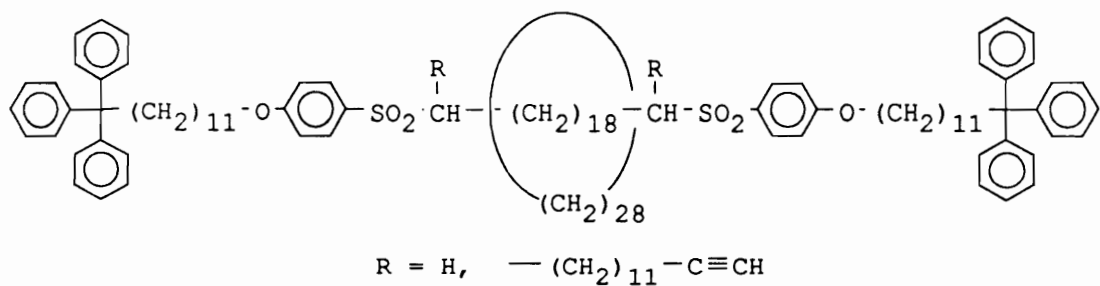
B = Bulky Group (e.g. Trityl)

Harrison *et al.* reported the synthesis of "hooplane" (**I-16**) from decamethylene diol, trityl chloride, and a 28-membered acyloin bonded to a polymeric resin.²⁷ The yield was 6% and the structure was proven by degradation. Later they also prepared rotaxane **I-17** via statistical

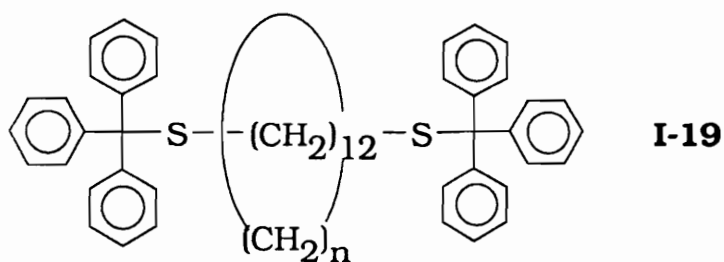
threading method, e.g., equilibration of the linear and cyclic species, and studied the thermal stability of the rotaxane.²⁸ They found that stable compounds were formed when $n = 25$ to 29 . Their further work revealed that rings with less than 22 methylene units can not be threaded and rings with more than 33 methylene units can not be retained by the trityl capped chains.²⁹



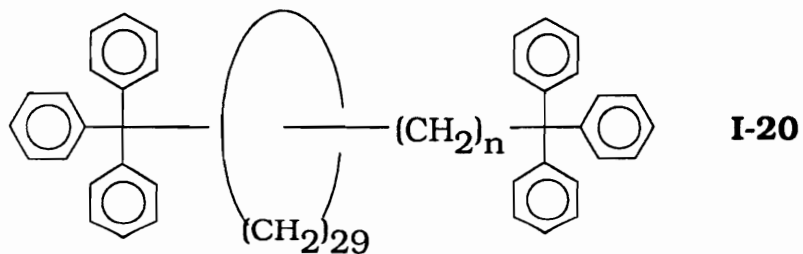
Using the statistical threading method, Schill *et al.* have synthesized rotaxane **I-18** in 10% yield in 1983³⁰ and they also prepared rotaxanes **I-19** and **I-20**.³¹ For **I-19** system, the ring size ranged from $n = 21$ to $n = 29$; while for **I-20** system, the chain length ranged from $n = 10$ to $n = 38$. The yields of rotaxanes increased from 0.35 to 6.8% and 4.5 to 11.3%, respectively, as a function of ring size and chain length of the dumbbell as determined by HPLC analyses.



I-18

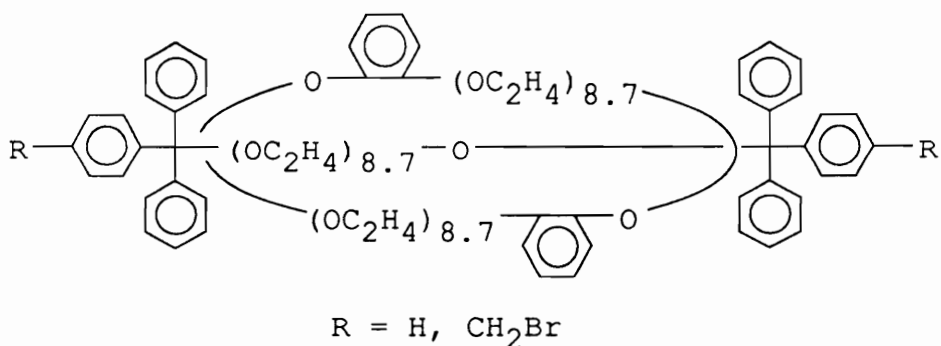


I-19



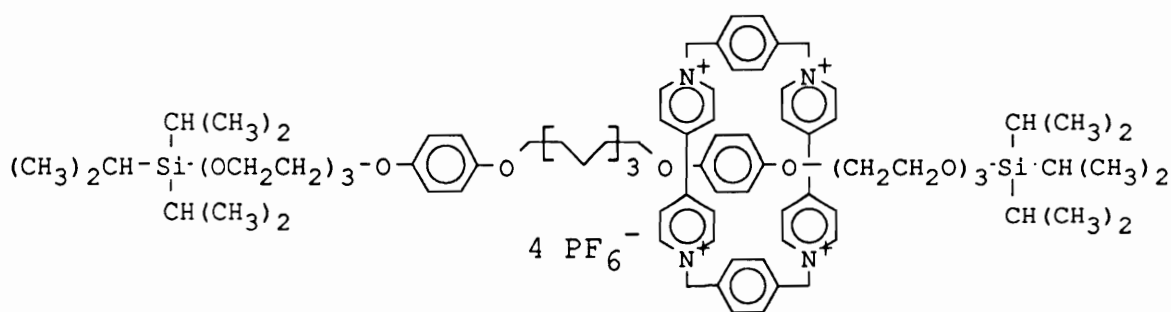
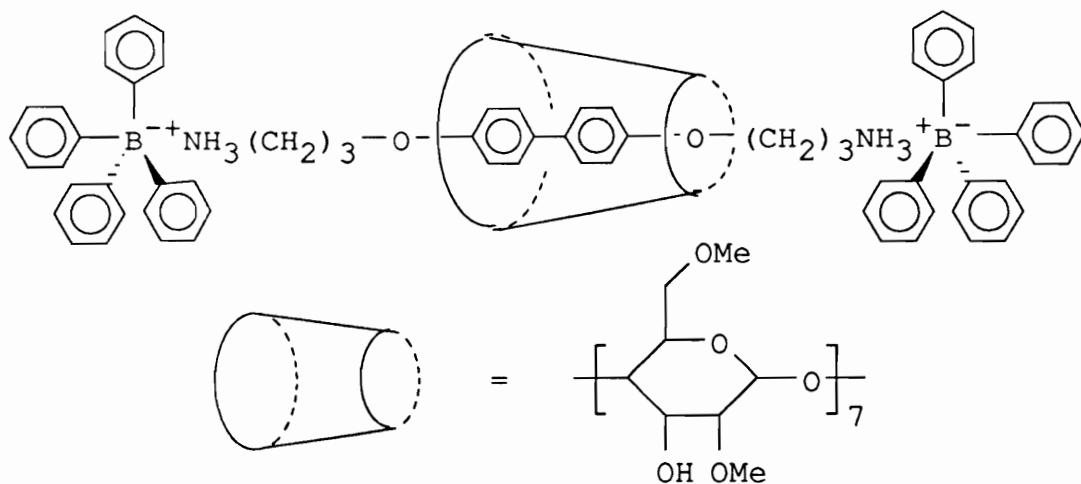
I-20

Agam *et al.* studied the statistical threading method theoretically. They set up a mathematical model and equations relating the amount of threading to concentration, chain length and ring size. Based on their calculation, they optimized the reaction conditions and obtained a 15% yield of rotaxane **I-21** from the crown ether, the oligomeric ethylene glycol and trityl chloride.³²



I-21

Recently the template directed syntheses have become actively studied. This method gives the highest yields of rotaxanes. Ogino synthesized and studied some properties of rotaxanes consisting of cyclodextrins threaded by α,ω -diaminoalkanes coordinated to cobalt(III) complexes.³³ Lawrence *et al.* reported the self-assembly of a threaded molecular loop, rotaxane **I-22**.³⁴ This was a template directed self-assembly process between the diammonium chloride salt and heptakis(2,6-*O*-methyl)- β -cyclodextrin in aqueous solution. The rotaxane was obtained in 71% yield. A few months ago, Stoddart *et al.* synthesized a rotaxane **I-23** they called a "molecular shuttle".³⁵ This rotaxane was synthesized via host-guest complexation of the paraquat tetracationic macrocycle and an oligomeric ethylene glycol chain containing two hydroquinone moieties. Because complexation was used as a driving force, the yield of the rotaxane was high.



Even though numbers of rotaxanes have been synthesized and various synthetic methodologies have been studied, the investigation of rotaxane physical properties is still in the primary stage. It has been found that rotaxanes show thin layer chromatographic (TLC) behavior different from that of a mixture of the components.²³ The thermal properties of some rotaxanes have been reported. The rotaxane **I-16** is stable up to 200°C,²⁷ while **I-17** ($n = 29$) decomposed at 120°C by thermally extruding the linear molecule from the macrocycle.²⁸ Rotaxanes also show mass spectral (MS) characteristic parent ion peaks

representing the molecular weight summation of the two components.^{25,28} It seems that the melting point of rotaxanes fall in between those of the two components,²⁹ and so does the solubility.

Most rotaxanes, especially when the complexation occurs between the linear and cyclic species, show nuclear magnetic resonance (NMR) chemical shift changes (different from that in the spectrum of its two components) for some characteristic peaks. For example, in the **I-17** system when there were 13 methylene units in the linear chain and $n = 32$, the shift was observed for methylene ring protons.²⁹

It is very interesting that in the "molecular shuttle" **I-23**, because of the charge-transfer interaction of the paraquat salt with hydroquinone moieties, the ring moves between the two identical "stations" (hydroquinone linkages) like a bead on a string.³⁵ The activation free energy for the ring motion from one station to the other is 13 kcal per mole. It may be possible to replace one of the hydroquinone moieties with another electron rich unit so that the shuttle can be driven electronically in a particular manner and hence it may be possible to process information as a molecular-scale computer.

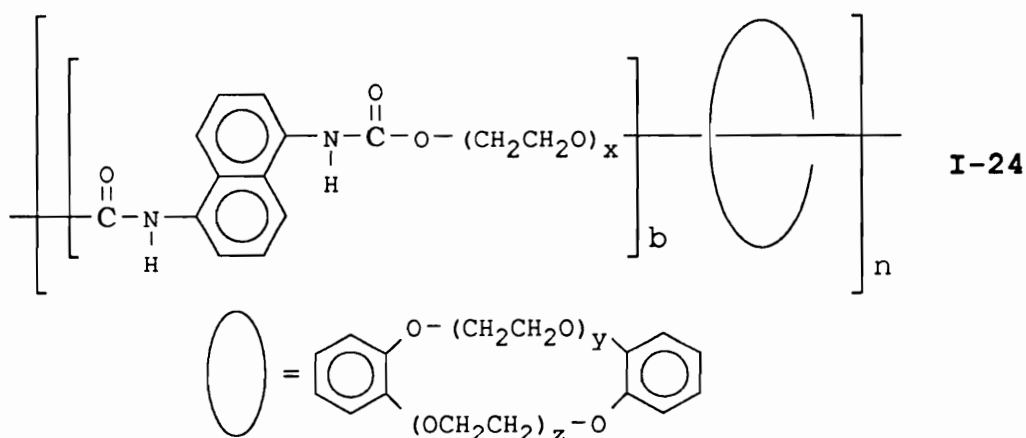
I-3-2: POLYROTAXANES

Harrison first demonstrated that macrocycles can thread onto polymer chains. He carried out the experiment with gas chromatography.³⁶ When a macrocycle gaseous phase was passed through the column, threading of the macrocycle onto the polymeric

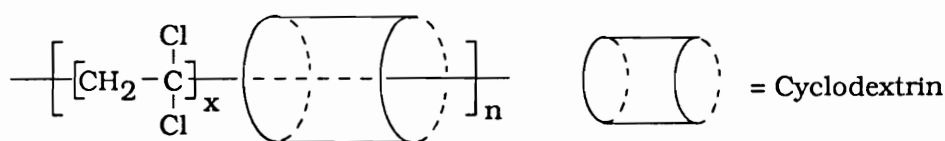
stationary phase took place and the vapor pressure of the macrocycle decreased upon threading.

There are a limited number of polyrotaxanes which have been reported. The topic refers to only a few names like Agam, Maciejewski and Lipatova.

By the addition of naphthalene-1,5-diisocyanate to an equilibrium system of oligomeric ethylene glycols (DP = 3 - 22) and crown ethers (15, 30, 44 and 58 membered rings), Agam *et al.* synthesized the first polyrotaxanes **I-24** in 1976.³⁷ They studied threading efficiency (number of threaded crown ethers per repeat unit) variation with ring size of the crown ether and chain length of the linear glycol. When the ring sizes vary from 30 to 44 to 58, b value varies from 10 to 30 to 50. When x varies from 3 to 4 to 7 to 13.2 to 22.3 at fixed y and z values of 8.7, b value varies from 10 to 3.1 to 1.9 to 1.6 to 2.1. Unfortunately, the polymers were not completely isolated and purified and molecular weights were not obtained. Note that there were no blocking groups used in this polyrotaxane system. Later Agam *et al.* used trityl moieties as end blockers to synthesize an oligomeric rotaxane via anionic oligomerization of ethylene oxide in the 58-membered crown ether. The rotaxane was obtained in 11% yield. However, Schill *et al.* have proven that the trityl group can not block macrocycles larger than 33 membered.²² Therefore, in the oligomeric rotaxane system, the macrocycle dethreaded upon heating to 150°C or during the gel chromatographic elution.³⁷

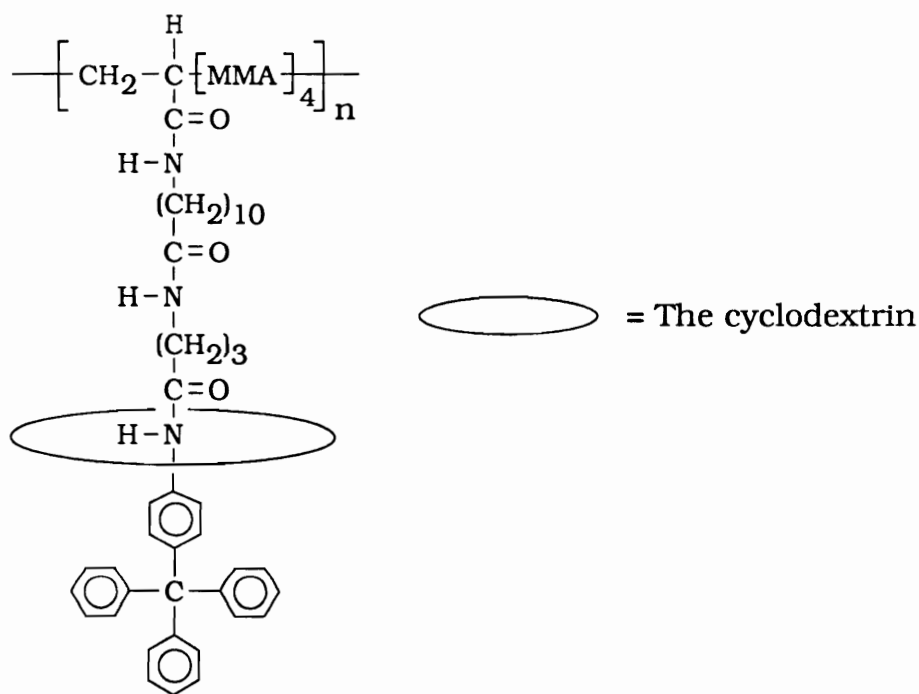


Maciejewski *et al.* reported the synthesis of polyrotaxanes **I-25** from the polymerization of vinylidene chloride and β -cyclodextrin in 1979.³⁸⁻⁴⁰ The polymer contained 80 wt% cyclodextrin linked to the vinylidene chloride polymer chain (20 wt%). The molecular weight was ca. 20,000. Note that this was a crystalline adduct polymerization where interaction between the cyclic and linear species acted as a driving force for threadings. That is different from the work by Agam *et al.* who used the statistical threading method.



Lipatova *et al.* synthesized polyrotaxanes **I-26** from swollen cyclic urethanes (34 and 40 membered rings) and neat styrene monomer by thermal polymerization.^{41,42} For the 34-membered ring, the x value was 18, while for the 40-membered ring, the x value was 21. They found

crystalline.^{41,42} Polyrotaxanes **I-25** with $x = 4.5$ to 21 were soluble in dimethylformamide (DMF), while the model polymers (the linear backbone without macrocycle) were not.³⁹ However, polyrotaxanes **I-26** were not soluble in benzene or dimethyl sulfoxide (DMSO), while the model polymer was soluble in benzene and the macrocycle was soluble in DMSO.^{41,42} Again, polyrotaxane **I-27** was soluble in diethyl ether, while the model polymer was not.⁴³



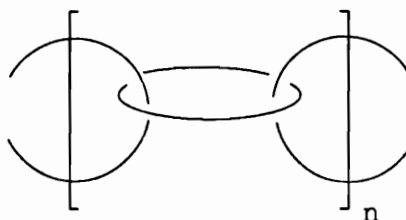
More solution properties of **I-27** have been studied.⁴³ For example, chemical shift changes for some protons in the ¹H-NMR spectrum were observed; the reduced viscosities of polyrotaxanes were found to be lower than that of the model polymer.

I-3-3: RAPID DEVELOPMENT IN CATENANE SYNTHESIS

As rotaxane related compounds, especially due to their synthetic similarities, it is necessary to discuss catenanes briefly. A catenane (Latin: *catena* = the chain) is a linked chain in which macrocyclic molecules are held together only mechanically without the aid of a covalent bond as represented by **I-28**, a catenane containing two rings. The number of rings can be as many as a polymer, polycatenane **I-29**.



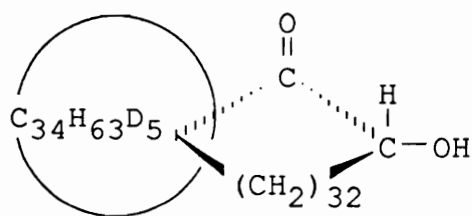
I-28



I-29

Compared with rotaxane chemistry, catenane chemistry is older and studied more extensively. Back to some time between 1900 and 1912, long before macrocycles were even known, Prelog and Willstätter have mentioned the compounds in a seminar at Zürich.⁴⁴ However, the thought had not become realistic until the advances made in synthesis of macrocycle compounds. Lüttringhaus *et al.* in Germany made the first report on experimental work in the synthesis of catenanes in 1958;⁴⁵ but the first isolated catenane was obtained by Wasserman in 1960.^{46,47} He synthesized "a few milligrams" of catenane **I-30** from a macrocyclic acyloin in the presence of a macrocyclic hydrocarbon. Oxidation of **I-30** cleaved the acyloin containing ring and yielded the

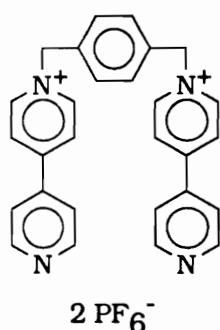
linear species. In the paper by Frisch and Wasserman entitled "chemical topology",²⁰ compounds which can be classified in this manner (include catenanes, rotaxanes and knots) were first called topological isomers, e.g., interlocked and uninterlocked, knotted and unknotted. Calculations were also given for the probability of formation and the stability of these materials.



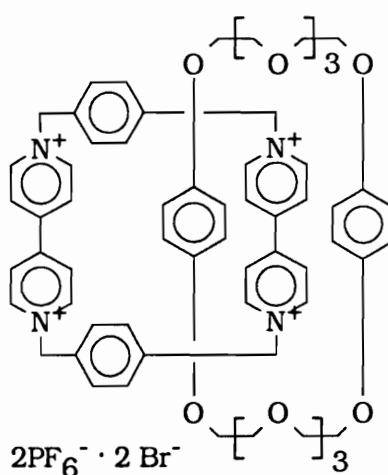
I-30

Since 1960, many catenanes have been synthesized via different methods such as chemical conversion,^{48,49} Möbius strip synthesis⁵⁰⁻⁵³ and statistical⁵⁴ approaches. Schill *et al.* first synthesized [3]-catenanes, catenanes comprised of three interlocking rings, by chemical conversion and translational isomerization was observed.^{55,56} However, they have not been high yielding (below 14%) until recently; synthesis of catenanes with high yields has been achieved via the template method. Using a phenanthroline-based macrocycle and difunctional molecules with Cu^{++} and Cs^+ as templates, Sauvage *et al.* have synthesized and characterized phenanthroline based [2]-catenanes in 27% yield^{57,58} and [3]-catenanes in 58% yield.⁵⁹ Stoddart *et al.* have extensively studied the host-guest

complexation between bis(paraphenylene)-(3n+4)-crown-n and the paraquat and diquat dications (see discussion in Chapter V). Based on this principle, they reported the synthesis of **I-32** in a one-step reaction from precursor **I-31** and α,α' -dibromo-p-xylene in the presence of bis(paraphenylene)-34-crown-10 in a 70% yield!⁶⁰



I-31



I-32

There have been no polycatenanes with unique structures as **I-29** synthesized except some reports on network systems which trapped macrocycles by threading onto linear chains between two crosslinking points as shown by **I-33**. Actually the systems should be classified as crosslinked polyrotaxanes; however, they have been called polymeric catenanes by Frisch *et al.* They studied a crosslinked polybutadiene containing a cyclic depsipeptide (Valinomycin), a 36-membered ring.⁶¹

Mark *et al.* studied some crosslinking systems containing cyclic poly(dimethylsiloxane).⁶²⁻⁶⁴

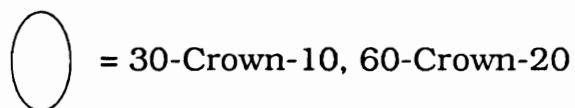
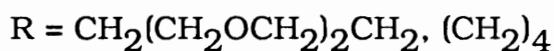
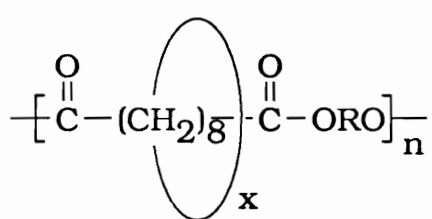
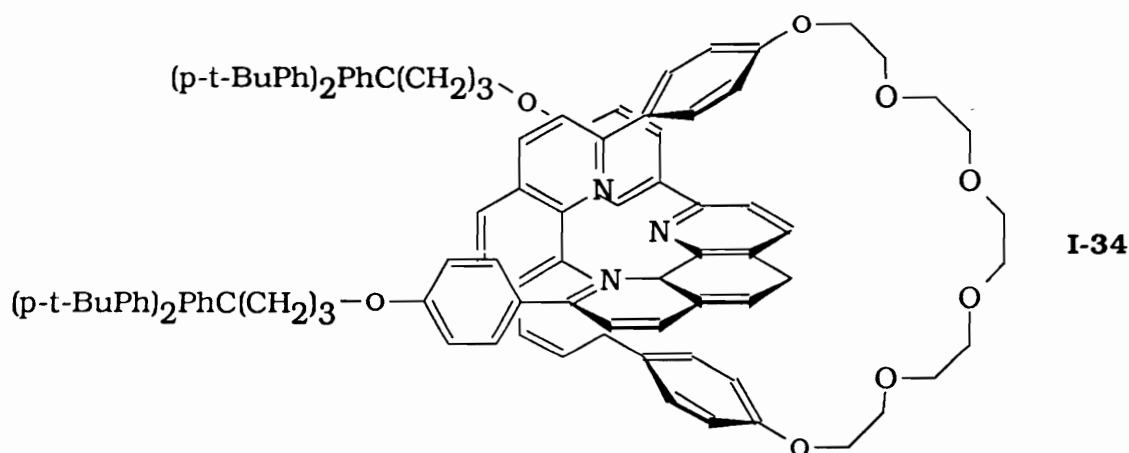


I-33

I-3-4: OTHER WORK ON ROTAXANE CHEMISTRY DONE IN OUR LABORATORY

Gibson *et al.* started the research on monomeric and polymeric rotaxanes in 1986 and have made significant contributions to rotaxane chemistry. Besides polyurethane-based polyrotaxanes, the other systems studied include polyester, polyamide, polystyrene and polyacrylonitrile based polyrotaxanes and some monomeric rotaxanes.⁶⁵ Following the method used by Sauvage *et al.*, a phenanthroline based rotaxane **I-34** has been synthesized in 42% yield and characterized by ¹H-NMR and MS analyses.⁶⁶ Significant chemical shift differences were observed between the protons on **I-34** and those on its two components. The mass spectrum showed three major peaks, corresponding to the parent ion of the rotaxane, fragmentation of the linear component and fragmentation of the cyclic component, respectively. The polyester based

polyrotaxane **I-35**,⁶⁷ synthesized from dimethyl sebacate, tri(ethylene glycol), and crown ethers via the statistical threading approach, showed only one peak on GPC trace, while the blend made by physical mixing of the model polymer and the macrocycle showed two peaks corresponding to the two separated components. Also the macrocycle in the blend can be removed easily by reprecipitation several times, but not in the case of the polyrotaxane system where the macrocycle is threaded; this revealed that reprecipitation is an effective method to remove unthreaded macrocycle from a rotaxane system.



$n/x = 1.8 - 7.7$

Recently, work on poly(butylene sebacate)-60C20 based polyrotaxanes has shown some interesting behavior of this unique polymer.⁶⁸⁻⁷⁰ For examples, the polyrotaxane has lower glass transition temperature and is more soluble in common solvents; most strikingly crystallization of 60C20 and the polyester backbone occur, producing two crystalline phases. Kinetics of crystallization of 60C20 in the polyrotaxane system have also studied and some potential applications of this new material have been proposed.

I-4: SYNTHETIC METHODOLOGIES

Generally there are three synthetic approaches leading to the interlocking systems: chemical conversion, statistical threading and template synthesis.

I-4-1: CHEMICAL CONVERSION

As illustrated by Scheme I-1, a well-designed molecule called a prerotaxane (**I-36**) has a special topological structure in which a difunctionalized linear backbone is encircled by a cyclic species and the two species are chemically bonded. A rotaxane (**I-38**) is generated when the covalent bond between the two species is cleaved after the ends of the linear species are blocked with blocking group (**I-37**). An example is rotaxane **I-13** which is generated by the hydrolysis of **I-14**. A

polyrotaxane **I-39** can be obtained from the polymerization involving in the prerotaxane. The key point of this method is synthesis of the prerotaxane **I-36**, which could be very difficult.

I-4-2: STATISTICAL THREADING

As illustrated by Scheme I-2, a difunctionalized linear species (**I-40**) is stirred with a melted macrocycle until an equilibrium is reached. A stoichiometric amount of monofunctionalized blocking group (**I-41**) is added to block the ends of the linear species. A certain percentage of rotaxane (**I-42**) can be isolated from the product mixture. A polyrotaxane (**I-43**) can also be prepared by conventional polymerization in the presence of a macrocycle or using it as the solvent.

This is the most widely used method. Many rotaxanes such as those numbered from **I-16** to **I-21**, and polyrotaxanes such as **I-24**, **I-26**, **I-35** were synthesized via this method.

Agam *et al.* have found that the yield of a rotaxane is controlled by several variables as shown by Equation (I-1),³² where N is the number of

$$N = \{k M_e M_g [1 - \exp(-N_e / \pi N_g)] N_e N_g \theta\} / V \quad \text{Eq. I-1}$$

threadings; M_e and M_g are the number of moles of the ring and the chain, respectively; V is the total volume; θ is threading angle which depends on the radius of the ring (r) and diameter of the chain (d) and is determined by Equation (I-2) and k is a constant related to characteristics of the system.

$$\text{Cos}\theta = d/2r$$

Eq. I-2

It can be seen from Equation (I-1) that the number of threadings increases with increases in concentrations of the ring and the chain. Therefore, a pure macrocycle used as solvent is the limiting case that the highest threading can be obtained. In considering threading and dethreading, the number of threadings changes with ring size and chain length in the fashion of a curve with the maximum value of N . However, in this mathematical model the rings were assumed to be rigid cycles and chains were rigid rods and the threading is directly related to the chain diameter and ring radius. The case could be very different practically. Because of the flexibility of the long chain and large ring, the dethreading may not be significant, especially for high molecular weight polyrotaxanes. This is consistent with experimental results. Dethreading was not observed for polyester-crown ether based polyrotaxanes.⁶⁷

I-4-3: TEMPLATE SYNTHESIS

In general, the template approach can be classified into two categories. Schemes I-3 represents the template synthesis using a third species (usually a metal ion) as the template. Scheme I-4 represents the template synthesis via host-guest complexation, the linear and the cyclic molecules serve as templates for each other.

In Scheme I-3, both linear species (**I-44**) and cyclic species (**I-45**) are electron donors. They coordinate to a metal ion (M) to form an

interlocking molecule **I-46** which is a prerotaxane. The molecular planes of **I-46** are perpendicular to each other due to the steric dictates of the coordination sites on M, i.e., tetrahedral for Cu⁺⁺. The prerotaxane can either react with two moles of monofunctionalized blocking group and then be demonstrated to form a rotaxane **I-47** or be polymerized to a polyrotaxane **I-48**. Rotaxane **I-34** was synthesized via this approach.⁶⁶

In Scheme I-4, a host-guest complexation between an electron rich (or deficient) macrocycle (**I-49**) and an electron deficient (or rich) difunctionalized linear species (**I-50**) yields a threaded union **I-51**, which is a prerotaxane. A rotaxane **I-52** is generated by reacting of **I-51** with a monofunctionalized blocking group. On the other hand, **I-51** can be directly used as a polyrotaxane precursor leading to polyrotaxanes **I-53**. Rotaxanes **I-22**,³⁴ **I-23**³⁵ and polyrotaxanes **I-25**,³⁸⁻⁴⁰ **I-27**⁴³ were synthesized via this approach.

I-4-4: DRIVING FORCES FOR THREADING

The Gibbs free energy change associated with the threading process is determined by enthalpy and entropy changes according to

$$\Delta G = \Delta H - T \Delta S \quad \text{Eq. I-3}$$

In the statistical threading approach, ΔH is essentially zero or even positive (repulsive force between the linear and the cyclic species). Therefore, entropy change plays a major role as the driving force. The threading efficiency is affected by several variables such as ring size and ring rigidity, chain length and chain rigidity, ring-chain compatibility,

etc.. In the template approach, the negative ΔH from the electronic interaction between the donor and receptor offers a strong driving force. Very high threading efficiency, even quantitative, can be achieved with this approach.

REFERENCES

1. (a) Flory, P. J. "*Principles of Polymer Chemistry*", Cornell University Press, Ithaca, New York, **1953**; (b) Odian, G. "*Principles of Polymerization*", 2nd. Ed., Wiley, New York, **1981**; (c) Rudin, A. "*Elements of Polymer Science and Engineering*", Academic Press, New York, **1982**; (d) Hiemenz, P. C. "*Polymer Chemistry, the Basic Concepts*", Marcel Dekker, Inc., New York, **1984**; (e) McGrath, J. E. "*Encyclopedia of Physical Science and Technology*", Academic Press, New York, **1987**, Vol. 11, p120-142.
2. Roovers, J. "*Encyclopedia of Polym. Sci. and Eng.*", John Wiley & Sons, Inc., New York, **1987**, Vol. 2, p478.
3. Manaresi, P.; Parrini, P.; Semeghini, G. L.; de Fornasari, E. *Polymer* **1976**, 17, 595.
4. Kurata, M.; Abe, M.; Iwama, M.; Matsushima, M. *Polym. J.* **1972**, 3, 729.
5. Thurmond, C. D.; Zimm, B. H. *J. Polym. Sci.* **1952**, 8, 477.
6. Kamada, K.; Sato, H. *Polym. J.* **1971**, 2, 489.
7. Schaefgen, J. R.; Flory, P. J. *J. Am. Chem. Soc.* **1948**, 70, 2709.
8. Pfannemüller, B.; Burchard, W.; Franken, I. *Starch* **1976**, 28, 1.

9. Kennedy, J. P.; Guhaniyogi, S. C.; Percec, V. *Poly. Bull.* **1982**, *8*, 563.
10. Eschwey, H.; Burchard, W. *Polymer* **1975**, *16*, 180.
11. Wooley, K. L.; Hawker, C. J.; Fréchet, J. M. J. *J. Am. Chem. Soc.* **1991**, *113*, 4252.
12. Kennedy, J. P. *Appl. Polym. Symp.* **1977**, *30*, 1.
13. (a). Flory, P. J. "*Encyclopedia of Poly. Sci. and Eng.*", John Wiley & Sons, Inc., New York, **1987**, Vol. 10, p95; (b). Gillham, J. K. *ibid*, Vol. 4, p519.
14. (a). Noshay, A.; McGrath, J. E. "*Block Copolymers: Overview and Critical Survey*" **1977**, Academic Press, New York; (b). Riess, G.; Hurtrez, G.; Bahadur, P. "*Encyclopedia of Polym. Sci. and Eng.*", John Wiley & Sons, New York, **1985**, Vol. 2, p324; (c). McGrath, J. E. *Pure and Appl. Chem.* **1983**, *55*, 1573. (d). McGrath, J. E. *J. Chem. Ed.* **1981**, *58*, 914.
15. "Cyclic Polymers", Edited by Semlyen, J. A., Elsevier, New York, **1986**.
16. Hiraoka, M. "*Crown Compounds, Their Characteristics and Applications*", *Study in Org. Chem. Vol. 12*, Elsevier, New York, **1982**, p241
17. de Gennes, P. G. *Macromolecules* **1984**, *17*, 703.

18. (a). Wilkes, G. L.; Orlor, B.; Huang, H. *Polym. Prepr.* **1985**, 26(2), 300; (b). Huang, H.; Orlor, B.; Wilkes, G. L. *Macromolecules* **1987**, 20(6), 1322.
19. Schill, G. "Catenanes, Rotaxanes, and Knots", *Organic Chem.-A series of Monographs, Vol. 22*, Academic Press, New York, **1971**.
20. Frisch, H. L.; Wasserman, E. *J. Am. Chem. Soc.* **1961**, 83, 3789.
21. (a). Stetter H.; Lihotzky, R. *unpublished data* **1962**; (b). Lihotzky, R. *Dissertation* **1962**, Technische Hochschule, Aachen.
22. Schill, G.; Zollenkopf, H. *Nachr. Chem. Techn.* **1967**, 79, 149.
23. Schill, G.; Zollenkopf, H. *Ann. Chem.* **1969**, 721, 53.
24. Schill, G.; Zürcher, C.; Vetter, W. *Chem. Ber.* **1973**, 106, 228.
25. Schill, G.; Beckmann, W.; Vetter, W. *Chem. Ber.* **1980**, 113, 941.
26. Schill, G.; Beckmann, W.; Vetter, W. *Ang. Chem. Int. Ed. Engl.* **1973**, 12, 665.
27. Harrison, I. T.; Harrison, S. *J. Am. Chem. Soc.* **1967**, 89, 5723.
28. Harrison, I. T. *J. Chem. Soc., Chem. Commun.* **1972**, 231.
29. Harrison, I. T. *J. Chem. Soc., Perkin I* **1974**, 301.
30. Schill, G.; Scheveikert, N.; Fritz, H.; Vetter, W. *Angew. Chem. Int. Ed. Engl.* **1983**, 22, 889.

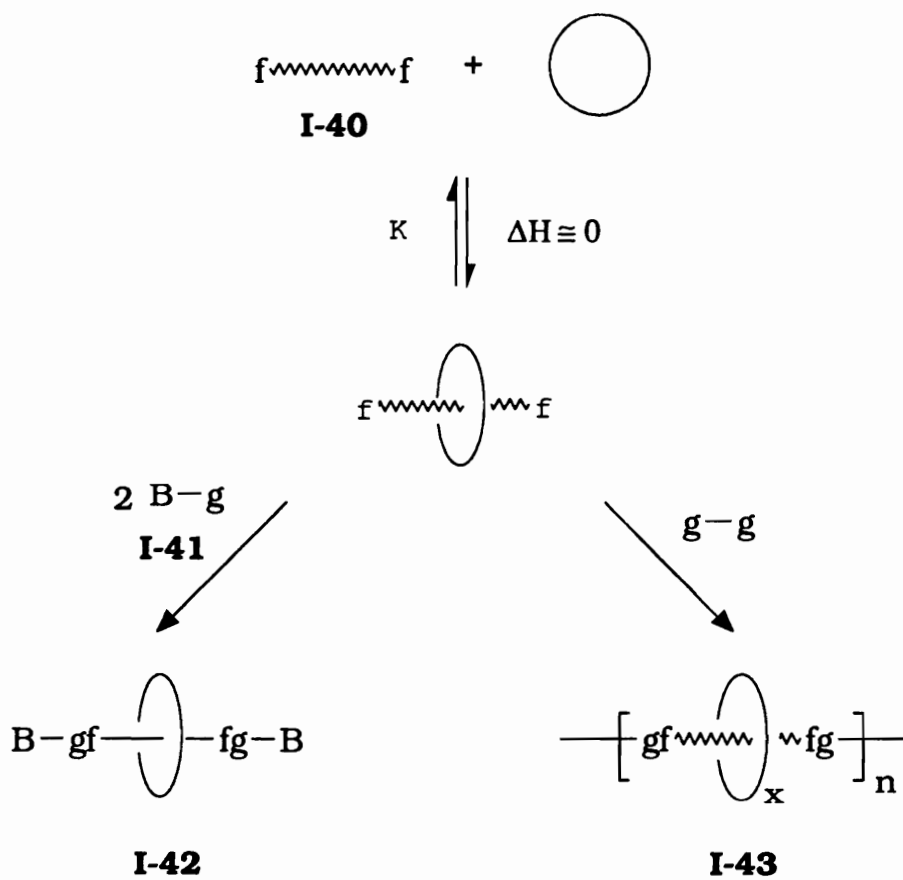
31. Schill, G.; Beckmann, W.; Schweickert, N.; Fritz, H. *Chem. Ber.* **1986**, *119*, 2647.
32. Agam, G.; Graiver, D.; Zilkha, A. *J. Am. Chem. Soc.* **1976**, *98*, 5206.
33. Ogino, H. *J. Am. Chem. Soc.* **1981**, *103*, 1303.
34. Venkata T.; Rao, S.; Lawrence, D. S. *J. Am. Chem. Soc.* **1990**, *112*, 3614.
35. Ashton, P. R.; Groguz, M.; Slawin, A. M. Z.; Stoddart, J. F.; Williams, D. J. *Tetrahedron Lett.* **1991**, *32*, 6235; *J. Am. Chem. Soc.* **1991**, *113*, 5131.
36. Harrison, I. T. *J. Chem. Soc., Chem. Commun.* **1977**, 384.
37. Agam, G.; Zilkha, A. *J. Am. Chem. Soc.* **1976**, *98*, 5214.
38. Maciejewski, M. *J. Macromol. Sci.-Chem.* **1979**, *A13(1)*, 77.
39. Maciejewski, M.; Gwizdowski, A.; Peczak, P.; Pietrzak, A. *J. Macromol. Sci.-Chem.* **1979**, *A13(1)*, 87.
40. Maciejewski, M. *J. Macromol. Sci.-Chem.* **1979**, *A13(8)*, 1175.
41. Lipatova, T. E.; Kosyanchuk, L. F.; Gomza, Yu. P.; Shilov, V. V.; Lipatov, Yu. P. *Dokl. Akad. Nauk SSSR, (Eng. Tr.)* **1982**, *263*, 140.
42. Lipatova, T. E.; Kosyanchuk, L. F.; Shilov, V. V.; Gomza, Yu. P. *Poly. Sci. USSR, (Eng. Tr.)* **1985**, *27*, 622.

43. Born, M.; Ritter, H. *Makromol. Chem., Rapid Commun.* **1991**, *12*, 471.
44. Footnote 5 in reference 20.
45. Lüttringhaus, A.; Cramer, F.; Prinzbach, H.; Henglein, F. M.; *Justus Liebigs Ann. Chem.* **1958**, *613*, 185.
46. Wasserman, E. *J. Am. Chem. Soc.* **1960**, *82*, 4433.
47. Wasserman, E. *Sci. Am.* **1962**, *207*, 94.
48. Schill, G.; Lüttringhaus, A. *Angew. Chem.* **1964**, *76*, 567.
49. Schill, G.; Doerjter, G.; Logemann, E.; Vetter, W. *Chem. Ber.* **1980**, *113*, 3697.
50. Wasserman, E.; Ben-Efraim, D. A.; Wolovsky, R. *J. Am. Chem. Soc.* **1968**, *90*, 3286.
51. Wolovsky, R. *J. Am. Chem. Soc.* **1970**, *92*, 2132.
52. Ben-Efraim, D. A.; Batich, C.; Wasserman, E. *J. Am. Chem. Soc.* **1970**, *92*, 2133.
53. E. Wasserman, C. Batich, S. Barer, D. A. Ben-Efraim, *Polym. Prepr.*, *13*(2), 920(1972).
54. Agam, G.; Zilkha, A. *J. Am. Chem. Soc.* **1976**, *98*, 5214.
55. Schill, G.; Zürcher, C. *Chem. Ber.* **1977**, *110*, 2046.

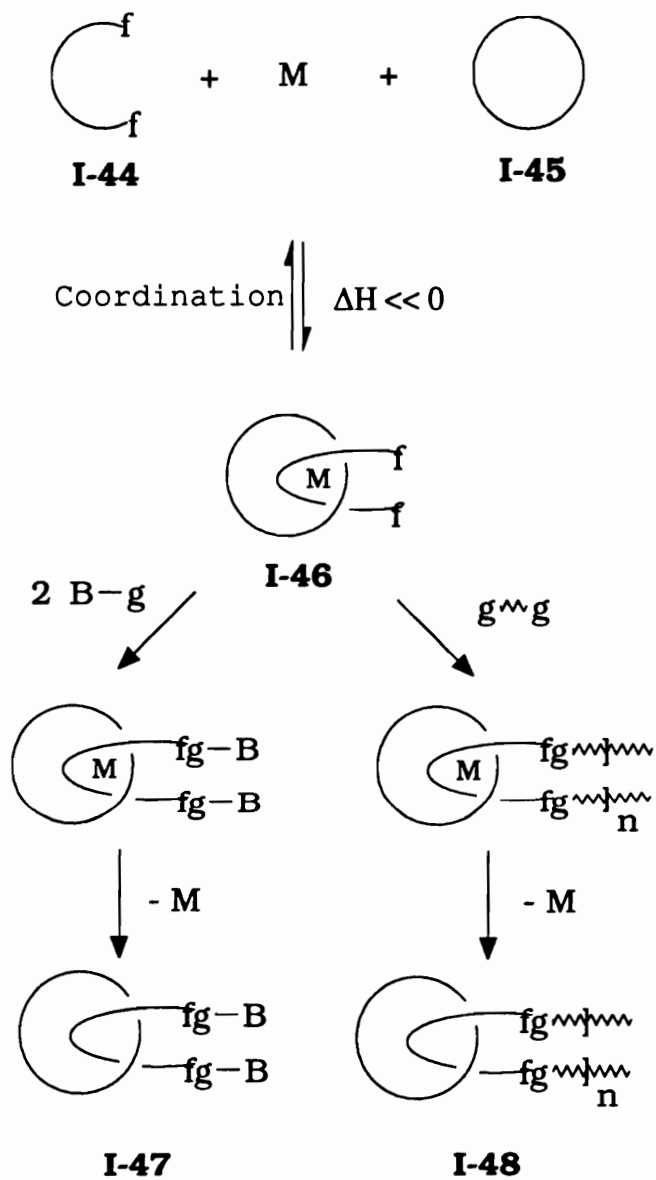
56. Schill, G.; Ressler, K.; Fritz, H.; Vetter, W. *Angew. Chem., Chem., Int. Ed. Engl.* **1981**, *20*, 187.
57. Dietrich-Buchecker, C. O.; Sauvage, J-P. *J. Am. Chem. Soc.* **1984**, *106*, 3043.
58. Dietrich-Buchecker, C. O.; Sauvage, J-P.; Weiss, J. *Tetrahedron Lett.* **1986**, *27*, 2257.
59. Dietrich-Buchecker, C. O.; Khemiss, A.; Sauvage, J-P. *J. Chem. Soc., Chem. Commun.* **1986**, 1376.
60. Ashton, P. R.; Goodnow, T. T.; Kaifer, A. E.; Reddington, M. V.; Slawin, A. M. Z.; Spencer, N.; Stoddart, J. F.; Vicent, C.; Williams, D. J. *Angew. Chem., Int. Ed. Engl.* **1989**, *28*, 1396.
61. Callahan, D.; Frisch, H. L.; Klempner, D. *Poly. Eng. Sci.* **1975**, *15*, 70.
62. Fyvie, T. J.; Frisch, H. L.; Semlyen, J. A.; Clarson, S. J.; Mark, J. E. *J. Poly. Sci., Part A, Poly. Chem.* **1987**, *25*, 2503.
63. Garrido, L.; Mark, J. E.; Clarson, S. J.; Semlyen, J. A. *Poly. Commun.* **1985**, *26*, 53.
64. Garrido, L.; Mark, J. E.; Clarson, S. J.; Semlyen, J. A. *Poly. Commun.* **1985**, *26*, 55.

65. Gibson, H. W.; Bheda, M.; Engen, P.; Shen, Y. X.; Sze, J.; Wu, C.; Joardar, S.; Ward, T. C.; Lecavalier, P. R. *Makromol. Chem., Macromol. Symp.* **1991**, 42/43, 395.
66. Wu, C.; Lecavalier, P. R.; Shen, Y. X.; Gibson, H. W. *Chem. Mater.* **1991**, 3, 569.
67. Wu, C.; Bheda, M. C.; Lim, C.; Shen, Y. X.; Sze, J.; Gibson, H. W. *Poly. Commun.* **1991**, 32, 204.
68. Gibson, H. W.; Wu, C.; Shen, Y. X.; Bheda, M.; Sze, J.; Engen, P.; Prasad, A.; Marand, H.; Loveday, D.; Wilkes, G. L. *Polym. Preprints* **1991**, 32(3), 593.
69. Gibson, H. W.; Wu, C.; Shen, Y. X.; Bheda, M.; Sze, J.; Engen, P.; Prasad, A.; Marand, H.; Loveday, D.; Wilkes, G. L. *Polym. Preprints* **1991**, 32(3), 637.
70. Marand, H.; Prasad, A.; Wu, C.; Bheda, M.; Gibson, H. W. *Polym. Preprints* **1991**, 32(3), 639.

Scheme I-2: Statistical Threading Approach to Rotaxanes and Polyrotaxanes



**Scheme I-3: Template Synthesis of Rotaxanes and Polyrotaxanes:
Metal Ion as Template**



CHAPTER II:

CROWN ETHER MACROCYCLES

The term "crown" generally refers to macrocyclic polyethers having the ethyleneoxy units as the basic repeating structure. This family of compounds has been extensively studied. Many books have been published in review of this field.¹

II-1: CONCEPTS OF DESIGNING MACROCYCLES FOR ROTAXANES AND POLYROTAXANES

One of the critical points in rotaxane and polyrotaxane design and synthesis is the design and synthesis of macrocycles. There are several basic concepts for design of macrocycles.

II-1-1: EFFECTIVE CAVITY SIZE

Effective cavity size is a critical requirement for macrocycles used in the rotaxane and polyrotaxane synthesis. The effective cavity of the macrocycle (actual cavity available for threading) must be larger than the effective chain diameter of the linear species to allow threading to occur.

On the other hand, it should not be so big as to allow easy dethreading since an equilibrium exists between the threaded and the unthreaded states. However, dethreading has not been observed in polyrotaxane systems even when a crown ether as large as 60C20 was used.² The effective cavity of a macrocycle is determined by the ring size (number of atoms in the ring), ring flexibility (conformation) and ring configuration (stereochemistry of the ring members). The ring flexibility is not very important unless the ring size is extremely large. Since we are dealing with polyethylene oxide and phenylene based crown ethers, the configuration is also not considered. The only variable now to be considered is the ring size.

Harrison has demonstrated that rings with less than 22 methylene units for hydrocarbon macrocycles cannot be threaded by 1,11-undecanediol. But those with more than 33 methylene units can dethread from the undecane backbone even when blocked with a trityl group.³ Agam *et al.*, based on a mathematical model, have theoretically derived an expression relating the amount of threading to several variables, including ring size.⁴ He pointed out that the ring size affects the threading more than other parameters. To our knowledge from previous results,¹⁻⁵ it seems that crown ethers with ring sizes of 30-membered to 60-membered are suitable for polyrotaxane syntheses with reasonable threading efficiency and the resulting polymers show significant differences in properties from their corresponding model polymers, the polymer backbones without macrocycles.

II-1-2: ABILITY TO COMPLEX A GUEST MOLECULE

If the template method is used, it is required that the macrocycle possesses the ability to form a so-called host-guest complex with another species. The macrocycle acts as a host and the other species is a guest. In order to form a host-guest complex, a strong interaction must exist between the host and the guest molecules with significant enthalpy changes. The interaction may be coordination (Scheme I-3) where the macrocycle and the linear molecule offer electron pairs or charge transfer (Scheme I-4) where the macrocycle can either be the donor or acceptor. Generally the guest can be a metal ion and then the metal ion binds with a linear species as represented by Scheme I-3 or it can be a suitable linear species only via a molecular self-assembly process as shown in Scheme I-4. The examples of macrocycles which can be used in the template synthesis include phenanthroline based, phenylene based, paraquat based, cyclodextrin derivatives, etc.

II-1-3: FUNCTIONALIZED MACROCYCLES

To synthesize polyrotaxanes having schematic structures **I-12c**, **I-12d**, and **I-12e**, functionalized macrocycles are required. They can be either monofunctionalized (precursors for **I-12d** and **I-12e**) or difunctionalized (precursors for **I-12c**). Functionalized macrocycles are usually prepared from functionalized starting materials. If the functional group is affected during the cyclization, it should be protected prior to the reaction and deprotected afterward.

II-1-4: MELTING POINT, SOLUBILITY AND STABILITY

In the statistical threading approach, macrocycles are used as solvents in most of the cases. Therefore, it is required that the melting point of the macrocycle is below the reaction (polymerization) temperature. To provide a low viscosity for the polymerization system, generally the melting point of the macrocycle is expected to be 30°C or more below the polymerization temperature. Of course, the macrocycles should be able to dissolve the monomers. Crown ethers with ring sizes of 30 to 60 membered are polar in nature and their melting points are in the range of 30 to 50°C. They, therefore, are good candidates for many rotaxane and polyrotaxane systems.

If one or more co-solvents are used in the synthesis, sometimes in the statistical threading but mostly in the template approaches, it is required that the macrocycle is soluble in or miscible with the co-solvents.

Macrocycles should be thermally and chemically stable under the reaction conditions. For example, the decomposition temperature of crown ethers and phenylene based crown ethers are around 180°C and 275°C, respectively; they can be used for polyurethanes.

Table II-1 listed some examples of macrocycles with ring sizes from 25-membered to 60-membered.⁶⁻¹³ They are crown ether and analog candidates for polyrotaxanes.

II-2: SYNTHETIC APPROACHES

The first crown compound was synthesized in 1967 by Pedersen⁷ when he was preparing a diphenyl ether from the reaction of tetrahydropyran (THP) monoprotected catechol and di(ethylene glycol) dichloride. After the deprotection, he unexpectedly obtained dibenzo-18-crown-6 as a by-product. Since then he has synthesized many examples of the compounds we know as "crown ethers".

II-2-1: SYNTHETIC METHODS

Crown ethers are usually synthesized via Williamson ring closure reactions involving a diol and another species having leaving groups at the ends. Synthetic approaches can be generalized as four principal methods named "V", "W", "X" and "Y", respectively.

"V" Method: This is the "one plus one" method as represented by an example shown in Scheme II-1. A single diol is allowed to react with a single oligo(ethylene glycol) having leaving groups at each end. The diol can be ethylene glycol, hydroquinone, hydrocarbon diols, bis-phenol-A, phenanthroline-based bisphenol, etc. Introduction of a functional group from R leads to monofunctionalized crown ethers.

"W" Method: The example for "W" method is shown in Scheme II-2. In this method, the two hydroxyl groups are separated by a portion of the chain. The R group could be any segment (rigid in most cases) such as

aromatic ring, hydrocarbon chain, etc. The R' group, of course, could be the same as R or different or it also can be oligo(ethylene oxide)s. By variation of R, R', a, and b groups, symmetrical and unsymmetrical crown ethers can be prepared. Also functional groups can be introduced from R and R' groups leading to mono or difunctionalized crown ethers.

"X" Method: As shown by Scheme II-3, the stoichiometry of this method is the same as that of "V" method. However, the product is produced by "four-piece combination" instead of "two-piece combination". Of course, the crown ether formed by "two-piece combination" would also be produced as a side-product. In fact, it is not the intent of the synthesis but the reaction dynamics (size of crown) which determine the product. Again, there are many choices of R and R' groups.

"Y" Method: This is a self-cyclization process involving only one starting material which has a hydroxyl group at one end and a leaving group at the other end as represented by Scheme II-4. Of course, the crown ether with twice the ring size is also produced. As in the "V" and "X" methods, the ring size of the crown determines the outcome of the reaction.

In the Schemes II-1 to II-4, the leaving group is not necessarily chloride. It also could be bromide, iodide, tosylate, methanesulfonate, etc. The tosylate seems to be the best choice of leaving group since oligo(ethylene glycol)s are very easily converted to the ditosylates by reacting with tosyl chloride.

II-2-2: TEMPLATE EFFECT

It has been known that higher yields of macrocycles can be achieved under high dilution conditions so that the probability of the two ends meeting exceeds the probability of linear polymer formation. However, this is not the only way to improve the yields. Another even more efficient method is the use of a template in the synthesis. The templates are usually metal ions or other cations with specific sizes. The effect is illustrated in Scheme II-5, the formation of 18-crown-6 (18C6). The first C-O bond formation may not be effected by the presence of the templating cation (M^+). However, the second C-O bond formation is largely effected. The cation is ion-paired with the alkoxide anion and the remainder of the chain wraps around it. It is clear from Scheme II-5 that the geometry of the complex favors the ring formation by bringing the ends close together.

Many studies have shown that the ring size of the crown ether produced (i.e., Scheme II-1 vs Scheme II-3) depends on the size of the template used.^{10, 4-18} For example, Masci *et al.* have shown that in the presence of a metal ion, the yield of a unsubstituted crown ether was related to its ring size in the fashion of a bell-shaped curve. The curve shifted to larger sizes of crown ethers when larger sizes of templating metal ions were used (Figure II-1).¹⁷ Therefore, by choice of template, a desired size of crown ether can be obtained in relatively high yield.

II-3: RESULTS AND DISCUSSION

II-3-1: PREPARATIONS OF PRECURSORS FOR CROWN ETHERS

The precursors used for syntheses of the crown ethers are oligo(ethylene glycol)s and oligo(ethylene glycol) ditosylates or the diiodides.

II-3-1-1: Oligo(ethylene glycol)s

One of the disadvantages of "V" method (Scheme II-1) to synthesize macrocyclic crown ethers is that relatively high molecular weight starting materials are required. For instance, deca(ethylene glycol) and deca(ethylene glycol) ditosylate were used by Chênevert *et al.* to prepare 60C20.¹⁰ The difficulties faced are the preparation and purification of the oligo(ethylene glycol)s. In the syntheses of oligo(ethylene glycol)s from lower molecular weight precursors, one generally obtains a mixture of products containing oligo(ethylene glycol)s with several different molecular weights. Multiple distillations are usually used to separate and purify these oligo(ethylene glycol)s. The distillations have to be done under high vacuum at very high temperatures. Even though some oligo(ethylene glycol)s such as penta- and hexa(ethylene glycol)s are commercially available, they are very expensive and not realistic for our case since we require large quantities.

To solve this problem, we adopted the "X" method (Scheme II-3) (by

using commercially available (very cheap) low molecular weight oligo(ethylene glycol)s such as ethylene glycol, di-, tri- and tetra(ethylene glycol)s to obtain desired crown ethers. Still the hexa(ethylene glycol) was synthesized from tetra(ethylene glycol) and ethylene glycol via a two-step route as shown by Scheme II-6. First, tetra(ethylene glycol) was converted to the dichloride which is an electrophile reactive toward ethylene glycol. This conversion was done with thionyl chloride and pyridine was added to capture by-product HCl to drive the reaction. In the second step, sodium (half equivalent to ethylene glycol) was used to mono-deprotonate ethylene glycol. An excess amount of the mono-deprotonated ethylene glycol was used to ensure the formation of hexa(ethylene glycol). However, still the yield of pure hexa(ethylene glycol) was quite low (29%). The loss of yield could be due to the side-reactions and also not all of the hexa(ethylene glycol) was separated from the product mixture by distillations.

The purity of the hexa(ethylene glycol) was proved by Gas Chromatography (GC) with a commercial standard sample as a reference. The GC traces are shown in Figure II-2. The structure was proved by $^1\text{H-NMR}$ (Figure II-3). Also FTIR shows the existence of hydroxyl groups.

II-3-1-2: Oligo(ethylene glycol) Ditosylates

It is known that tosylate is a good leaving group. I used oligo(ethylene glycol) ditosylates in my crown ether syntheses. The oligo(ethylene glycol) ditosylates were obtained by ditosylation of corresponding oligo(ethylene glycol)s in NaOH/H₂O/THF system as

shown in Scheme II-7. These reactions were reported by Ouchi *et al.*¹⁴ The reported reaction time was 2 hours. However, the reactions were found not to be complete in 2 hours and hence, I allowed them to go for 24 hours. Under that condition, the reactions were complete and isolation and purification were simplified, i.e., no column separation was necessary. A slightly excess amount of tosyl chloride was used in all reactions and yields were over 90%.

The oligo(ethylene glycol) ditosylates with chain length more than three ethylene oxide units were obtained as oils. The purification procedures were basically extractions and washings to remove salts and unreacted starting materials. However, tri(ethylene glycol) ditosylate and ethylene glycol ditosylate were crystalline solids, which were purified by recrystallizations. Figure II-4 shows ¹H-NMR spectra of tri- and tetra(ethylene glycol) ditosylates. They are consistent with their structures. Also FTIR spectra show no hydroxyl groups.

II-3-1-3: Penta(ethylene glycol) Diiodide

Penta(ethylene glycol) diiodide was also prepared via a multistep route starting from ethylene glycol. This compound was used in the synthesis of a phenanthroline-based macrocycle. The macrocycle synthesis was done by Wu *et al.* in our laboratory.¹⁹ Therefore, it will not be reported here.

The synthetic route is shown in Scheme II-8. The first step was the preparation of penta(ethylene glycol); both the synthesis and

purification were the same in principle as those of hexa(ethylene glycol) discussed above. Then the diol was converted to dichloride by treatment with thionyl chloride. Further, the dichloride was converted to the diiodide by refluxing in acetone with an excess amount of sodium iodide. The last two steps gave very good yields.

Both the dichloride and diiodide were purified by multiple vacuum distillations. The functional group conversions were monitored by FTIR analyses and further proved by $^1\text{H-NMR}$ analyses. Figure II-5 clearly shows that the chemical shift of $-\text{CH}_2\text{-X}$ methylene protons changed from 3.70 ppm to 3.30 ppm when X was changed from $-\text{Cl}$ to $-\text{I}$.

II-3-2: SYSTEMATIC SYNTHESSES OF m-CROWN-n

The syntheses of 30C10, 36-crown-12 (36C12), 42-crown-14 (42C14), 48-crown-16 (48C16) and 60C20 have been reported by Chênevert *et al.*¹⁰ The method they used was the "V" method ("two-piece combination") with R = oligo(ethylene oxide) (Scheme II-1). By variation of the chain lengths of the two reactants, crown ethers with different ring sizes were obtained. They used NaH as base and tetrahydrofuran (THF) as the reaction solvent. The reported yields were 55% (30C10), 28% (36C12), 20% (42C14), 22% (48C16) and 26% (60C20). 30C10 and 36C12 were reported as oils. The melting points of the other crown ethers were 28.5 - 31°C (42C14), 40 - 43°C (48C16) and 46 - 50.5°C (60C20). Crown ethers showed single peaks on $^1\text{H-NMR}$ spectra (chloroform-d). The chemical shifts were 3.67 ppm (30C10), 3.66 ppm (36C12), 3.66 ppm (42C14), 3.66 ppm (48C16) and 3.64 (60C20). In this

section, the systematic syntheses of these crown ethers in large quantities (20 - 50 gram scales) using relatively low molecular weight starting materials are reported.

The one-pot systematic synthesis of crown ethers is illustrated in Scheme II-8. The reaction was nucleophilic substitution in a NaH/THF system with tosylate as leaving group. Two crowns were obtained from each reaction. One was formed by "two-piece combination" and the other (twice the ring size) was formed by "four-piece combination". The total yield of the two crown ethers ranged from 30% to 60% depending on the system. Of course, the reaction dynamics determine the outcome of the reactions. It is known that the relative yields of the cyclic versus open chain products depend on reaction conditions, especially concentration. Generally dilution favors the formation of cyclic species. Therefore, the reactions were carried out in relatively high dilution systems to enhance the yield of crown ethers. Also the relative yields of the two crown ethers ($m/2$ -crown- $n/2$ versus m -crown- n) (Scheme II-8) is determined by several variables such as ring sizes, concentrations, temperature and template used. Assuming the ring strain effect is negligible, generally the yield of $m/2$ -crown- $n/2$ is higher than that of m -crown- n . This is probably because the shorter chain has shorter end-to-end distance and higher collision probability. Based on this idea, higher temperature should favor the larger ring formation. It was true that a higher yield of 42C14 was obtained at higher temperature when tri(ethylene glycol) reacted with tetra(ethylene glycol) ditosylate.²⁰ Another efficient method to obtain high yields of a crown ether with desired ring size is the use of

template. Unfortunately, I did not investigate the template effect on these reaction systems.

All crown ethers used in the syntheses of polyrotaxanes were prepared from the corresponding low molecular weight oligo(ethylene glycol)s and oligo(ethylene glycol) ditosylates. For examples, the reaction of tri(ethylene glycol) and tri(ethylene glycol) ditosylate produced 36C12 and 18C6; tetra(ethylene glycol) and tri(ethylene glycol) ditosylate produced 42C14 and 21-crown-7 (21C7); tetra(ethylene glycol) and tetra(ethylene glycol) ditosylate produced 48C16 and 24-crown-8 (24C8), while tetra(ethylene glycol) and hexa(ethylene glycol) ditosylate produced 60C20 and 30C10. Alternate syntheses using the shorter glycols and the longer ditosylates produced much lower yields, especially when the glycols are shorter than tri(ethylene glycol). This phenomenon was also observed by Ouchi *et al.* in the syntheses of 20-crown-6 from butanediol and penta(ethylene glycol) ditosylate. The yield increased from 26% to 42% when the diol and ditosylate were reversed.¹⁴

The isolation and purification of crown ethers were very difficult since the reaction products were mixtures of crown ethers with different ring sizes and open chain diols and ditosylates with different molecular weights. Vacuum distillations were not practical because decomposition of crown ethers begins to occur at 175°C. Column separations were also not efficient since the polarity of the products and by-products are so close. Fortunately, the crown ethers were isolated and purified by multiple recrystallizations in acetone at low temperature. Most of

impurities such as the diols and ditosylates are soluble in acetone and different crown ethers can recrystallize out at different temperatures. Therefore, by controlling the recrystallization conditions, the crown ethers were isolated and purified.

All the crown ethers show a single peak on $^1\text{H-NMR}$ spectra (Figure II-6). It was difficult to identify the chemical shifts differences between them when the $^1\text{H-NMR}$ spectra were taken separately because the instrumental conditions were not exactly the same (Figure II-6a - Figure II-6e). However, the differences became significant on the $^1\text{H-NMR}$ spectrum of a synthetic mixture of pure crown ethers (Figure II-6f).

Differential scanning calorimetric (DSC) analysis was done with 60C20 and the trace is shown in Figure II-7. The glass transition temperature is -66°C and melting point is 49°C . The other crown ethers are expected to have similar thermal transitions.

II-3-3: BIS(*p*-PHENYLENE) BASED CROWN ETHERS

In this section, the syntheses and characterization of two semirigid macrocycles, bis(*p*-phenylene)-34-crown-10 (BPP34C10) and bis(*p*-phenylene)-32-crown-4 (BPP32C4) are reported.

Even though BPP34C10 is a known compound, it is necessary to study different synthetic methods for the purpose of seeking an economic and efficient synthetic route because a large quantity of the material is required in the polyrotaxane syntheses; however, most of the reported work was done on small scales with low yields. Therefore, optimizations

of reported literature procedures for one step and four step syntheses have been carried out routinely on relatively large scales (2 - 3 g of pure product). A new two step procedure and application of the template effect for the first time to the one step process were also investigated.

BPP32C4 is a new compound. The synthesis is the same as that of BPP34C10 in principle. This compound was prepared using only the one step method.

II-3-3-1: BPP34C10

Theoretically there are several synthetic routes by which BPP34C10 could be obtained. This compound was first reported by Cram *et al.*^{21,22} via a one-step reaction of hydroquinone and tetra(ethylene glycol) ditosylate; the yield was reported as 8%. Stoddart *et al.* employed a four-step procedure to synthesize BPP34C10 starting from hydroquinone and tetra(ethylene glycol) ditosylate which included the monoprotection of hydroquinone.²³ The overall yield reported by them was 12.8%, which was higher than that by the one-step synthesis. It is known that one hardly obtains high yields in the synthesis of macrocycles because of the formation of many by-products, including linear and cyclic oligomers. In order to optimize the synthesis, I have examined five synthetic methods for this macrocycle: a four-step route, a two-step route, a one-step route in two different solvents, and a one-step route with Cs⁺ as template.

Based on Stoddart *et al.*'s four-step procedure, I used a modified

route described in Scheme II-10. In this method, a protecting benzyl group was used. The monoprotected compound **II-6** was obtained in 54%, which is close to the theoretical value for this monoprotection reaction. The appearance of a singlet benzyl proton peak at 5.00 ppm in the $^1\text{H-NMR}$ spectra was the evidence of the benzyl ether bond formation. In the second-step, an excess amount of 4-benzyloxyphenol **II-6** and a strong base (NaH) were used to ensure the disubstitution. This step yielded 74% of a disubstituted product **II-7**. Because the C-O bond of a benzyl ether is weaker than that of an aliphatic ether, catalytic hydrogenation was adopted to remove the benzyl protective group without breaking other ether bonds. The FTIR spectrum showed the appearance of a phenol peak after the hydrogenation (Figure II-8) and the $^1\text{H-NMR}$ spectrum showed the disappearance of benzyl proton peaks. A quantitative yield of the diphenol **II-8** was obtained. The reaction conditions of the last step (cyclization) were the same as those in the second step (disubstitution) except that a one to one molar ratio of the diphenol **II-8** to tetra(ethylene glycol) ditosylate was used. Since the yield of the cyclization depends on the concentration of the reaction system, the cyclization reaction was carried out in a dilute system (0.05 M); this produced pure BPP34C10 in 28% yield. The structure of BPP34C10 was proved by its FTIR spectrum which showed no hydroxyl peak and its $^1\text{H-NMR}$ spectrum which is consistent with the structure (Figure II-9). Also its melting point is close to the reported value.²³

In another hand, I used a two-step synthetic route without the monoprotection of hydroquinone (Scheme II-11). The reaction conditions

in step 1 were controlled precisely by dropwise adding base to the solution of hydroquinone and tetra(ethylene glycol) ditosylate in which hydroquinone was in large excess. The main product was expected to be the diphenol **II-8** and also some macrocycle. The excess of hydroquinone was removed from the products by extraction with water. The resultant product mixture showed three major peaks on HPLC (Figure II-10). The largest peak, identified as **II-8** by spiking with an authentic sample, was 54.6% by area, corresponding to 49% yield. The cyclization was carried out with this product mixture, without isolation and purification of the diphenolic compound, by reaction with one equivalent of tetra(ethylene glycol) ditosylate using NaH/DMF. The product from the cyclization reaction was a mixture containing BPP34C10 (**II-9**) which was isolated by column chromatography and purified by recrystallization from toluene/n-hexane (70:30/v:v) mixture. The overall yield of BPP34C10 with this two step method was 14.2%.

The one-step route was performed in two different solvents (Scheme II-12). I first carried out this one-pot reaction of hydroquinone and tetra(ethylene glycol) ditosylate in refluxing 1-butanol/1,4-dioxane. 1,4-Dioxane was used to dissolve tetra(ethylene glycol) ditosylate which is not very soluble in 1-butanol. Again, the reaction solution was dilute (0.1 M) to increase the probability of cyclization. This one-pot reaction gave a mixture of products including monosubstituted, oligomeric and cyclic compounds. Fortunately, column chromatography on acidic alumina with ethyl ether as eluting solvent is able to separate macrocycle from other by-products which are more polar open chain compounds and

have much longer retention times. A 10.5% yield of macrocycle was found with this method.

The one-step synthesis of BPP34C10 was also investigated in refluxing ethanol. A poor yield (3.5%) of BPP34C10 was obtained in this case. The decrease in yield is probably due to the lower reaction temperature.

The yield of BPP34C10 increased significantly with this one-step method when the template effect was applied. In the case of 1-butanol/1,4-dioxane, the yield increased to 12.5% when equimolar Cs_2CO_3 was present in the reaction system, corresponding to a 19% relative increase. This indicates that the formation of macrocycle is stepwise and the coordination of Cs^+ to oxygen atoms on the ether chain helps the orientation toward the formation of the cyclic species in the process.

In summary, the yield of BPP34C10 associated with different synthetic routes are listed in Table II-2. It can be seen that the yield is determined by the cyclization step. In the one-step route, "four pieces" are brought together to form the macrocycle. But there are only "two pieces" required for cyclizations in four-step and two-step routes which offer higher cyclization yields. However, the overall yields are comparable.

BPP34C10 was analyzed by DSC and the trace is shown in Figure II-7b. As a normal crystalline compound, BPP34C10 shows a glass

transition temperature of 258^oK and a crystallization temperature of 291^oK. Interestingly, two melting peak at 367^oK and 373^oK were observed, indicating that BPP34C10 exists in two different crystal structures (or two different molecular conformations). This result is consistent with crystal structures of BPP34C10 determined by X-ray single crystal analysis (see Chapter V-2-1). It can be estimated that ratio of the two crystals is approximately 3:1 based the peak areas.

II-3-3-2: BPP32C4

A bis(para-phenylene) based hydrocarbon macrocycle, BPP32C4 (**II-10**), was synthesized via a one step reaction of hydroquinone and 1,10-dibromodecane as shown in Scheme II-13. As in the one-step synthesis of BPP34C10, the ring was formed by "four-piece combination". The reaction conditions and work-up procedures were also the same as that of the one-step synthesis of BPP34C10 in 1-butanol/1,4-dioxane system. The ¹H-NMR spectrum (Figure II-11) is consistent with its structure. Its MS spectrum (Figure II-12) has a parent ion peak at 496 which corresponds to the macrocycle molecular weight. Further, elemental analysis gives correct contents of the elements.

II-4: CONCLUSION

Crown ethers m-crown-n can be systematically synthesized via

one-pot reactions of the corresponding oligo(ethylene glycol)s and oligo(ethylene glycol) ditosylates. This is a combination of "V" and "X" methods. The total yields of the two crown ethers from each reaction ranged from 30% to 60%. However, the relative yield of each crown depends on the reaction dynamics (ring size, concentration, temperature, template, etc.).

Comparing the yields of BPP34C10 among the five methods discussed above, the one-step route with a solvent mixture of 1-butanol and 1,4-dioxane is the most simple (20 hour reaction), economical [cheaper solvent (1-butanol vs. DMF), cheaper base (NaOH vs. NaH), no benzyl chloride, no Cs₂CO₃] and efficient method to synthesize BPP34C10, even though the other methods offer higher yields.

The same method (one-step route) can be applied to the synthesis of other bis(para-phenylene) based crown ethers. A new crown ether BPP32C4 was synthesized with similar yield as that of BPP34C10.

II-5: EXPERIMENTAL

Ethylene glycol (99%), di(ethylene glycol) (99%), tri(ethylene glycol) (99%), tetra(ethylene glycol) (99%), tri(ethylene glycol) dichloride (99%), hydroquinone (99%), thionyl chloride (99%) and sodium iodide (98%) were purchased from Aldrich Chemical Co. and used without further

purifications. Sodium hydride (60%) in mineral oil was purchased from Aldrich Chemical Co. and washed with n-hexane before use. *p*-Toluenesulfonyl chloride (98%) was purchased from Aldrich Chemical Co. and recrystallized once in n-hexane. 1,10-Dibromodecane was also purchased from Aldrich Chemical Co. and recrystallized once from petroleum ether.

Melting points were determined on a HAAKE BUCHLER capillary melting point apparatus and are corrected. The FTIR spectra were recorded on a Nicolet MX-1 FTIR spectrometer. The ¹H-NMR spectra were recorded on a Bruker WP 270 MHz instrument using tetramethylsilane (TMS) as the internal standard. GC analyses were performed using an a Varian 3400 Gas Chromatograph instrument. HPLC experiments were performed using an ISCO model 2350 equipped with computer controlled dual pumps and a UV detector. The mass spectrum was measured with a VGA 7070E analytical mass spectrometer by the Biochemistry Department of Virginia Polytechnic Institute and State University. The elemental analysis was done by Atlantic Microlab Inc., Norcross, GA.

II-5-1: HEXA(ETHYLENE GLYCOL)

II-5-1-1: Tetra(ethylene glycol) Dichloride

A mixture of tetra(ethylene glycol) (239.5 mL, 1.39 mol), pyridine (250 mL, 3.10 mol) and benzene (1.3 L) in a 3-L, 3-necked flask was heated to reflux under nitrogen with magnetic stirring. Thionyl chloride

(225.5 mL, 3.10 mol) was added dropwise over 3 hours. The mixture was refluxed for 24 hours.

The product was extracted 2 times with benzene (2 x 400 mL) after the mixture was cooled down to room temperature. The combined organic phase was washed 3 times with water (3 x 800 mL), dried with MgSO_4 , filtered and rotary evaporated down to a yellow oil. The product was purified by vacuum distillation (1.7 torr, 148°C) 3 times and 251.5 g of slightly yellow oil was obtained.

Yield: 78.3% (reported: 92%);⁷ b.p. 148°C at 1.7 torr (reported⁷: b.p. 95°C at 0.4 mm); IR ($\nu/\text{max}, \text{cm}^{-1}$): 2905, 1450, 1380, 1342, 1280, 1224, 1110, 1080, 1051, 1000, 950, 900, 832, 748, 661; $^1\text{H-NMR}$ (chloroform- d /TMS, ppm): 3.65 (t, 4 H, $-\underline{\text{CH}_2}\text{-Cl}$), 3.70 (s, 8 H, $-\text{OCH}_2\text{CH}_2\text{OCH}_2\text{CH}_2\text{O}-$), 3.81 (t, 4 H, $\text{Cl-CH}_2\underline{\text{CH}_2}\text{O-}$).

II-5-1-2: Hexa(ethylene glycol)

To ethylene glycol (724 g, 11.7 mol) in a 3-L, 3-necked flask with mechanical stirring and gentle warming, sodium (106 g, 4.61 mol) was added partwise over 3 hours under nitrogen with the temperature at 91°C . The mixture was stirred for 30 min. after the addition of sodium. Tetra(ethylene glycol) dichloride (273 g, 1.18 mol) was added dropwise. The mixture was stirred for 12 hours and then cooled down to room temperature.

Water (300 mL) was added. The solution was acidified to $\text{pH} = 7$ with 10% HCl. The salt was filtered and discarded and water was

removed by rotary evaporation. The yellow oil was subjected to vacuum distillation (0.15 torr, 180 - 200°C) 3 times and 96 g of slightly yellow oil was obtained. GC indicated high purity (Figure II-2).

Yield: 29% (reported: 35%²⁴, 80%²⁵ with a different method); b.p. 190°C at 0.15 torr (reported²⁶: b.p. 217°C at 4 mm); IR ($\nu/\text{max}, \text{cm}^{-1}$): 3449, 2898, 1976, 1453, 1349, 1308, 1239, 1116, 948, 891, 844; ¹H-NMR (Figure II-3, chloroform-d/TMS, ppm): 3.31 (t, 2 H, -OH), 3.63 (t, 4 H, -CH₂-OH), 3.70 (s, 8 H, -OCH₂CH₂OCH₂CH₂O-), 3.75 (t, 4 H, HO-CH₂CH₂O-).

II-5-2: OLIGO(ETHYLENE GLYCOL) DITOSYLATES

II-5-2-1: Tetra(ethylene glycol) Ditosylate

NaOH (53.0 g, 1.33 mol) in water (300 ml) was mixed with tetra(ethylene glycol) (80.5 g, 0.400 mol) in THF (200 mL) in a 2-L, 3-necked flask. The flask was placed in an ice bath. Tosyl chloride (171.6 g, 0.900 mol) in THF (300 mL) was added into the flask dropwise. The mixture was mechanically stirred for 24 hours.

The mixture was poured into 10% HCl (500 mL) at 0°C. The product was extracted two times with toluene (2 x 500 mL). The combined organic phase was washed two times with water (2 x 800 mL), one time with dilute (0.5 wt%) aqueous K₂CO₃ solution (400 mL), one more time with water (400 mL) and dried with MgSO₄. A slightly yellow oil (197 g) was obtained after the solvent was removed by rotary evaporation. The oil was washed with hot n-hexane to remove unreacted

tosyl chloride. A colorless viscous oil (195 g) was obtained.

Yield: 100%; IR ($\nu/\text{max}, \text{cm}^{-1}$): 2960, 1596, 1464, 1420, 1344, 1176, 1140, 1100, 1080, 1025, 955, 923, 898, 829, 749, 675, 665, 570, 540; $^1\text{H-NMR}$ (Figure II-4a, chloroform-d/TMS, ppm): 2.45 (s, 6 H, -CH₃), 3.55 (m, 8 H, -OCH₂CH₂OCH₂CH₂O-), 3.68 (t, 4 H, -CH₂O-); 4.15 (t, 4 H, TsO-CH₂-), 7.35 (d, 4 H, arom.), 7.80 (d, 4 H, arom.).

II-5-2-2: Tri(ethylene glycol) Ditosylate

To a 5-L, 3-necked flask, NaOH (80.0 g, 2.00 mol) and water (1 L) were added. The flask was placed in an ice bath. Tri(ethylene glycol) (100 g, 0.666 mol) was added and the mixture was mechanically stirred for 30 min. Tosyl chloride (317 g, 1.67 mol) in THF (1 L) was added dropwise. The mixture was stirred for 48 hours.

The two phases were separated with a separation funnel. The residual product left in the water phase was extracted 2 times with methylene chloride (2 x 300 mL). All organic phases were combined and rotary evaporated down to a white solid which was recrystallized two times in acetone to give 250 g of pure white crystals.

Yield: 82%; m.p. 80.8 - 81.9°C (reported²⁶: 80 - 82°C); $^1\text{H-NMR}$ (Figure II-4a, chloroform-d/TMS, ppm): 2.44 (s, 6 H, -CH₃), 3.52 (s, 4 H, -OCH₂CH₂O-), 3.65 (t, 4 H, -CH₂O-), 4.13 (t, TsOCH₂-), 7.34 (d, 4 H, arom.), 7.78 (d, 4 H, arom.).

II-5-3: PENTA(ETHYLENE GLYCOL) DIODIDE

II-5-3-1: Penta(ethylene glycol)

To ethylene glycol (621 g, 10.0 mol) in a 3-L, 3-necked flask with mechanical stirring and gentle warming, sodium (92.0 g, 4.00 mol) was added partwise over 3 hours under nitrogen with a reaction temperature of 91°C. The mixture was stirred for 30 min. after the addition of sodium. Tri(ethylene glycol) dichloride (187 g, 1.00 mol) was added dropwise. The mixture was stirred for 12 hours and then cooled to room temperature.

Water (250 ml) was added. The solution was acidified to pH = 7 with 10% HCl. The salt was filtered and discarded and water was removed by rotary evaporation. A yellow oil was obtained and subjected to vacuum distillation (0.6 torr, 170 - 180°C) two times and 49.7 g of slightly yellow oil was obtained.

Yield: 28%; b.p. 170 - 180°C at 0.6 torr (reported²⁶: b.p. 184°C at 2 mm).

II-5-3-2: Penta(ethylene glycol) Dichloride

A mixture of penta(ethylene glycol) (41.0 g, 0.172 mol), pyridine (43.5 g, 0.550 mol) and benzene (300 mL) in a 500-mL, 3-necked flask was heated to reflux under nitrogen with magnetic stirring. Thionyl chloride (65.7 g, 0.550 mol) was added dropwise over 3 hours. The mixture was refluxed for 24 hours.

The solution was cooled down to room temperature. Water (300 ml) was added. The product was extracted with benzene two times (2 x 300 mL). The combined organic phase was washed 3 times with water (3 x 500 mL), dried with MgSO₄, filtered and rotary evaporated down to a yellow oil which was subjected to vacuum distillation (0.75 torr, 180 - 190°C). A slightly yellow oil (30 g) was obtained.

Yield: 63%; b.p. 180 - 190°C at 0.75 torr; ¹H-NMR (Figure II-5a, chloroform-d/TMS, ppm): 3.65(t, 4 H, Cl-CH₂-), 3.70(s, 12 H, -OCH₂CH₂OCH₂CH₂OCH₂CH₂O-), 3.80(t, 4 H, -OCH₂-).

II-5-3-3: Penta(ethylene glycol) Diiodide

To a mixture of penta(ethylene glycol) dichloride (28.1 g, 0.102 mol) and NaI (90.0 g, 0.600 mol) in a 1-L, 1-necked flask, acetone (700 ml) was added and the solution was stirred for 20 hours at reflux.

The salt was filtered and discarded and acetone was removed by rotary evaporation. The product was extracted 2 times with methylene chloride (2 x 250 mL). The combined phase was washed 3 times with water (3 x 500 mL), dried with MgSO₄, filtered and rotary evaporated down to a reddish brown oil (50.0 g) which showed one spot on TLC. No purification was attempted because of the known thermal instability of alkyl iodides.

Yield: 100%; ¹H-NMR (Figure II-5b, chloroform-d/TMS, ppm): 3.30 (t, 4 H, I-CH₂-), 3.70 (s, 12 H, -OCH₂CH₂OCH₂CH₂OCH₂CH₂O-), 3.80 (t, 4 H, -CH₂O-).

II-5-4: 60C20 AND 30C10¹⁰

The syntheses of 30C10 and 60C20 were done in collaboration with C. Lim in our laboratory.²⁷

NaH (60%) (42.8 g, 1.07 mol) was washed two times with n-hexane (2 x 100 ml) and transferred into a 5-L, 3-necked flask with THF (freshly opened) (2.5 L) under nitrogen. Hexa(ethylene glycol) (60.3 g, 0.210 mol) was added slowly and the mixture was mechanically stirred for 2 hours at room temperature. Tetra(ethylene glycol) ditosylate (106 g, 0.210 mol) in 300 ml THF was added dropwise over 9 hours. The mixture was stirred for 3 days under the same conditions.

Water (100 ml) was added dropwise to destroy unreacted NaH. Bubbles were observed upon the addition of water. The precipitates were filtered and discarded and THF was removed by rotary evaporation. The crude crown mixture (90.2 g of oil) was passed through a short silica gel (90 g) column with methylene chloride. The eluted crown mixture (63 g of brown solid) was subjected to recrystallization 4 times in acetone at -20°C. The white crystalline solid was 60C20 (15.07 g). The mother solution contained 30C10 which was further purified by recrystallization in n-hexane at room temperature. The recrystallization was performed by dissolving the crude compound in hot n-hexane and the solution was kept at room temperature in a round bottom flask open to air for 7 days. Clear crystals of 30C10 were formed (6.0 g).

Yields: 16% (60C20), 6.0% (30C10); m.p. 52.2 -53.9°C (60C20,

reported¹⁰: 46.0 - 50.5°C), 34.0 - 36.0°C (30C10, reported as an oil¹⁰); IR (v/max,cm⁻¹) (30C10): 2878, 2735, 1762, 1457, 1347, 1299, 1251, 1135, 1115, 1040, 992, 944, 855, 732; ¹H-NMR (chloroform-d/TMS, ppm): 3.64 (s) (60C20, Figure II-6e), 3.68 (s) (30C10, Figure II-6a). DSC transitions (60C20, Figure II-7b): T_g = - 66°C, T_m = 49°C.

II-5-5: 36C12

NaH (60%, 32.0 g, 0.8 mol) was washed 2 times with n-hexane (2 x 60 ml) and transferred into a 5-L, 3-necked flask with dry THF (1.5 L) under nitrogen. Tri(ethylene glycol) (42.6 g, 0.284 mol) in THF (500 ml) was added slowly and the mixture was mechanically stirred for 30 min. at room temperature. Tri(ethylene glycol) ditosylate (130 g, 0.284 mol) in THF (1 L) was added. The mixture was stirred for 24 hours under the same conditions.

Water (100 ml) was added to destroy the unreacted NaH. Bubbles were observed upon the addition of water. The precipitates were filtered and discarded and THF was removed by rotary evaporation. A brown oil (150 g) was obtained and passed through a short silica gel column (500 g) with methylene chloride. The eluted light brown oil (125 g) was dissolved in 200 ml of methylene chloride. The solution was kept in a round bottom flask open to air at room temperature for 5 days. Clear crystals were formed. The crystals were picked up, rinsed with acetone with immediate vacuum drying and weighed 14.3 grams.

Yield: 19%; m.p. 37.0 - 37.5°C (reported as an oil¹⁰); ¹H-NMR

(Figure II-6b, chloroform-d/TMS, ppm): 3.67 (s).

II-5-6: 42C14

NaH (60%, 40.0 g, 1.00 mol) was washed 2 times with n-hexane (2 x 60 ml) and transferred into a 5-L 3-necked flask with dry THF (500 ml) under nitrogen. Tetra(ethylene glycol) (63.5 g, 0.327 mol) in THF (500 ml) was added slowly and the mixture was mechanically stirred for 2 hours. Tri(ethylene glycol) ditosylate (150 g, 0.327 mol) in THF (2 L) was added. The system was further diluted to a total volume of 4 L. and the mixture was stirred for 48 hours under the same conditions.

Water (20 ml) was added to destroy the unreacted NaH. Bubbles were observed upon the addition of water. The precipitates were filtered and discarded and THF was removed by rotary evaporation. A reddish-purple oil (83.8 g), which solidified in 30 min., was obtained. The solid was recrystallized in acetone at -20°C. A white powder (61.1 g) was obtained. The powder was further recrystallized 5 times in acetone at -4°C and a white crystalline solid (25 g) was obtained.

Yield: 22%; m.p. 49.6 - 50.4°C (reported¹⁰: 28.5 - 31.0°C); ¹H-NMR (Figure II-6c, chloroform-d/TMS, ppm): 3.65 (s).

II-5-7: 48C16

NaH (60%, 60.0 g, 1.50 mol) was washed 2 times with n-hexane (2 x 100 ml) and transferred into a 5-L 3-necked flask with dry THF (1.5 L) under nitrogen. Tetra(ethylene glycol) (100 g, 0.515 mol) in THF (1 L)

was added slowly and the mixture was mechanically stirred for 30 min. at room temperature. Tetra(ethylene glycol) ditosylate (261 g, 0.520 mol) in THF (1 L) was added. The mixture was stirred for 24 hours under the same conditions.

Water (80 ml) was added to destroy the unreacted NaH. Bubbles were observed upon the addition of water. The precipitates were filtered and discarded and THF was removed by rotary evaporation. A brown oil (35 g), which solidified in hours, was obtained and subjected to recrystallization 5 times in acetone at -20°C . A white crystalline solid (19.5 g) was obtained.

Yield: 15%; m.p. $49.6 - 50.8^{\circ}\text{C}$ (reported¹⁰: $40.0 - 43.0^{\circ}\text{C}$); $^1\text{H-NMR}$ (Figure II-6d, chloroform-d/TMS, ppm): 3.65 (s).

II-5-8: SYNTHESIS OF BPP34C10

II-5-8-1: Four-Step Route (Scheme II-10)

II-5-8-1-1: p-Benzyloxyphenol (II-6) ---- Monoprotection

Hydroquinone (165 g, 1.50 mol) was placed in a 2-liter 3-necked flask under nitrogen atmosphere at room temperature. DMF (1 L) was added to dissolve the hydroquinone. Potassium carbonate (207 g, 1.50 mol) was added and the solution was mechanically stirred. Benzyl chloride (173 g, 1.50 mol) was added into the flask dropwise over three hours. The solution was stirred for two days at room temperature.

The precipitate was filtered and discarded. The filtrate was

neutralized with 10% HCl solution to pH = 7. The product was extracted three times with ethyl ether (3 x 500 mL) and the combined organic phase was washed eight times with water (8 x 600 mL) to remove DMF and then dried with magnesium sulfate. A solid was obtained after the solvent was rotary evaporated. Recrystallization was done twice with 80% ethyl acetate and 20% n-hexane mixture. White mica crystals (164 g) were obtained and dried under vacuum overnight.

Yield: 55%; m.p. 119.8 - 121.1°C (reported²⁸: 122°C); FTIR (v/max,cm⁻¹): 3400, 2896, 1512, 1468, 1424, 1376, 1280, 1256, 1160, 1100, 1038, 935, 815, 766, 749, 693, 532, 517; ¹H-NMR (chloroform-d/TMS, ppm): 4.60 (s, 1 H, -OH), 5.00 (s, 2 H, PhCH₂O-), 6.75 - 6.90 (m, 4 H, arom.), 7.20 - 7.50 (m, 5 H, arom.).

**II-5-8-1-2: 1,11-Bis(para-benzyloxyphenoxy)-3,6,9-trioxaundecane
(II-7) ---- Disubstitution**

NaH (60%) (6.56 g, 0.164 mol) was washed three times with n-hexane (3 x 20 mL) and transferred into a 500-mL 3-necked flask with DMF (200 mL) under nitrogen. p-Benzyloxyphenol (II-6) (24.0 g, 0.119 mol) in DMF (150 mL) was added into the flask dropwise over 30 min. and the solution was magnetically stirred for another 30 min. Tetra(ethylene glycol) ditosylate (30.1 g, 0.0595 mol) in DMF (100 mL) was added dropwise over one hour and the solution was stirred for three days at room temperature.

Water (100 ml) was added into the flask dropwise to remove

unreacted NaH. Bubbles were observed upon the addition of water. The product was extracted three times with ethyl acetate (3 x 300 mL). The combined organic phase was washed with water eight times (8 x 600 mL) to remove DMF and then dried with magnesium sulfate. A solid was obtained after the solvent was removed by rotary evaporation. Recrystallization was done three times with ethyl acetate/n-hexane (4:1/v:v) mixture. A white crystalline solid (26.1 g) was obtained and dried under vacuum overnight.

Yield: 74.3%; m.p. 82.6 - 83.0°C (reported²³: oil); FTIR (Figure II-8a, $\nu/\text{max}, \text{cm}^{-1}$): 2952, 2896, 1510, 1452, 1404, 1376, 1296, 1232, 1136, 1108, 1095, 1088, 1078, 1070, 982, 930, 836, 829, 756, 738, 693; ¹H-NMR (chloroform-d/TMS, ppm): 3.60 (m, 8 H, -OCH₂CH₂OCH₂CH₂O-), 3.75 (m, 4 H, arom.-OCH₂CH₂O-aliph.), 4.10 (m, 4 H, arom.-OCH₂CH₂O-aliph.), 5.00 (s, 4 H, PhCH₂O-), 6.80 - 6.90 (m, 8 H, arom.), 7.40 - 7.50 (m, 10 H, arom.).

II-5-8-1-3: 1,11-Bis(para-hydroxyphenoxy)-3,6,9-trioxaundecane (II-8)

---- Deprotection

A calibrated Parr 3911 hydrogenation apparatus was used to carry out the catalytic hydrogenation. Compound **II-7** (19.7 g, 0.0330 mol) was dissolved in toluene (300 mL) in the reaction vessel. 10% Pd/C catalyst (2.00 g) was added into the vessel. For safety, the catalyst was added very slowly and partwise. The reaction was carried out for 18 hours at room temperature under a starting pressure of 35.5 psi. The catalyst was filtered and reused after it was washed with methanol three

times. The filtrate was rotary evaporated down to a viscous oil (13.0 g) which was dried under vacuum overnight.

Yield: 100% (reported²³: 100% as an oil); FTIR (Figure II-8b, $\nu/\text{max}, \text{cm}^{-1}$): 3500, 3008, 2960, 2920, 1509, 1460, 1340, 1304, 1260, 1228, 1148, 1116, 1082, 1075, 975, 948, 833, 755, 745, 693, 514; ¹H-NMR (chloroform-d/TMS, ppm): 3.65 (m, 8 H, -OCH₂CH₂OCH₂CH₂O-), 3.70 (m, 4 H, arom.-OCH₂CH₂O-aliph.), 4.00 (m, 4 H, arom.-OCH₂CH₂O-aliph.), 6.80 (m, 8 H, arom.).

II-5-8-1-4: Bis(para-phenylene)-34-crown-10 (II-9) --- Cyclization

NaH (60%, 5.00 g, 0.122 mol) was washed three times with n-hexane (3 x 20 mL) and transferred into a 500-mL 3-necked flask under nitrogen with DMF (150 mL). Compound **II-8** (6.04 g, 0.0160 mol) in DMF (100 mL) was added into the flask dropwise over 30 min. The mixture was stirred for another 30 min. Tetra(ethylene glycol) ditosylate (7.48 g, 0.0149 mol) in DMF (50 mL) was added dropwise over one hour. The reaction mixture was stirred for two days at room temperature.

Water (100 ml) was added dropwise to remove unreacted NaH. Bubbles were observed upon the addition of water. The product was extracted with ethyl acetate three times (3 X 300 mL). The combined organic phase was washed with water eight times (8 X 600 mL) to remove DMF and then dried with magnesium sulfate. The solvent was removed by rotary evaporation. A slightly brown solid was obtained. The first recrystallization was done with methanol. The solid was then dissolved

in ethyl acetate (20 ml). To the solution, a relatively large amount of methanol (60 ml) was added and a white precipitate was observed. The precipitate (2.20 g) identified as BPP34C10 was filtered and dried under vacuum overnight.

Yield: 27.5% (reported²³: 30%); m.p. 84.0 - 86.0°C [reported²³: 87.0 - 89.0°C (from this method)]; FTIR (v/max,cm⁻¹): 2960, 2920, 1509, 1460, 1349, 1340, 1311, 1304, 1235, 1140, 1120, 1105, 1075, 1038, 975, 948, 900, 833, 745, 515; ¹H-NMR (Figure II-9, chloroform-d/TMS, ppm): 3.60 (m, 16 H, -OCH₂CH₂OCH₂CH₂O-), 3.75 (m, 8 H, arom.-OCH₂CH₂O-aliph.), 4.03 (m, 8 H, arom.-OCH₂CH₂O-aliph.), 6.85 (s, 8 H, arom.).

II-5-8-2: Two-Step Route (Scheme II-11)

II-5-8-2-1: 1,11-Bis(para-hydroxyphenoxy)-3,6,9-trioxaundecane (II-8)

---- Disubstitution

In a 500-mL 3-necked flask, sodium dithionite (0.1 g) was added to 95% ethanol (100 mL), which had been previously deaerated with nitrogen. Then hydroquinone (55.1 g, 0.500 mol) was added and dissolved by warming. Tetra(ethylene glycol) ditosylate (25.1 g, 0.0500 mol) was added and the mechanically stirred solution was heated to reflux. To this refluxing solution was added over 15 min. a solution of KOH (8.42 g, 0.150 mol) in 95% ethanol (50 mL). The mixture was stirred at reflux for 4 hours under nitrogen.

The mixture was cooled down to room temperature and neutralized

with 30% sulfuric acid. The product was extracted two times with methylene chloride (2 X 300 mL). The combined organic phase was washed with water two times (2 X 500 mL) and dried with magnesium sulfate. A brown oil (17.0 g) was obtained after the solvent was removed by evaporation. HPLC (Figure II-10, mobile phase: 80:20/v:v ratio of 2-propanol and n-hexane; stationary phase: normal silica) was run on the mixture of products. Three peaks [retention times (sec.): 3.03, 192, 301] were shown and the one for the diphenol **II-8** (at 301 sec.) was identified by spiking. Area% of the peak for **II-8** was 54.6% and the calculated pure yield was 49%. The product mixture was subjected to the next reaction without further purification.

II-5-8-2-2: Bis(para-phenylene)-34-crown-10 (II-4) ---- Cyclization

The cyclization was carried out with the product mixture from step 1 (disubstitution). The stoichiometry is based on HPLC data. NaH (60%, 5.00 g, 0.075 mol) was washed three times with n-hexane (3 x 20 mL) and transferred to a 500-mL 3-necked flask with DMF (150 mL) under nitrogen. The crude product **II-8** (from step 1) (8.90 g) in DMF (50 mL) was added into the flask dropwise. The mixture was magnetically stirred for another 30 min. Tetra(ethylene glycol) ditosylate (7.48 g, 0.0149 mol) was added dropwise over one hour. The reaction mixture was stirred overnight at room temperature.

Water (100 ml) was added to the mixture to remove the unreacted NaH; bubbles were observed upon the addition of water. The product was extracted two times with ethyl acetate (2 X 250 mL). The combined

organic phase was washed two times with water (2 x 400 ml) and dried with magnesium sulfate. A brown solid (13.0 g) was obtained. Column chromatographic separation was done on 900 grams of silica gel with ethyl acetate-hexane (1:1/v:v) as eluting solvent. Recrystallization of the solid third component of elution (the first and second were oils) with toluene/n-hexane (7:3/v:v) gave BPP34C10 (2.30 g) as clear crystals which were dried under vacuum overnight.

Yield: 29%; m.p. 94.3 - 95.6°C (reported²²: 93.5 - 94.0°C); FTIR (v/max,cm⁻¹): 2961, 2920, 1060, 1460, 1350, 1341, 1311, 1304, 1236, 1140, 1120, 1103, 1075, 1038, 975, 948, 902, 833, 745, 514; ¹H-NMR (chloroform-d/TMS, ppm): 3.70 (m, 16 H, -OCH₂CH₂OCH₂CH₂O-), 3.80 (m, 8 H, arom.-OCH₂CH₂O-aliph.), 4.00 (m, 8 H, arom.-OCH₂CH₂O-aliph.), 6.80 (s, 8 H, arom.).

II-5-8-3: One-step Route (Scheme II-12)

Hydroquinone (14.7 g, 0.100 mol) in 1-butanol (450 mL) was mixed with NaOH (9.10 g, 0.228 mol) in H₂O (10 mL) in a 2-L 3-necked flask under nitrogen. The solution was mechanically stirred for 30 min. at reflux. A deep blue color was observed. Tetra(ethylene glycol) ditosylate (50.2 g, 0.100 mol) in 1,4-dioxane/1-butanol (3:2/v:v) mixture (500 mL) was added into the flask. The reaction mixture was stirred at reflux for 20 hours.

The system was cooled down to room temperature. The precipitates (NaOTs and some other 1-butanol insoluble by-products)

were filtered and discarded. The filtrate was rotary evaporated down to a brown solid (50.0 g). The solid was dissolved in methylene chloride (100 mL) and passed through a short filtration silica gel column with ethyl acetate to remove some impurities. A light brown solid (25.0 g) was obtained after the solvent was removed from the eluted solution by rotary evaporation. This was subjected to a regular column separation. The column used was an acidic alumina column with ethyl ether as eluting solvent. The first eluted component was a colored oil and then BPP34C10 eluted next. Recrystallization from toluene/n-hexane (3:2/v:v) mixture gave clear crystalline BPP34C10 (2.85 g), which was dried under vacuum overnight.

Yield: 10.5%; m.p. 95.0 - 96.8°C (reported²²: 93.5 - 94.0°C); FTIR (v/max,cm⁻¹): 2960, 2920, 1509, 1460, 1349, 1341, 1310, 1300, 1235, 1140, 1120, 1105, 1077, 1038, 975, 950, 901, 833, 745, 514; ¹H-NMR (chloroform-d/TMS, ppm): 3.70 (m, 16 H, -OCH₂CH₂OCH₂CH₂O-), 3.80 (m, 8 H, arom.-OCH₂CH₂O-aliph.), 4.00 (m, 8 H, arom.-OCH₂CH₂O-aliph.), 6.75 (s, 8 H, arom.).

II-5-8-4: Template One-step Route (Scheme II-12)

Hydroquinone (11.1 g, 0.100 mol) in 1-butanol (450 mL) was mixed with NaOH (9.10 g, 0.228 mol) in H₂O (10 mL) in a 2-L 3-necked flask under nitrogen. The solution was mechanically stirred for 30 min. at reflux. A dark blue color was observed. Tetra(ethylene glycol) ditosylate (50.2 g, 0.100 mol) and Cs₂CO₃ (32.6 g, 0.100 mol) in 1,4-dioxane/1-butanol (3:2/v:v) mixture (500 mL) were added into the flask. The

mixture was stirred for 20 hours at reflux.

The work-up and purification procedures were the same as those in one-step route described above. BPP34C10 was obtained as clear crystals (3.35 g).

Yield: 12.5%; Melting point, FTIR and $^1\text{H-NMR}$ results were the same as those in the one-step route.

II-5-9: SYNTHESIS OF BPP32C4

Hydroquinone (14.7 g, 0.100 mol) in 1-butanol (450 mL) was mixed with NaOH (9.10 g, 0.228 mol) in H_2O (20 mL) in a 2-L 3-necked flask under nitrogen. The solution was mechanically stirred for 30 min. at reflux. A deep blue color was observed. 1,10-Dibromodecane (30.0 g, 0.100 mol) in 1-butanol/1,4-dioxane (3:2/v:v) mixture (500 mL) was added into the flask. The reaction mixture was stirred for 20 hours at reflux.

The work-up and purification procedures were the same as those in the one-step synthesis of BPP34C10. BPP32C4 was obtained as white crystals (1.30 g).

Yield: 7.5%; m.p. 101.5 - 102.0°C; $^1\text{H-NMR}$ (Figure II-11, chloroform-d/TMS, ppm): 1.29 (s, 16 H, $-\text{OCH}_2\text{CH}_2\text{CH}_2-(\text{CH}_2)_4-\text{CH}_2\text{CH}_2\text{CH}_2\text{O}-$), 1.41 (m, 8 H, $-\text{OCH}_2\text{CH}_2\text{CH}_2-(\text{CH}_2)_4-\text{CH}_2\text{CH}_2\text{CH}_2\text{O}-$), 1.72 (m, 8 H, $-\text{OCH}_2\text{CH}_2\text{CH}_2-(\text{CH}_2)_4-\text{CH}_2\text{CH}_2\text{CH}_2\text{O}-$), 3.92 (t, 8 H, $-\text{OCH}_2\text{CH}_2\text{CH}_2-(\text{CH}_2)_4-\text{CH}_2\text{CH}_2\text{CH}_2\text{O}-$), 6.81 (s, 8 H, arom.); MS (Figure

II-12, m/z): EI+ = 496; elemental analysis (%): calculated for C₃₂H₄₈O₄.

C: 77.38, H: 9.74, O: 12.88; found: C: 77.12, H: 9.64.

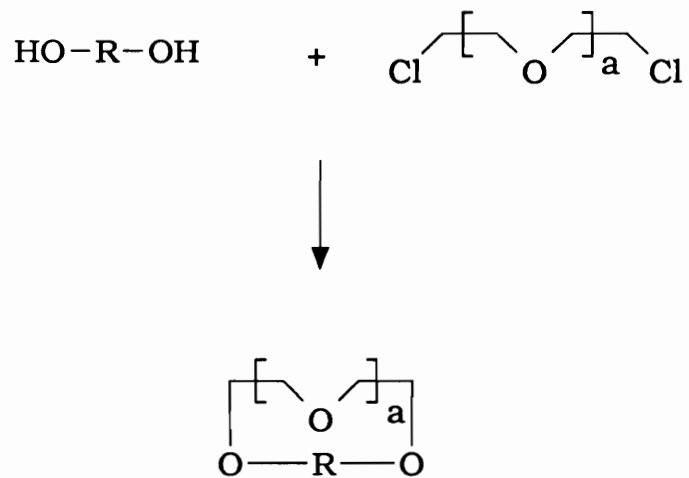
REFERENCES

1. Gokel, G. W.; Korzeniowski, S. H. "*Macrocyclic Polyether Synthesis*", Springer-Verlag, New York, **1982**.
2. Wu, C.; Bheda, M.; Lim, C.; Shen, Y. X.; Sze, J.; Gibson, H. W. *Polym. Commun.* **1991**, *32*, 204.
3. Harrison, I. T. *J. Chem. Soc., Perkin I* **1974**, 301
4. Agam, G.; Gravier, D.; Zilkha, A. *J. Am. Chem. Soc.* **1976**, *98*, 5206.
5. Gibson, H. W.; Bheda, M.; Engen, P. T.; Shen, Y. X.; Sze, J.; Wu, C.; Saikat, J.; Ward, T. C.; Lecavalier, P. R. *Makromol. Chem., Macromol. Symp.* **1991**, *42/43*, 395.
6. Ashton, P. R.; Slawin, A. M. Z.; Spencer, N.; Stoddart, J. F.; Williams, D. J. *J. Chem. Soc., Chem. Commun.* **1987**, 1066.
7. Pedersen, C. J. *J. Am. Chem. Soc.* **1967**, *89*, 7017.
8. Dietrich-Beuchecker, C. O.; Sauvage, J. P.; Kintzinger, J. P. *Tetrahedron Lett.* **1983**, *24*, 5095.
9. Kyba, E. P.; Helgeson, R. C.; Madan, K.; Gokel, G. W.; Tarnowski, T. L.; Moore, S. S.; Cram, D. J. *J. Am. Chem. Soc.* **1977**, *99*, 2564.
10. Chênevert, R.; D'Astous, L. *J. Heterocyclic Chem.* **1986**, *23*, 1785.

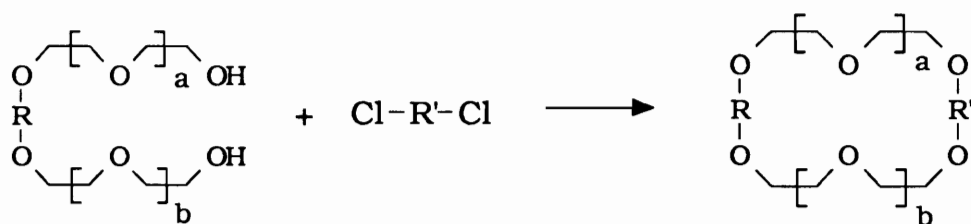
11. Allwood, B. L.; Spencer, N.; Shahriari-Zavareh, H.; Stoddart, J. F.; Williams, D. J. *J. Chem. Soc., Chem. Commun.* **1987**, 1061.
12. Thompson, M. D.; Bradshaw, J. S.; Nielsen, S. F.; Bishop, C. T.; Cox, F. T.; Fore, P. E.; Maas, G. E.; Izatt, R. M.; Christinasen, J. J. *Tetrahedron* **1977**, 3317.
13. Newkome, G. R.; Nayak, A.; McClure, G. L.; Danesh-Khoshboo, F.; Broussard-Simpson, J. *J. Org. Chem.* **1976**, 42, 1500.
14. Ouchi, M.; Inoue, Y.; Kanzaki, T.; Hakuski, T. *J. Org. Chem.* **1984**, 49, 1408.
15. Laidler, D. A.; Stoddart, J. F. in "*The Chemistry of Ethers, Crown Ethers, Hydroxyl Groups and Their Sulphur Analogues*", Edited by S. Patai, John Wiley & Sons, New York, **1980**, p1.
16. Vitali, C. A.; Masci, B. *Tetrahedron* **1989**, 45, 2201.
17. Vitali, C. A.; Masci, B. *Tetrahedron* **1989**, 45, 2213.
18. Reinhoudt, D. N.; Gray, R. T.; Smit, C. J.; Veenstra, Ms. I. *Tetrahedron* **1976**, 32, 1161.
19. Wu, C. Lecavalier, P. R.; Shen, Y. X.; Gibson, H. W. *Chem. Mater.* **1991**, 3, 569.
20. Engen, P. T. *PhD Dissertation* **1991**, Virginia Polytechnic Institute and State University.

21. Helgeson, R. G.; Timko, J. M.; Cram, D. J. *J. Am. Chem. Soc.* **1973**, *96*, 7380.
22. Helgeson, R. C.; Tarnowski, T. L.; Timko, J. M.; Cram, D. J. *J. Am. Chem. Soc.* **1977**, *99*, 6411.
23. Allwood, B. L.; Spencer, N.; Shahriari-Zavareh, H.; Stoddart, J. F.; Williams, D. J. *J. Chem. Soc., Chem. Commun.* **1987**, 1061, The synthesis is summarized in a footnote.
24. Perry et al. *Can. J. Res.* **1936**, *14*, 77.
25. Bartsch, R.; Cason, C. V.; Czech, B. P. *J. Org. Chem.* **1989**, *54*, 857.
26. *Aldrich catalog* 1990 - 1991.
27. Lim, C. *MS Thesis* **1991**, Virginia Polytechnic Institute and State University.
28. "CRC Handbook of Data for Org. Comp.", Edited by Weast, R. C.; Grassell, J. G., 2nd Ed., CRC Press, Boca Raton, Florida, **1989**, Vol. V, p3418.

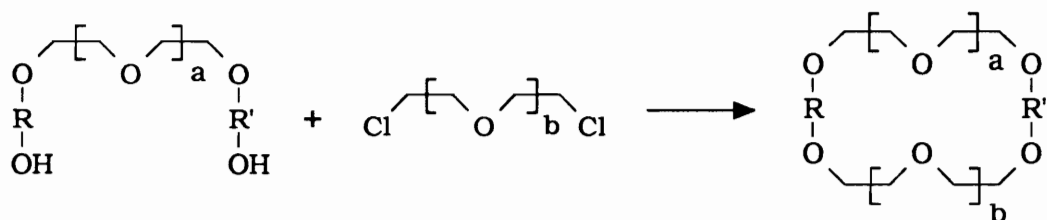
Scheme II-1: Example of "V" Method



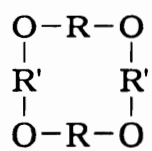
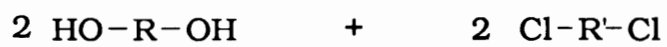
Scheme II-2: Example of "W" Method



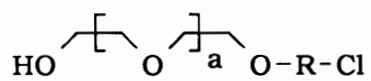
or



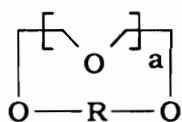
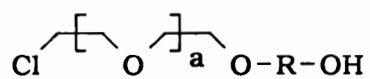
Scheme II-3: Example of "X" Method



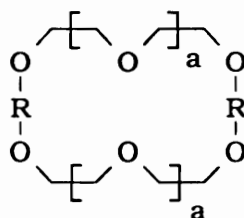
Scheme II-4: Examples "Y" Method



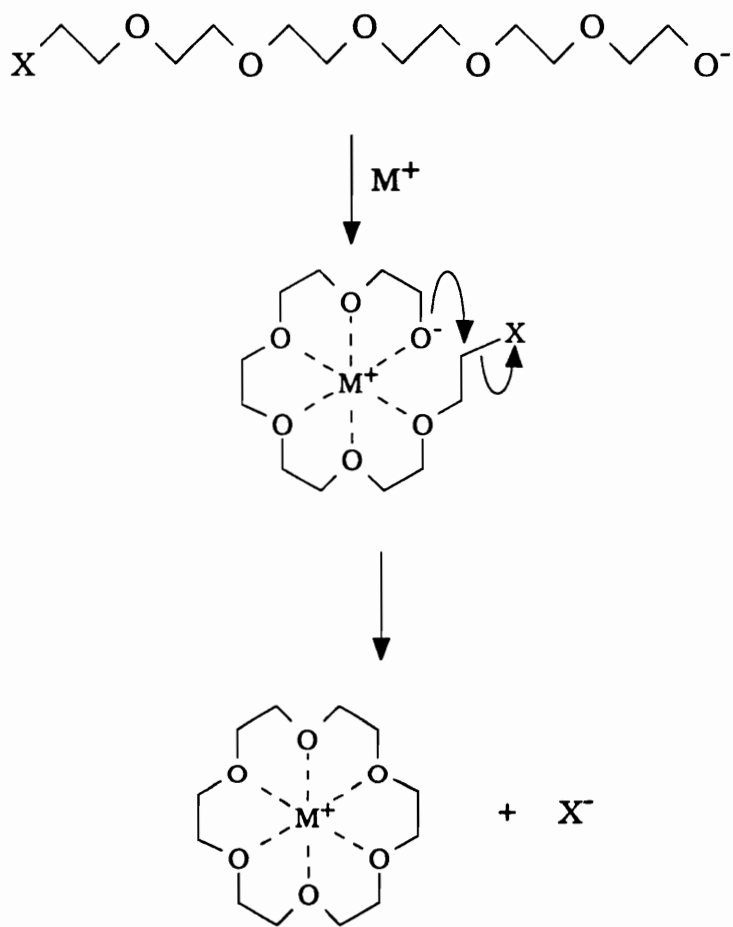
OR



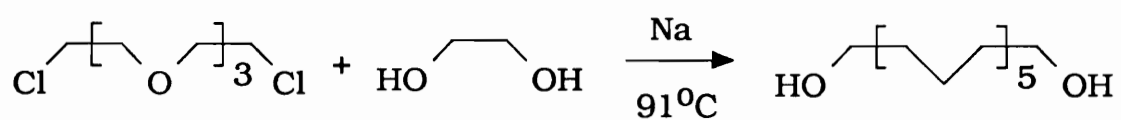
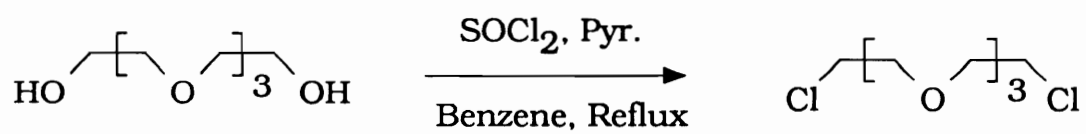
+



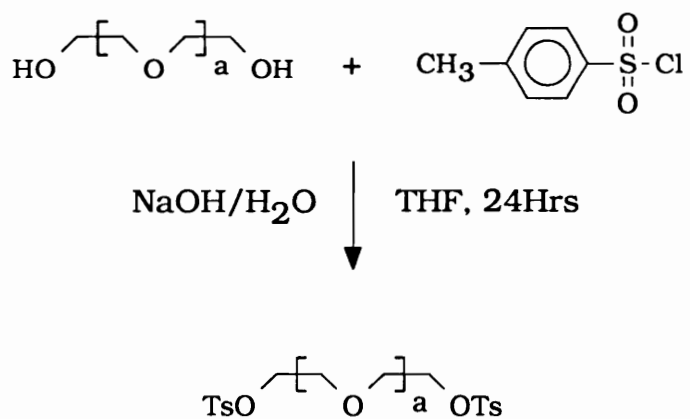
Scheme II-5: Template Effect in the Crown Ether Synthesis



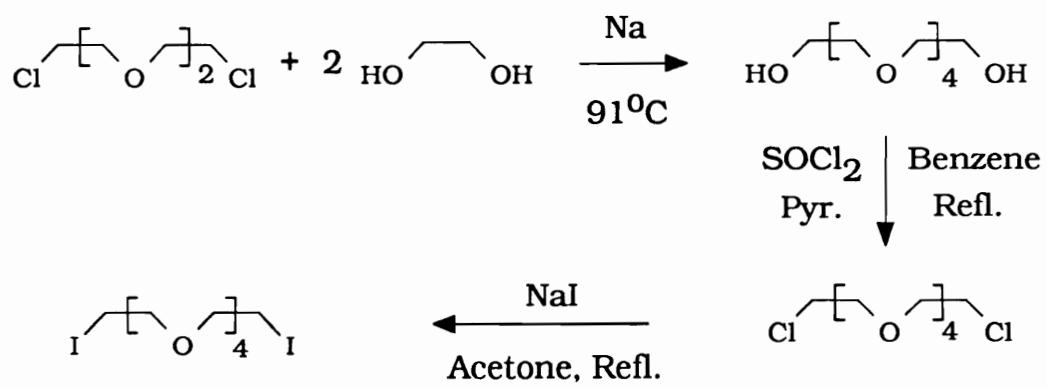
Scheme II-6: Synthesis of Hexa(ethylene glycol)



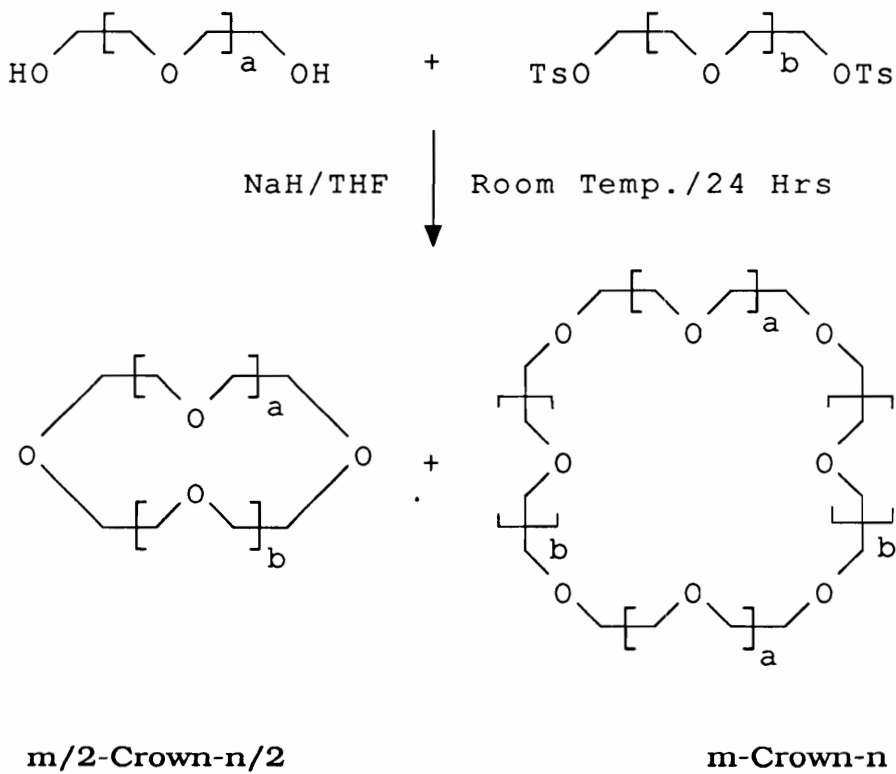
Scheme II-7: Syntheses of Oligo(ethylene glycol) Ditosylates



Scheme II-8: Synthesis of Penta(ethylene glycol) Diiodide



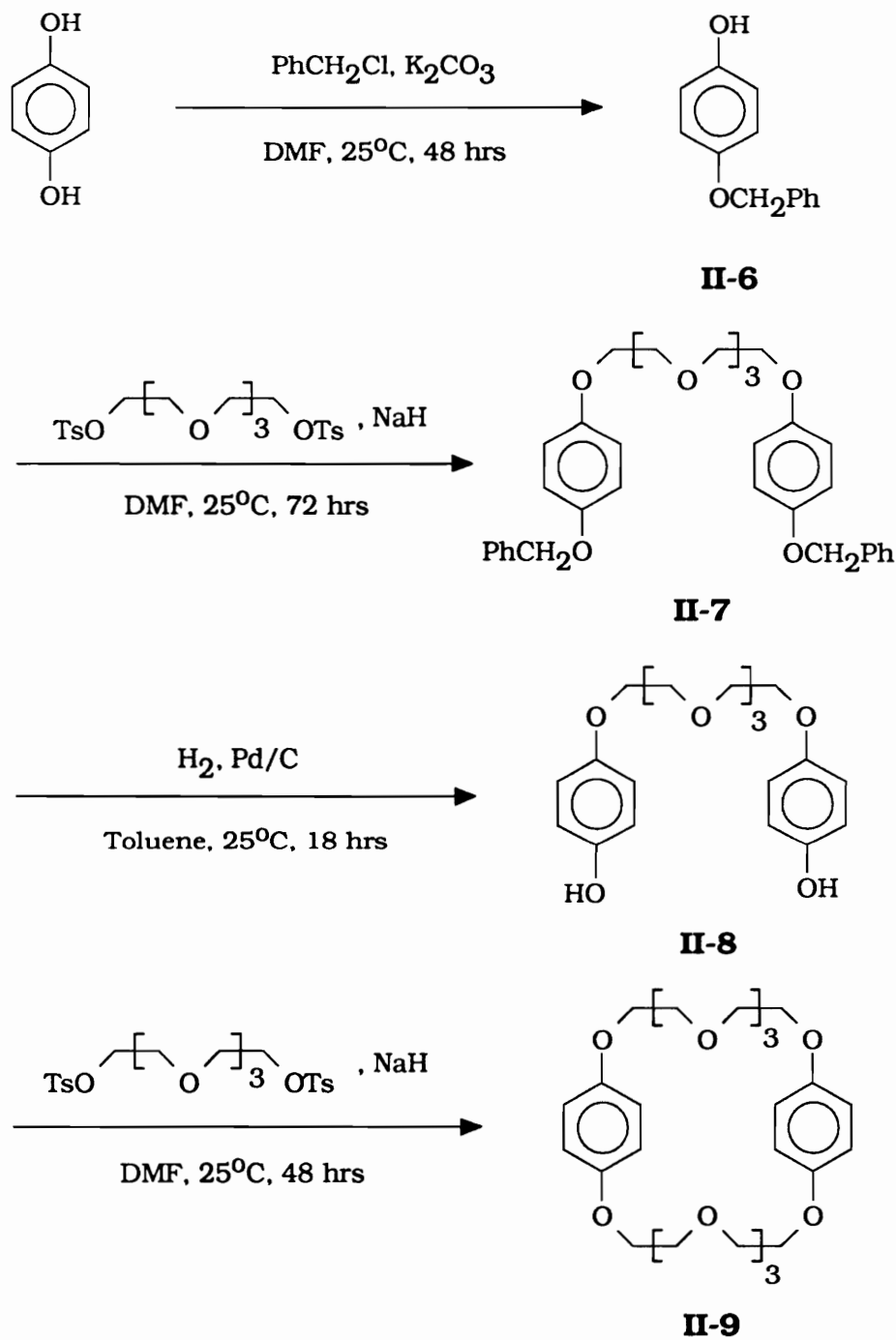
Scheme II-9: Systematic Synthesis of Crown Ethers



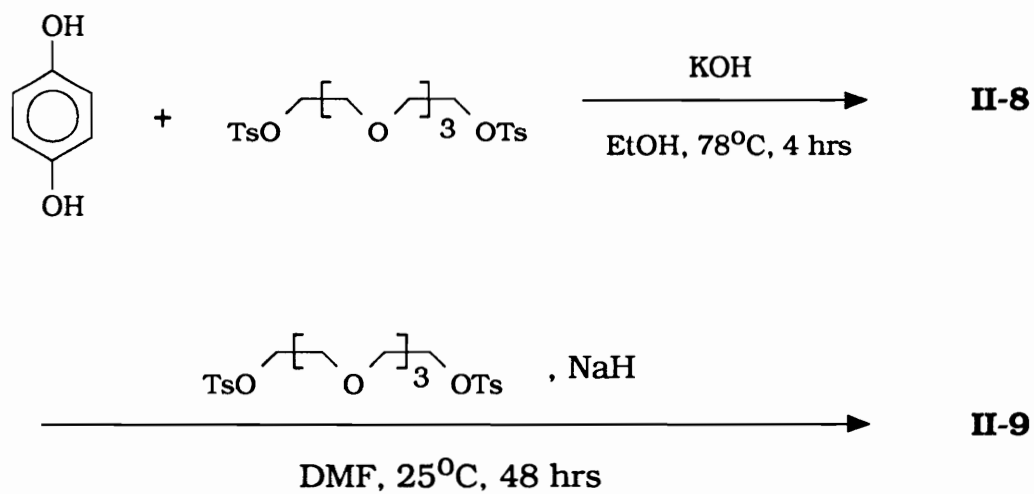
$$m = 6(a + b) + 12; \quad n = 2(a + b) + 4$$

II-1. 30C10, **II-2.** 36C12, **II-3.** 42C14, **II-4.** 48C16, **II-5.** 60C20

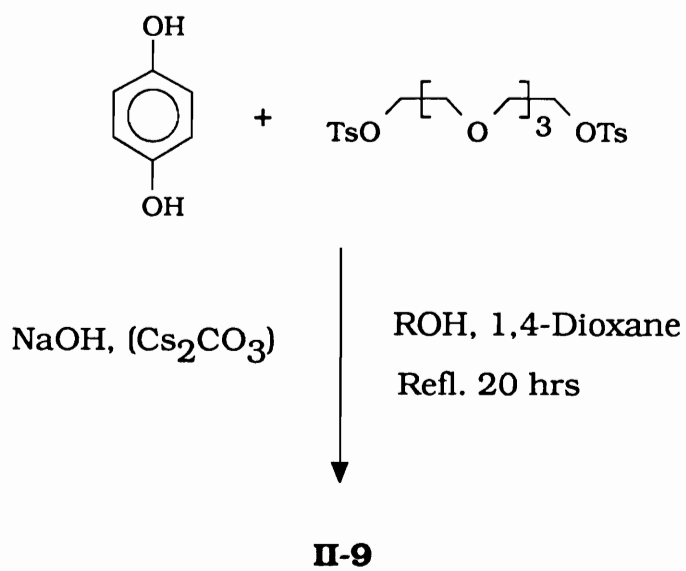
Scheme II-10: Four Step Synthesis of BPP34C10



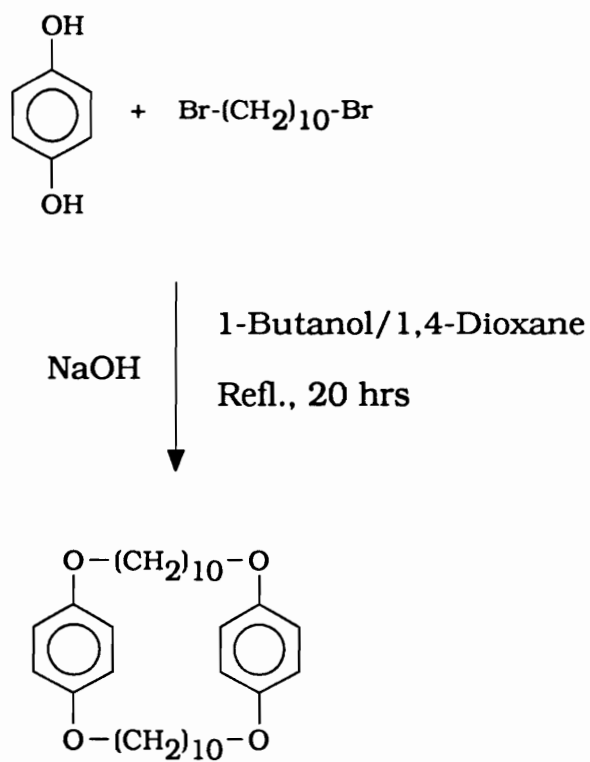
Scheme II-11: Two Step Synthesis of BPP34C10



Scheme II-12: One Step Synthesis of BPP34C10

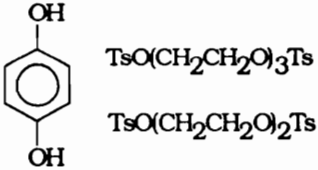
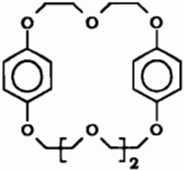
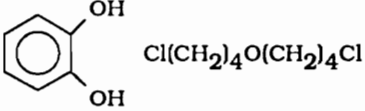
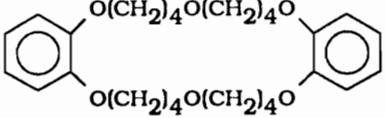
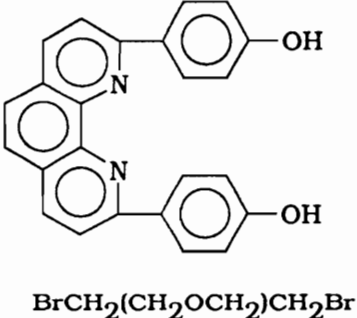
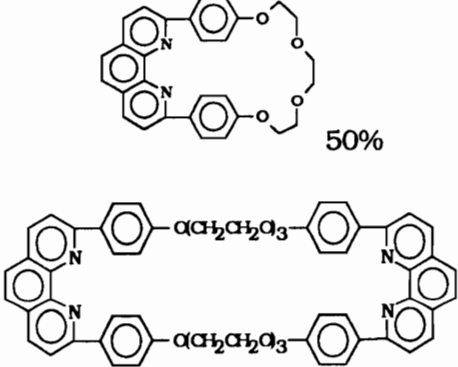
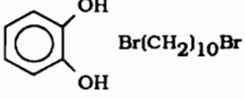
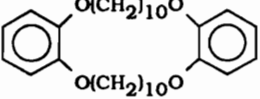
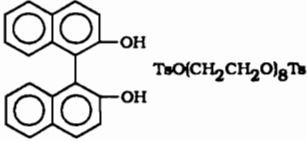
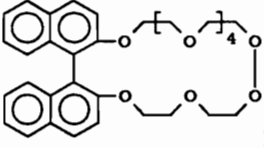


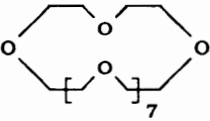
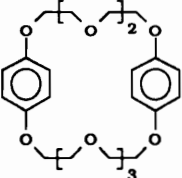
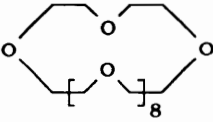
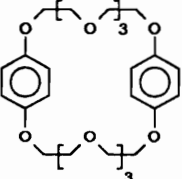
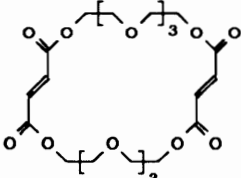
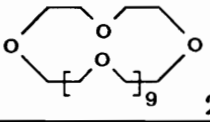
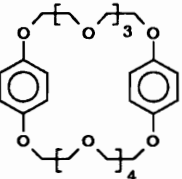
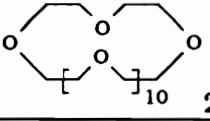
Scheme II-13: Synthesis of BPP32C4



II-10

**Table II-1: Some Examples of Macrocycles
with Ring Size from 25 to 60 Atoms**

Starting Materials	Macrocyclic Products and Yield	Ring Size	Refs
 <p>TsO(CH₂CH₂O)₃Ts TsO(CH₂CH₂O)₂Ts (4 Steps)</p>	 <p>7.5%</p>	25	6
 <p>Cl(CH₂)₄O(CH₂)₄Cl</p>	 <p>17%</p>	26	7
 <p>BrCH₂(CH₂OCH₂)CH₂Br</p>	 <p>50%</p> <p>14%</p>	27	8
 <p>Br(CH₂)₁₀Br</p>	 <p>3%</p>	28	7
 <p>TsO(CH₂CH₂O)₆Ts</p>	 <p>25%</p>	29	9

$\text{HO}(\text{CH}_2\text{CH}_2\text{O})_5\text{H}$ $\text{TsO}(\text{CH}_2\text{CH}_2\text{O})_5\text{Ts}$	 55%	30	10
 $\text{TsO}(\text{CH}_2\text{CH}_2\text{O})_3\text{Ts}$ (4 Steps) $\text{TsO}(\text{CH}_2\text{CH}_2\text{O})_4\text{Ts}$	 11%	31	6
$\text{HO}(\text{CH}_2\text{CH}_2\text{O})_6\text{H}$ $\text{TsO}(\text{CH}_2\text{CH}_2\text{O})_5\text{Ts}$	 19%	33	10
 $\text{TsO}(\text{CH}_2\text{CH}_2\text{O})_4\text{Ts}$ (4 Steps)	 13%	34	11
	 2%	35	12
$\text{TsO}(\text{CH}_2\text{CH}_2\text{O})_6\text{Ts}$ $\text{HO}(\text{CH}_2\text{CH}_2\text{O})_6\text{H}$	 28%	36	10
 $\text{TsO}(\text{CH}_2\text{CH}_2\text{O})_4\text{Ts}$ $\text{TsO}(\text{CH}_2\text{CH}_2\text{O})_5\text{Ts}$ (4 Steps)	 15%	37	6
$\text{HO}(\text{CH}_2\text{CH}_2\text{O})_7\text{H}$ $\text{TsO}(\text{CH}_2\text{CH}_2\text{O})_6\text{Ts}$	 24%	39	10

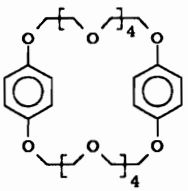
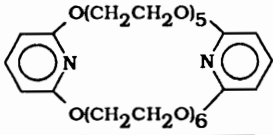
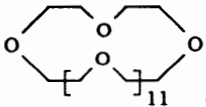
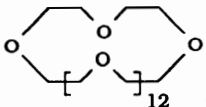
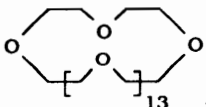
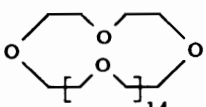
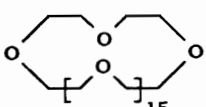
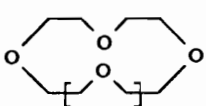
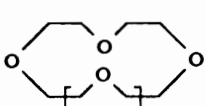
 $\text{TsO}(\text{CH}_2\text{CH}_2\text{O})_5\text{Ts}$ (4 Steps)	 12%	40	6
	 4%	41	13
$\text{HO}(\text{CH}_2\text{CH}_2\text{O})_7\text{H}$ $\text{TsO}(\text{CH}_2\text{CH}_2\text{O})_7\text{Ts}$	 20%	42	10
$\text{HO}(\text{CH}_2\text{CH}_2\text{O})_8\text{H}$ $\text{TsO}(\text{CH}_2\text{CH}_2\text{O})_7\text{Ts}$	 24%	45	10
$\text{HO}(\text{CH}_2\text{CH}_2\text{O})_8\text{H}$ $\text{TsO}(\text{CH}_2\text{CH}_2\text{O})_8\text{Ts}$	 22%	48	10
$\text{HO}(\text{CH}_2\text{CH}_2\text{O})_9\text{H}$ $\text{TsO}(\text{CH}_2\text{CH}_2\text{O})_8\text{Ts}$	 22%	51	10
$\text{HO}(\text{CH}_2\text{CH}_2\text{O})_9\text{H}$ $\text{TsO}(\text{CH}_2\text{CH}_2\text{O})_9\text{Ts}$	 24%	54	10
$\text{HO}(\text{CH}_2\text{CH}_2\text{O})_{10}\text{H}$ $\text{TsO}(\text{CH}_2\text{CH}_2\text{O})_9\text{Ts}$	 28%	57	10
$\text{HO}(\text{CH}_2\text{CH}_2\text{O})_{10}\text{H}$ $\text{TsO}(\text{CH}_2\text{CH}_2\text{O})_{10}\text{Ts}$	 26%	60	10

Table II-2: Yields (%) of BPP34C10 with Different Synthetic Routes

Synthetic Routes	Step 1	Step 2	Step 3	Step 4	Overall
Four-Step (Scheme II-10)	54.0	74.0	100	27.5	10.2
Two-Step (Scheme II-11)	49.0	29.0	-	-	14.2
One-Step (Scheme II-12)	A	10.5	-	-	10.5
	B	12.5	-	-	12.5
	C	3.5	-	-	3.5

A: In 1-butanol/1,4-dioxane system, without template,

B: In 1-butanol/1,4-dioxane system, with Cs₂CO₃ as template,

C: In ethanol system, without template.

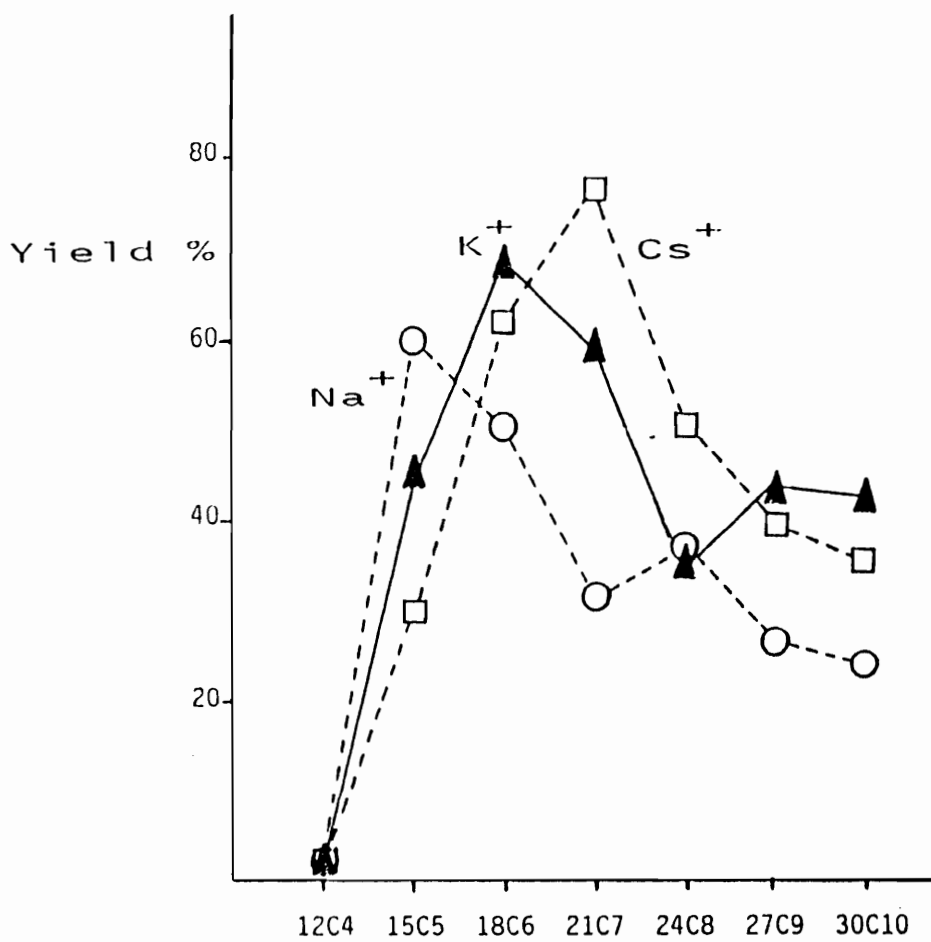


Figure II-1: Yields of Unsubstituted Crown Ethers in the Presence of NaOH (O), KOH (Δ), CsOH (\square)¹⁷.

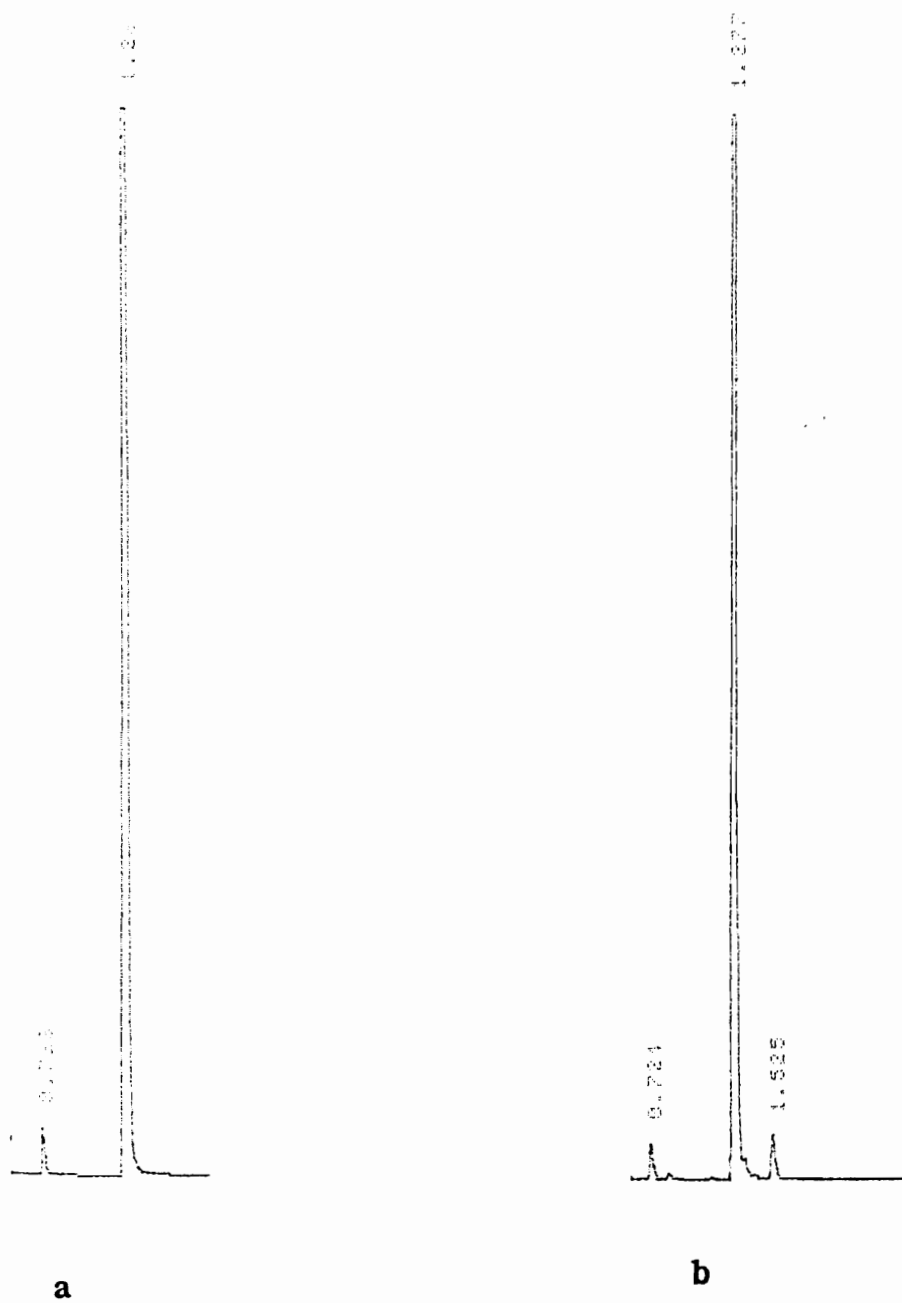


Figure II-2: GC Traces of (a) Hexa(ethylene glycol) (Synthesized) and (b) Hexa(ethylene glycol) (Commercial Standard).

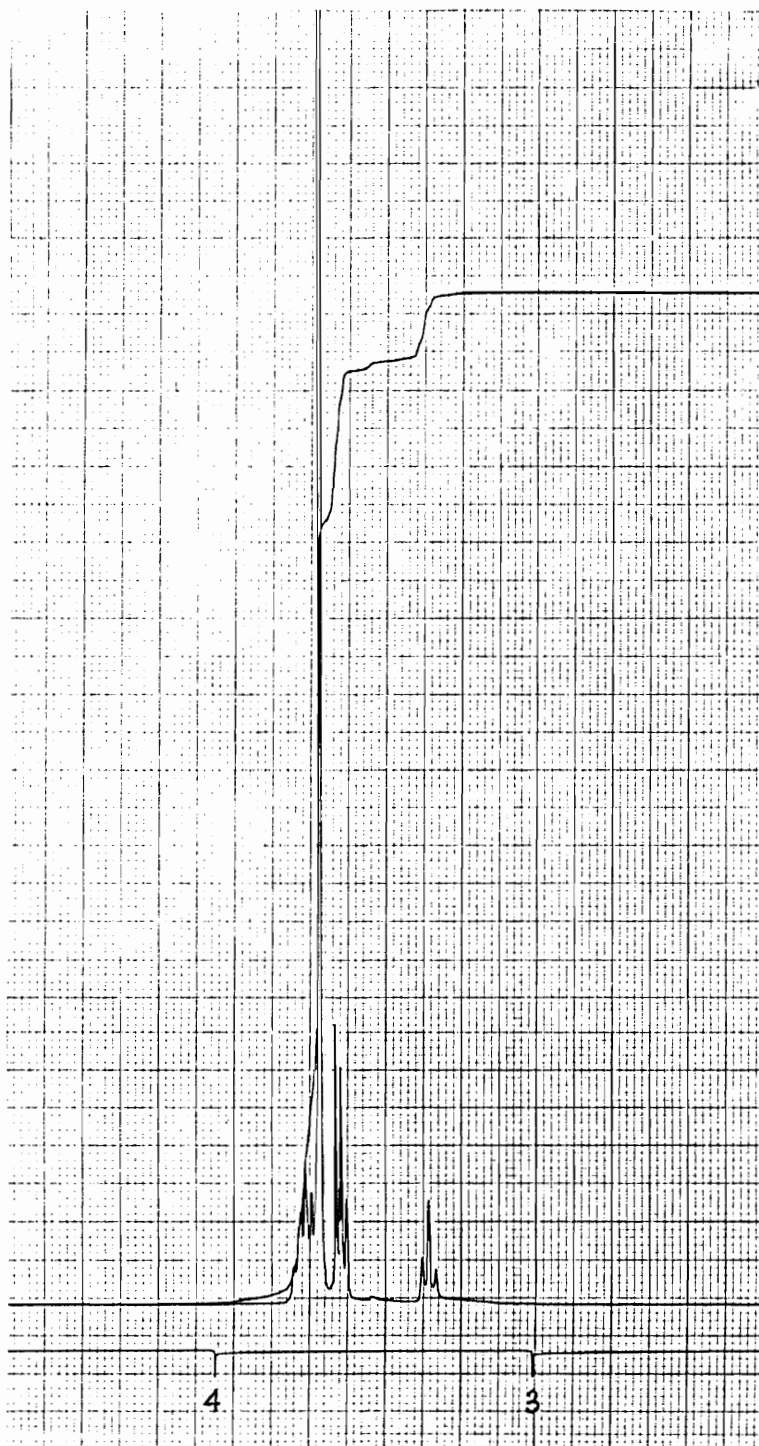


Figure II-3: $^1\text{H-NMR}$ Spectrum of Hexa(ethylene glycol).

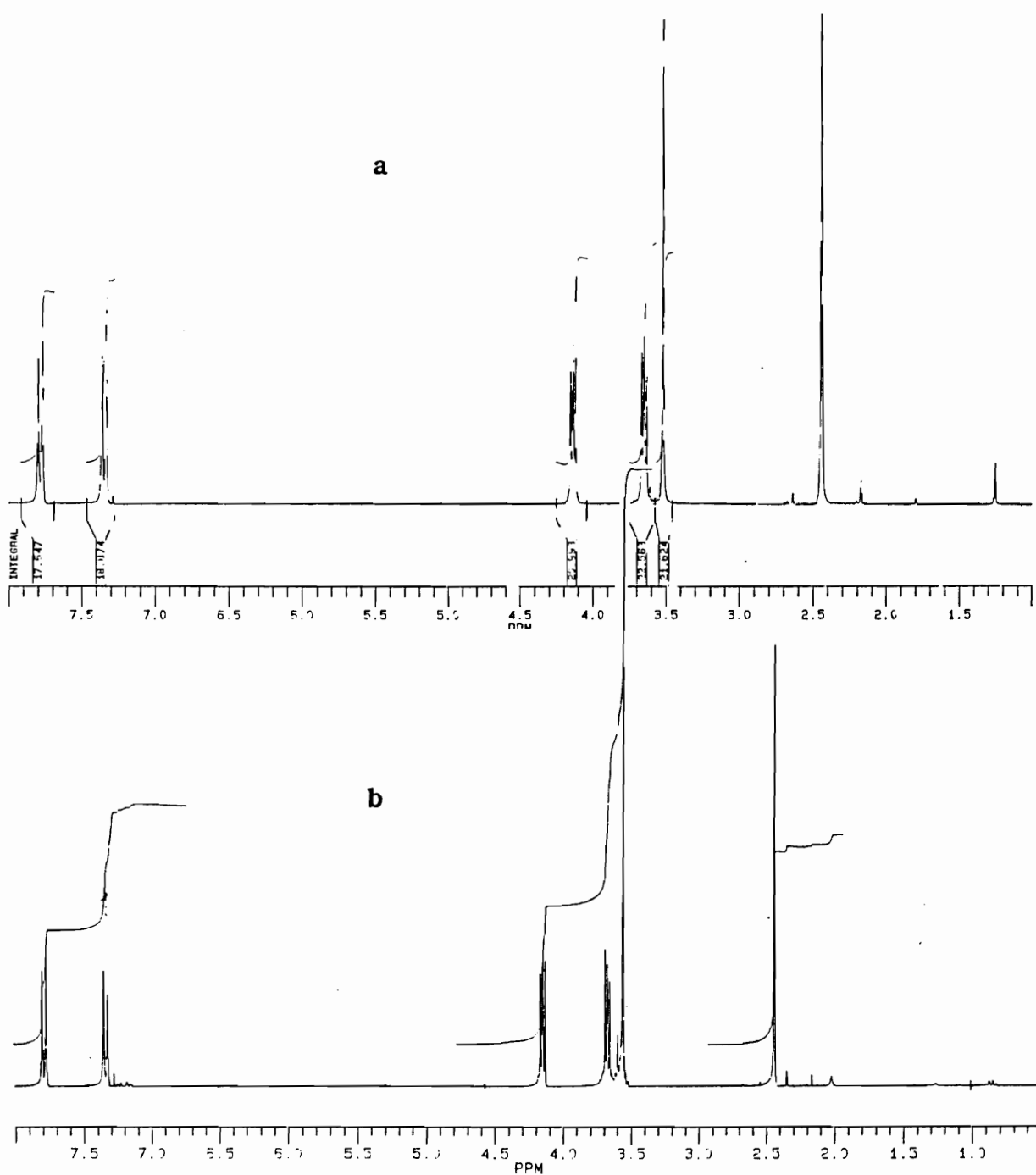


Figure II-4: $^1\text{H-NMR}$ Spectra of (a) Tri(ethylene glycol) Ditosylate and (b) Tetra(ethylene glycol) Ditosylate.

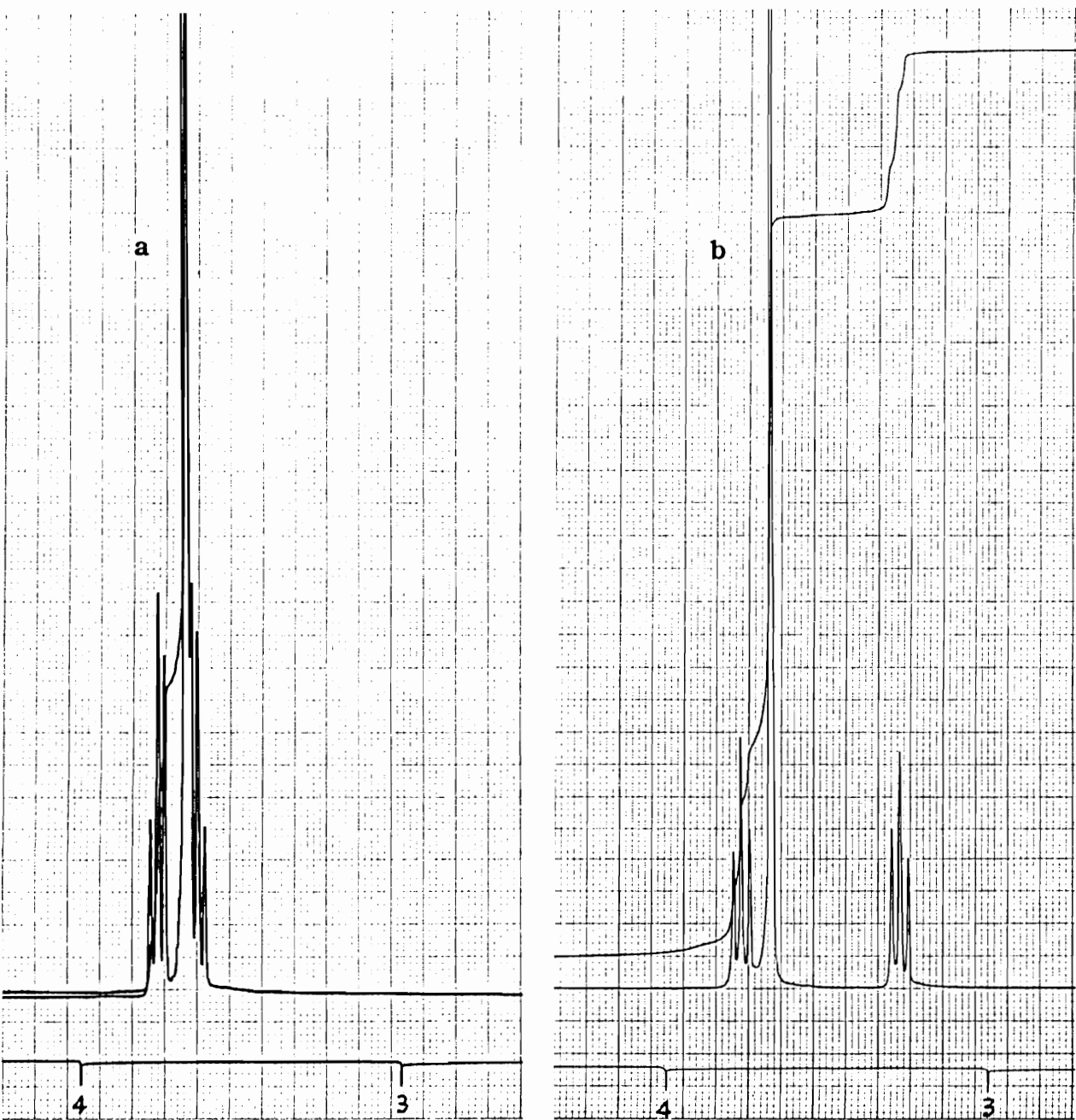


Figure II-5: $^1\text{H-NMR}$ Spectra of (a) Penta(ethylene glycol) Dichloride and (b) Penta(ethylene glycol) Diiodide.

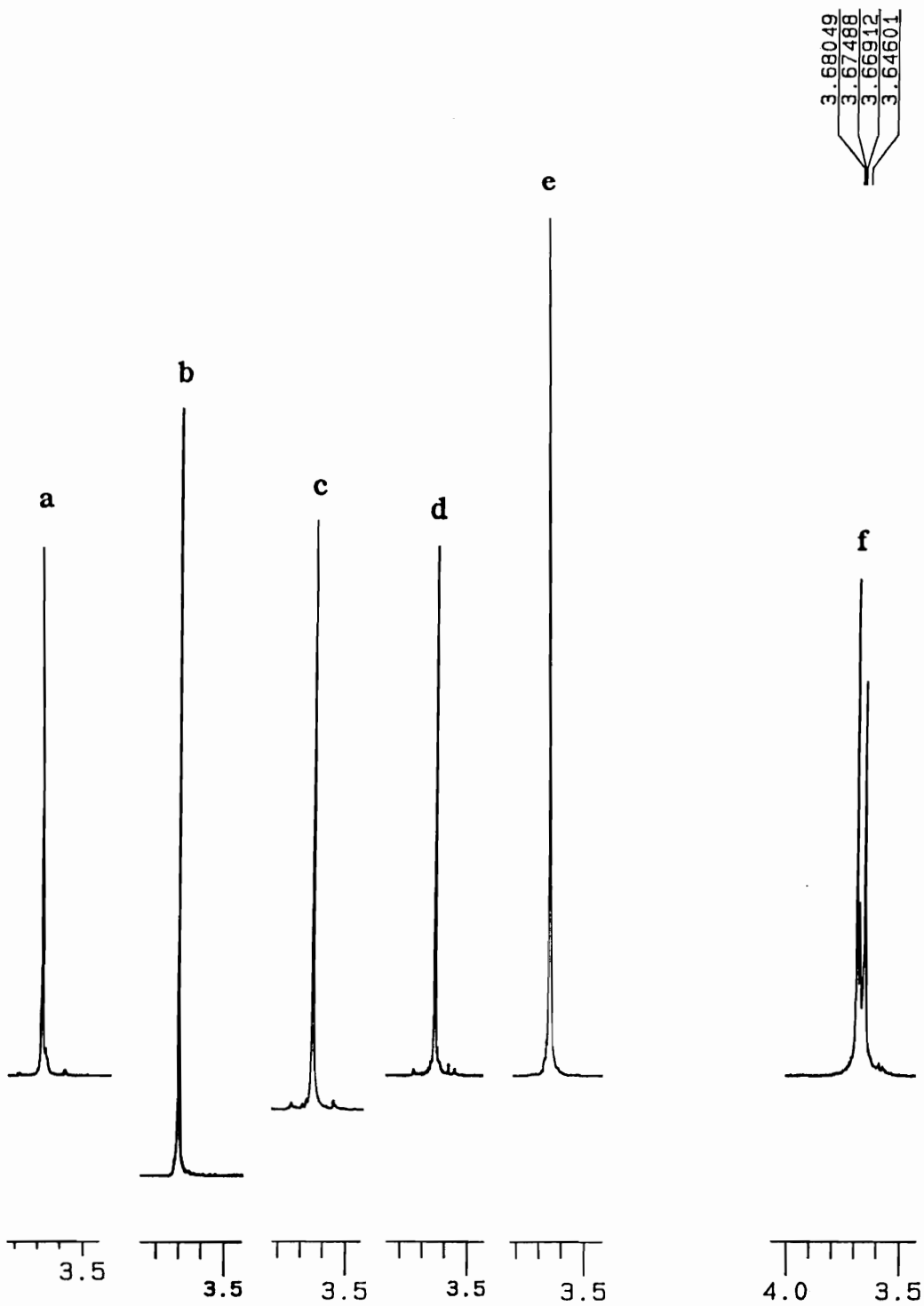


Figure II-6: $^1\text{H-NMR}$ Spectra of (a) 30C10, (b) 36C12, (c) 42C14, (d) 48C16, (e) 60C20 and (f) Mixture of Crown Ethers.

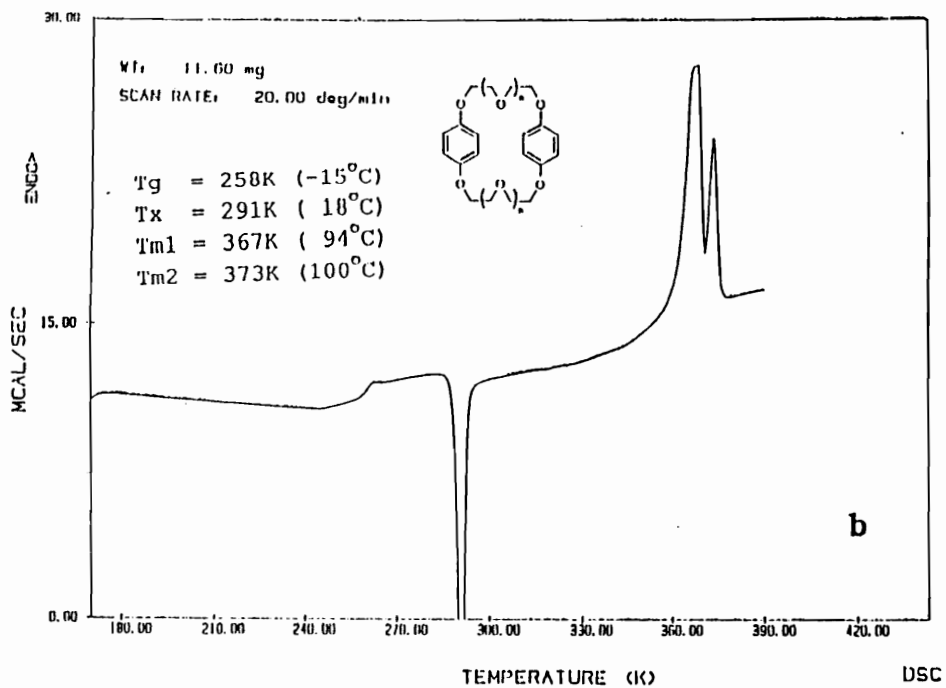
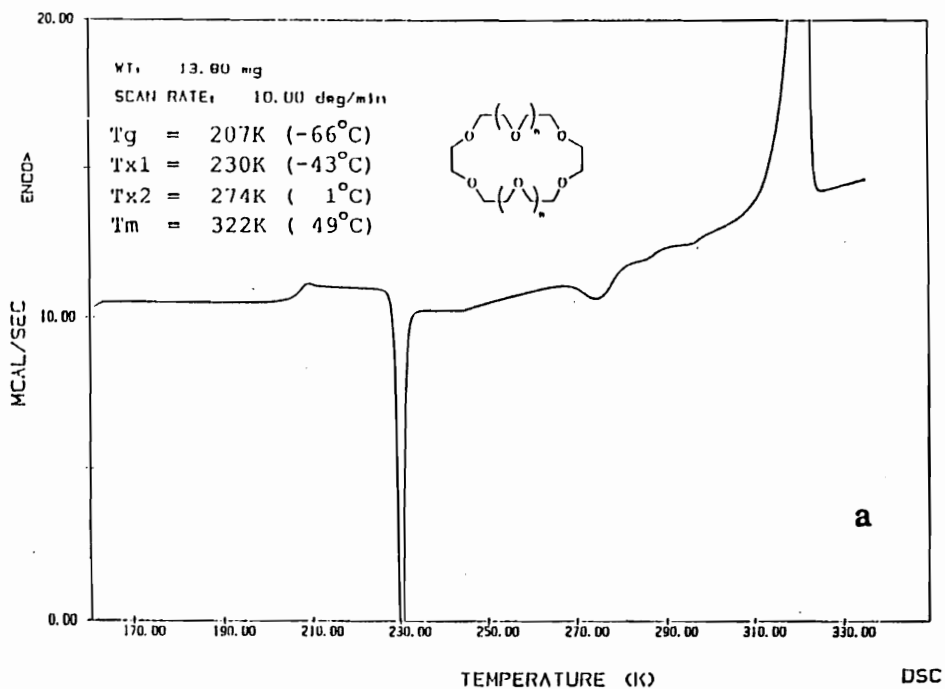


Figure II-7: DSC Trace of (a) 60C20 and (b) BPP34C10.

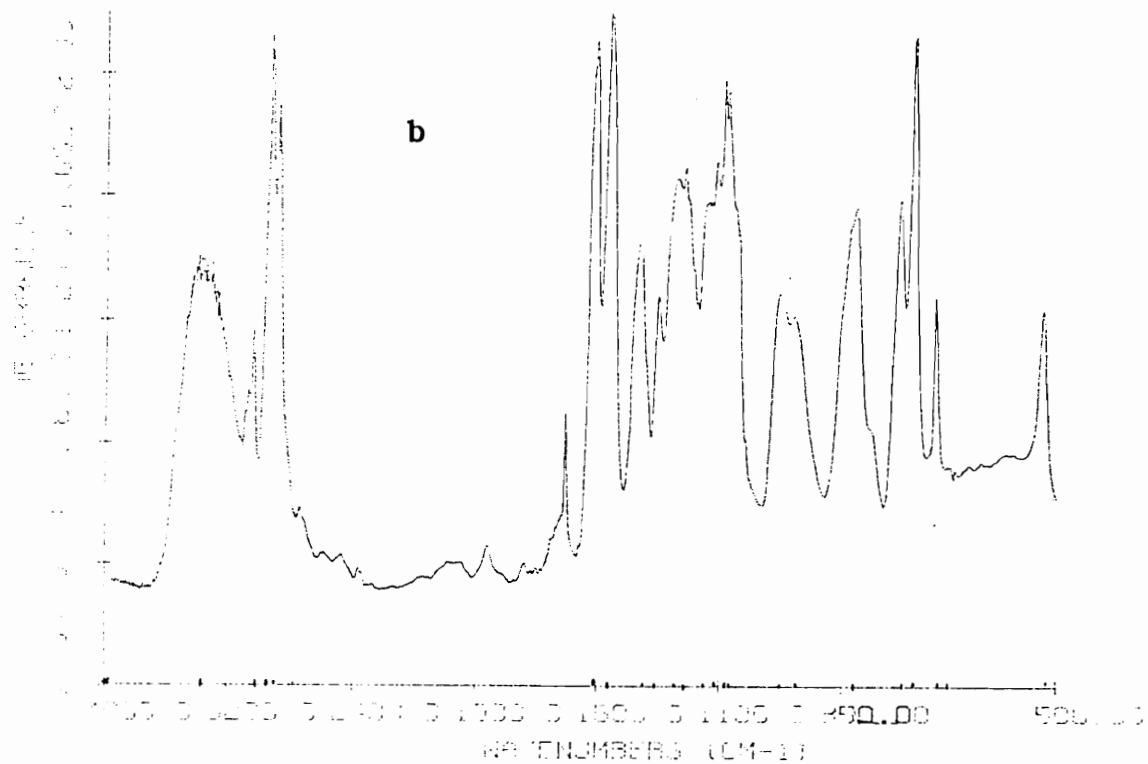
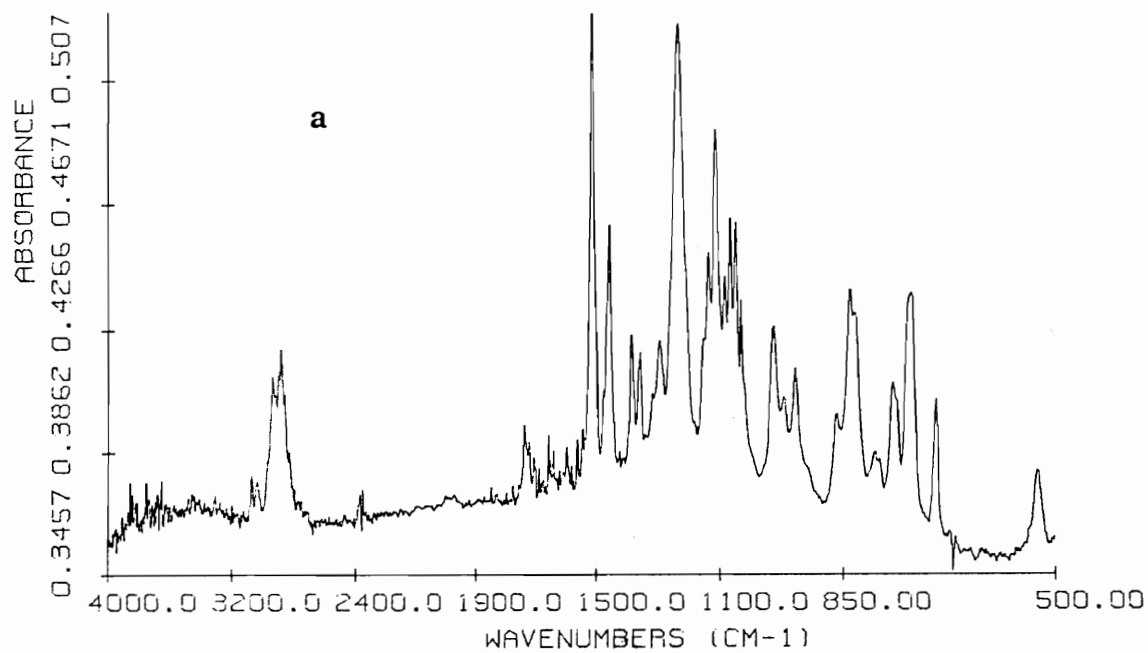


Figure II-8: FTIR Spectra of (a) the Disubstituted compound (II-7) and (b) the diphenol (II-8). Notice the Appearance of the O-H Stretch at 3500 cm⁻¹.

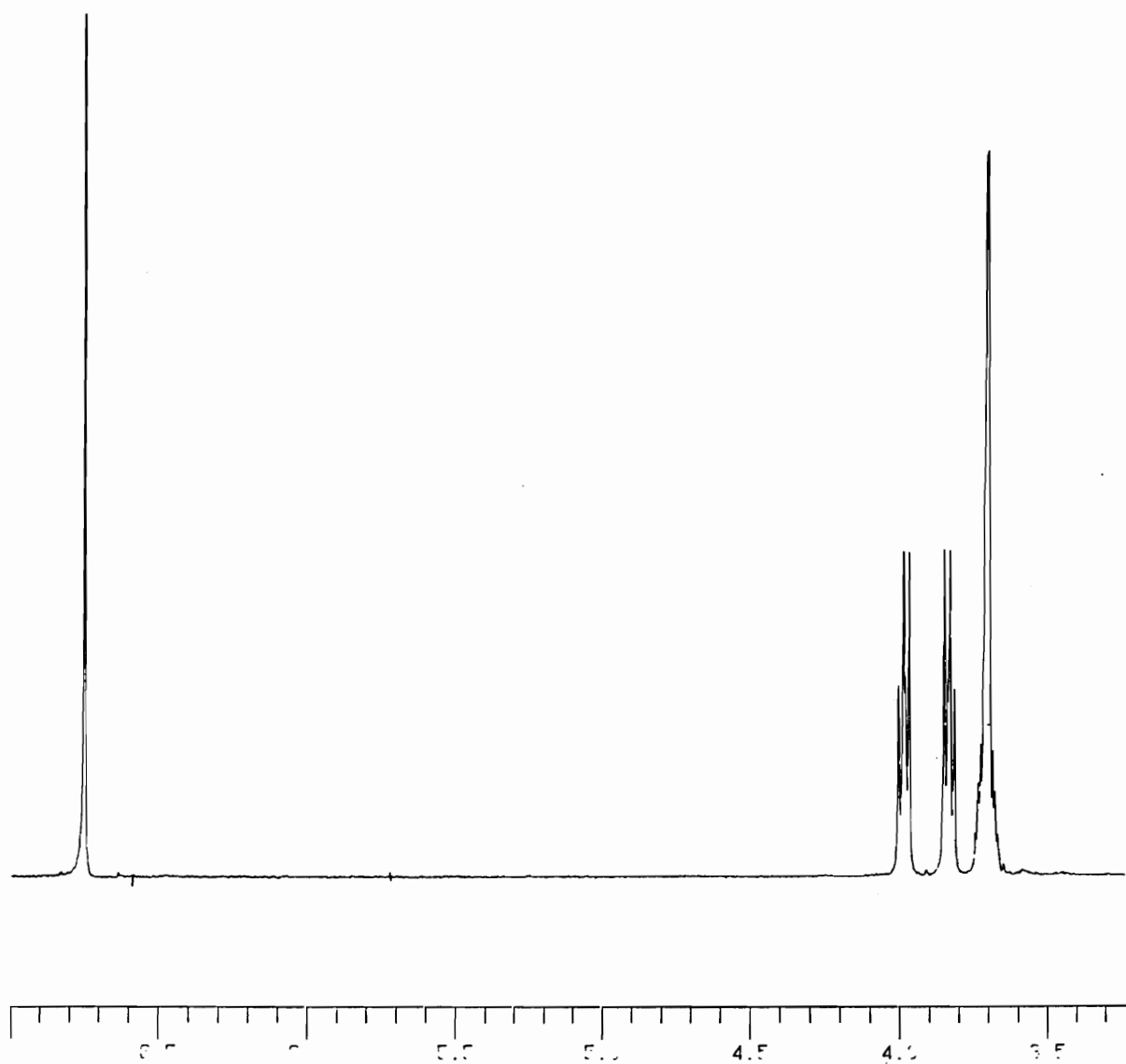


Figure II-9: $^1\text{H-NMR}$ Spectrum of BPP34C10 (II-9) Obtained from One-Step Synthesis.

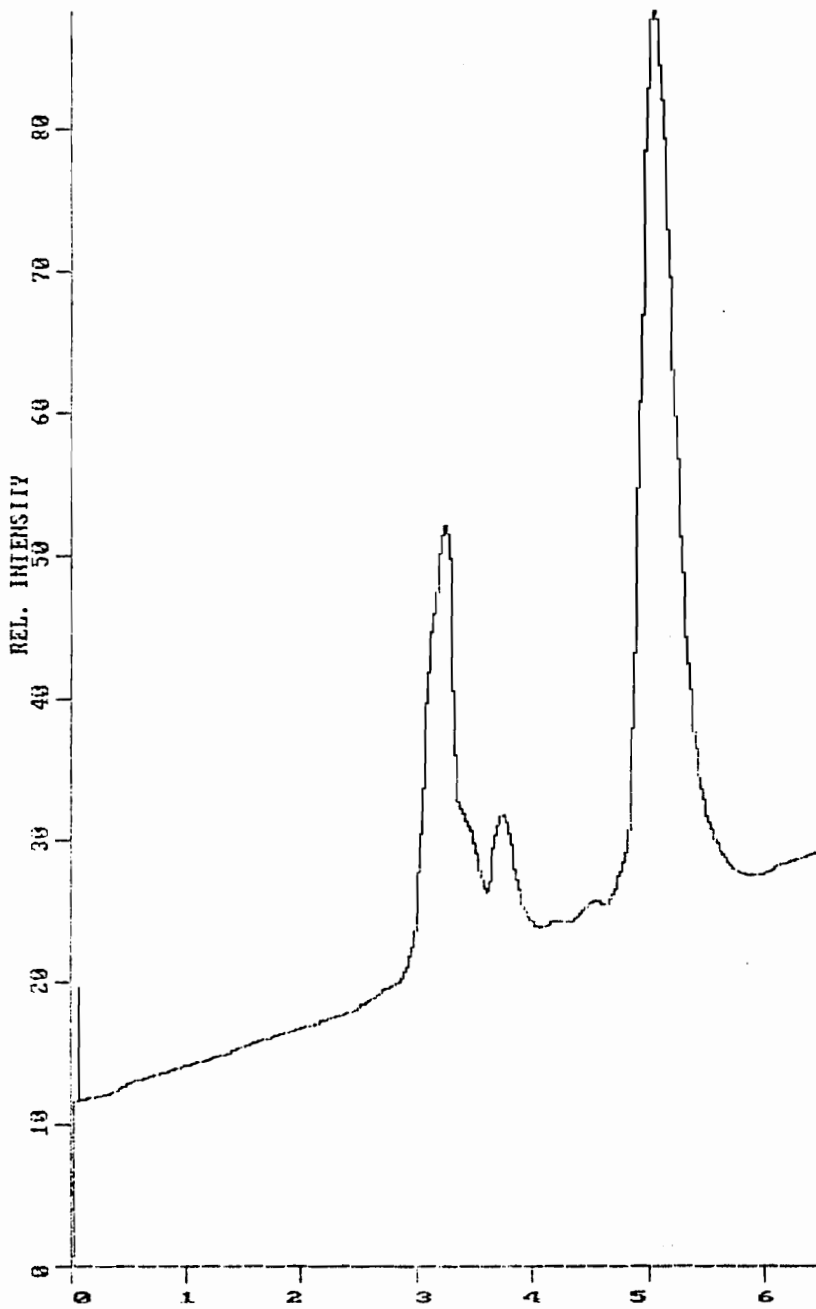


Figure II-10: HPLC Trace of the Product Mixture from Step 1 of the Two-Step Route.

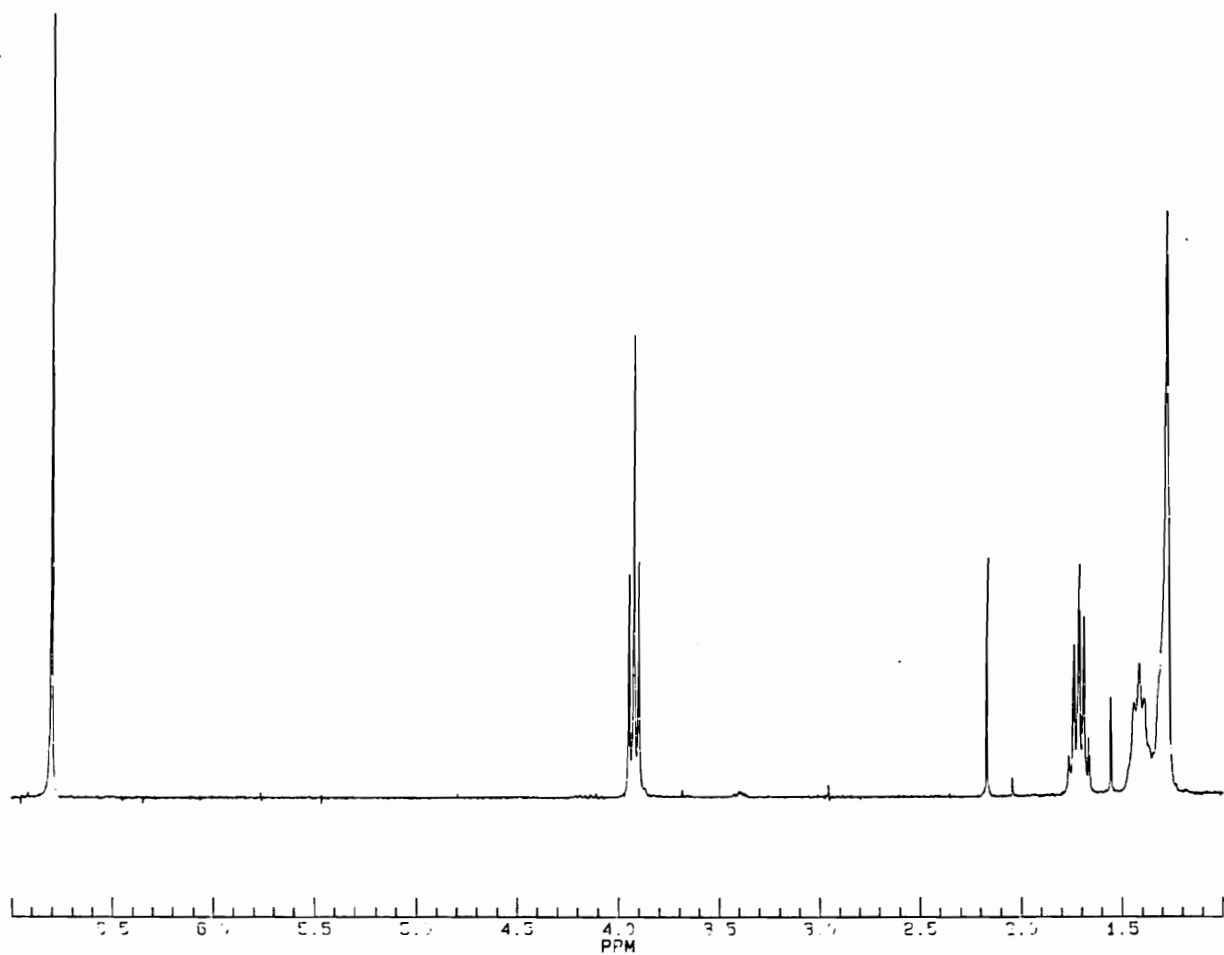


Figure II-11: $^1\text{H-NMR}$ Spectrum of BPP32C4 (II-10).

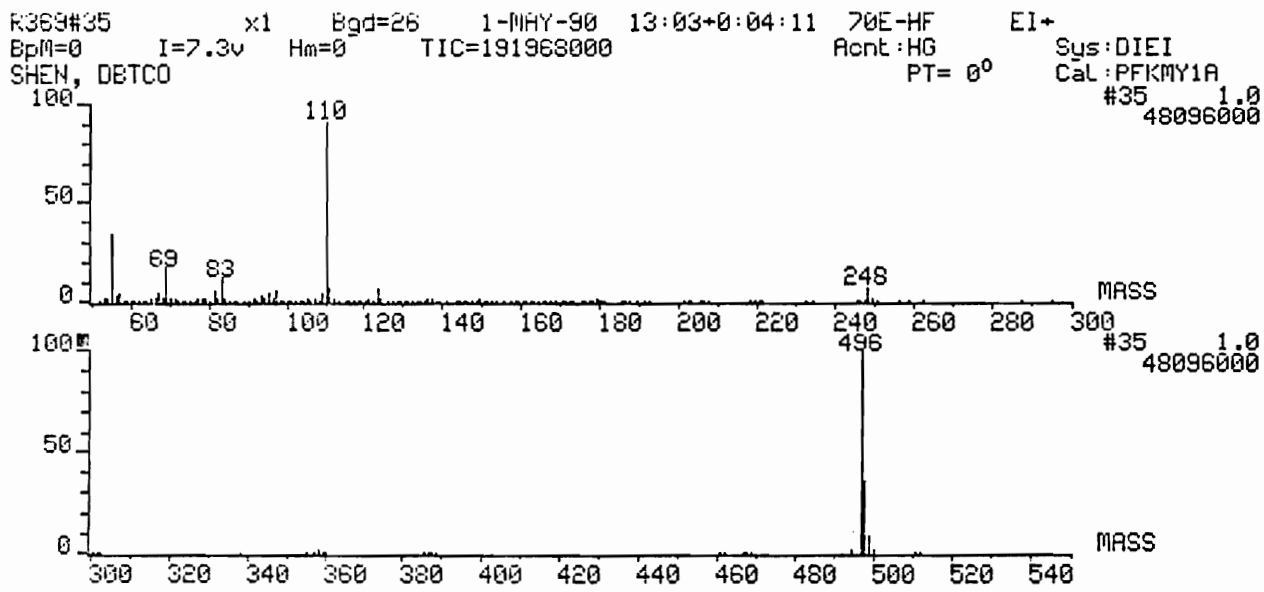


Figure II-12: MS Spectrum of BPP32C4 (II-10).

CHAPTER III: MONOFUNCTIONALIZED TRIARYL DERIVATIVES (BLOCKING GROUPS)

In this chapter, the syntheses and characterization of several types of functionalized bulky compounds are discussed. These compounds were used as blocking groups to prevent permanently the loss of the threaded cyclics.

III-1: DESIGN AND USE OF BLOCKING GROUPS

III-1-1: DESIGN CONCEPTS

The purpose of introducing blocking groups into rotaxane and polyrotaxane molecules is to prevent the dethreading of macrocycles from the linear backbone. Even though the blocking groups may not be necessary for "temporarily stable" polyrotaxanes,¹ monomeric and oligomeric rotaxanes always have to have blocking groups at ends of or along the linear backbone. The term "temporarily stable" means that the dethreading is not significant in certain period of time which is long

enough to carry out various characterizations. However, for "permanently stable" polyrotaxanes, blocking groups are always required.

The most important parameter considered in the design of blocking groups is their sizes, which, of course, have to be bigger than the cavities of the macrocycles to be blocked. The size of a blocking group required to block a specific macrocycle can be theoretically calculated and demonstrated with a CPK molecular model or computer simulation. However, few experimental demonstrations have been reported. Harrison reported that the hydrocarbon macrocycles with more than 29 methylene units can pass over the trityl end blocker at 120°C;² the one with 28 membered ring passed over the bis(cyclohexyl) acetyl group. While the tris(*p-t*-butylphenyl)methyl end group can prevent threading of the hydrocarbon macrocycle with methylene units less than 34 at 250°C; unfortunately no larger rings were tested.³ It seems that there have been no clear experimental results correlating the ring cavity and blocking group size. I intend to synthesize blocking groups as big as I can for more applications.

Another factor to consider is their functionality. In order to chemically introduce a blocking group into a rotaxane or polyrotaxane molecule, the functionality of the blocking group is required to be compatible with the reaction system. For example, the functional group of a blocking group has to be highly reactive toward the end groups of the linear species under the same conditions as those for the other reactions such as polymerization in the system. Blocking groups may be

designed as monofunctionalized or difunctionalized as represented by **III-1** and **III-2**, respectively, where the solid ball represent a bulky group. The use of these two different types of blocking groups will be discussed in the next section.



III-1



III-2

Solubility of blocking groups should also be compatible with the reaction system. In other words, blocking groups have to be soluble in the reaction solvent which may be either a melted macrocycle or a mixture of macrocycle and another solvent.

III-1-2: USE OF BLOCKING GROUPS

Monofunctionalized blocking groups are used as end blockers for both monomeric and polymeric rotaxanes. To prepare monomeric rotaxanes, blocking groups can be added into the reaction system when the threading equilibrium is reached. To prepare polymeric rotaxanes, blocking groups can either be added after the polymerization or used as an initiator and molecular weight control agent added at the beginning of

the polymerization as represented by Scheme III-1. Polyrotaxanes resulting from this method have schematic structure **I-12a**.

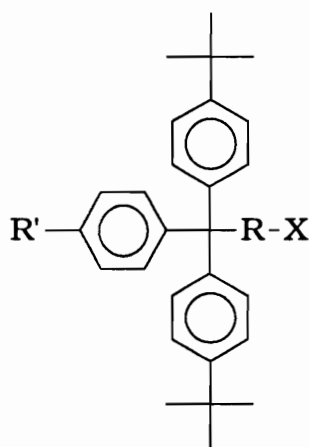
Difunctionalized blocking groups can be used as comonomers in the polymerizations as shown by Scheme III-2. In that case, blocking groups are incorporated into the polymer backbone as spacers among macrocycle molecules, which leads to the formation of polyrotaxane **I-12b**.

In this chapter, I report monofunctionalized triaryl derivatives used as monofunctionalized blocking groups. Difunctionalized blocking groups were not used in my studies. Therefore, they are not reported here. However, their syntheses will be discussed in chapter VII.

III-2: RESULTS AND DISCUSSION

The triaryl derivatives synthesized and characterized are shown in **III-3**. These compounds have not been reported in the literature. However, tris-*p-t*-butylphenylmethanol was used by Harrison in his synthesis of monomeric rotaxanes.³ But he did not report the preparation of this compound. Marvel *et al.* used tris-*p-t*-butylphenylmethanol and di-(*p-t*-butylphenyl)phenylmethanol in their syntheses of alkyl substituted hexaarylethanes.⁴ They prepared the alcohols via the reactions of *p-t*-butylbromobenzene Grignard reagent

and ethyl benzoate or ethyl *p-t*-butylbenzoate. They reported tri-*p-t*-butylphenylmethanol as a crystalline compound with melting point of 212 - 213°C in about 40% yield from the reaction. Unfortunately di-(*p-t*-butylphenyl)phenylmethanol was not purified and no characterization data was reported.



III-3a: R' = H, R = (CH₂)₃, X = OH

III-3b: R' = H, R = (CH₂)₃, X = Cl

III-3c: R' = H, R = (CH₂)₃, X = I

III-3d: R' = H, R = (CH₂)₆, X = OH

III-3e: R' = H, R = (CH₂)₆, X = Cl

III-3f: R' = H, R = (CH₂)₆, X = I

III-3g: R' = H, R = *p*-C₆H₄, X = OH

III-3h: R' = *t*-butyl, R = *p*-C₆H₄, X = OH

III-3i: R' = *t*-butyl, R = *p*-C₆H₄OCH₂CH₂OCH₂CH₂, X = OH

III-3j: R' = *t*-butyl, R = *p*-C₆H₄OCH₂-*p*-C₆H₄CH₂, X = Br

According to Marvel *et al.*, a bulky triaryl group can be built up by the Grignard reaction of a bromobenzene derivative and a benzoate ester. With this principle, I synthesized series **III-3** starting from the Grignard reaction of *p-t*-butylbromobenzene and methyl benzoate or methyl *p-t*-butylbenzoate followed by several modification steps.

III-2-1: GRIGNARD REACTIONS

Di-(*p-t*-butylphenyl)-phenylmethanol and tris-*p-t*-butylphenylmethanol were synthesized via Grignard reaction as shown in Scheme III-3. An attempt was first made with ethyl ether as solvent which is a common solvent for the preparation of Grignard reagents. However, the reaction did not proceed, probably due to the lower refluxing temperature of ethyl ether. Thus, the *p-t*-butylphenyl Grignard reagent was prepared *in-situ* in refluxing THF. The Grignard reagent then reacted with half an equivalent of methyl benzoate or methyl *p-t*-butylbenzoate to produce di-(*p-t*-butylphenyl)-phenylmethanol or tris-*p-t*-butylphenylmethanol. This reaction was via a two-step mechanism as shown in Scheme III-4. First, the Grignard reagent attacked the carbonyl and a diaryl ketone was generated. The ketone was further attacked by the Grignard reagent to give the triaryl alcohol after hydrolysis. The reaction gave 80% - 90% yields. A major by-product was a fluorescent compound, which may be the coupling product (hexaaryl dimethyl ether).

Tris-*p-t*-butylphenylmethanol has a higher melting point and recrystallizes easier than di-(*p-t*-butylphenyl)-phenylmethanol since it is more symmetrical. However, both alcohols can be purified via

recrystallization by proper choice of solvent system. The alcohols were characterized by melting point measurement, FTIR, $^1\text{H-NMR}$ and elemental analyses. A peak from O-H stretch was seen in FTIR spectra [Figure III-1a for di-(*p-t*-butylphenyl)-phenylmethanol] and $^1\text{H-NMR}$ spectra [Figure III-2a for di-(*p-t*-butylphenyl)-phenylmethanol and Figure III-2b for tris-*p-t*-butylphenylmethanol] gave correct integrations of *t*-butyl and aromatic protons. The elemental analysis results are within accepted errors.

III-2-2: MODIFICATION METHOD 1 (SCHEME III-5)

Di-(*p-t*-butylphenyl)-phenylmethanol and tris-*p-t*-butylphenylmethanol can not be directly used as blocking groups because the steric hindrance reduces the reactivities and also the resultant trityl ether type compounds are hydrolytically unstable. Therefore, it is necessary to have the functional group remote from the steric hindrance region. This can be achieved by adding a linear chain to lead the functional group out. The method is illustrated in Scheme III-5.

III-2-2-1: Reduction

In order to generate a carbanion for a nucleophilic substitution reaction, di-(*p-t*-butylphenyl)-phenylmethanol was reduced to di-(*p-t*-butylphenyl)phenylmethane by formic acid in toluene. The mechanism of this reaction is illustrated in Scheme III-6. The reaction of the alcohol and formic acid generated a carbocation which abstracted a hydride from the formate anion to form the triaryl methane and carbon dioxide was

released. This is a quantitative reaction and the product was easily separated and purified.

FTIR analysis showed the disappearance of the O-H stretch (Figure III-1). ¹H-NMR showed the appearance of a singlet at 5.49 ppm which is from 3^o aliphatic proton of the methane (Figure III-2c). The compound was also characterized by melting point measurement and elemental analysis, which gave satisfactory results.

III-2-2-2: Addition of a Linear Chain by Nucleophilic Substitution

The di-(*p-t*-butylphenyl)phenylmethane was allowed to react with tetrahydropyran-protected (THP-protected) 3-chloropropanol-1 or 6-chlorohexanol-1 to form chain extended THP-protected alcohols which underwent deprotection with HCl to produce hydroxyl-terminated blocking groups **III-3a**, and **III-3d** (Scheme III-5). These reactions were carried out in THF with *n*-BuLi as base at 0^oC. A triarylcabanion was generated when *n*-BuLi abstracted the 3^o proton from the triarylmethane and then the carbanion attacked the chloride on the THP-protected chloroalcohol in S_N2 fashion resulting in a C-C bond formation. The appearance and disappearance of a deep red color during the reaction indicated the formation and consumption of the triarylcabanion. The yields of these reactions ranged from 40% - 50%. The low yields were probably due to the carbanion abstraction of protons from the chloride leading to elimination or from other species in the reaction system such as moisture, residual alcohol in the THP-protected chloroalcohols, etc.

Compounds **III-3a** and **III-3d** are not crystallizable. However, they were easily purified by column separations on silica gel since the impurities were much less polar and had smaller retention volumes than the alcohols. The compounds were characterized by melting point measurement, FTIR, $^1\text{H-NMR}$ and elemental analyses. FTIR traces showed a large peak from OH stretch. Both $^1\text{H-NMR}$ (Figure III-3a and Figure III-4a) and elemental analyses gave satisfactory results.

III-2-2-3: Conversion of Functional Groups

Blocking groups **III-3a** and **III-3d** can be used in rotaxane and polyrotaxane syntheses. However, to apply the blocking groups more widely, hydroxyl groups were converted to iodide, a good leaving group. This conversion was done via a two-step path (Scheme III-5). First, the hydroxyl groups were converted into chloride by reaction with thionyl chloride in benzene and pyridine.^{5,6} The mechanism of this reaction is probably as shown in Scheme III-7. Thionyl chloride first reacts with pyridine to form a pyridine salt which increase the electrophilicity of S atom. The S atom is then attacked by the oxygen of the alcohol (**III-3a** or **III-3d**) resulting in the formation of a intermediate **III-4** which further decomposes to **III-5**. The compound **III-5** undergoes a $\text{S}_{\text{N}}\text{I}$ reaction according to a mechanism discussed by J. March.⁷ This is a two step process with an alkyl chloride as the product and release of SO_2 . Second, the chloride was further converted into iodide by reacting with sodium iodide in acetone.⁸ Both are known reactions with high yields (85% - 100%).

The chloro-terminated compounds **III-3b** and **III-3e** were not purified before they were subjected to iodinations. Therefore, no analyses were done except TLC and $^1\text{H-NMR}$. However, the crude compounds were quite pure after separation procedures according to TLC and $^1\text{H-NMR}$ (Figure III-3b and Figure III-4b) results. The iodo-terminated blocking groups **III-3c** and **III-3f** are viscous oils and no melting points and boiling points were obtained. However, FTIR and $^1\text{H-NMR}$ (Figure III-3c and Figure III-4c) gave satisfactory results.

The functional group conversions were clearly seen from $^1\text{H-NMR}$ spectra shown in Figure III-3 ($n = 3$) and Figure III-4 ($n = 6$). When the functional group changed from -OH to -Cl to -I, the chemical shift of methylene protons on the carbon bonded to the functional group changed upfield from 3.63 to 3.50 to 3.13 ppm for the $n = 3$ system and 3.67 to 3.54 to 3.20 for the $n = 6$ system. These upfield shifts are consistent with the order of decrease in electronegativities of the functional groups from -OH to -Cl to -I.

III-2-3: MODIFICATION METHOD 2 (SCHEME III-8)

III-2-3-1: Addition of Phenyl Ring by Aromatic Electrophilic

Substitutions

Since the reactions of the triarylmethyl carbanions and THP-protected alcohols were not high yielding, a phenyl ring was added via a carbocationic process to achieve the remoteness of the functional group from the steric hindrance region. This method was based on a literature

report by Mikroyannidis who used a similar reaction to prepare bis(4-hydroxyphenyl)-diphenylmethane.⁹ Reactions of triarylmethanols and phenol offered much higher yields (85% - 98%). This method also simplified the synthetic route (no reduction step).

As shown in Scheme III-8, the reactions were carried out in refluxing phenol with HCl as the catalyst and produced phenol type blocking groups **III-3g** and **III-3h**. They are aromatic electrophilic substitution reactions. The carbocations formed by the acid catalyzed ionization of the triarylmethanols attacked the para-position of phenol to form the desired products. After the reaction, the large excess of phenol was removed by washing with aqueous NaOH solution. Compounds **III-3g** and **III-3h** were easily purified by recrystallizations since the crystallizabilities were largely increased by introducing a phenyl ring.

Again, **III-3g** and **III-3h** gave satisfactory characterization results from melting point measurement, FTIR, ¹H-NMR and elemental analyses. Figure III-5 shows ¹H-NMR spectra of these two compounds. Notice that the phenol proton was clearly seen at 4.89 ppm for **III-3g** and 4.72 ppm for **III-3h** and also the aromatic protons most close to the phenoxy show up as a doublet around 6.70 ppm.

III-2-3-2: Further Chain Extension by Williamson Reactions

The phenol type hydroxyl groups are of low reactive toward MDI in the polyurethane synthesis since the aromatic ring decreases the nucleophilicity and also produce thermally labile urethane linkages.

Therefore, it is necessary to convert the phenoxy group to an aliphatic hydroxyl. This can be done by further chain extension as illustrated in Scheme III-8. Phenol type blocking group **III-3h** was allowed to react with an excess amount of THP-protected di(ethylene glycol) monochloride in KOH/1-butanol system followed by deprotection with HCl; a hydroxyl terminated blocking group **III-3i** was obtained in 95% yield.

The purification of **III-3i** was straightforward. The only impurity left after extraction was unreacted di(ethylene glycol) monochloride. Since this impurity is acetone soluble, it was removed by carrying out recrystallization of **III-3i** in acetone.

¹H-NMR (Figure III-6) and FTIR gave satisfactory results. The melting point of **III-3i** is 80°C lower than that of starting material **III-3h** because a flexible ethylene oxide chain was added. Therefore, it is possible to adjust the melting point (as well as solubility) of a hydroxyl terminated blocking group by proper choice of chain length of the ethylene oxide segment. This adjustment is necessary when the blocking group is subjected to different reaction conditions.

On the other hand, **III-3h** was allowed to react with large excess of α,α' -dibromo-*p*-xylene to form the benzyl bromide terminated blocking group **III-3j** (I used NaH as base, actually it is not necessary to use such a strong base for this reaction). This blocking group can be used in Menschutkin reactions to prepare paraquat dication containing rotaxanes and polyrotaxanes and some other reactions in which the bromide serves as a leaving group. The rotaxanes and polyrotaxanes

incorporating this blocking group are unstable since the benzyl ether bond in the blocking group can be cleaved by treatment with acid or by catalytic hydrogenation. This property is important in the verification of rotaxane formation and study of dethreading process. After removal of the blocking group from a rotaxane or polyrotaxane by acid treatment or hydrogenolysis, dethreadings take place and, therefore, free linear and cyclic species are expected to be detected by TLC, HPLC or other analytical methods either qualitatively or quantitatively.

Compound **III-3j** was characterized by melting point measurement and $^1\text{H-NMR}$ analysis. $^1\text{H-NMR}$ spectra shown in Figure III-7 clearly demonstrated the formation the desired product. Figure III-7a shows the spectrum of the crude product after the reaction. Three singlets are shown for benzylic protons: 4.47 ppm (from unreacted α,α' -dibromoxylene), 4.52 ppm (benzyl protons next to bromide on **III-3j**) and 5.02 ppm (benzyl ether protons on **III-3j**). After washing several times with acetone, the peak at 4.47 ppm disappeared (Figure III-7c) indicating the removal of unreacted α,α' -dibromoxylene by washing. The equal integration of peaks at 4.52 ppm and 5.20 ppm shows that none of the compound with two triarylmethyl groups formed in the reaction.

III-3: EXPERIMENTAL

p-t-Butylbromobenzene, magnesium turnings and 2,3-dihydropyran were purchased from Lancaster Synthesis, Inc. and used without further purification. Methyl benzoate (reagent grade) and phenol (loose crystals) were purchased from Fisher Scientific Company and also used without further purification. *p-t*-Butylbenzoic acid (98%), formic acid (99%), 3-chloropropanol (99%), 6-chlorohexanol (99%), 2-(2-chloroethoxy)ethanol (99%), *n*-butyllithium (solution in hexanes, 2.5M), thionyl chloride (99+%), sodium iodide (98%), pyridine (99+%) and α,α' -dibromo-*p*-xylene (98%) were purchased from Aldrich Chemical Company. The *n*-butyllithium was titrated as 2.4 M. α,α' -Dibromo-*p*-xylene was recrystallized once from *n*-hexane; the others were used without further purification.

The THP-protected 3-chloropropanol and 6-chlorohexanol were prepared from the reactions of 2,3-dihydropyran with 3-chloropropanol and 6-chlorohexanol, respectively. The preparation of these two compound were done in collaboration with P. Engen (THP-protected 3-chloropropanol¹⁰) and C. Lim (THP-protected 6-chlorohexanol¹¹) in our laboratory.

Melting points were determined on a HAAKE BUCHLER capillary melting point apparatus and are corrected. The FTIR spectra were recorded on a Nicolet MX-1 FTIR spectrometer. The ¹H-NMR spectra

were recorded on a Bruker WP 270 MHz instrument using TMS as the internal standard. Elemental analyses were done by Atlantic Microlab, Inc., Norcross, Georgia.

III-3-1: GRIGNARD REACTIONS

III-3-1-1: Di-*p-t*-butylphenyl phenylmethanol

In an oven-dried 2-L 3-necked flask equipped with a condenser, dropping funnel, mechanical stirring and nitrogen system, magnesium turnings (12.2 g, 0.500 mol) were placed with dry THF (800 mL) (dried with Na/benzophenone). *p-t*-Butylbromobenzene (100 g, 0.469 mol) in dry THF (200 mL) was added dropwise over one hour with gentle heating (heating was removed when the reaction started). The reaction was allowed to go for two hours. A brown color was observed. Methyl benzoate (30.0 g, 0.220 mol) in dry THF (100 mL) was added dropwise over one hour. The mixture was stirred overnight at reflux under nitrogen.

The system was cooled to room temperature. The solution was neutralized with 10% HCl. Product was extracted 2 times with n-hexane (2 x 350 mL). The combined organic phase was washed 3 times with water (3 x 500 mL) and dried with MgSO₄. A yellow solid (80.0 g) was obtained after removal of the solvent by rotary evaporation. The solid was subjected to recrystallization two times in methanol and 78.0 g of white powder was obtained.

Yield: 95%; m.p. 94.0 - 95.0°C; FTIR (Figure III-1a, $\nu/\text{max}, \text{cm}^{-1}$): 3590, 2950, 2873, 1510, 1499, 1475, 1463, 1395, 1360, 1306, 1259, 1201, 1162, 1123, 1046, 1026, 912, 848, 828, 768, 698, 668, 616, 588, 540; $^1\text{H-NMR}$ (Figure III-2a, chloroform- d /TMS, ppm): 1.27 (s, 18 H, *t*-butyl), 7.15 - 7.35 (m, 13 H, arom.); elemental analysis (%): calculated for $\text{C}_{27}\text{H}_{32}\text{O}$, C: 87.05, H: 8.66, O: 4.29; found, C: 86.34, H: 8.49.

III-3-1-2: Tris-*p-t*-butylphenylmethanol

To an oven-dried 500-mL 3-necked flask equipped with a condenser, magnetic stirring, dropping funnel and nitrogen system, magnesium turnings (7.39 g, 0.304 mol) were added with dry THF (85 mL) (dried with Na/benzophenone) and a small iodine crystal. *p-t*-Butylbromobenzene (43.2 g, 0.203 mol) in dry THF (65 mL) was added dropwise over 2 hours. The disappearance of the brown color of iodine indicated the beginning of the reaction. The solution became brown again after the reaction started. The mixture was stirred for another 2 hours at room temperature with gentle heating. Ethyl *p-t*-butylbenzoate (20.9 g, 0.101 mol) in dry THF (85 mL) was added dropwise over 2 hours. The mixture was stirred overnight at reflux.

The system was cooled down to room temperature. The product was precipitated into 1 L of 10% HCl aqueous solution. The precipitate was filtered and washed with 100 mL of hot *n*-hexane (the product residue that remained in the hexane phase was recovered and washed again). The combined solid was subjected to recrystallization in cyclohexane three times and 25 g of white powder was obtained.

Yield: 58% (some product was lost during the washing) (reported⁴: \cong 40%); m.p. 201.5 - 205.7°C (reported⁴: 212 - 213°C); FTIR ($\nu/\text{max}, \text{cm}^{-1}$): 3590, 3012, 2935, 2851, 1610, 1518, 1509, 1490, 1471, 1399, 1360, 1314, 1308, 1271, 1205, 1176, 1118, 1022, 1004, 927, 912, 850, 840, 823, 801, 755, 702, 610, 581, 545, 524; ¹H-NMR (chloroform-d/TMS, ppm): 1.32 (s, 27 H, *t*-butyl), 7.19 (d, 6 H, aromatic), 7.33 (d, 6 H, aromatic); elemental analysis (%): calculated for C₃₁H₄₀O, C: 86.86, H: 9.41, O: 3.73; found: C: 86.79, H: 9.39.

III-3-2: MODIFICATION METHOD 1

III-3-2-1: Di-(*p-t*-butylphenyl)phenylmethane

Di-(*p-t*-butylphenyl)phenylmethanol (80.0 g, 0.210 mol) was dissolved in toluene (800 mL) in a 2-L 3-necked flask equipped with a condenser and mechanical stirring. The solution was heated to reflux and formic acid (350 mL) was added. The mixture was allowed to reflux overnight.

The system was cooled to room temperature. Two layers were observed. The organic phase was separated and more product in the formic acid and water phase was extracted 2 times with toluene (2 x 200 mL). The combined organic phase was washed three times with water (3 x 500 mL) and dried with MgSO₄. An oil (75.5 g) was obtained after removal of the solvent by rotary evaporation. The first recrystallization was done in *n*-hexane and the second recrystallization was done in

toluene, both at -20°C. A white powder (60.0 g) was obtained after it was vacuum dried overnight.

Yield: 80% (some compound was lost during recrystallizations); m.p. 99 - 100°C; FTIR (Figure III-1b, $\nu/\text{max}, \text{cm}^{-1}$): 2950, 2873, 1510, 1495, 1475, 1468, 1395, 1360, 1259, 1201, 1138, 1123, 1088, 1040, 862, 850, 828, 780, 768, 698, 605, 588, 553, 545, 535; $^1\text{H-NMR}$ (Figure III-2c, chloroform- d /TMS, ppm): 1.30 (s, 18 H, *t*-butyl), 5.49 [s, 1 H, (aryl) $_3$ -CH], 7.03 - 7.32 (m, 13 H, arom.); elemental analysis (%): calculated for $\text{C}_{27}\text{H}_{32}$, C: 90.95, H: 9.05; found: C: 90.70, H: 9.04.

III-3-2-2: 4,4-Di-*p-t*-butylphenyl-4-phenylbutanol-1 (III-3a)

In an oven-dried 500-mL 3-necked flask equipped with magnetic stirring and nitrogen system, di-*p-t*-butylphenylphenylmethane (19.4 g, 0.0543 mol) was placed with dry THF (200 mL) (dried with Na/benzophenone). The flask was immersed in an ice-bath. *n*-BuLi (2.5 M, 21.8 mL, 0.0543 mol) was syringed into the flask over 15 minutes. A red color was observed upon the addition of *n*-BuLi. The reaction was allowed to go for 45 minutes. THP-protected 3-chloropropanol-1 (9.70 g, 0.0543 mol) was syringed into the flask over 15 minutes. The solution was stirred for 20 hours. The red color disappeared.

Water (15 mL) was added. The product was extracted 3 times with diethyl ether (3 x 200 mL). The combined organic phase was washed 3 times with water (3 x 500 mL) and dried with MgSO_4 . A yellow oil (30.8 g) was obtained after the removal of solvent by rotary evaporation. TLC

showed one major spot. This oily product was subjected to the deprotection reaction without further analysis and purification.

The oil (30.0 g) was dissolved in a mixture of methanol and methylene chloride (1:1/v:v, 240 mL) in a 500-mL 1-necked flask. HCl (36%, 3.5 mL) was added. The solution was magnetically stirred for 2 hours at room temperature.

Most of solvents were rotary evaporated. The residue was dissolved in 200 mL of methylene chloride. The solution was washed 3 times with water (3 x 300 mL) and dried with MgSO₄. A yellow solid (20 g) was obtained after removal of the solvent by rotary evaporation. This solid was subjected to column separation on silica gel with eluting solvent grading from pure n-hexane to a mixture containing 60% n-hexane and 40% ethyl acetate. A white solid (8.00 g) was obtained as the third component eluted.

Yield: 36%; m.p. 77.0 - 79.0°C; FTIR (v/max,cm⁻¹): 3440, 3040, 2961, 2840, 1739, 1620, 1540, 1516, 1460, 1417, 1376, 1280, 1259, 1221, 1160, 1139, 1088, 1070, 1053, 1025, 970, 955, 925, 874, 843, 818, 763, 742, 707, 647, 608, 584, 570, 546; ¹³C-NMR (chloroform-d/TMS, ppm): 21.5, 25.7, 31.8, 34.6, 37.5, 65.2, 125.0, 126.0, 128.0, 129.1, 129.8, 144.6, 148, 148.9; ¹H-NMR (Figure III-3a, chloroform-d/TMS, ppm): 1.30 (s, 18 H, *t*-butyl), 1.40 (m, 2 H, CH₂CH₂CH₂OH), 2.63 (m, 2 H, CH₂CH₂CH₂OH), 3.63 (t, 2 H, CH₂CH₂CH₂OH), 7.20 - 7.35 (m, 13 H, aromatic); elemental analysis (%): calculated for C₃₀H₃₈O, C: 86.90, H: 9.25, O: 3.86; found: C: 86.78, H: 9.26.

III-3-2-3: 6,6-Di-*p-t*-butylphenyl-6-phenylhexanol-1 (III-3d)

In an oven-dried 500-mL 3-necked flask equipped with magnetic stirring and nitrogen system, di-*p-t*-butylphenyl-phenylmethane (20.0 g, 0.0560 mol) was placed with dry THF (200 mL) (dried with Na/benzophenone). The flask was immersed in a ice-bath. *n*-BuLi (2.5 M, 22.4 mL, 0.0560 mol) was syringed into the flask over 15 minutes. A red color was observed upon the addition of *n*-BuLi. The reaction was allowed to go for 45 minutes. THP-protected 6-chlorohexanol-1 (12.4 g, 0.056 mol) was syringed into the flask over 15 minutes. The solution was stirred for 20 hours. The red color disappeared.

Water (15 mL) was added. The product was extracted 3 times with diethyl ether (3 x 200 mL). The combined organic phase was washed 3 times with water (3 x 500 mL) and dried with MgSO₄. A yellow oil (28.2 g) was obtained after the removal of solvent by rotary evaporation. TLC showed one major spot. This oily product was subjected to the deprotection reaction without further analysis and purification.

The oil (28.0 g) was dissolved in a mixture of methanol and methylene chloride (1:1/v:v, 200 mL) in a 500-mL 1-necked flask. HCl (36%, 3.0 mL) was added. The solution was magnetically stirred for 2 hours at room temperature.

Most of the solvents were rotary evaporated. The residue was dissolved in 200 mL of methylene chloride. The solution was washed 3 times with water (3 x 300 mL) and dried with MgSO₄. A yellow oil (19.5

g) was obtained after the removal of solvent by rotary evaporation. This oil was subjected to column separation on silica gel with eluting solvent grading from pure n-hexane to a mixture containing 60% n-hexane and 40% ethyl acetate. A light yellow oil (12.0 g) was obtained as the third component eluted.

Yield: 47%; FTIR ($\nu/\text{max}, \text{cm}^{-1}$): 3380, 3015, 2955, 2841, 1609, 1511, 1471, 1403, 1375, 1330, 1280, 1207, 1128, 1083, 1065, 1038, 1020, 952, 909, 845, 824, 767, 758, 749, 710, 695, 652, 618, 581, 570, 550, 542, 502; $^1\text{H-NMR}$ (Figure III-4a, chloroform-d/TMS, ppm): 1.32 (s, 18 H, t-butyl), 1.45 [m, 2 H, $(\text{CH}_2)_2\text{CH}_2(\text{CH}_2)_3\text{OH}$], 1.58 [m, 2 H, $(\text{CH}_2)_3\text{CH}_2(\text{CH}_2)_2\text{OH}$], 1.78 [m, 2 H, $\text{CH}_2\text{CH}_2(\text{CH}_2)_4\text{OH}$], 2.55 [m, 2 H, $\text{CH}_2(\text{CH}_2)_5\text{OH}$], 3.56 [m, 2 H, $(\text{CH}_2)_4\text{CH}_2\text{CH}_2\text{OH}$], 3.65 [t, 2 H, $(\text{CH}_2)_5\text{CH}_2\text{OH}$], 7.13 - 7.25 (m, 13 H, aromatic).

III-3-2-4: 4,4-Di-*p-t*-butylphenyl-4-phenyl-1-iodobutane (III-3c)

Hydroxyl terminated blocking group **III-3a** (2.00 g, 4.82×10^{-3} mol) was placed in an oven-dried 250-mL 3-necked flask equipped with a condenser, dropping funnel and nitrogen system. Benzene (50.0 mL) and pyridine (15.0 mL) were added. Thionyl chloride (4.89 g, 0.0411 mol) in benzene (10.0 mL) was added dropwise over 45 minutes at room temperature. The mixture was stirred for one hour at room temperature and then heated at reflux for overnight.

The system was cooled down to room temperature and product was extracted with benzene three times (3 x 75 mL). The combined

organic phase was washed with water three times (3 x 200 mL) and dried with MgSO₄. A dark brown oil (2.34 g) was obtained after the removal of solvent by rotary evaporation. Some dark colored impurities were removed by filtration on silica gel. A brown viscous oil (2.00 g) was obtained and TLC showed one major spot.

The crude yield of **III-3b** is 85%. ¹H-NMR analysis (Figure III-3b) was done with the crude sample and the chemical shifts are: 1.30 ppm (s, 18 H, t-butyl), 1.58 (m, 2 H, CH₂CH₂CH₂Cl), 2.68 (m, 2 H, CH₂CH₂CH₂Cl), 3.47 (t, 2 H, CH₂CH₂CH₂Cl), and 7.15 - 7.30 (m, 13 H, aromatic). This crude product was subjected to the next reaction without further purification.

NaI (3.50 g, 0.0231 mol) was dissolved in acetone (75.0 ml) in a 250-mL 1-necked flask. The crude **III-3b** (2.00 g, 4.62 x 10⁻⁴ mol) in acetone (25.0 mL) was added. The mixture was stirred at reflux for 72 hours.

The system was cooled down to room temperature and the solvent was removed by rotary evaporation. The product was extracted with methylene chloride three times (3 x 75 mL). The combined organic phase was washed with water three times (3 x 200 mL) and dried with MgSO₄. A brown sticky solid (2.00 g) was obtained.

Yield of **III-3c**: 83%; ¹H-NMR (Figure III-3c, chloroform-d/TMS, ppm): 1.30 (s, 18 H, t-butyl), 1.60 (m, 2 H, CH₂CH₂CH₂l), 2.65 (m, 2 H,

CH₂CH₂CH₂l), 3.12 (t, 2 H, CH₂CH₂CH₂l), 7.15 - 7.30 (m, 13 H, aromatic).

III-3-2-5: 6,6-Di-4-t-butylphenyl-6-phenyl-1-iodohexane (III-3f)

Hydroxyl terminated blocking group **III-3d** (8.06 g, 0.0177 mol) was placed in an oven-dried 500-mL 3-necked flask equipped with a condenser, dropping funnel and nitrogen system. Toluene (300 mL) and pyridine (60 mL) were added. Thionyl chloride (20.0 g, 0.168 mol) in toluene (20 mL) was added dropwise over 1 hour at room temperature. The mixture was stirred for one hour at room temperature and then heated at reflux overnight.

The system was cooled down to room temperature and product was extracted with toluene three times (3 x 100 mL). The combined organic phase was washed with water three times (3 x 300 mL) and dried with MgSO₄. A yellow oil (8.50 g) was obtained after decolorizing with activated carbon and removal of solvent by rotary evaporation. TLC showed one major spot.

The crude yield of **III-3e** is quantitative. ¹H-NMR analysis (Figure III-4b) was done with the crude sample and the chemical shifts are: 1.30 ppm (s, 18 H, t-butyl), 1.46 ppm [m, 2 H, (CH₂)₂CH₂(CH₂)₃Cl], 1.69 ppm [m, 2 H, (CH₂)₃CH₂(CH₂)₂Cl], 1.80 ppm [m, 2 H, CH₂CH₂(CH₂)₄Cl], 2.54 ppm [m, 2 H, CH₂(CH₂)₅Cl], 3.47 ppm [t, (CH₂)₄CH₂CH₂Cl], 3.55 ppm [t, 2 H, (CH₂)₅CH₂Cl], 7.15 - 7.27 ppm (m,

13 H, aromatic). This crude product was subjected to the next reaction without further purification.

NaI (10.0 g, 0.0667 mol) was dissolved in acetone (150 mL) in a 500-mL 1-necked flask. The crude **III-3e** (8.20 g, 0.0173 mol) in acetone (50 mL) was added. The mixture was stirred at reflux for 72 hours.

The system was cooled down to room temperature and the solvent was removed by rotary evaporation. The product was extracted with methylene chloride three times (3 x 150 mL). The combined organic phase was washed with water three times (3 x 300 mL) and dried with MgSO₄. A brown oil (9.02 g) was obtained.

Yield: 92%; FTIR (ν /max, cm⁻¹): 3011, 2890, 1602, 1529, 1506, 1465, 1400, 1370, 1300, 1237, 1215, 1198, 1135, 1122, 1040, 1019, 970, 908, 845, 830, 761, 697, 653, 622, 589, 570, 542, 505; ¹H-NMR (Figure III-4c, chloroform-d/TMS, ppm): 1.32 (s, 18 H, t-butyl), 1.45 [m, 2 H, (CH₂)₂CH₂(CH₂)₃I], 1.75 [m, 2 H, (CH₂)₃CH₂(CH₂)₂I], 1.85 [m, 2 H, CH₂CH₂(CH₂)₄I], 2.53 [m, 2 H, CH₂(CH₂)₅I], 3.14 [t, 2 H, (CH₂)₄CH₂CH₂I], 3.19 [t, 2 H, (CH₂)₅CH₂I].

III-3-3: MODIFICATION METHOD 2

III-3-3-1: *p,p'*-Di(*t*-butyl)-*p'*-hydroxytetraphenylmethane (III-3g)

Di-*p-t*-butylphenylphenylmethanol (26.0 g, 0.0700 mol) and phenol (20 g, 0.213 mol) were placed in a 250-mL 1-necked flask equipped with a condenser and nitrogen system. THF (50 mL) was added. HCl (36%, 2

mL) was added as a catalyst. A deep red color was observed immediately. The mixture was refluxed for 24 hours.

The system was cooled down to room temperature and THF was rotary evaporated. The product was extracted three times with n-hexane (3 x 250 mL) and NaOH aqueous solution (20 g/L) (250 mL). The combined organic phase was washed three times with the NaOH aqueous solution (3 x 300 mL) and three times with water (3 x 300 mL) and dried with Na₂SO₄. A white solid (23.6 g) was obtained after it was decolorized with activated carbon and the solvent was rotary evaporated. The product was recrystallized four times from acetone and fine crystals (16.5 g) were obtained.

Yield: 53% [the low yield was probably due to the addition of THF in the system (the ring opening of THF could take place by attack of the triaryl carbocation) and also some product was lost during recrystallizations]; m.p. 210.0 - 210.9°C; FTIR (ν/max,cm⁻¹): 3320, 2958, 2920, 1705, 1611, 1510, 1525, 1445, 1400, 1373, 1283, 1245, 1221, 1188, 1109, 1021, 881, 847, 821, 754, 712, 705, 700, 600, 581, 549, 542; ¹H-NMR (Figure III-5a, chloroform-d/TMS, ppm): 1.29 (s, 18 H, t-butyl), 4.89 (s, 1 H, OH), 6.72 (d, 2 H, aromatic most close to OH), 7.05 - 7.28 (m, 15 H, aromatic).

III-3-3-2: Tris-*p-t*-butylphenyl-4-hydroxyphenylmethane (III-3h)

Tris-*p-t*-butylphenylmethanol (13.0 g, 0.0303 mol) was dissolved in phenol (50 g) by warming in a 250-mL 1-necked flask equipped with a

condenser and nitrogen system. HCl (36%, 1 mL) was added as a catalyst. A deep reddish-blue color was observed immediately. The mixture was refluxed for 24 hours.

The system was cooled down to room temperature. The product was extracted three times with toluene (3 x 150 mL) and NaOH aqueous solution (20 g/L) (250 mL). The combined organic phase was washed three times with the NaOH aqueous solution (3 x 250 mL) and three times with water (3 x 250 mL) and dried with Na₂SO₄. A white solid (13.7 g) was obtained after it was decolorized with activated carbon and the solvent was rotary evaporated. The solid was boiled in n-hexane for 30 minutes, filtered, dried under vacuum and weighed (11.5 g).

Yield: 85%; m.p. 301.0 - 301.8°C; FTIR ($\nu/\text{max}, \text{cm}^{-1}$): 3605, 3425, 2960, 2920, 1611, 1510, 1505, 1445, 1425, 1400, 1373, 1285, 1250, 1221, 1188, 1109, 1021, 847, 821, 703, 700, 600, 585, 580, 570; ¹H-NMR (Figure III-5b, chloroform-d/TMS, ppm): 1.30 (s, 27 H, t-butyl), 4.72 (s, 1 H, OH), 6.70 (d, 2 H, aromatic most close to OH), 7.05 - 7.25 (m, 14 H, aromatic); elemental analysis (%): calculated for C₃₇H₄₄O, C: 88.03, H: 8.79, O: 3.17; found: C: 88.00, H: 8.60.¹²

III-3-3-3: Mono-[*p*-tris(*p*'-*t*-butylphenyl)methylphenyl Ether of Di(ethylene glycol) (III-3i)

The phenol type blocking group **III-3h** (5.00 g, 9.90 x 10⁻³ mol) was dissolved in 1-butanol (100 mL) by heating in a 250-mL 1-necked flask equipped with a condenser and magnetic stirring. KOH (1.00 g,

0.0178 mol) in H₂O (5 mL) was added and the mixture was refluxed for 30 minutes. THP-protected di(ethylene glycol) monochloride (4.00 g, 0.0192 mol) in 1-butanol (20 mL) was added. The solution was refluxed for 36 hours. A white precipitate was observed after 5 hours.

Methylene chloride (100 mL) was added. The precipitate was filtered and discarded. The filtrate was rotary evaporated down to a solid (8.30 g). The solid was dissolved in a mixture of methylene chloride and methanol (2:1/v:v, 150 mL) in a 250-mL 1-necked flask. HCl (36%, 2.00 mL) was added and the solution was magnetically stirred for 2.5 hours at room temperature.

Solvents were rotary evaporated and a white solid was obtained (6.88 g). The solid was dissolved in methylene chloride (200 mL). The solution was washed with water three times (3 x 200 mL) and dried with Na₂SO₄. A white solid (5.92 g) was obtained after the removal of solvent. This solid was subjected to recrystallization in acetone two times and gave white fine crystals that weighed (5.58 g).

Yield: 95%; m.p. 218.3 - 218.6°C; FTIR (ν/max,cm⁻¹): 3425, 2910, 2860, 1603, 1505, 1470, 1445, 1400, 1375, 1273, 1240, 1205, 1195, 1133, 1109, 1070, 1021, 939, 915, 847, 821, 703, 700, 632, 580, 570, 540, 422; ¹H-NMR (Figure III-6, chloroform-d/TMS, ppm): 1.30 (s, 27 H, t-butyl), 3.69 (m, 2 H, CH₂CH₂OCH₂CH₂OH), 3.76 (m, 2 H, CH₂CH₂OCH₂CH₂OH), 3.87 (m, 2 H, CH₂CH₂OCH₂CH₂OH), 4.11 (m, 2 H, CH₂CH₂OCH₂CH₂OH), 6.79 (d, 2 H, aromatic most close to OH), 7.08 (m, 6 H, aromatic), 7.23 (m, 6 H, aromatic); elemental analysis (%):

calculated for C₄₁H₅₂O₃, C: 83.06, H: 8.84, O: 8.10; found: C: 82.14, H: 8.76.

III-3-3-4: α -[*p*-(Di-*p'*-*t*-butylphenylphenylmethyl)phenoxy- α' -bromo-*p*-xylene (III-3j)

The phenol type blocking group **III-3h** (6.00 g, 0.0119 mol) was dissolved in dry THF (dried with Na/benzophenone) (50 mL) in a 250-mL 1-necked flask equipped with nitrogen system and magnetic stirring. NaH (60%) (0.83 g, 0.0208 mol) was added and the mixture was stirred for 20 minutes. α,α' -Dibromo-*p*-xylene (10.6 g, 0.0402 mol) in dry THF (25 mL) was added. The solution was stirred for 20 hours at room temperature.

A few drops of water were added to destroy the unreacted NaH. Bubbles were observed upon the addition of water. The product was extracted three times with methylene chloride (3 x 75 mL). The combined organic phase was washed three times with water (3 x 100 mL) and dried with Na₂SO₄. The solution was passed through a silica gel filtration column. A white solid (9.50 g) was obtained after the removal of solvent.

The solid was dissolved in methylene chloride (70 mL) and acetone (100 mL) was added during heating. The product precipitated out upon the removal of methylene chloride by heating. The precipitate was filtered and the above procedure was repeated. A white powder (4.20 g) was obtained after vacuum drying.

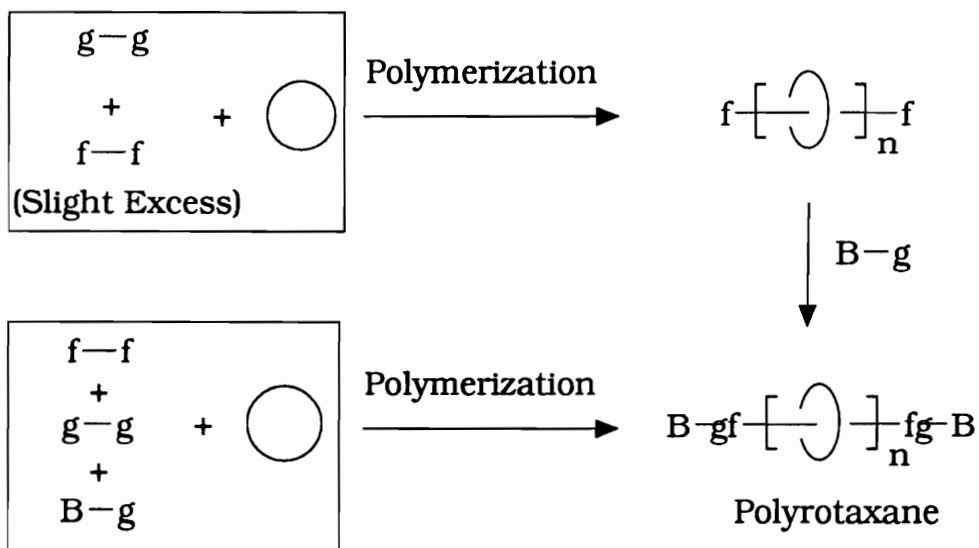
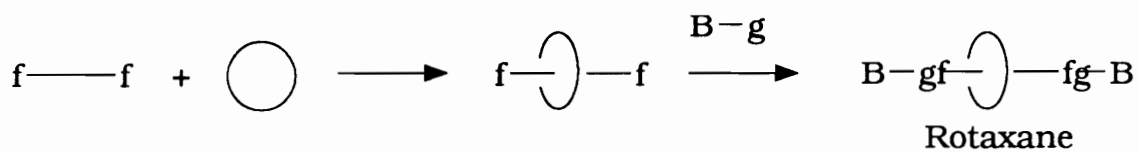
Yield: 51%; m.p. 230.1 - 230.8°C; ¹H-NMR (Figure III-7, chloroform-d/TMS, ppm): 1.29 (s, 18 H, t-butyl), 4.52 (s, 2 H, CH₂Br), 5.02 (s, 2 H, PhOCH₂-Ph), 6.86 (d, 2 H, aromatic most close to OCH₂-), 7.05 - 7.26 (m, 15 H, aromatic), 7.43 (s, 4 H, aromatic of xylene unit).

REFERENCES

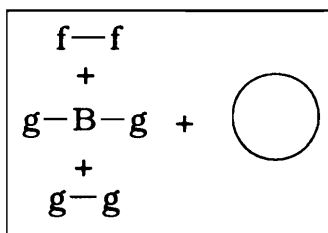
1. Wu, C.; Bheda, M. C.; Lim, C.; Shen, Y. X.; Sze, J.; Gibson, H. W. *Polymer Commun.* **1991**, 32, 204.
2. Harrison, I. T. *J. Chem. Soc., Chem. Commun.* **1972**, 231.
3. Harrison, I. T. *J. Chem. Soc., Perkin Trans. I* **1974**, 301.
4. Marvel, C. S.; Kaplan, J. F.; Himel, C. M. *J. Am. Chem. Soc.* **1941**, 63, 1892.
5. Rapoport, H.; Campion, J. E. *J. Am. Chem. Soc.* **1951**, 73, 2239.
6. Shinkai, S.; Inuzuka, K.; Miyazaki, O.; Manabe, O. *J. Am. Chem. Soc.* **1985**, 107, 3950.
7. March, J. "*Advanced Organic Chemistry*", 3rd. Ed., John Wiley & Sons, N. Y., **1985**, p286 -287.
8. Schroder, C.; Wolf, S.; Agosta, W. C. *J. Am. Chem. Soc.* **1987**, 109, 5491.
9. Mikroyannidis, J. A. *Eur. Poly. J.* **1985**, 21, 895.
10. Engen, P. "*Ph. D. Dissertation*", Virginia Polytechnic Institute and State University, Blacksburg, Virginia, **1991**.

11. Lim, C. "*M. S. Thesis*", Virginia Polytechnic Institute and State University, Blacksburg, Virginia, **1991**.
12. Sze, J. "*M. S. Thesis*", Virginia Polytechnic Institute and State University, Blacksburg, Virginia, **1992**.

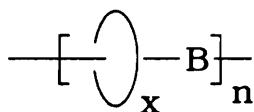
Scheme III-1: Use of Monofunctional Blocking Groups



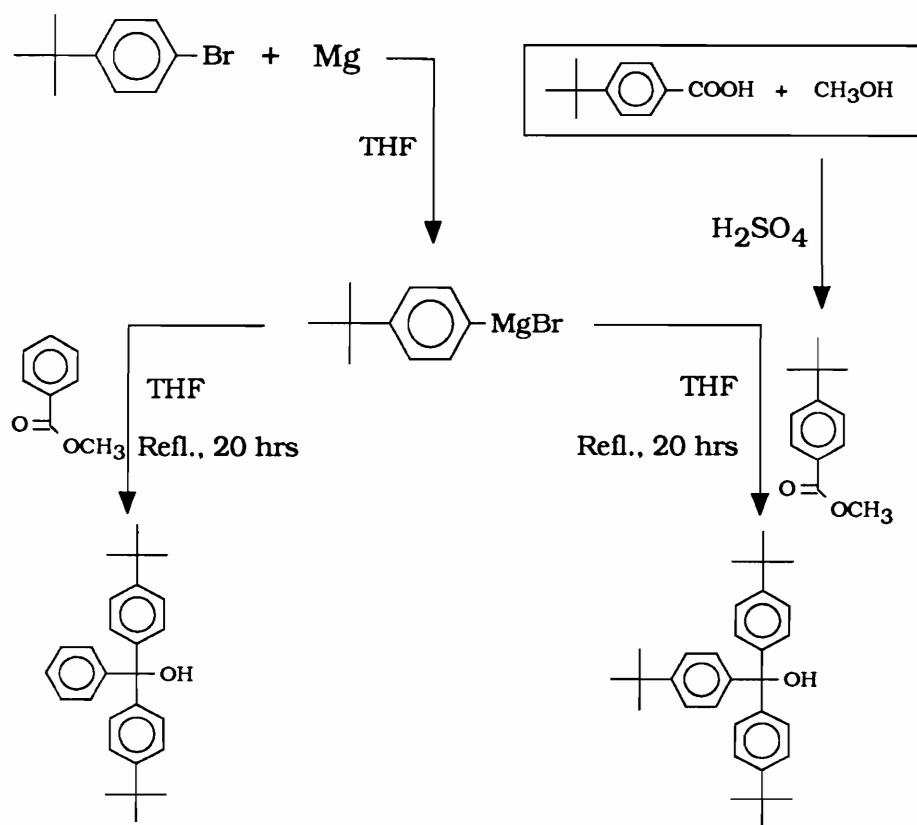
Scheme III-2: Use of Difunctional Blocking Groups



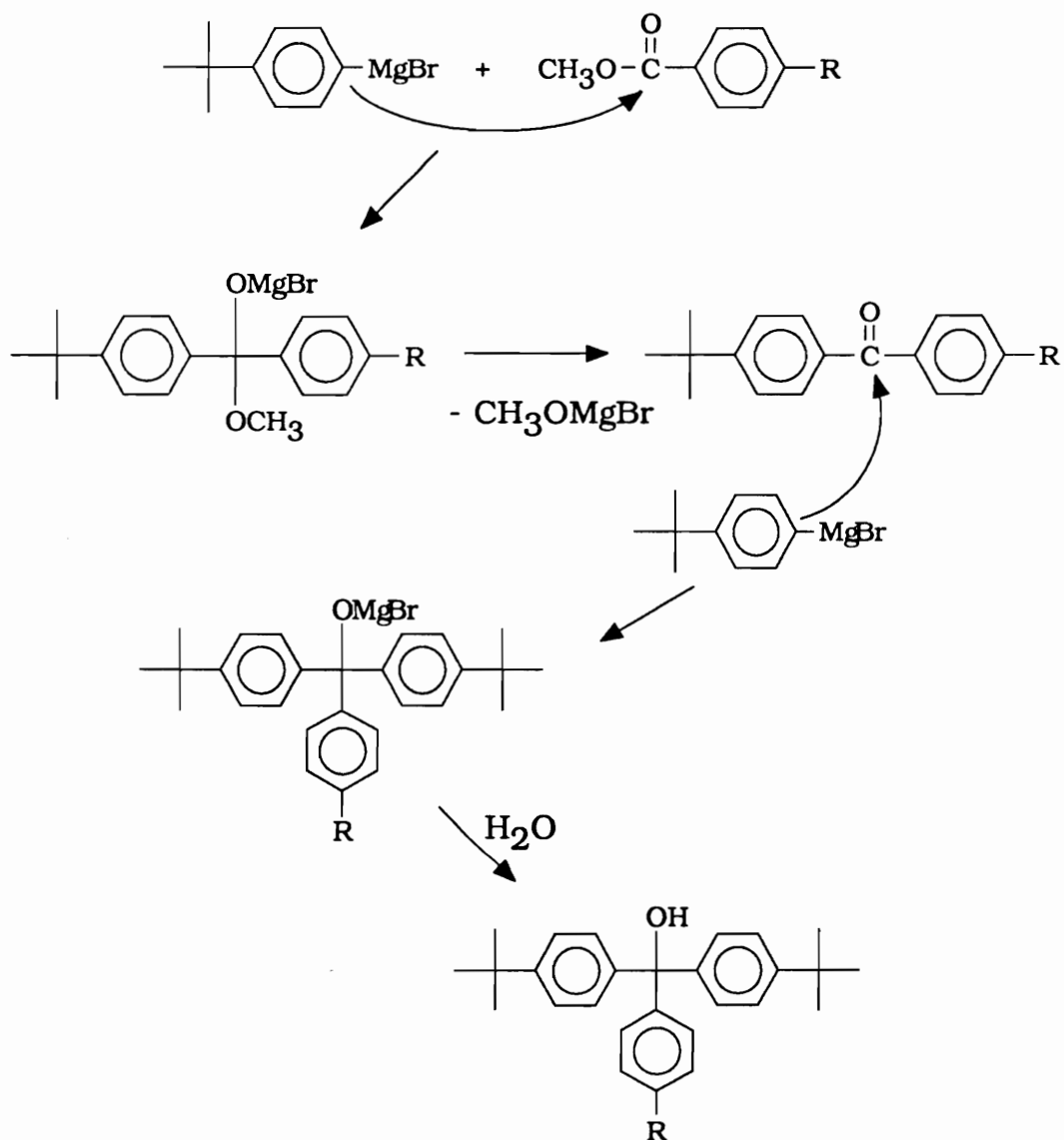
Polymerization



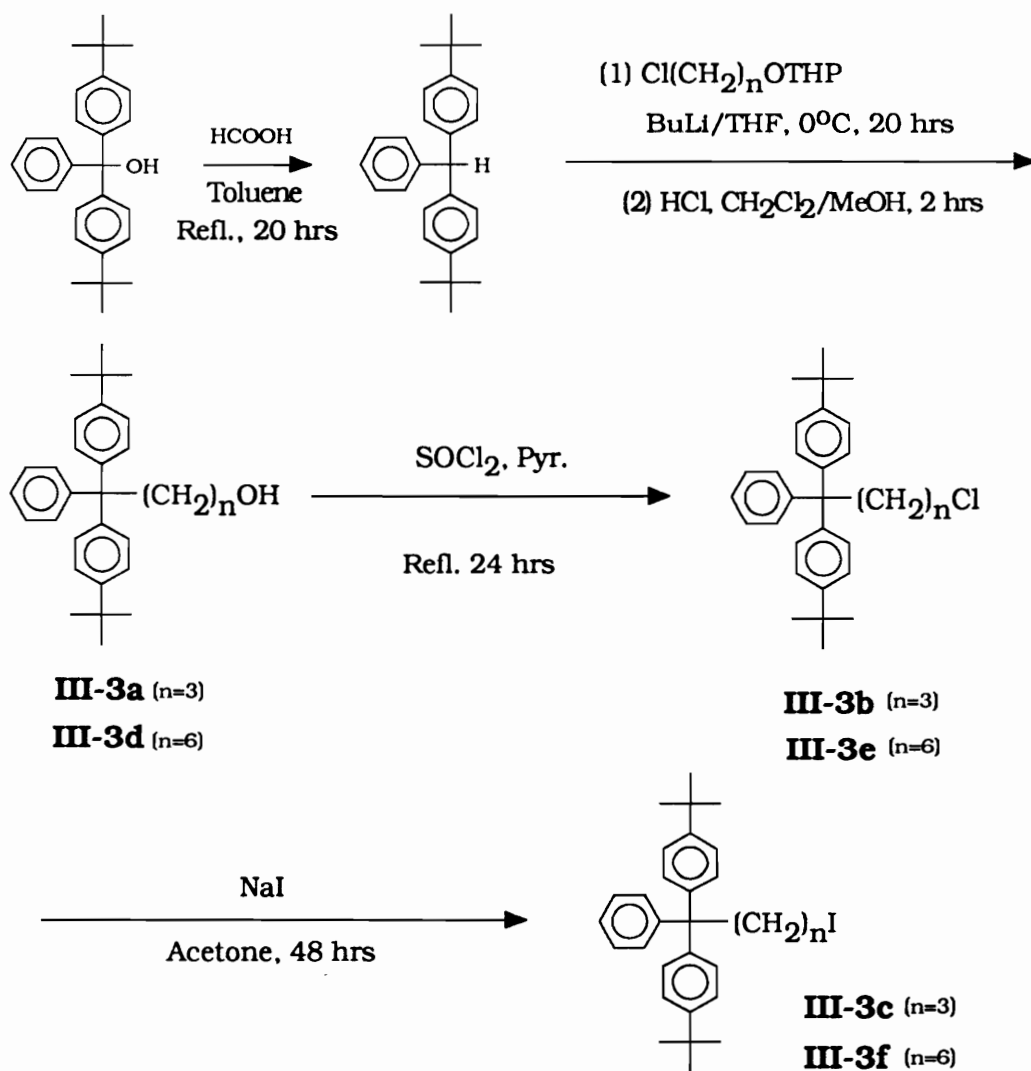
Scheme III-3: Syntheses of Blocking Groups (Triarylmethanols)



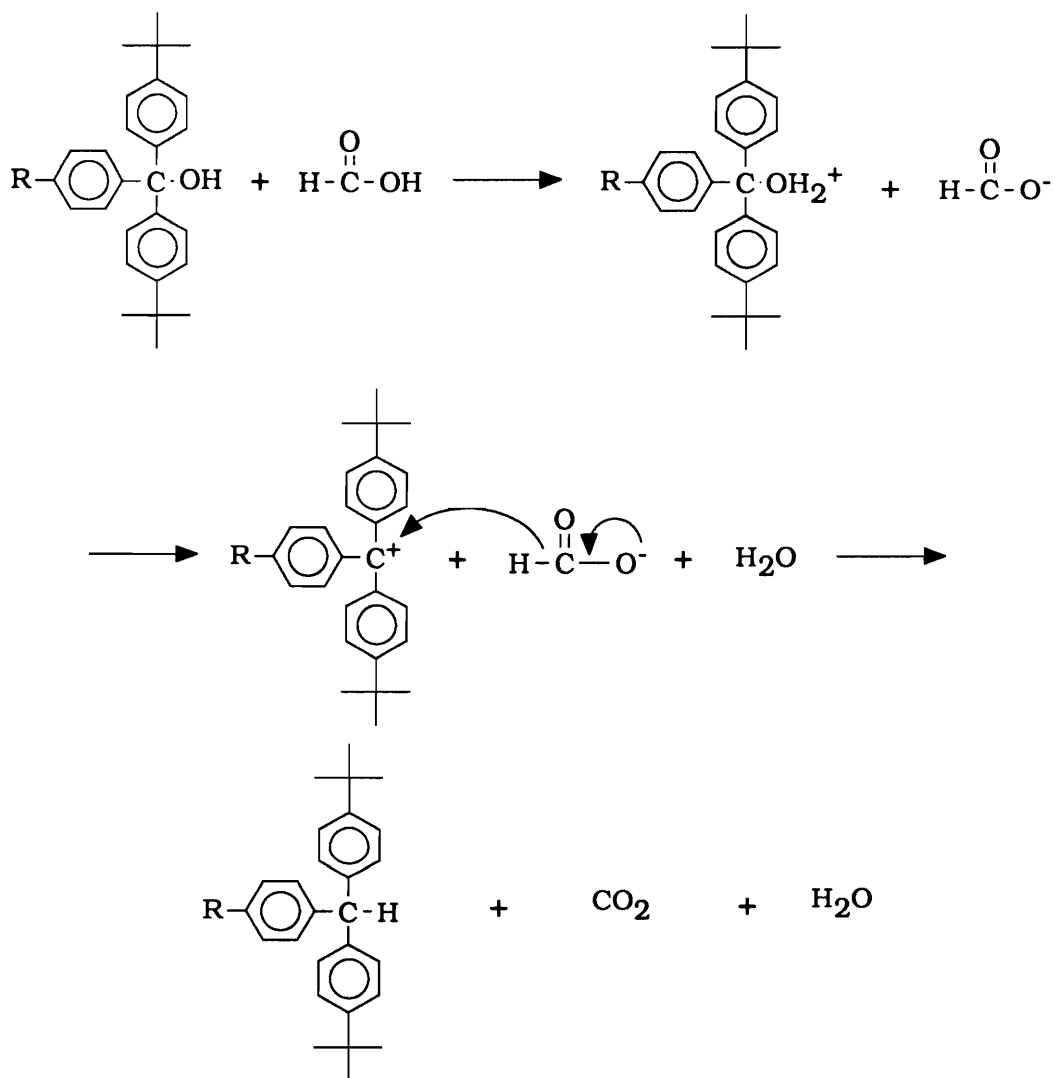
Scheme III-4: Mechanism of Grignard Reactions



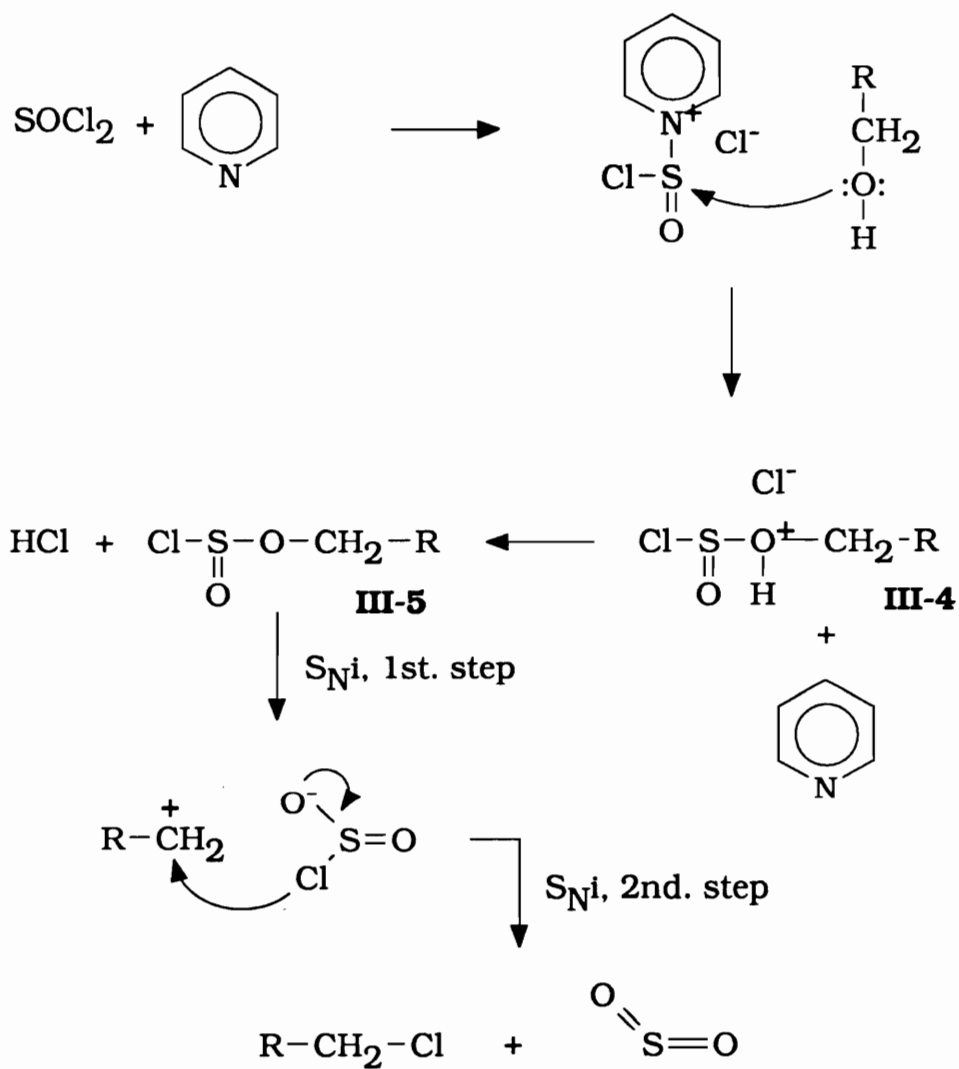
Scheme III-5: Modification of Blocking Groups (Method 1)



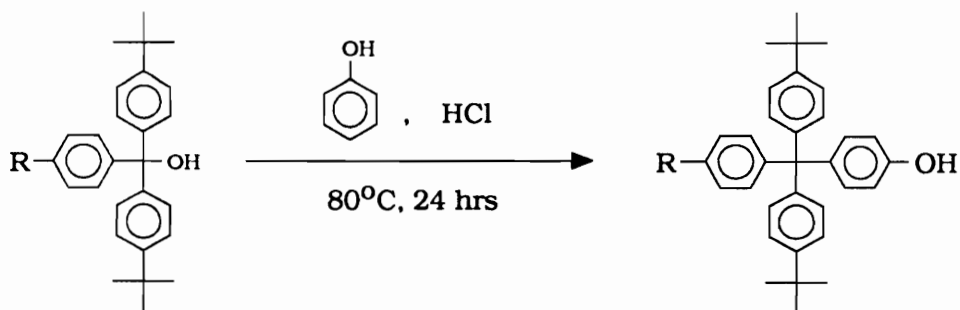
Scheme III-6: Mechanism of the Alcohol Reduction by Formic Acid



**Scheme III-7: Mechanism of the Reactions of Alcohols
and Thionyl Chloride**

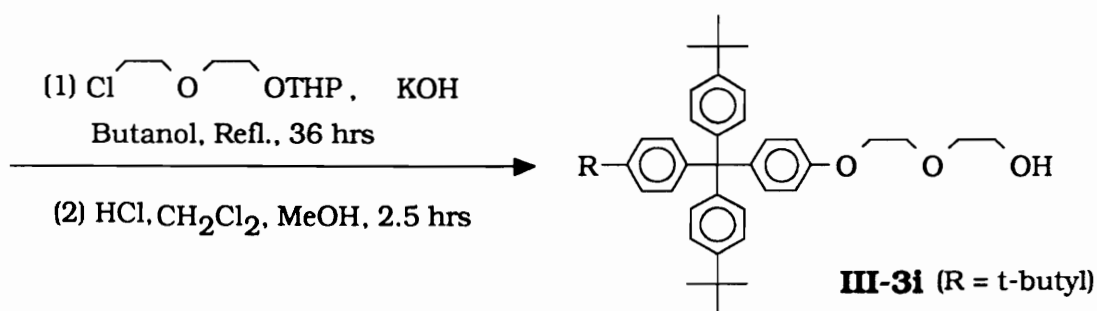


Scheme III-8: Modification of Blocking Groups (Method 2)

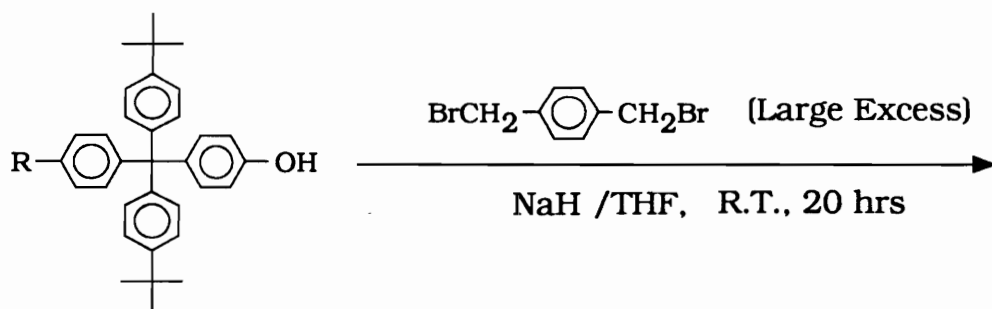


III-3g (R = H)

III-3h (R = t-butyl)



III-3i (R = t-butyl)



III-3j (R = t-butyl)

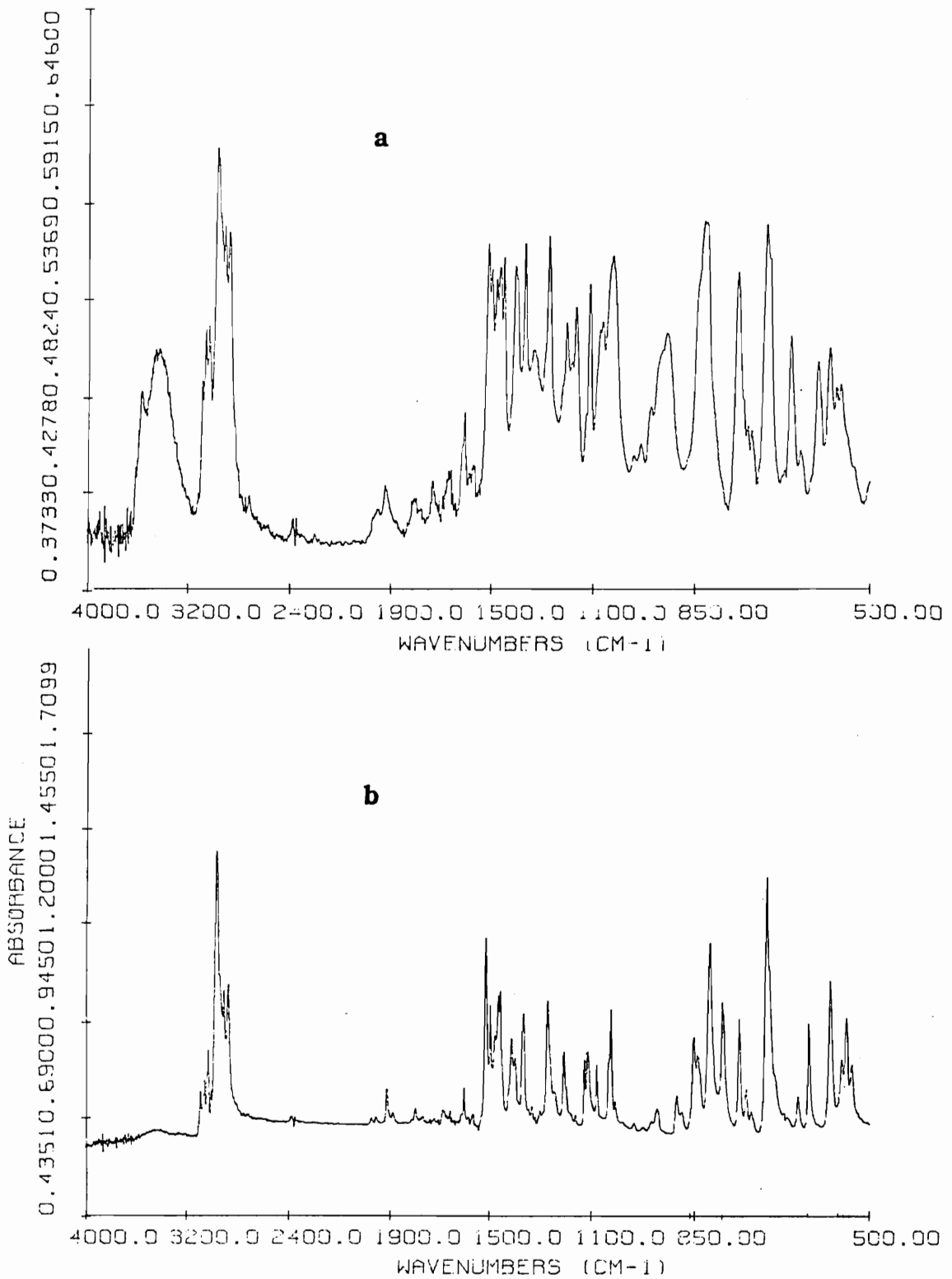


Figure III-1: FTIR Spectra of (a) Di-(*p-t*-butylphenyl)phenylmethanol and (b) Di-(*p-t*-butylphenyl)phenylmethane.

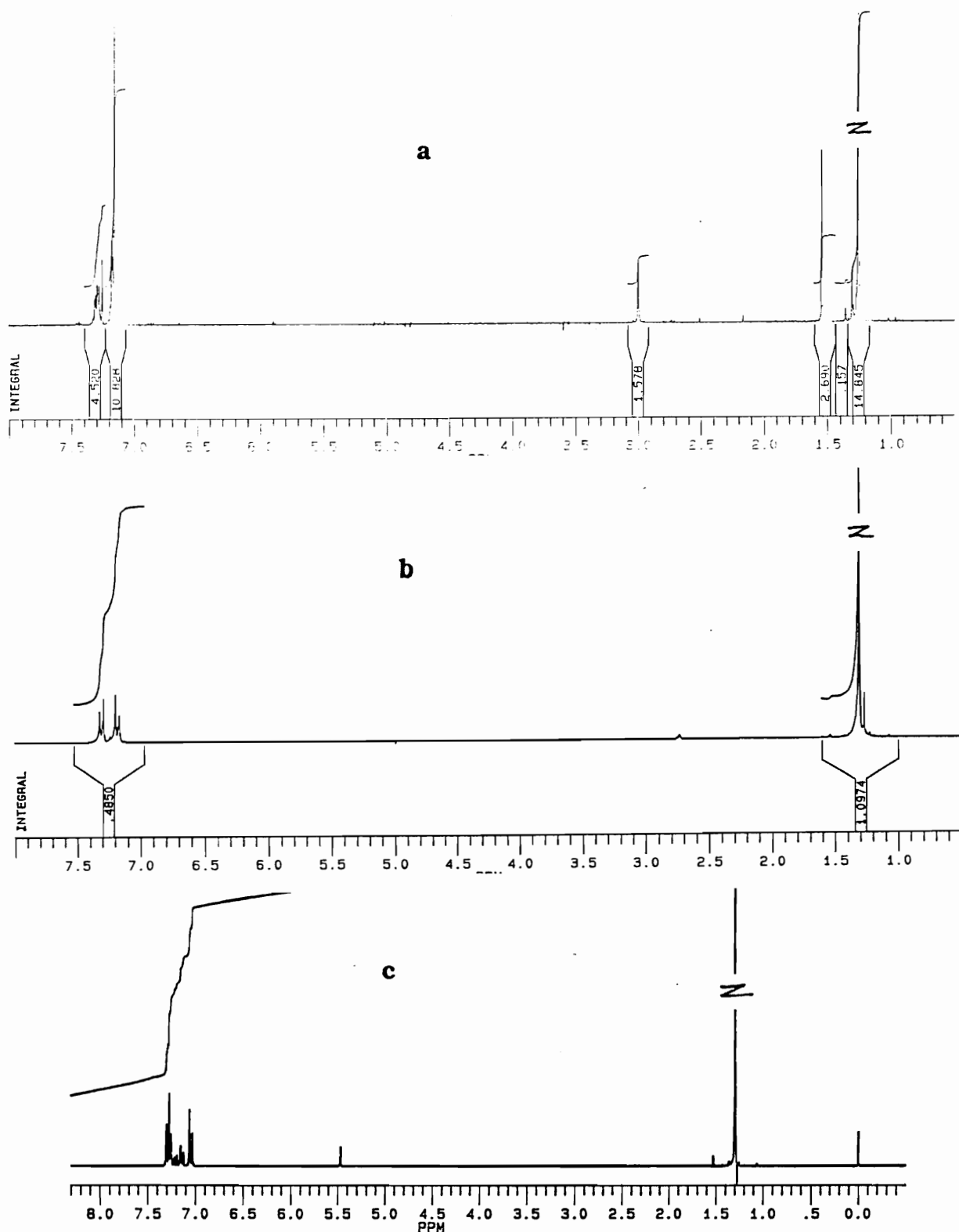


Figure III-2: ¹H-NMR Spectra of (a) Di-(*p-t*-butylphenyl)-phenylmethanol, (b) Tris-*p-t*-butylphenylmethanol and (c) Di-(*p-t*-butylphenyl)phenylmethane.

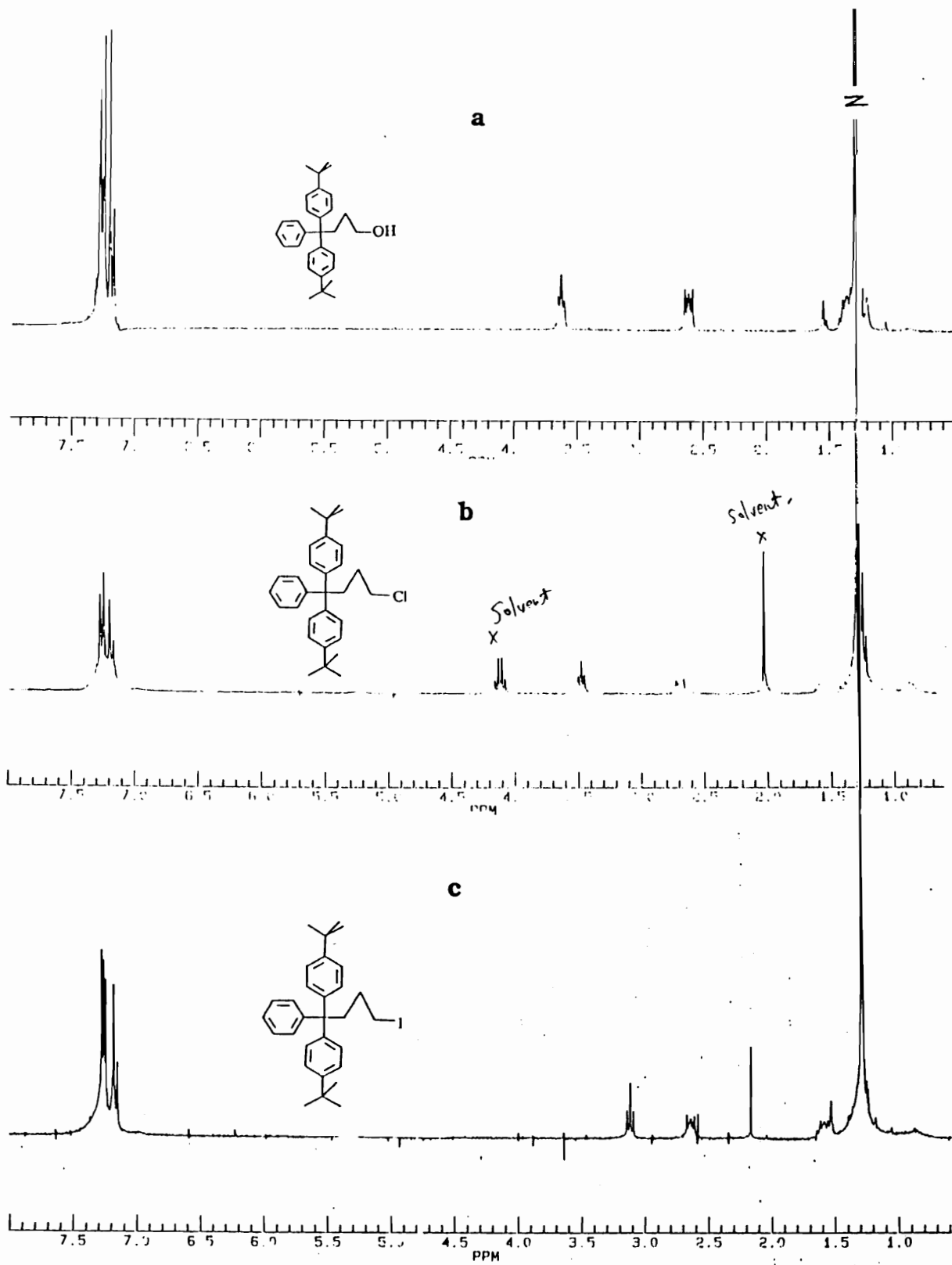


Figure III-3: $^1\text{H-NMR}$ Spectra of (a) III-3a, (b) III-3b and (c) III-3c.

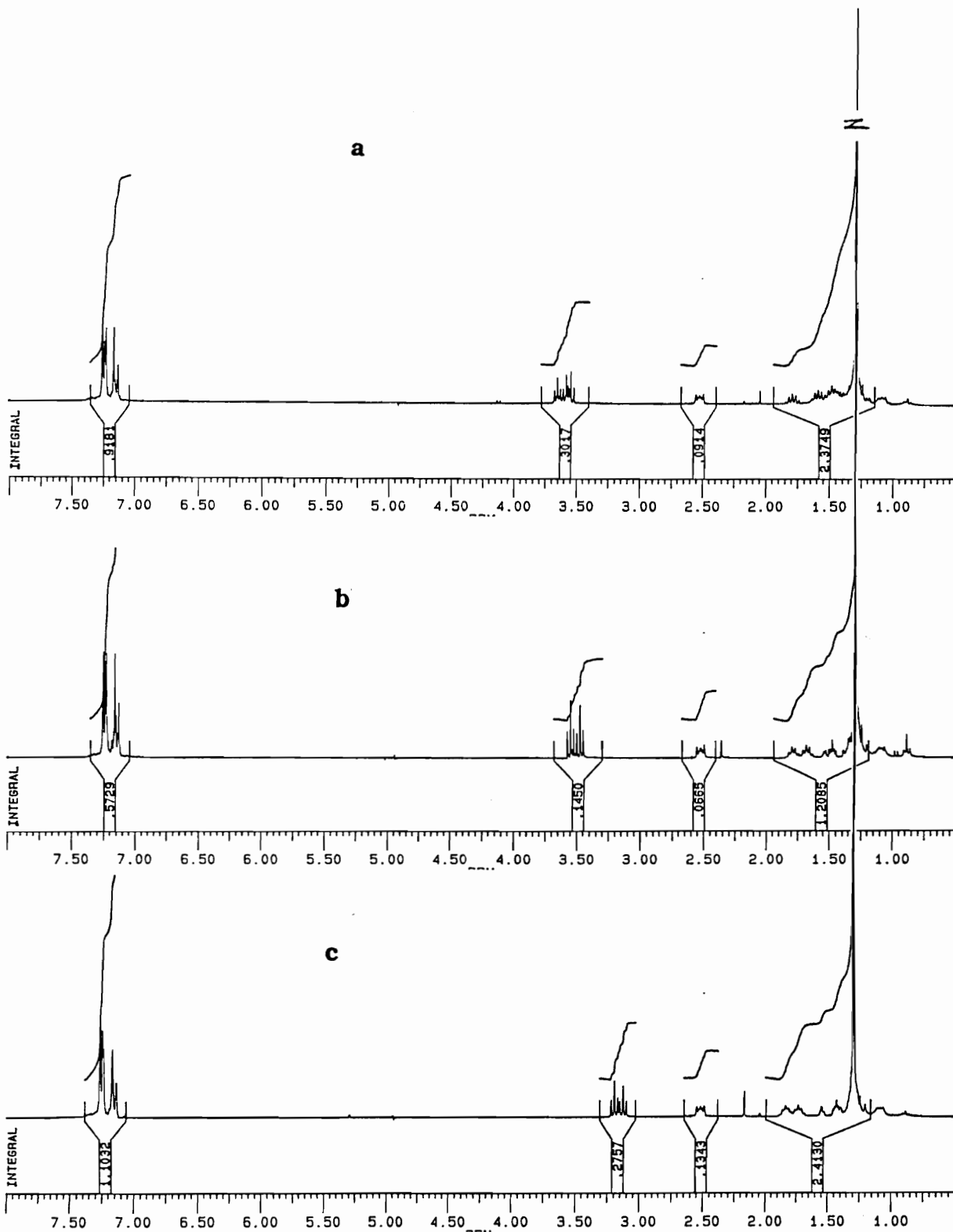
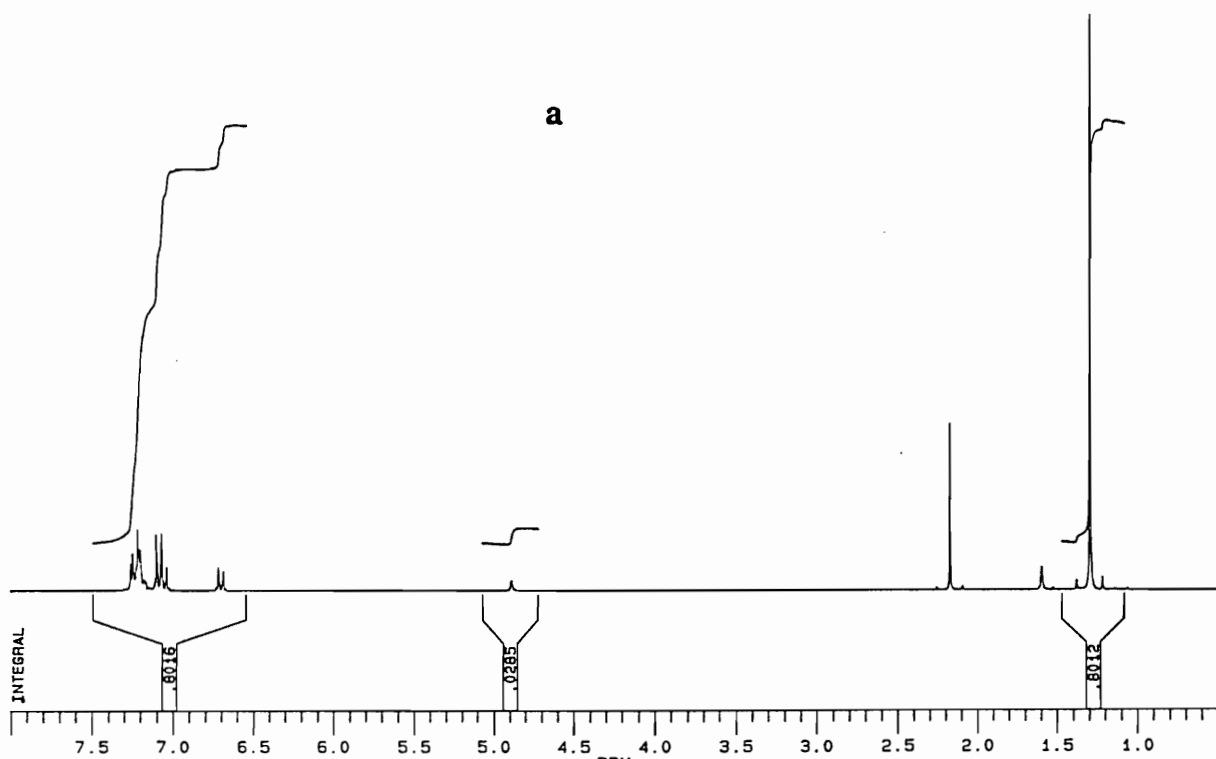


Figure III-4: $^1\text{H-NMR}$ Spectra of (a) III-3d, (b) III-3e and (c) III-3f.

a



b

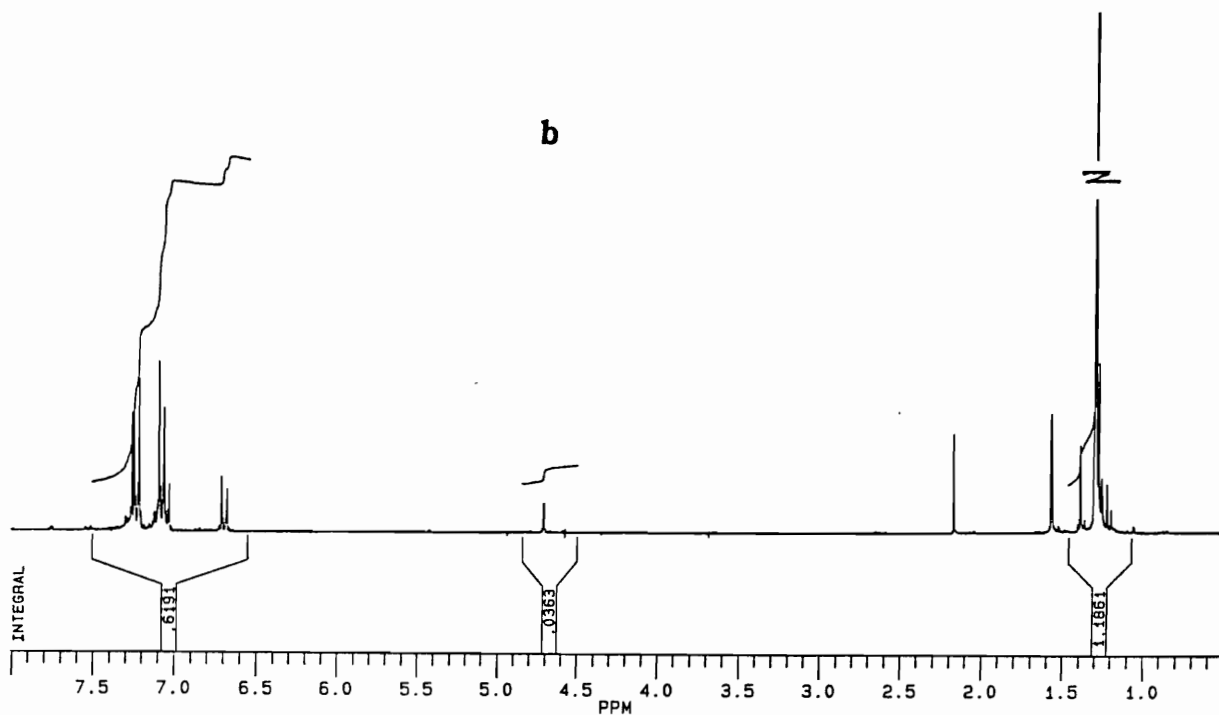


Figure III-5: ^1H -NMR Spectra of (a) III-3g and (b) III-3h.

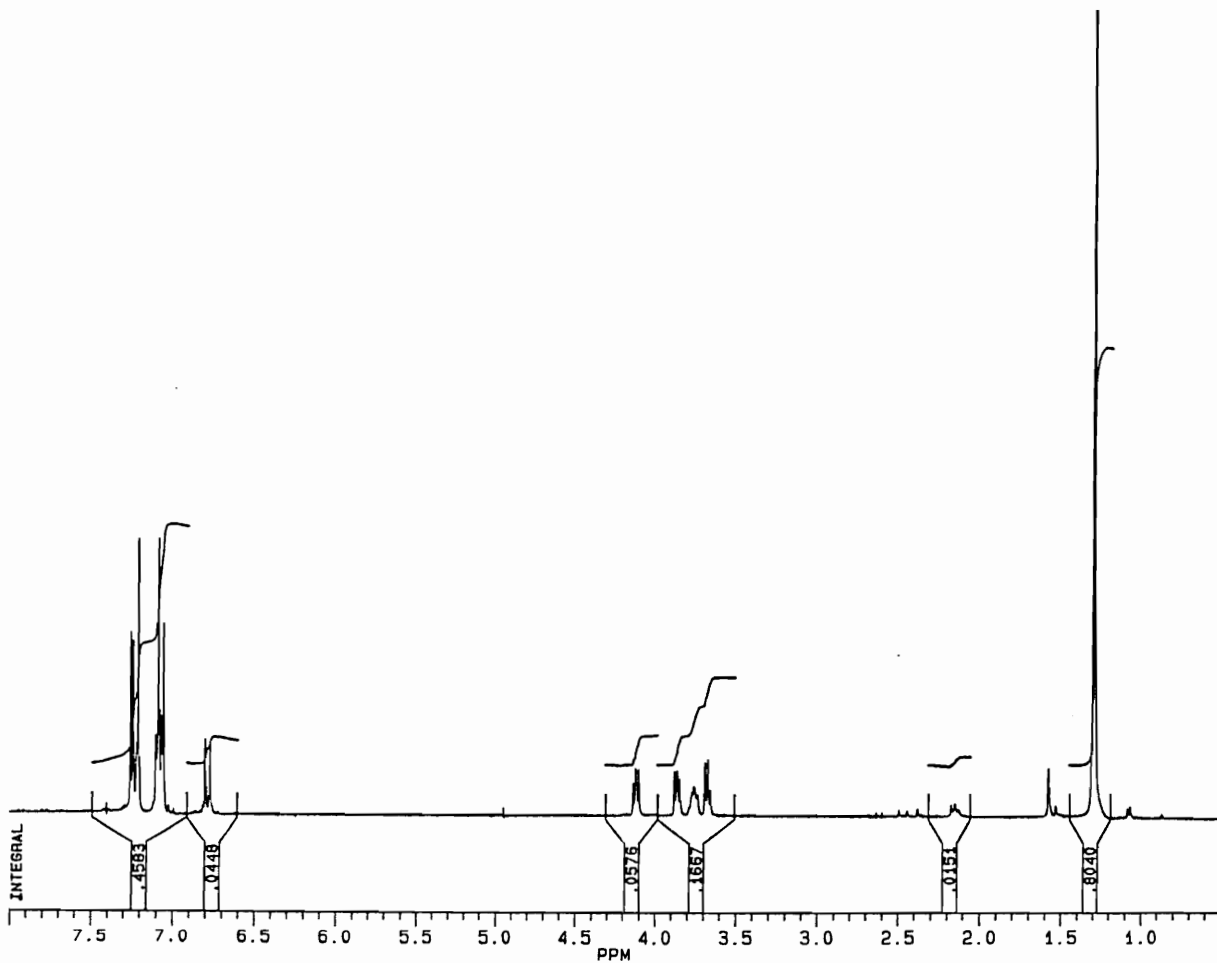


Figure III-6: $^1\text{H-NMR}$ Spectrum of III-3i.

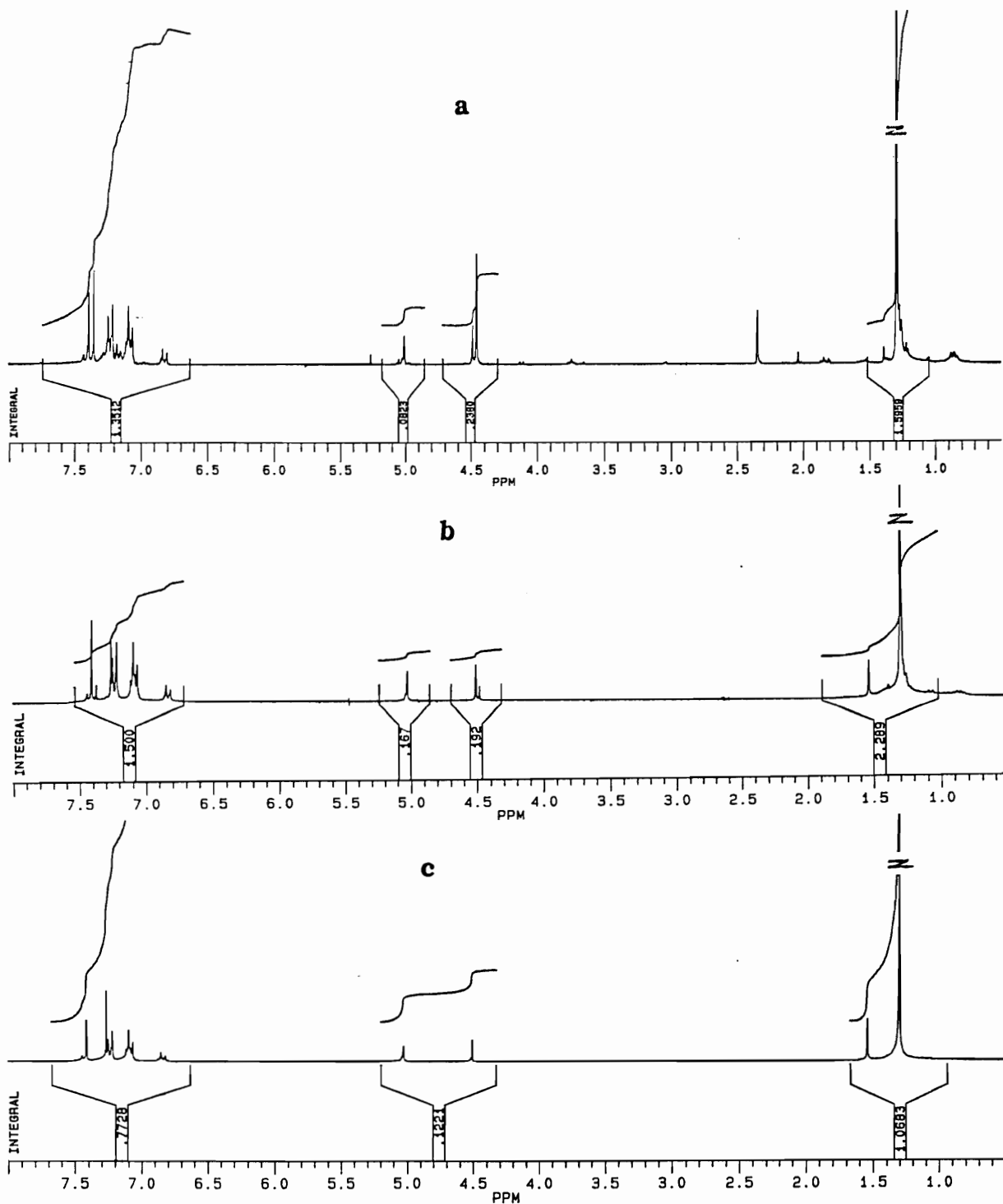


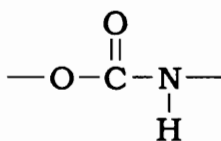
Figure III-7: $^1\text{H-NMR}$ Spectrum of III-3j: (a) Crude compound from the reaction, (b) after Washed Once with Acetone and (c) after Washed Twice with Acetone.

CHAPTER IV:
POLY(URETHANE-CROWN ETHER)
ROTAXANES VIA THE STATISTICAL
THREADING APPROACH

As a general approach in polyrotaxane synthesis, statistical threading can be applied to any polymer and macrocycle system in principle, as long as the critical requirements for the formation of a polyrotaxane such as ring size and chain length are met. In my study, I chose polyurethane as the polymer backbone and crown ethers as the cyclic components. This choice was made based on several important features: polyurethanes are well known as industrial and commercially important materials; in comparison with chain-growth polymerization, the step-growth process favors threading since the slow process allows threading to take place during the polymerization; it is also expected that the hydrogen bonding between urethane linkage and crown ethers could enhance the threading efficiency.

IV-1: POLYURETHANES

First discovered by Bayer *et al.* in 1930s,¹ polyurethanes are a class of polymers that incorporate the carbamate linkage (IV-1) as a character functional group. Of course, other functional groups such as ether, ester, urea, amide, etc. may also incorporate. Born during World War II, polyurethane science and technology were greatly retarded in their early years. Polyurethane products were not commercially produced until 1950s when the raw materials such as toluene diisocyanate (TDI) and polyester polyols became commercially available, even though the subject was described clearly on the scientific basis and applications by the authors of early patents on polyurethanes.²⁻⁴



IV-1

IV-1-1: STARTING MATERIALS

The materials used for laboratory synthesis and industrial manufacture of polyurethanes include two class of materials:

polyfunctional isocyanates and hydroxy compounds with active hydrogen atoms.

Polyfunctional isocyanates used for polyurethane synthesis are generally diisocyanates and some triisocyanates. They are either aromatic or aliphatic. Table IV-1 lists some examples of common used polyfunctional isocyanates. Isocyanates are highly toxic and sensitive to moisture. They are stored and handed under nitrogen.

The compounds with active hydrogen atoms used for polyurethane synthesis are polyols, generally diols or triols. They may be polyester, polyether or hydrocarbon polyols. In polyurethane structures, segments introduced from polyols serve as flexible spacers. The higher the molecular weights of polyols used, the lower the concentrations of urethane groups and consequently the more flexible the polyurethane chains. For examples, polyurethanes derived from lower molecular weight or less flexible diols such as ethylene glycol, di(ethylene glycol), 1,4-butanediol, 1,6-hexanediol and 1,10-decanediol are hard and stiff. But those polyurethanes derived from higher molecular weight flexible diols such as poly(ethylene oxide)s with molecular weights higher than tetra(ethylene glycol), poly(tetramethylene oxide)s with molecular weights 650, 1000 and 2000 are soft and show much lower glass transition temperatures. Some examples of polyols common used for the laboratory syntheses and industrial manufacture of polyurethanes are listed in Table IV-2 and Table IV-3, respectively. For the laboratory syntheses of thermoplastic polyurethanes, usually a single or mixture of diols are

used. However, industrially used polyol raw materials are mixtures of polyols with different structures and functionalities. The recipes are made for different applications. In the use of polyester type of polyols, for example, a mixture of adipic acid, di(ethylene glycol) and a small amount of trimethylolpropane with average molecular weight 2,400 is used for flexible foams; a mixture of adipic acid, phthalic acid, oleic acid and trimethylolpropane with average molecular weight 930 is used for rigid foams; while elastomers use a mixture of adipic acid and ethylene glycol.

The flash points and ignition temperatures are also important data for industrial polyols. They are required to be reasonable high. The flash points of polyether type of polyols are over 100°C and those of polyester type of polyols are over 200°C. Both type of polyols have very high ignition temperatures; they are over 300°C for polyether type and 400°C for polyester type.

Aromatic polyols such as hydroquinone and bisphenol-A are generally not preferred for polyurethane syntheses due to their lack of reactivity toward polyfunctional isocyanates and also form unstable urethane linkages.

Polyfunctional amines are, in some cases, used as comonomers to produce urea group containing polyurethanes called polyureaurethanes. Especially diamines are often used as chain extenders in the segmented elastomer syntheses since stronger molecular interactions in the hard segments are introduced by the presence of the urea group which is

more polar than the urethane linkage. Unlike phenols, because of high reactivity between amine and cyanate groups, aromatic polyfunctional amines are also used in the syntheses.

IV-1-2: CHEMICAL REACTIONS OF POLYFUNCTIONAL ISOCYANATES

The key reactions leading to the formation of urethane groups are the reactions of isocyanate and hydroxyl groups. The high reactivity of the isocyanate group with nucleophilic reagents results from the pronounced positive character of the carbon induced by the electron resonance effect between the two double bonds consisting of nitrogen, carbon and oxygen. In fact, nitrogen and oxygen at ends of the " π -bridge" serve as electro-withdrawing atoms, resulting in positive charge on the carbon atom. This resonance sequence is illustrated in Scheme IV-1. It can be seen that the carbon atom is positively charged in the resonance states **IV-2b** and **IV-2c**.

IV-1-2-1: Reactions with Polyols to Form Polyurethanes

Scheme IV-2 shows the syntheses of polyurethanes from diisocyanates and diols. This is a step growth polymerization without releasing a small molecule. The mechanism of the formation of urethane group is illustrated in Scheme IV-3. The electron rich oxygen on the diol attacks the positively charged carbon of the isocyanate group giving maybe two products: **IV-4** and **IV-5**. The enol **IV-4** is unstable and undergoes proton rearrangement resulting in **IV-5** as the final product.

This reaction can either be carried out with or without catalysts. The catalysts are amine and acetate types of alkaline species which enhance nucleophilicity of the hydroxyl group on the polyols. The common used catalysts are triethylamine, triethylenediamine, ferric acetylacetonate, tri-n-butyltin acetate, di-n-butyltin diacetate, dibutyltin dilaurate, tin octoate, etc. General solvents for the polymerization are polar solvents such as THF, DMSO, NMP, DMAC, etc. Toluene is also used in some cases. The reaction temperatures are required to be below 110°C since more side reactions occur at higher temperature.

IV-1-2-2: Other Reactions

Besides the reaction with hydroxyl group, isocyanate groups can react with many other functional groups containing active hydrogen. Scheme IV-4 gives some examples of these reactions. Amines are more reactive than alcohols toward isocyanates. The reactions of isocyanates and amines give ureas. Carboxylic acids are less reactive than alcohols toward isocyanates; the reactions produce amides through an unstable intermediate, carbamate anhydride, which releases one carbon dioxide molecule immediately. Isocyanates can also react with water to form ureas as final product. This reaction undergoes several steps. First, isocyanate reacts with water to form a carbamic acid which is an unstable enol type structure and loses one molecular carbon dioxide with an amine and isocyanate as products. Consequently a urea results due to the high reactivity of amine with isocyanate.

IV-1-2-3: Synthesis of High Molecular Weight Linear polyurethanes

In order to synthesize high molecular weight linear polyurethanes, attention must be paid to several important factors.

(1) **Functionality of Starting Materials:** Difunctional isocyanates and diols are required.

(2) **Purity of Starting Materials:** Starting materials have to be very pure, especially no moisture and other active hydrogen containing impurities. High purity of diisocyanates may be achieved by multiple vacuum distillations under nitrogen. Lower molecular weight diols can also be purified with the same method. Higher molecular weight diols may be purified by some other methods such as drying with drying agents in solution, multiple recrystallizations, etc.

(3) **Stoichiometry:** The overall molar ratio of isocyanate group to hydroxyl group should be equal to one.

(4) **Temperature and Side Reactions:** During the polymerization, there are many side reactions that may take place, especially at higher polymerization temperature. The major side reaction is the reaction of isocyanate with the product polymer in which the hydrogen on nitrogen acts as a active hydrogen. These side reactions result in the formation of branching and crosslinking. To avoid side reactions, the polymerization temperature is required to be low (usually below than 110°C).

(5) Others: There are some other factors such as extent of reaction, solvent and catalyst which also effect the molecular weight of linear polyurethanes.

IV-1-3: POLYURETHANE PRODUCTS AND THEIR APPLICATIONS

As a class of important commercial materials, polyurethanes are produced worldwide in different application forms.

Polyurethane foams (soft, semirigid and rigid) are produced based on two types of reactions: isocyanate group reacts with hydroxyl group to form urethane linkages and isocyanate group reacts with added water to form urea linkages. Generally two types of starting materials are mixed: (1) isocyanate and (2) a mixture of glycol, chain extender (a low molecular weight diol), catalyst, water, blowing agent and surfactant. For the flexible foam, the carbon dioxide generated from the reaction of isocyanate and water expand the reaction mixture to a foam. For the rigid foam, an additional blowing agent which usually is monofluorotrichloromethane is used and also, polymeric MDI is used as the isocyanate component to improve the foam properties. Polyurethane foams are used as materials in the following areas: furniture and household goods, refrigeration technology and appliances, textile, technical articles, energy management, construction industry, technical insulation, automotive, ship and aircraft industry, transportation, packaging, etc.

Polyurethane thermoplastic elastomers are produced via two reactions: (1) an excess amount of isocyanate is reacted with a polymeric diol (usually a polyether or polyester) to form an isocyanate terminated prepolymer and (2) a chain extender is used to interconnect the prepolymer molecules, resulting in a high molecular weight segmented polymer with soft segments introduced from the diol and hard segments from MDI and the chain extender. Polyurethane elastomers are used in the automotive industry, engineering applications, construction industry, shoe industry, film and tubes, etc.

Polyurethanes are also used widely as paints, coatings, adhesives and so on. Figure IV-1 shows the percentage of polyurethane applications in different areas.

IV-2: RESULTS AND DISCUSSION

IV-2-1: SYNTHESSES OF POLYROTAXANES

In this section, I report the synthetic part of a series of polyrotaxanes containing linear polyurethane backbone derived from MDI and tetra(ethylene glycol) threaded crown ethers with different ring sizes. Total urethane polymers will be reported; they are the polyurethane backbone threaded with: 16% 36C12 (**IV-6**), 29% 42C14 (**IV-7**), 45% 48C16 (**IV-8**), 63% 60C20 (**IV-9**) (all percentages are weight

based). Another polyrotaxane containing polyurethane-urea backbone and 53 wt% 60C20 (IV-10) will also be reported.

IV-2-1-1: Threading Equilibrium

Let us consider a simple case. The dynamic threading of a linear molecule "L" and a macrocycle "M" to form a rotaxane "R" with equilibrium constant K is depicted in Scheme IV-5. As discussed in section I-4-4 (Chapter I), two extreme cases are possible: (1) statistical threading in which ΔH is zero or positive (repulsive) and entropy changes drive the process and (2) directed or template threading, an enthalpically driven process resulting from attractive forces (negative ΔH) between the linear species and the cyclic species. The Equations IV-1 to IV-2 describe the basis of the equilibrium thermodynamically.

$$K = [R]/[L][M] \quad \text{Eq. IV-1}$$

$$- RT \ln K = \Delta H - T \Delta S \quad \text{Eq. IV-2}$$

For the statistical threading process, assume ΔH is zero. Equation IV-3 can be obtained by combining Equation IV-1 and IV-2.

$$\ln[R] = \ln[L][M] + \Delta S/R \quad \text{Eq. IV-3}$$

Equation IV-3 clearly shows that the concentration of the rotaxane formed increases with increasing concentration of linear and cyclic species in the fashion of natural logarithm and also with increasing ΔS . If the concentrations of the linear and the cyclic species in monomer feed are fixed, the concentration of the rotaxane increases with increase

in ΔS only. ΔS is related to the characteristics of the linear and the cyclic species such as ring size, ring conformation, chain length, chain diameter, chain flexibility, etc.

IV-2-1-2: Polymerizations

The synthetic route leading to the polyurethane-based polyrotaxanes is illustrated in Scheme IV-6. According to the equilibrium assumption discussed in the previous section, the concentration of a rotaxane increases with an increase in concentration of linear and cyclic monomer feed. Therefore, my statistical threadings were performed in the pure melted crown ethers without the addition of another co-solvent. In other words, a crown ether was used as the solvent in which the polymerization was preformed.

The mixture of tetra(ethylene) glycol and a melted crown ether was stirred for one hour before the polymerization for allowance of prethreading to reach the equilibrium. The reaction temperature was controlled at 90°C; about 30 to 50°C above the the melting temperatures of the crown ethers. This temperature provided reasonable solvent viscosities; of course, they are still higher than those of common solvents. It was believed that the polymerization proceed more slowly in the presence of macrocycle since the chain orientations are retarded by the higher solvent viscosity and because they are carrying a burden, threaded macrocycle molecules. Hence the polymerization was allowed to proceed for 24 hours which is relatively long for this type of reaction.

The synthetic approach to the polyurethane-urea-based polyrotaxane (**IV-10**) is shown in Scheme IV-7. The 60C20 had been exposed to air for several days before it was used. It is known that crown ethers absorb moisture from air. Therefore, the 60C20 used for this synthesis contained a trace amount of water which joined the polymerization reaction, resulting in the formation of some urea linkages in the polymer backbone (see section IV-1-2-2). The $^1\text{H-NMR}$ chemical shift of the proton on the urethane nitrogen is more downfield than that on urea nitrogen; this provided an experimental method to determine the percentage content of urea groups incorporated into the polymer backbone.

IV-2-1-3: Purification

The polyrotaxanes were purified by multiple reprecipitations into a relatively large amount of solvent in which the crown ether is very soluble but the polyrotaxane is not. As a matter of fact, polyrotaxanes have different solubilities when the macrocycles and their contents are different. Different nonsolvents, therefore, were used to precipitate different polyrotaxanes: **IV-6** was reprecipitated into methanol and water; **IV-7** was reprecipitated into methanol; **IV-8** and **IV-10** were reprecipitated into ethyl acetate; **IV-9** was first reprecipitated into a mixture of ethyl acetate followed by reprecipitations into pure ethyl acetate. The reprecipitation for each polymer was continued until a constant composition (x/n value, number of macrocycles per repeat unit) of the polymer was reached. Table IV-4 shows the polymer compositions

(x/n values) obtained from $^1\text{H-NMR}$ analyses (to be discussed later in this chapter) after each reprecipitation for each polyrotaxane. However there were some materials lost during the reprecipitations. This is because fractionation took place as a result of solubility increases with polyrotaxanes containing a large amount of macrocycle. For example, when **IV-10** was reprecipitated from ethyl acetate, the polyrotaxane fractions containing higher amount of 60C20 were soluble in ethyl acetate and only lower fractions were obtained. For all cases of polyrotaxane reprecipitations, especially for **IV-8**, **IV-9** and **IV-10**, residual polyrotaxanes remaining in the mother solutions were detected by $^1\text{H-NMR}$ analyses.

It can be seen from Table IV-4 that a constant ratio of crown ether to repeat unit for all of the polyrotaxanes was reached after the first or second reprecipitations. Therefore, I expect no free (unthreaded) crown ethers remaining in the systems. Even though there were no blocking groups at ends of the polyrotaxane chains, dethreading of macrocycles was not significant. Before each reprecipitation, samples were dissolved in THF for about 30 minutes to 1 hour; however, I found no composition changes by dethreading. This could result from the random coiling of the chains and attractive intra-annular hydrogen bonding between crown ethers and polyurethane chains.

IV-2-1-4: Threading Efficiencies

The threading efficiency is defined as the number of rings per repeat unit in the polyrotaxane backbone. Assuming the polymerization

conversion is 100%, thus, the threading efficiency is defined as the rotaxane repeat unit yield assuming a maximum of one ring per repeat unit, based on the limiting reagent, the glycol (in our case). Calculated threading efficiencies are listed in Table IV-5. It is interesting to see that when the crown/glycol ratio was kept at 1.5 in the feed there is a tremendous increase in threading efficiency with increases in ring size represented by the number of skeletal atoms of the rings.

The threading process could be very complicated. There are many possible kinetic steps leading to the formation of polyrotaxane macromolecules. Scheme IV-8 illustrates some of the steps. In summary, any linear species in the system, monomer, dimer, trimer, etc., with and without already threaded rings, may thread with a cyclic species and equilibria exist between the linear and cyclic species. These equilibria have different equilibrium constants K since K is related to the length of linear species. It can be understood that the threading decreases with increasing chain length of the linear species and there is a critical chain length at which the threading approaches zero, e.g. $K = 0$. In other words, threading preferentially takes place with lower molecular weight species (monomers and oligomers). On the other hand, condensation reaction occurs simultaneously with threadings. All monomers and oligomers in the system, with and without threaded rings react to form a high molecular weight polymer, polyrotaxane.

Even though the threading process is so complicated, the problem can be simplified by making some assumptions: (1) the threading process

is slower than the polymerization reaction; (2) rings are fully open rigid cycles and (3) the enthalpy change for the threading is zero (no significant interaction between the linear and cyclic species). The first assumption leads to a conclusion that threading takes place only between one of the monomers [tetra(ethylene glycol) in our case] and macrocycle during the prethreading period and no threadings occur during the polymerization. The threading which occurs before the polymerization is called primary threading and that which occurs during the polymerization is called secondary threading. Obviously the assumptions are very rough; however, from this point we could obtain some basic information on a threading system.

Based on assumptions addressed above, a very simple dynamic equilibrium between a linear, a cyclic and a rotaxane as shown in Scheme IV-5 can be used to describe the statistical result of my systems and from this starting point a relative relationship between the threading efficiency and ring size of crown ether may be obtained. Agam *et al.* have worked on a similar approach.¹² By considering the probabilities of a chain positioned inside the threading area of a macrocycle at equilibrium, they derived an equation to describe the threading system (Equation IV-4); where N is the number of threading; V is total volume; L_0 and M_0 are number of moles of initial linear and cyclic species, respectively. n_C and n_L are the number of atoms of the cyclic and linear species, respectively, and θ is the threading angle.

$$NV = 0.195 L_0 M_0 n_C n_L^{1.3} \theta [1 - \exp(-n_C/\pi n_L)] \quad \text{Eq. IV-4}$$

However, this equation does not fit my experimental results well. I have modified this equation to fit our experiments. The factor $[1 - \exp(-n_C/\pi n_L)]$ in Equation IV-4 is related to the dynamics of the threading. But, it seems to be more realistic if this term is modified as follows. The origin of the term has the form: $[1 - \exp(-2r/l)]$; where $2r$ is ring diameter and l is chain length. If $2r \gg l$, $[1 - \exp(-2r/l)]$ approaches one representing maximum threading; if $2r \ll l$, the factor approaches zero representing no threading. If the average length of each bond of the $(\text{CH}_2\text{CH}_2\text{O})_n$ segment is estimated as 1.7 \AA , then $l = 1.7 n_L$ and the circumference of the ring $C = 1.7 n_C$. Assuming that the bond angle is 109.5° and the bond length is 1.7 \AA , I calculated that the average chain diameter (D) of polyethylene oxide is approximately 1.96 \AA . Since the chain and ring frame have the same diameter, the actual ring diameter $2r = (C/\pi) - 1.96$. Therefore,

$$2r/l = (1.7 n_C - 1.96 \pi)/1.7 \pi n_L$$

For tetra(ethylene glycol), $n_L = 13$; then

$$2r/l = (1.7 n_C - 6.16)/69.4 \quad \text{Eq. IV-5}$$

Replacing $n_C/\pi n_L$ in Equation IV-4 by $2r/l$ in Equation IV-5 with substitution of $n_L = 13$, we have

$$NV = 5.48 L_0 M_0 n_C \theta \{1 - \exp[-(1.7 n_C - 6.16)/69.4]\}$$

$$NV = 5.48 L_0 M_0 n_C \theta [1 - \exp(0.0888 - 0.0245 n_C)] \quad \text{Eq. IV-6}$$

In the polymerization reactions under discussion, a constant molar ratio (1.50) of crown ether per glycol (and per MDI) was used; thus the total reaction volumes vary. The total volume can be estimated based on the volume contributions from each component; where $(Mt)_C$ and $(Mt)_L$ are the molecular weights of cyclic and linear species, respectively; ρ_C and ρ_L are the densities of cyclic and linear species, respectively.

$$V = M_0(Mt)_C/\rho_C + L_0(Mt)_L/\rho_L \quad \text{Eq. IV-7}$$

Assuming the cyclic and the linear species have the same density of 1.3 as estimated, then $\rho_C = \rho_L = \rho = 1.3$. The molecular weights can be represented by number of atoms: $(Mt)_C = b n_C$ and $(Mt)_L = b n_L$; where b is the molecular weight contribution of each skeletal atom and taken as 14.6, which is one third of molecular weight of the repeat unit ($\text{CH}_2\text{CH}_2\text{O}$). Therefore,

$$V = 11.23 L_0 (i n_C + n_L) \quad \text{Eq. IV-8}$$

where i is molar ratio of monomer feed and defined as $i = M_0/L_0$. Figure IV-2 illustrated the critical threading angle θ beyond which chains can thread into the ring. The value of θ is related to chain diameter (D) and ring radius. The maximum threading occurs at $\theta_m = 90^\circ$ requiring an infinite ring size if D is fixed. Therefore, θ/θ_m represents that fraction of threadings that can actually take place. Equation IV-9 gives the relationship among θ , D and ring radius r .

$$\text{Cos } \theta = D/2r \quad \text{Eq. IV-9}$$

Since $2r = (C/\pi) - 1.96 = (1.7 n_C/\pi) - 1.96 = 0.541 n_C - 1.96$ and $D = 1.96$, we have

$$\cos \theta = 1.96/(0.541 n_C - 1.96) \quad \text{Eq. IV-10}$$

or $\theta = \cos^{-1}[1.96/(0.541 n_C - 1.96)] \quad \text{Eq. IV-11}$

Equation IV-6 now becomes Equation IV-12 after replacing θ by θ/θ_m , M_0 by iL_0 , n_L by 13 and substitutions of Equations IV-8 , IV-11 and $i = 1.5$.

$$\frac{N}{L_0} = \frac{8.13 \times 10^{-3} n_C \cos^{-1}[1.96/(0.541 n_C - 1.96)] [1 - \exp(0.0888 - 0.0245 n_C)]}{1.5 n_C + 13}$$

Eq. IV-12

The ratio of the number of threadings to the total number of linear species (N/L_0) is the threading efficiency assuming the polymerization conversion is 100%. Hence Equation IV-12 gives a relationship between the threading efficiency and ring size in terms of the number of skeletal atoms n_C . Figure IV-3 shows two plots of threading efficiency versus ring size: the upper curve is experimental results and the lower one is the theoretical plot based on equation IV-12.

It is seen that the two curves have the same profile. Theoretical and experimental results match for the macrocycle having lowest ring

size, 36-membered. However, deviations are observed for larger rings. The threading efficiency increases more rapidly with ring size than that theoretically predicted. This deviation is probably the direct result from the secondary threadings which are more pronounced in our system because the hydrogen bonding between crown ether and urethane group could serve as a driving force for threading.

Threading takes time. The rate of threading increases with increasing ring size. I believe that for smaller macrocycles such as 36C12 the rate of threading is slower than the rate of polymerization. Therefore, no secondary threadings could take place and the experimental result matches the theoretical result which is based on the primary threading only. However, the rate of threading could be faster than that of polymerization for larger rings and of course, the experimental threading efficiencies are higher than those from the theoretical prediction and the bigger the ring, the larger the difference.

IV-2-2: SYNTHESIS OF MODEL POLYURETHANE

The model polymer of a polyrotaxane is the linear component of the polyrotaxane with the similar molecular weight as the polyrotaxane. Generally a model polymer can be prepared via the same polymerization under similar conditions as those for synthesis of the polyrotaxane performed without the presence of a macrocycle. In order to simulate the reaction conditions for the polyrotaxane synthesis, a noncyclic solvent which has similar polarity and other properties as those of the macrocycle is added in the same amount by weight.

My model polyurethane (**IV-11**) was synthesized by carrying out the same reaction under the same conditions as those for the polyurethane-based polyrotaxanes except 2-methoxyethyl ether (diglyme), which has similar polarity as crown ethers, was used as the polymerization solvent. The reaction is shown in Scheme IV-9. A slightly excess amount of MDI was used to achieve higher polymer molecular weight that would be comparable with the polyrotaxanes. The polymerization was allowed to proceed for 24 hours at 90°C and the polymer was purified by multiple reprecipitations into methanol in which the monomers are soluble.

IV-2-3: CHARACTERIZATION OF THE POLYMERS

In this section, solution, thermal and spectroscopic characterization of polyurethane-based, polyurethane-urea-based polyrotaxanes and the model polyurethane will be reported. The properties of the polyurethane-based polyrotaxanes will be discussed against those of the model polyurethane.

IV-2-3-1: Physical Behavior of the Polymers

First of all, the room temperature physical behaviors of all polyrotaxanes with different ring sizes and ring contents and the model polymer are different, indicating that they have different thermal and morphological properties. These behaviors are described as follows.

Model Polyurethane (**IV-11**): glassy solid, brittle transparent film.

Polyurethane-rotaxa-36-crown-12 (IV-6): hard amorphous solid, slightly turbid ductile film.

Polyurethane-rotaxa-42-crown-14 (IV-7): soft amorphous elastomer-like solid, turbid elastomeric film.

Polyurethane-rotaxa-48-crown-16 (IV-8): Tar-like sticky material.

Polyurethane-rotaxa-60-crown-20 (IV-9): wax-like solid, turbid film.

Polyurethane-urea-rotaxa-60-crown-20 (IV-10): rubbery solid, rubbery film.

The room temperature physical behaviors of the polymers reveal that they have different glass transition temperatures and crystallinities which will be discussed in the following sections.

IV-2-3-2: $^1\text{H-NMR}$ Analyses

IV-2-3-2-1: Polyurethane-Based Polyrotaxanes and the Model

Polyurethane

Figure IV-4 shows the $^1\text{H-NMR}$ spectrum of the model polyurethane. The chemical shifts are: 3.51 ppm (singlet, $\text{OCH}_2\text{CH}_2(\text{OCH}_2\text{CH}_2)_2\text{OCH}_2\text{CH}_2\text{O}$, 8n protons), 3.62 ppm (multiplet, $\text{OCH}_2\text{CH}_2(\text{OCH}_2\text{CH}_2)_2\text{OCH}_2\text{CH}_2\text{O}$, 4n protons), 4.19 ppm (multiplet, $\text{OCH}_2\text{CH}_2(\text{OCH}_2\text{CH}_2)_2\text{OCH}_2\text{CH}_2\text{O}$, 4n protons), 3.79 ppm (singlet, arom.- CH_2 -arom., 2n protons), 7.10 ppm (doublet, aromatic, 4n

protons), 7.38 ppm (doublet, aromatic, 4n protons) and 9.66 ppm (singlet, NH, 2n protons).

The $^1\text{H-NMR}$ spectra of polyurethane-based polyrotaxanes are shown in Figure IV-5. As matters of fact, two points need to be mentioned: (1) all the polyrotaxanes have the same spectra as that of the model polymer except that there is an extra singlet characteristic of the crown ether and (2) the characteristic crown ether peak can only be seen separate in polyurethane-rotaxa-36-crown-12 (**IV-6**) system and overlaps with the one for the ethyleneoxy protons in the polymer backbone in the other polyrotaxane systems; this is because the chemical shift of 36C12 protons is a little more downfield than those of the other crown ethers. Integrations of these crown ether signals (with correction for the ethyleneoxy protons in the polymer backbone) relative to the aromatic protons enable the compositions of the polyrotaxanes to be determined.

Notice that there is a very small singlet at about 8.50 ppm on all $^1\text{H-NMR}$ spectra (Figure IV-5), indicating that all polymers contain a very small amount (negligible) of urea linkage (about 1 - 2%).

IV-2-3-2-2: Polyurethane-urea-rotaxa-60-crown-20

The $^1\text{H-NMR}$ spectrum of polyurethane-urea-rotaxa-60-crown-20 (**IV-10**) is shown in Figure IV-6. The chemical shifts are: 3.45 ppm (singlet, $\text{OCH}_2\text{CH}_2(\text{OCH}_2\text{CH}_2)_2\text{OCH}_2\text{CH}_2\text{O}$ in the backbone plus 60C20 protons, $8n + 45.6n$ protons), 3.54 ppm (multiplet, $\text{OCH}_2\text{CH}_2(\text{OCH}_2\text{CH}_2)_2\text{OCH}_2\text{CH}_2\text{O}$ in the backbone, 4n protons), 4.09

ppm (multiplet, $\text{OCH}_2\text{CH}_2(\text{OCH}_2\text{CH}_2)_2\text{OCH}_2\text{CH}_2\text{O}$ in the backbone, $4n$ protons), 3.70 ppm (singlet, arom.- CH_2 -arom., $3.10n$ protons), 7.01 ppm (doublet, aromatic, $6.21n$ protons), 7.28 ppm (doublet, arom.- CH_2 -arom., $6.21n$ protons), 8.44 ppm (singlet, NH on urea group, $1.10n$ protons) and 9.55 ppm (singlet, NH on urethane group, $2n$ protons). Integration of the urea NH peak relative to urethane NH peak gives the a/n value, urea group content. Similarly, integration of the 60C20 peak (with correction for the ethyleneoxy protons in the polymer backbone) gives the x/n value, crown ether content.

IV-2-3-3: Solubilities

In the purification processes, I faced many problems with choice of reprecipitation non-solvents. Model polyurethane (IV-11) and the polyrotaxanes containing less and smaller crown ethers (IV-6 and IV-7) can be reprecipitated into methanol or water easily. However, those containing more and larger crown ethers (IV-8, IV-9 and IV-10) were very difficult to reprecipitate. They either formed emulsions or homogeneous solutions with most solvents, even water. Generally speaking, the polyrotaxanes are more soluble in common solvents than the model polyurethane and the solubility increases with increasing weight percent and size of crown ethers.

IV-2-3-3-1: Solubilities at Room Temperature

Solubilities of all polymers in some common solvents were roughly observed in a test-tube at room temperature by treating 0.001 g of

sample with 1 mL of solvent. The results are listed in Table IV-6. It can be seen that the model polyurethane (**IV-11**) is insoluble in water, methanol and acetone, as expected, and only slightly soluble in methylene chloride. However, all the polyrotaxanes are soluble in methylene chloride and acetone. More interestingly, the polyrotaxanes with highest weight percentage of 60C20, **IV-8** and **IV-9**, are water soluble.

Regarding the solubility differences between polyrotaxanes and the model polymer, discussion could be based on Flory equations (Equations IV-13, IV-14 and IV-15); where $[\eta]$ is intrinsic viscosity, M is molecular weight, $\langle r_0 \rangle$ is unperturbed chain end-to-end distance, n is the number of segments (related to the number of the repeat units), l is length of the segment, θ is bond angle, ϕ is rotational angle, α is expansion factor, χ is interaction parameter, V is the volume and Φ_0 is a constant.

$$[\eta] M = \Phi_0 (\langle r_0 \rangle^2)^{3/2} \alpha^3 \quad \text{Eq. IV-13}$$

$$\langle r_0 \rangle^2 = n l^2 f(\theta) f(\phi) \quad \text{Eq. IV-14}$$

$$\alpha^5 - \alpha^3 \text{ ----} \rightarrow [(1/2 - \chi) n^{1/2}] / V \quad \text{Eq. IV-15}$$

The product $[\eta] M$ in Equation IV-13 represents the hydrodynamic volume of a polymer in terms of the variables at the right hand side. The expansion factor α is related to the solvation and, of course, molecular weight. Under Θ conditions, α equals 1. Under non- Θ conditions, α is described according to Equation IV-15. The interaction parameter χ measures the interactions between the macromolecules and solvent

molecules. Different from the model polymer, χ of a polyrotaxane-solvent system is more complicated. It is driven from two different interactions: polymer backbone-solvent interaction and macrocycle-solvent interaction. These interactions are determined by their respective solubility parameters (δ). In my case, macrocycles are more soluble in common solvents than the polymer backbone (model polymer). The strong interaction between crown ethers and solvent can largely increase α and hence the hydrodynamic volumes of our polyrotaxanes. According to Equation IV-14, the unperturbed end-to-end distance of a polymer chain is determined by bond angle (θ) and rotational angle (φ), besides the number of segments (n) and their length (l). Bond angles of a polyrotaxane backbone are not expected to be very different from the model polymer if the macrocycles are big enough. However, with small macrocycles, the steric hindrance and rotational barriers could be important factors in polyrotaxane systems. As one can imagine, backbone rotation with macrocycles hanging on is much more difficult than that without them. In other words, backbone rotation is restricted in a polyrotaxane system by the threaded macrocycles. Generally, a polyrotaxane would have a bigger $f(\varphi)$ and hydrodynamic volume than the model polymer. On the other hand, loose packing of macromolecules and weaker inter-molecular interactions in the solid state are also expected in polyrotaxane systems due to the presence of macrocycles. In conclusion, the polyrotaxanes are more soluble in common solvents than the model polymer and also the solubility increases with increase in size and content of macrocycle.

IV-2-3-3-2: Critical Solution Temperatures

The polyurethane-based polyrotaxanes **IV-8** and **IV-9** were found to be soluble in water as reported in the previous section. To my surprise, the solutions became cloudy when they were heated up and returned back to homogeneous when they were cooled down. This interesting phase behavior was further investigated for the solutions with different concentrations by heating the solutions from 0°C to 100°C and naturally cooling down. An average value of cloud points read by heating and cooling was taken. The lower critical solution temperature (LCST) can be observed in this range; however, the upper critical solution temperature (UCST) can not be observed. Table IV-7 lists the LCST at different concentrations for **IV-9**. It was surprisingly seen that the LCST was not effected significantly by concentration. In the case of **IV-8**, there was no sharp upper cloud point. It seems that the solution gradually became cloudy when the temperature was raised and became complete cloudy at about 75°C, more than 10°C lower than that of **IV-9**.

At this stage, I do not quite understand why these two polyrotaxanes have such solution property. It may have something to do with backbone-crown intra-annular hydrogen bonding which could be temperature dependent. This phenomenon is currently under detailed investigation.

IV-2-3-4: Intrinsic Viscosity Measurements

The viscosity measurements were carried out with NMP as solvent at 25.8°C controlled by a constant temperature water bath. The viscosities at various concentrations were taken and the calculated reduced and inherent viscosities were plotted against concentrations. The intrinsic viscosities were obtained by extensions of the straight lines to zero concentration and results are shown in Table IV-8.

It is seen that polyurethane-rotaxa-42-crown-14 and the model polyurethane have high intrinsic viscosities. All other polyrotaxanes have lower intrinsic viscosities. These results are consistent with molecular weights (see next section) except that of polyurethane-rotaxa-42-crown-14 (IV-7). This particular sample has a comparable molecular weight with the others but displays the highest intrinsic viscosity; this will be further discussed in the next section.

IV-2-3-5: GPC Analyses and Molecular Weights

The reprecipitation experiments revealed that there were no free crown ethers in the polyrotaxane systems. In other words, all crown ethers detected by ¹H-NMR analyses were threaded on polymer chains. This was further proved by GPC analyses.

I have run GPC analyses under two different conditions. (1) I used NMP containing 0.006 M of LiBr as solvent and two different detectors: a differential refractive index detector originally incorporated into the system and a Viscotek Differential Viscometer Model 100 connected to

the system as an additional detector. The calibration was based on both universal calibration and polystyrene standards. (2) I used THF as solvent with only the differential refractive index detector; this calibration was based on polystyrene standards only.

Consider firstly the GPC results under the condition (1). Some GPC traces under this condition are shown in Figure IV-7a: model polyurethane (**IV-11**), Figure IV-7b: polyurethane-rotaxa-60-crown-20 (**IV-9**) and Figure IV-7c: a blend made of the model polyurethane and 60C20 in the same weight percent as that in the polyrotaxane. Let us now compare these traces. The model polymer and polyrotaxane have basically similar relatively sharp peaks; there is no peak corresponding to 60C20 with the RI detector. Even though the blend also shows no separated peak for 60C20, the broadness of the peak at higher elution volumes indicates the overlap of the model polymer and 60C20 peaks. The molecular weight averages of the blend are consistent with those calculated based on the blend composition, e.g. contributions from both the model polyurethane and 60C20. This result strongly supports our belief that in the polyrotaxane systems, crown ethers are threaded onto the polymer backbone to form a unified two component system; in the case of the blend, crown ethers are free (unthreaded) in the system and shown as a "long tail" in the GPC trace.

Secondly, let us consider the GPC results under the condition (2). Basically results are similar to those under the condition (1); however, the resolution seems to be better. Figure V-8 and Figure V-9 show GPC

traces of polyrotaxane, a blend containing the same weight percent of crown ether as that in the polyrotaxane, the model polymer and the crown ether itself in the overlap format, for 60C20 system and 36C12 systems, respectively. For the 60C20 system (Figure V-8), the results were similar as those under condition (1): the blend gave a broad peak without total separation of the polymer and 60C20, while polyrotaxane showed a narrow peak similar as that of the model polymer. The shift of 60C20 peak from the pure crown ether to the physical blend (Figure IV-8c versus IV-8d) indicates strong association of crown ether and polyurethane backbone. However, for the 36C12 system (Figure V-9), it is clearly seen that the crown ether peak is separated from that of the model polymer in the blend, while the rotaxane showed only one peak similar to that of model polymer. These results, again, reveal that, different from the physical blends in which polymer and crown ether are independent species, polyrotaxanes are homogeneous polymeric species containing a stable molecular union of linear polymer and crown ethers.

The GPC molecular weight averages (M_n and M_w) and polydispersities (M_w/M_n) determined under condition (1) and condition (2) are summarized in Tables IV-9 and IV-10, respectively. The molecular weight averages were calculated based on both the universal calibration and polystyrene calibration. Even though the molecular weights and polydispersities of all polymers were not the same, they are within a sufficiently narrow range to allow comparison of other polymer properties. Generally, the polyrotaxanes do not have very high molecular weights, which was probably caused by hydrolysis of MDI or trace

impurities (e.g. residual glycols) in the crown ethers which were used in relatively large amounts; or the calibration was probably incorrect for both the model polymer and polyrotaxanes since they may have different hydrodynamic volumes.

The viscosity molecular weight averages (M_v) along with Mark-Houwink coefficients obtained by the GPC analyses with universal calibration, intrinsic viscosities calculated based on the Mark-Houwink coefficients and M_v 's through equation $[\eta] = K M^a$ are listed in Table IV-11. First, the measured intrinsic viscosities (Table IV-8, see previous section) are slightly higher than those calculated from GPC except for polyurethane-rotaxa-42-crown-14 (**IV-7**) which has an unacceptably high calculated viscosity. Even for the measured viscosities, this particular sample has the highest value; however, notice that the GPC molecular weight from the universal calibration is comparable with the others, but by polystyrene standards, its molecular weight is higher by a factor of two. Why does it behave like that? A possible explanation is that this specific ring size of the crown ether (42-membered) can maximally expand the random coil of the polymer chain. As illustrated in Figure IV-10, if the ring size is smaller than 42-membered (Figure IV-10a), perhaps the rings are not big enough to cause significant chain extension as a result of their solvation. On the other hand, the presence of rings may reduce chain entanglements. If the ring size is bigger than 42-membered (Figure IV-10c), perhaps the ring flexibility would cause a minimal effect on the backbone as they become solvated. Thus, the polyrotaxane with 42-membered ring (Figure IV-10b) could have the highest intrinsic

viscosity as a result of intra-annular solvation and the consequent chain extension. In a plot of intrinsic viscosity versus ring size, a bell-shaped curve is obtained (Figure IV-11) and roughly, the maximum is located at the 42-membered ring size.

The numerical values of Mark-Houwink coefficients reflect the nature of the polymer and the nature of the solvent at a constant temperature. For a non-draining coil, a rigid body whose interior domain is unaffected by the solvent flow, the intrinsic viscosity is directly proportional to $M^{1/2}$. For a free-draining coil, in which each repeat unit of the polymer chain offers hydrodynamic resistance to the solvent flow, the intrinsic viscosity of such a coil is directly proportional to M^1 . Thus the values of Mark-Houwink coefficient $a = 0.5$ and 1 fix the two extremes of the non-draining and free-draining polymer molecular coils. The values offer information on the permeability of the coil to the flow streamlines. Back to my systems now; I have a values ranging from 0.312 to 0.792. The polyrotaxanes containing less and smaller rings (**IV-6**, **IV-7**, and **IV-8**) and the model polymer (**IV-11**) are more likely to form non-draining coils, i.e., the lowest a values. However, the polyrotaxanes containing 60C20 (**IV-9** and **IV-10**), the largest ring, in high percentage tend to form free-draining coils, i.e., the highest a values. The Mark-Houwink coefficient K may refer to coil expansion. It is clearly shown in Table IV-11 that the K value decreases with increase in ring size and ring content of the polyrotaxanes. That probably reveals that smaller rings are rigid enough to expand the coil. However, the large rings are too flexible to cause such expansion; instead, hydrogen bonding between the

crown ether and urethane group on the backbone may contract the coil. Thus, K values for the polyrotaxanes **IV-6**, **IV-7**, and **IV-8** are larger than that for the model polyurethane **IV-11**; but polyrotaxanes **IV-9** and **IV-10** have smaller K values than the model polyurethane.

It was seen that different molecular weight results were obtained under different calibration standards. Which are more reliable? I believe that molecular weights obtained under polystyrene standards are more reliable since they are more consistent with the viscosities. Therefore, the high viscosity of polyurethane-rotaxa-42-crown-14 (**IV-7**) could simply be a result of its high molecular weight. This would not, however, explain its anomalous Mark-Houwink a value (Table IV-11).

IV-2-3-6: FTIR Analysis

The goal of FTIR analysis was to investigate hydrogen bonding between urethane linkage and crown ether. Generally, polyether-based polyurethanes exhibit characteristic bands near 1700 cm^{-1} (C=O stretch), 1540 cm^{-1} (N- bending), 3300 cm^{-1} (N-H stretch), 1220 cm^{-1} (N-C-O stretch) and $1150 - 1060\text{ cm}^{-1}$ region (C-O-C stretch). In our studies, we focused on the bands near 1700 cm^{-1} (C=O stretch) and 3300 cm^{-1} (N-H stretch). Peak shifts are indicative of the formation of different hydrogen bonds.

Three samples were subjected to the analysis: the model polyurethane (**IV-11**), polyurethane-rotaxa-60-crown-20 (**IV-9**) and a blend made of **IV-11** and 60C20 in the same weight percentage as that in

the **IV-9**. Figure IV-12 shows the comparison of FTIR spectra of these three samples focused on two frequency ranges: 1675 - 1775 cm^{-1} where the signal of carbonyl stretch appears and 3150 - 3400 cm^{-1} where the signal of N-H stretch appears. Consider firstly the carbonyl stretch; two peaks are observed for the model polyurethane; their maximum absorbances are at 1725 cm^{-1} and 1705 cm^{-1} . The one at lower frequency is due to hydrogen bonded carbonyl groups. It is clearly seen that this peak shifts to 1725 cm^{-1} when 60C20 was present either by blending or by threading, indicating that less hydrogen bonding exists between the carbonyl in the polymer backbone and amide N-H groups. Secondly, the model polyurethane has a sharp peak with maximum absorbance at 3300 cm^{-1} and a weak absorption at 3200 cm^{-1} due to N-H stretch. The 3200 cm^{-1} peak and other lower frequencies increase in intensity for both blend and polyrotaxane, indicating that more extensive hydrogen bonding of N-H groups exists, presumably because of interactions between N-H groups of the polymer backbone and oxygens of the crown ether. However, the peak shift differences between the blend and the polyrotaxane reveal that in the polyrotaxane system hydrogen bonding is more efficient and perhaps a different type, e.g., intra-annular hydrogen bonding, exists besides the normal inter-molecular hydrogen bonding.

IV-2-3-7: DSC Analyses and Glass Transition Temperatures

IV-2-3-7-1: Polyurethane-Based Polyrotaxanes and the Model

Polyurethane

Figure IV-13 shows the first run DSC traces of polyurethane-based polyrotaxanes (**IV-6**, **IV-7**, **IV-8** and **IV-9**) and the model polyurethane (**IV-11**). It is seen that **IV-11**, **IV-6** and **IV-7** showed only one transition, the glass transition; however, **IV-8** and **IV-9** showed two transitions, a glass transition and a melting peak. We will discuss the glass transition temperatures in this section and the melting behavior in the next section.

The glass transition temperatures of the polymers are 324^oK (**IV-11**), 288^oK (**IV-6**), 273^oK (**IV-7**), 262^oK (**IV-8**), and 233^oK (**IV-9**). Generally all the crown ethers with ring sizes from 30 to 60-membered have T_g around 207^oK. It is clear that the glass transition temperatures of polyrotaxanes are much lower than that of the model polyurethane (**IV-11**) and decrease drastically with increase in ring size and weight percentage of crown ether incorporated. Figure IV-14 shows a plot of glass transition temperature versus ring size. Interestingly, a linear correlation is obtained. In a plot of $1/T_g$ of polyrotaxane against weight percent of crown ether incorporated also a linear relationship is obtained as shown Figure IV-15, indicating that the Fox equation can be applied to the polyrotaxane systems (the other crown ethers have similar glass transition temperatures as 60C20). Because the weight percentage of crown ethers in polyrotaxanes increase almost linearly with increasing

ring size (Figure IV-16), a plot of T_g against ring size gives a straight line with a negative slope (Figure IV-14), also indicating the application of Fox equation to the systems.

The lowering in glass transition temperatures of polymers through rotaxane formation may result from several different effects. The crown ether could act as a plasticizer which pushes polymer chains apart and effectively increases the free volume of the system. However, since crown ethers are threaded onto the polymer chains, this effect is not totally the same as that by a plasticizer. The plasticizer molecules, in general, have great mobility in the system, while the motions of threaded macrocycle molecules are restricted in certain ranges along the polymer backbone. In other words, their motions are greatly retarded by threading and their effect is more efficient. From this point of view, threaded macrocycle molecules act similarly as pendent groups which may decrease chain flexibility to allow more intimate alignment between macromolecules, resulting in an increase in T_g . However, this is a minor effect compared to the "chain separation" which decreases T_g in a large scale, especially in our polyurethane systems, this "separation" probably results in diminution of the hydrogen bonding between macromolecular chains through the entropically favored formation of intra-annular hydrogen bonding between the polymer backbone and threaded crown ether.

On the other hand, a polyrotaxane may be viewed as a random copolymer of the linear backbone and the macrocycle linear analog showing a T_g value which is intermediate between the value of the linear

polymer backbone and the macrocycle. In my case, crown ethers have very low T_g (about 207°K). Hence, the polyrotaxanes showed lower T_g than the model polymer.

IV-2-3-7-2: Polyurethane-urea-Based Polyrotaxane

DSC analysis was also done with polyurethane-urea-rotaxa-60C20 (**IV-10**). This polymer also showed two transitions, a glass transition at 245°K and the other was a melting peak at 313°K. It can be seen that this polymer also showed very low T_g . Since I have no corresponding model polyurethane-urea as a reference, I will not discuss the T_g in detail. The melting behavior will be discussed in the next section.

IV-2-3-8: Crystallization Behaviors

IV-2-3-8-1: Evidenced by DSC Analyses

Let us go back to look at the first run of DSC traces shown in Figure IV-13. The model polymer (**IV-11**) and polyrotaxanes with smaller crown ethers (**IV-6** and **IV-7**) showed only glass transitions without any other signals. However, those polyrotaxanes with larger crown ethers (**IV-8** and **IV-9**) showed a melting peak besides the glass transition signal. This is also true for the first run on **IV-10**, a polyurethane-urea-based polyrotaxane with 60C20, a relatively large crown ether (Figure IV-17a).

The melting temperatures observed were several degrees lower than melting points of the corresponding crown ethers. Table IV-12 lists

melting points of crown ethers in pure solid state and in polyrotaxanes. It is seen that even though 36C12 and 42C14 have melting points in their pure solid states of 37.0 - 37.5°C and 49.6 - 50.4°C, respectively, there are no melting signals observed in polyrotaxanes containing these two crown ethers (**IV-6** and **IV-7**). However, 48C16 and 60C20 showed melting peaks in their corresponding polyrotaxanes (**IV-8**, **IV-9** and **IV-10**), but 7 - 14°C lower than those measured in their pure solid states. It is now clear that (1) the polyurethane backbone is amorphous, (2) crystallization of the crown ether occurs and (3) this crystallization can only be observed with relatively large sizes of crown ethers (48C16 and 60C20).

A question raised is: does crystallization occur without dethreading of crown ethers? We will see that the answer is positive with some other interesting results. So far, the DSC traces discussed were obtained from first runs. However, those melting peaks were not seen in the second runs after the sample was naturally cooled down. Figure IV-17 clearly demonstrates this phenomenon. The polyurethane-urea-rotaxa-60C20 showed no melting peak in the first run done right after the polymer was synthesized; however, the melting peak was observed in the first run done on the same sample after it was aged at room temperature for two months, but this melting peak was not present in the second run. Furthermore, the same phenomenon was observed with the same sample after it was again aged at room temperature for six months. This reversible and time dependent crystallization strongly supports the

conclusion that the crown ether molecules were not dethreaded during the crystallization process.

The crystallization process is illustrated in Figure IV-18. When an amorphous polymer is aging at room temperature, 35 - 65°C above T_g , but about 15 to 20°C below the melting points of crown ethers, crown ether molecules diffuse along the linear polymer backbone and aggregate to form a crystalline phase. Upon heating, macrocycles diffuse apart and the polymer returns back to the amorphous state; recrystallization takes a relatively long time since the diffusion of the macrocycles along the backbone is kinetically retarded.

Why is the crystallization only observed with relatively larger crown ethers? The explanation could be focused on two points. Consider firstly that for the same linear polymer backbone the larger the crown ether, the higher the mobility along linear backbone. Secondly, the relatively larger $T_m - T_g$ (51 - 86°C) and $T_{\text{Room}} (298^\circ\text{C}) - T_g$ (35 - 65°C) windows of polyrotaxanes **IV-8**, **IV-9** and **IV-10** favor the diffusion of crown ether molecules along the linear backbone at room temperature relative to the smaller $T_m - T_g$ (probably ca. 25°C) and $T_{\text{Room}} (298^\circ\text{C}) - T_g$ (10 - 25°C) windows of **IV-6** and **IV-7**.

IV-2-3-8-2: Evidenced by X-Ray Analyses

The crystallization behavior and the proposed process (Figure IV-18) are further supported by the results from wide angle X-ray analyses.

Two samples were analyzed by X-ray: pure 60C20 and polyurethane-rotaxa-60C20; the latter was analyzed after two different thermal treatments: quenched from the melt to - 77°C and annealed at room temperature or annealed at 30°C. Figure IV-19 shows the X-ray patterns. Firstly, the crystalline phase observed in the polyrotaxane system was the crown ether crystalline phase as recognized by the same X-ray pattern in both cases. Secondly, the crystallinity of crown ether in the polyrotaxane was found to be higher at higher annealing temperature. That indicates that the rate of recrystallization was also temperature dependent; in other words, it was thermodynamically driven. This result, again, strongly supports my conclusion that the crystalline phase is formed by the diffusion of crown ether molecules along the linear polymer backbone and higher temperatures favor the process.

IV-2-3-8-3: Crystallization Kinetics

The 60C20 crystallization kinetics was studied by observing the spherulite growth rates under different crystallization temperature with a microscope. Two samples were subjected to the study: polyrotaxane **IV-9** and a physical blend containing model polyurethane **IV-11** and 60C20 which had the same weight percentage as that in the polyrotaxane **IV-9**.

Figure IV-20 shows the crystallization rate of 60C20 (spherulite growth rate) changes with crystallization temperature in the polyrotaxane and in the blend. It is interesting to see that 60C20 crystallizes much faster in the blend than in the polyrotaxane under the same

crystallization temperature. This result again reveals that the crystallization of threaded crown ether (in the polyrotaxane) is kinetically "retarded". Also from Figure IV-20 it can be noticed that the crystallization of 60C20 in the blend shows a common behavior, i.e., crystallization rate decrease with increasing crystallization temperature. However, this was not observed in the polyrotaxane, probably because the diffusion of 60C20 along polymer backbone is crystallization rate determining step in the polyrotaxane system.

IV-3: CONCLUSIONS

Some facts which are strongly supported by experimental results are summarized below.

IV-3-1: SYNTHESIS

- (1) The statistical threading method is efficient in our systems. The good compatibility of the polyether-based polyurethanes and crown ethers and hydrogen bonding between the urethane groups formed during the polymerization and crown ethers may favor the threadings.
- (2) Threading efficiency depends on many variables such as concentration, ring size, chain length, ring flexibility, chain flexibility, chain diameter, and so on. A mathematical equation was

derived to predict the threading efficiency changing with ring size of crown ether. Experimentally the threading efficiency increased drastically with ring size, which roughly matches the form of the theoretical prediction; the deviation was explained.

- (3) Multiple reprecipitation served as an efficient method to purify polyrotaxanes. Free macrocycles were removed by several reprecipitations.

IV-3-2: CHARACTERIZATION

- (1) The molecular structures of polyrotaxanes were proven by reprecipitations, $^1\text{H-NMR}$ and GPC analyses: reprecipitations were carried out until a constant macrocycle content was achieved; $^1\text{H-NMR}$ spectra showed macrocycle peaks and GPC traces showed no peak for free macrocycles.
- (2) All polymers have comparable molecular weights.
- (3) FTIR analyses showed that hydrogen bonding exist between the polyurethane backbone and the crown ether. It seems that hydrogen bonding is more efficient in polyrotaxane systems than that in the corresponding physical blend.
- (4) The solubility of the polyurethane was greatly enhanced through rotaxane formation: all polyrotaxanes are more soluble in common solvents than the model polymer. Water soluble polyurethane-

based polyrotaxanes have been prepared and they showed lower critical solution temperatures in aqueous solutions.

- (5) The glass transition temperature of the polyurethane was drastically decreased through rotaxane formation: all polyrotaxanes have lower glass transition temperatures than the model polymer. The Fox equation can generally be applied.
- (5) Crystallization of the threaded crown ether was observed with relatively larger crown ethers. This occurred without dethreading of the macrocycles and it was kinetically retarded. It was time and temperature dependent as evidenced by DSC analysis, wide angle X-ray scattering analysis and the study of crystallization kinetics.

IV-4: EXPERIMENTAL

MDI was purchased from Eastman Kodak Company. It was distilled two times under vacuum (b.p. 188°C/0.10 torr) and stored under nitrogen. Tetra(ethylene glycol) was purchased from Aldrich Chemical Company. It was also distilled two times under vacuum (b.p. 170°C/0.15 torr) and stored under nitrogen. All crown ethers were synthesized (see Chapter II) and dried under vacuum overnight at room temperature. Diglyme (99+%, anhydrous) was purchased from Aldrich Chemical Co. and used without further purification.

The $^1\text{H-NMR}$ spectra were recorded on a Bruker WP270 MHz instrument using tetramethylsilane as the internal standard. The solvent used was DMSO-d_6 for all analyses.

Viscosities of polyurethane-based polyrotaxanes and the model polyurethane were measured using a Cannon-Ubbelohde semi-micro dilute solution viscometer with 100 centipoise inner diameter capillary.

GPC analyses were done on a Waters 150C ALC/GPC system with Permagel $10^2 - 10^6$ Å polystyrene-divinylbenzene columns.

FTIR spectra were recorded on a Nicolet MX-1 FTIR spectrometer.

DSC analyses were done on Perkin-Elmer DSC-2C instrument.

The wide angle X-ray analyses were done on Scintag DMS 2000 Diffractometer with CuK_α radiation and Ni filter.

IV-4-1: POLYURETHANE-ROTAXA-36-CROWN-12 (IV-6)

Tetra(ethylene glycol) (1.0027 g, 5.1624×10^{-3} mol) and 36C12 (4.1000 g, 7.7436×10^{-3} mol) were mixed in an oven-dried 15-mL 1-necked flask which was immersed in an oil-bath with temperature 90°C . The mixture was magnetically stirred under nitrogen for 1 hour. MDI (1.2919 g, 5.1624×10^{-3} mol) was added. A yellowish-brown color was observed in about 30 minutes. A viscosity increase was also observed in about 5 hours. The reaction was allowed to proceed for a total of 24 hours under the same conditions.

The polymer was first precipitated into methanol (400 mL) from THF (15 mL). A viscous emulsion was obtained. The 2nd, 3rd and 4th reprecipitations were done into water (400 mL each) from THF (15 mL each). A yellowish-brown tar-like solid (2.21 g) was obtained. Weight per cent polymer recovered based on 0.16 threading efficiency : 81%.

IV-4-2: POLYURETHANE-ROTAXA-42-CROWN-14 (IV-7)

Tetra(ethylene glycol) (1.0883 g, 5.6032×10^{-3} mol) and 42C14 (5.1800 g, 8.4048×10^{-3} mol) were mixed in an oven-dried 15-mL 1-necked flask which was immersed in an oil-bath with temperature 90°C. The mixture was magnetically stirred under nitrogen for 1 hour. MDI (1.40226 g, 5.6032×10^{-3} mol) was added. A yellow color and viscosity increase were observed immediately. The stirring ceased in 5 minutes. The reaction was allowed to proceed for a total of 24 hours under the same conditions without stirring.

The polymer was reprecipitated 4 times into methanol (400 mL each) from THF (20 mL each). A yellow elastomeric solid (2.80 g) was obtained. Weight per cent polymer recovered based on 0.29 threading efficiency: 80%.

IV-4-3: POLYURETHANE-ROTAXA-48-CROWN-16 (IV-8)

Tetra(ethylene glycol) (0.99170 g, 5.1058×10^{-3} mol) and 48C16 (5.4800 g, 7.7749×10^{-3} mol) were mixed in an oven-dried 15-mL 1-necked flask which was immersed in an oil-bath with temperature 90°C. The mixture was magnetically stirred under nitrogen for 1 hour. MDI

(1.2777 g, 5.1058×10^{-3} mol) was added. A yellowish-brown color and viscosity increase were observed in 30 minutes. The reaction was allowed to proceed for a total of 24 hours under the same conditions.

The polymer was reprecipitated 4 times into ethyl acetate (400 ml each) from THF (20 mL each). A viscous tar-like solid (2.79 g) was obtained. Weight per cent polymer recovered based on 0.52 threading efficiency: 67%.

IV-4-4: POLYURETHANE-ROTAXA-60-CROWN-20 (IV-9)

Tetra(ethylene glycol) (1.0275 g, 5.2901×10^{-3} mol) and 60C20 (6.5000 g, 7.3864×10^{-3} mol) were mixed in an oven-dried 15-mL 1-necked flask which was immersed in an oil-bath with temperature 90°C. The mixture was magnetically stirred under nitrogen for 1 hour. MDI (1.3239 g, 5.2901×10^{-3} mol) was added. A yellow color was observed in a few minutes. A viscosity increase was also observed in 30 minutes and the stirring ceased in 30 minutes. The reaction was allowed to proceed for a total of 24 hours under the same conditions without stirring.

The polymer was first reprecipitated into a mixture of ethyl acetate and n-hexane (8:2/v:v, 400 mL) from THF (20 mL). A viscous emulsified liquid was obtained. The 2nd, 3rd and 4th reprecipitations were done into ethyl acetate (400 mL each) from THF (20 mL each). A slightly yellow wax-like solid (3.75 g) was obtained. Weight per cent polymer recovered based on 0.87 threading efficiency: 59%.

IV-4-5: POLYURETHANE-UREA-ROTAXA-60-CROWN-20 (IV-10)

Tetra(ethylene glycol) (1.0265 g, 5.2850×10^{-3} mol) and 60C20 which had been exposed to air for several days (5.0000 g, 5.6754×10^{-3} mol) were mixed in an oven-dried 15-mL 1-necked flask which was immersed in an oil-bath with temperature 90°C. The mixture was magnetically stirred under nitrogen for 1 hour. MDI (1.3427 g, 1.3652×10^{-3} mol) was added. A yellow color was observed in a few minutes. A viscosity increase was also observed in 30 minutes and the stirring ceased in 1 hour. The reaction was allowed to proceed for a total of 24 hours under the same conditions without stirring.

The polymer was reprecipitated 4 times into ethyl acetate (400 mL each) from THF (20 mL each). A slightly yellow amorphous solid (2.92 g) was obtained. Weight per cent polymer recovered based on 0.57 threading efficiency: 58%.

IV-4-6: MODEL POLYURETHANE (IV-11)

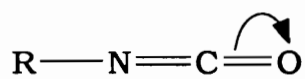
To an oven-dried 15-mL 1-necked flask, tetra(ethylene glycol) (1.4012 g, 7.2141×10^{-3} mol) was added with diglyme (5.00 mL). The flask was immersed in an oil-bath with temperature 90°C. MDI (1.8235 g, 7.2864×10^{-3} mol) was added and the solution was magnetically stirred under nitrogen. An orange color and increase in viscosity were observed in 20 minutes. The solution was continuously stirred for 24 hours.

The polymer was reprecipitated 2 times into methanol (400 mL each) from THF (20 mL each). A slightly yellow amorphous solid (2.98 g) was obtained. Weight per cent polymer recovered: 92%.

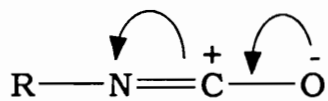
REFERENCES

1. Bayer, O. *Angew. Chem.* **1947**, 59(9), 257.
2. Farben, I. G. *German Patent* **1937**, 728.981.
3. Bayer, F. *German Patent* **1941**, 913.474.
4. Bayer, F. *German Patent* **1948**, 851.851.
5. Oertel, G. *Polyurethane Handbook*, Hanser Publishers, N.Y. **1985**, P69.
6. *Urethane Chemicals Bulletin*, 85-89, Akzo America, Inc., Enka, N. C., **1985**.
7. *TMXDI, Product Bulletin*, American Cyanamid Co., Wayne, N. J., **1983**.
8. Desmodur, W. *Bulk Handling and Storage*, Mobay Corp., Pittsburgh, P. A., **1982**.
9. Petterson, S. *Justus Liebigs Ann. Chem.* **1949**, 562, 205.
10. Siefken, W. *Justus Liebigs Ann. Chem.* **1949**, 562, 75.
11. Aldrich catalog **1990 - 1991**.
15. Agam, G.; Graiver, D.; Zilkha, A. *J. Am. Chem. Soc.* **1976**, 98, 5206.

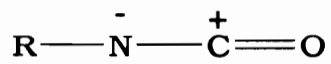
Scheme IV-1: Resonance Sequence of Isocyanate Group



IV-2a

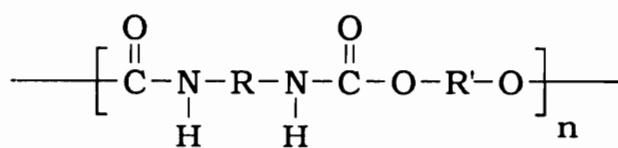
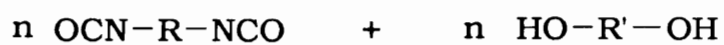


IV-2b



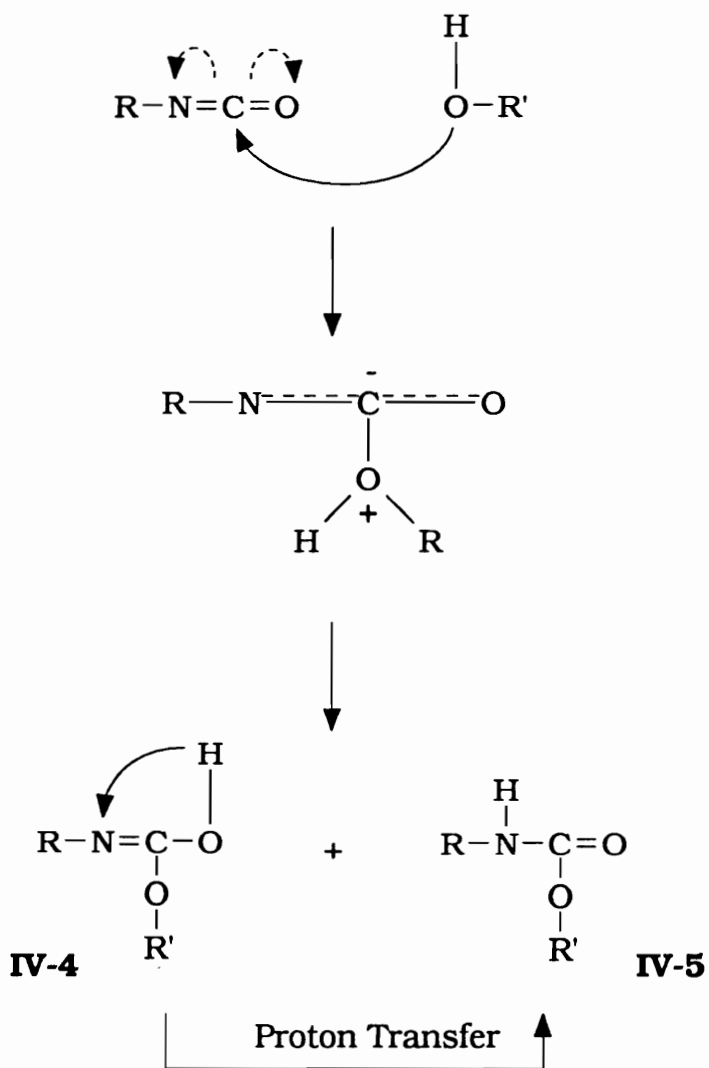
IV-2c

Scheme IV-2: The Formation of Polyurethanes

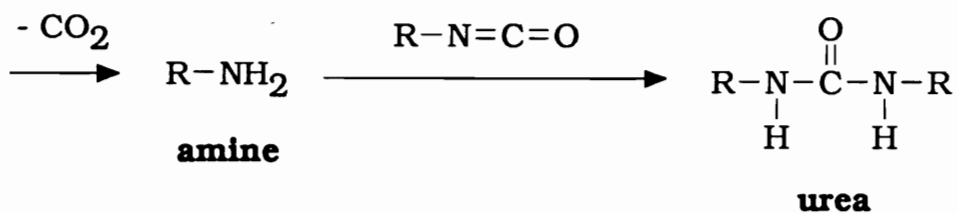
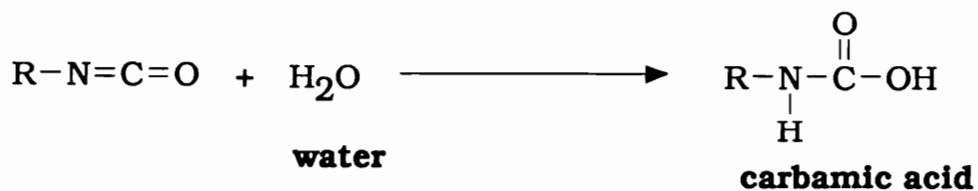
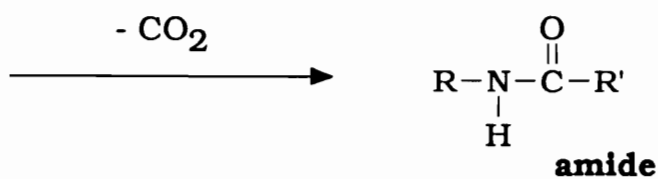
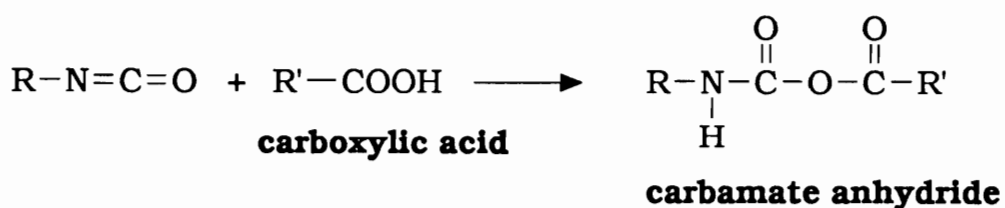
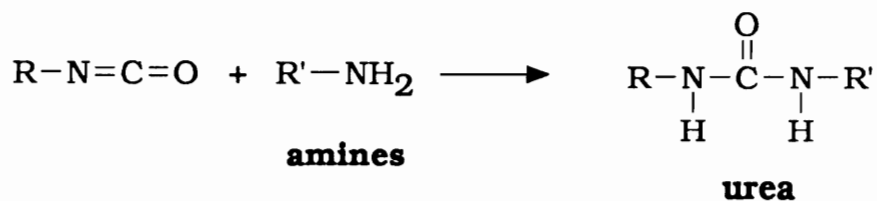


IV-3

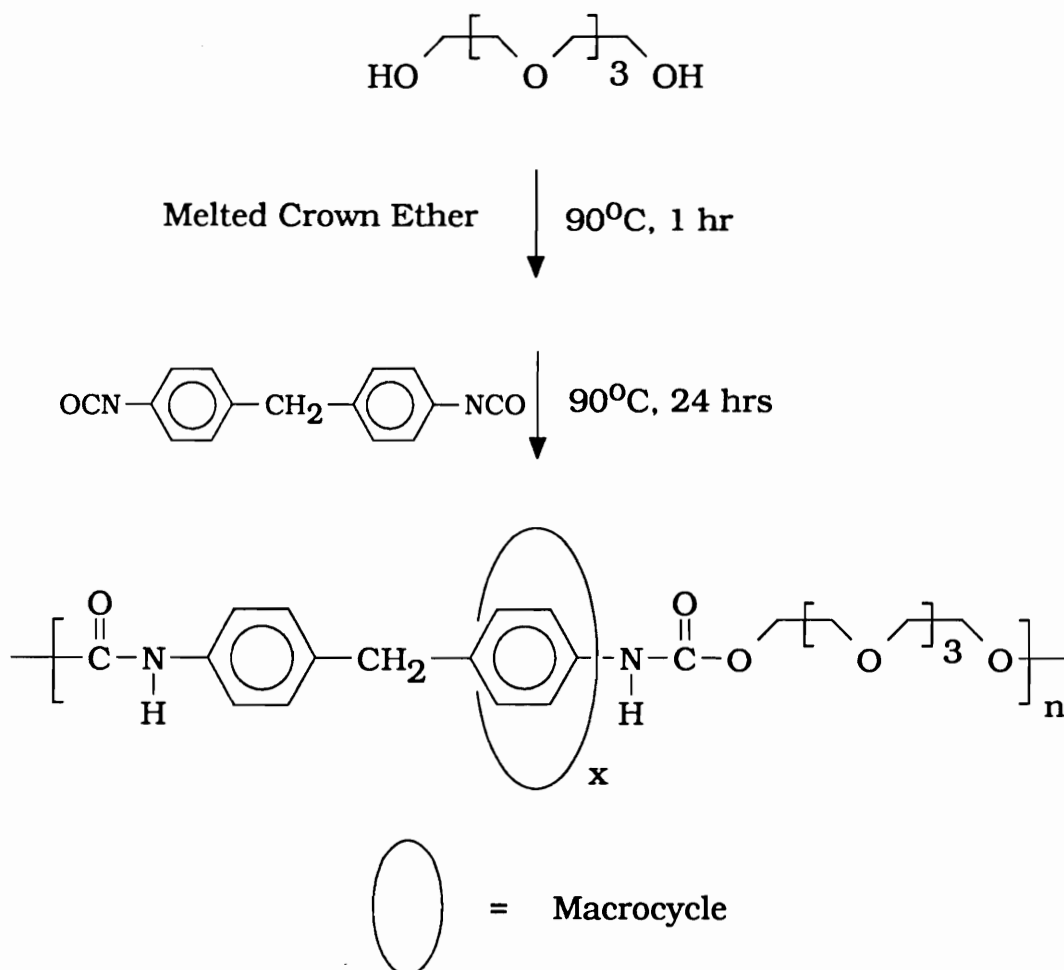
Scheme IV-3: Mechanism of Urethane Group Formation



Scheme IV-4: Other Reactions of the Isocyanate Group



Scheme IV-6: Syntheses of Polyurethane-Based Polyrotaxanes



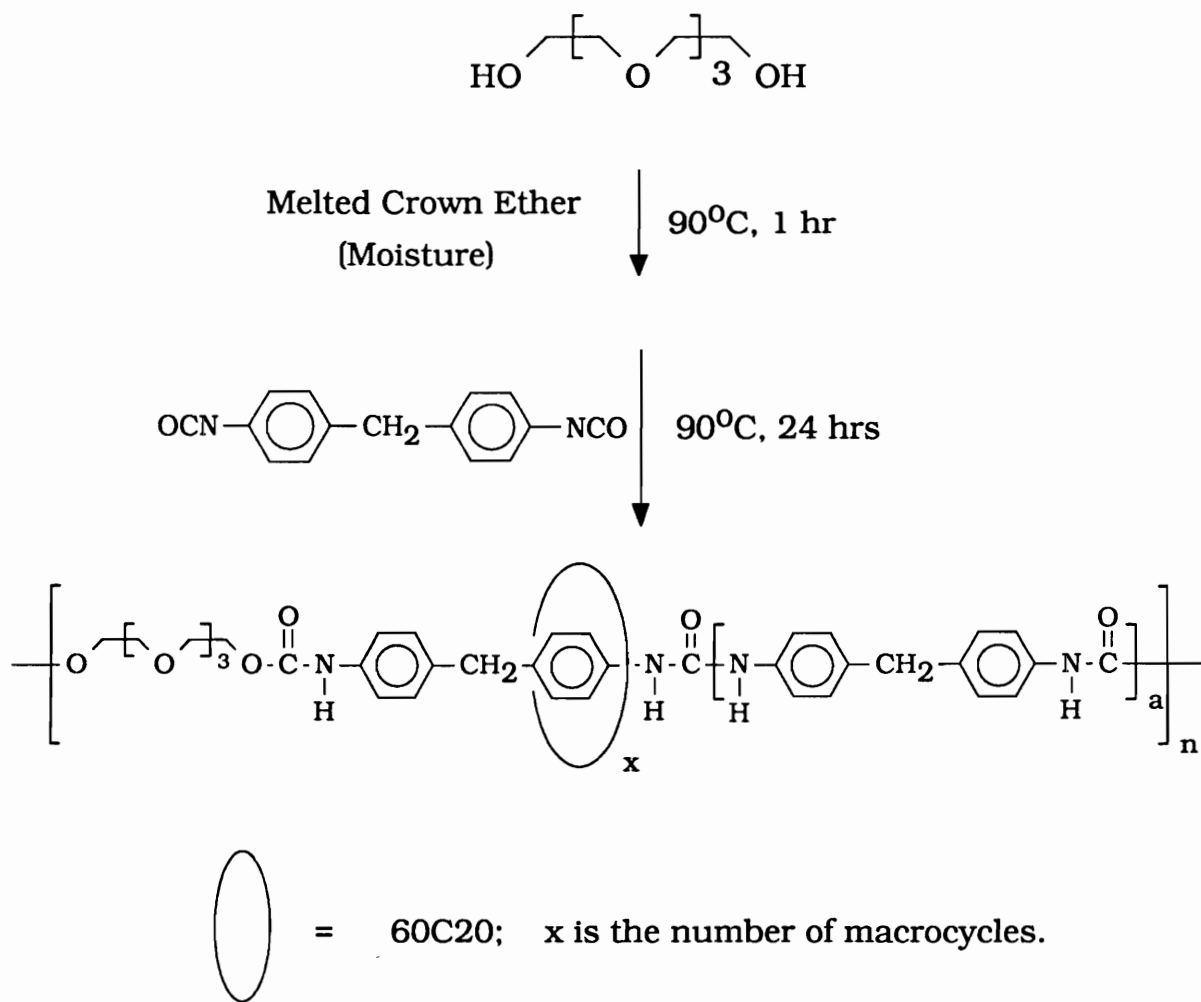
IV-6: Macrocycle = 36C12, $x/n = 0.16$

IV-7: Macrocycle = 42C14, $x/n = 0.29$

IV-8: Macrocycle = 48C16, $x/n = 0.52$

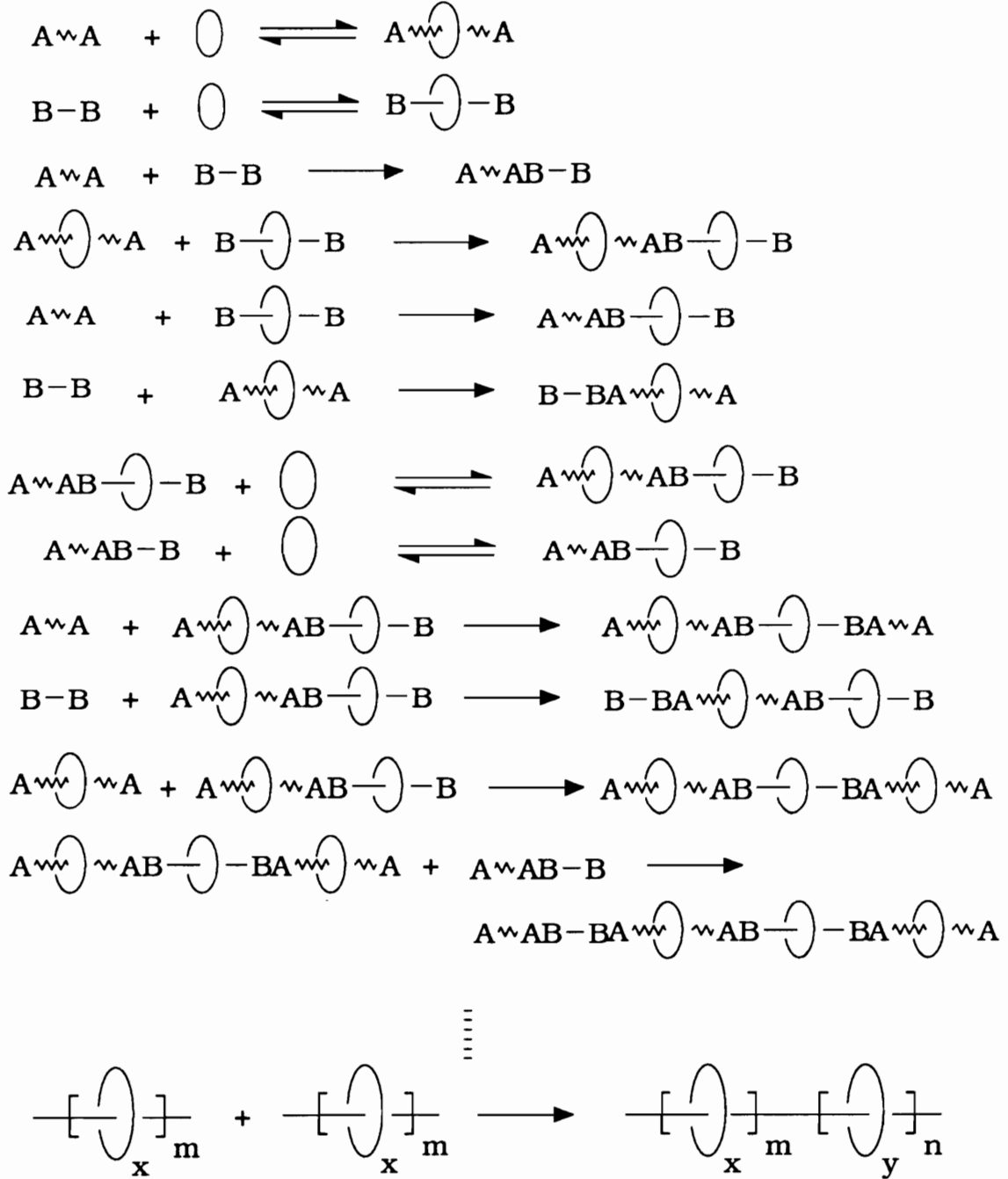
IV-9: Macrocycle = 60C20, $x/n = 0.87$

Scheme IV-7: Synthesis of a Polyurethane-urea-Based Polyrotaxane

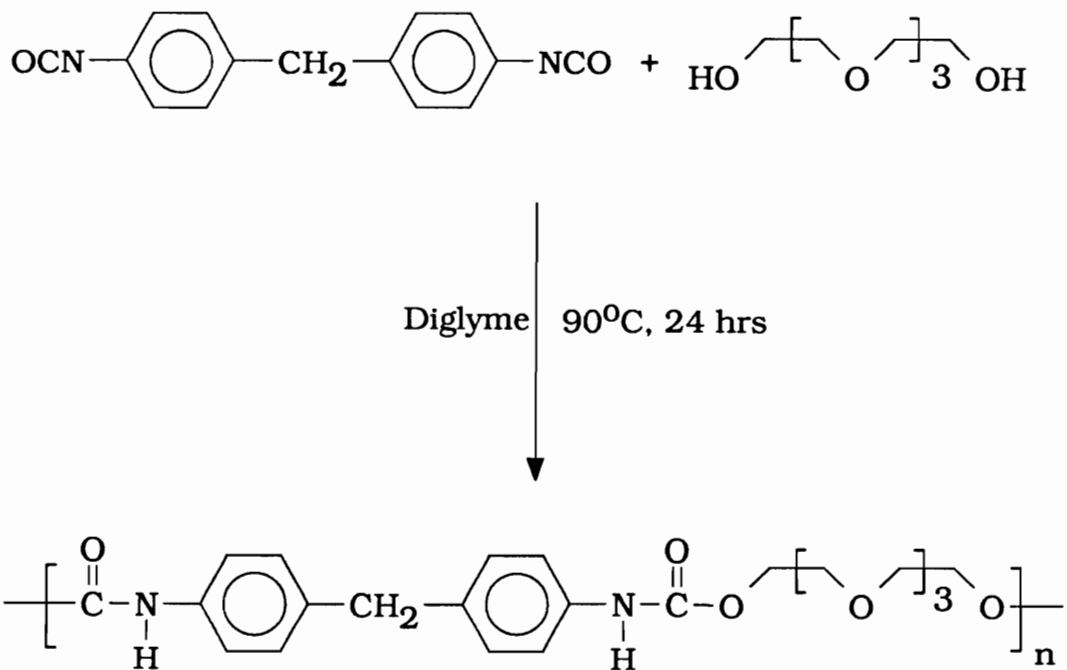


IV-10: $a/n = 0.55$, $x/n = 0.57$

Scheme IV-8: Threading Process

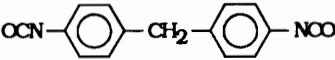
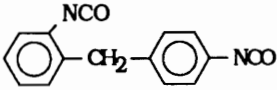
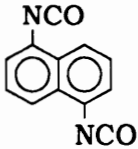
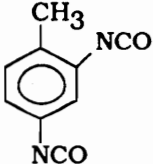
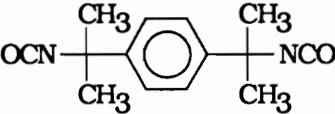


Scheme IV-9: Synthesis of Model Polyurethane



IV-11

Table IV-1: Some Examples of Polyfunctional Isocyanates

Name (abbreviation)	Structure	mp (°C)	bp(°C) (KPa)	Ref.
Diphenylmethane 4,4'- Diisocyanate (4,4'-MDI)		39.5	208 (1.33)	5
Diphenylmethane 2,4'- Diisocyanate (2,4'-MDI)		34.5	154 (0.17)	5
Naphthalene 1,5- Diisocyanate (NDI)		127	183 (1.33)	5
Toluene 2,4-Diisocyanate (TDI)		5.0	121 (1.33)	5
p-Phenylene Diisocyanate (PPDI)		94 - 95	260 (101.3)	6
p-Tetramethylylene Diisocyanate (p-TMXDI)		72	150 (0.40)	7

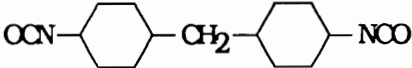
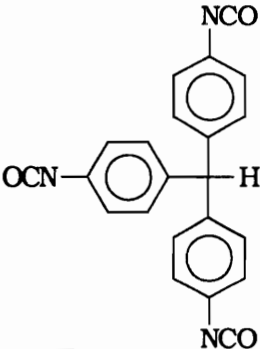
Dicyclohexylmethane 4,4'- Diisocyanate (H ₁₂ -MDI)		19 - 23	179 (0.12)	8 , 9
trans-cyclohexane 1,4- Diisocyanate (CHDI)		58 - 62	260 (101.5)	6
Hexamethylene Diisocyanate (HDI)	$\text{OCN}(\text{CH}_2)_6\text{NCO}$	- 67	127 (1.33)	5
Triphenylmethane 4,4',4''- Diisocyanate (Desmodur R ⁰)		89 - 90	-	10

Table IV-2: Some Examples of Polyols Used in Laboratory¹¹

Name	Structure	m.p. or b.p. (°C)
Ethylene glycol	$\text{HOCH}_2\text{CH}_2\text{OH}$	b.p. 196 - 198
Di(ethylene glycol)	$\text{HO}(\text{CH}_2\text{CH}_2\text{O})_2\text{H}$	b.p. 245
Tri(ethylene glycol)	$\text{HO}(\text{CH}_2\text{CH}_2\text{O})_3\text{H}$	b.p. 285
Tetra(ethylene glycol)	$\text{HO}(\text{CH}_2\text{CH}_2\text{O})_4\text{H}$	b.p. 314
Penta(ethylene glycol)	$\text{HO}(\text{CH}_2\text{CH}_2\text{O})_5\text{H}$	b.p. 184/2 mm
Hexa(ethylene glycol)	$\text{HO}(\text{CH}_2\text{CH}_2\text{O})_6\text{H}$	b.p. 217/4 mm
1,4-Butanediol	$\text{HO}(\text{CH}_2)_4\text{OH}$	b.p. 230
1,6-Hexanediol	$\text{HO}(\text{CH}_2)_6\text{OH}$	b.p. 250
1,10-Decanediol	$\text{HO}(\text{CH}_2)_{10}\text{OH}$	b.p. 170/8 mm

Poly(tetramethylene oxide) 650	$\text{HO}(\text{CH}_2\text{CH}_2\text{CH}_2\text{CH}_2\text{O})_{8.77}\text{H}$	-
Poly(tetramethylene oxide)- 1000	$\text{HO}(\text{CH}_2\text{CH}_2\text{CH}_2\text{CH}_2\text{O})_{13.62}\text{H}$	-
Poly(tetramethylene oxide)- 2000	$\text{HO}(\text{CH}_2\text{CH}_2\text{CH}_2\text{CH}_2\text{O})_{27.49}\text{H}$	-
Glycerin	$\text{HOCH}_2\text{CH}(\text{OH})\text{CH}_2\text{OH}$	b.p. 182/20 mm
Penterythritol	$\text{C}(\text{CH}_2\text{OH})_4$	

Table IV-3: Some Examples of Polyols Used in Industry⁵

Structure	MW Average	Hydroxyl number	Hydroxyl Content (%)
Propylene Glycol, Propylene Oxide	2,000 +/- 100	56 +/- 3	1.6 to 1.8
Trimethylolpropane, Ethylene Oxide, Propylene Oxide	4,800 +/- 300	35 +/- 2	1.00 to 1.13
Trimethylolpropane, Propylene Oxide	440 +/- 35	380 +/- 25	10.7 to 12.6
Sucrose, Propylene Glycol, Propylene Oxide	860 +/- 60	380 +/- 25	10.7 to 12.3
Glycerin, Propylene Oxide	3,000 +/- 200	56 +/- 3	1.6 to 1.8
Adipic Acid, Diethylene Glycol, Small Amount of Trimethylolpropane	ca. 2,400	57 to 63	1.7 to 1.9
Adipic Acid, Phthalic Acid, Glycerin, 1,2-Propylene Glycol	ca. 1,000	205 to 221	6.2 to 6.7
Adipic Acid, Phthalic Acid, Oleic Acid, trimethylolpropane	ca. 930	350 to 390	10.6 to 11.8
Phthalic Acid, Maleic Acid, Trimethylolpropane	ca. 2,450	250 to 270	7.6 to 7.9
Adipic Acid, Ethylene Glycol	ca. 2,000	52 to 58	1.5 to 1.7

* Data is obtained from "Polyurethane handbook" edited by G. Oertel (see ref. 5)

Table IV-4: Monomer Feed^a and Polyrotaxane Compositions^b after Reprecipitations

Polymer	IV-6	IV-7	IV-8	IV-9	IV-10
Monomer Feed^a	1.50	1.50	1.52	1.50	1.07
Repreci. Nonsolv.^c	Water	Methanol	Ethyl Acetate	Ethyl Acetate	Ethyl Acetate
1st. Repreci.	0.19	0.36	0.69	1.05	0.90
2nd. Repreci.	0.15	0.30	0.58	0.99	0.55
3rd. Repreci.	0.16	0.29	0.52	0.88	0.58
4th. Repreci.	0.16	0.29	0.52	0.87	0.57
Final wt% of Cyclic	16	29	45	63	53

a. Molar ratio of Crown Ether to Tetra(ethylene glycol)

b. Crown Ethers Per Repeat Unit (x/n value) Determined by ¹H-NMR analysis.

c. The solvent was THF in all cases.

Table IV-5: Threading Efficiencies

Polymer	Crown Ether	Monomer Feed Molar Ratio (Crown/Glycol)	Threading Efficiency (\bar{x}/n)
IV-6	36C12	1.50	0.16
IV-7	42C14	1.50	0.29
IV-8	48C16	1.52	0.52
IV-9	60C20	1.50	0.87
IV-10	60C20	1.07	0.57

Table IV-6: Solubilities of the Polymers in Some Solvents

Polymer	Crown Ether	Water	Methanol	Methylene Chloride	Acetone
IV-6	36C12	No	No	Yes	Yes
IV-7	42C14	No	No	Yes	Yes
IV-8	48C16	Yes*	No	Yes	Yes
IV-9	60C20	Yes*	No	Yes	Yes
IV-10	60C20	No	No	Yes	Yes
IV-11	-----	No	No	Slightly	No

* Exhibit Lower Critical Solution Temperature.

Table IV-7: Upper Cloud Points at Different Concentrations of Polyurethane-rotaxa-60-crown-20/Water System

C x 10³ (g/mL)	Cloud Point (+ °C)
3.50	86.5
2.63	87.0
2.10	87.0
1.05	88.0
0.70	88.0

Table IV-8: Intrinsic Viscosities of Polyurethane-Based Polyrotaxanes and the Model Polyurethane

Polymer	Crown Ether	[η] (dl/g)
IV-6	36C12	0.24
IV-7	42C14	0.45
IV-8	48C16	0.24
IV-9	60C20	0.27
IV-11	None	0.40

* Solvent: NMP; Temperature: 25.8°C.

Table IV-9: GPC Molecular Weights Determined Under Condition (1)^a

Polymer	$M_n \times 10^{-3}$		$M_w \times 10^{-3}$		M_w/M_n	
	Univ. ^b	PS ^c	Univ.	PS	PS	Univ.
IV-6	4.61	11.3	11.3	16.6	1.48	2.45
IV-7	6.69	29.6	10.6	59.7	2.02	1.58
IV-8	4.76	13.9	11.6	19.5	1.41	2.44
IV-9	6.34	16.5	13.2	21.3	1.29	2.08
IV-10	5.67	7.54	10.5	13.4	1.77	1.85
IV-11	8.82	14.8	16.5	32.4	2.19	1.87

a. The solvent used for GPC analyses was NMP.

b. Molecular weights based on universal calibration.

c. Molecular weights based polystyrene calibration.

**Table IV-10: GPC Molecular Weights Determined
Under Condition (2)^a**

Polymer	$M_n \times 10^3$	$M_w \times 10^3$	M_w/M_n
IV-6	7.24	10.8	1.50
IV-7	19.3	37.5	1.95
IV-8	7.01	10.6	1.51
IV-9	8.03	13.3	1.65
IV-11	12.1	27.0	2.24

* The solvent used for the GPC analyses was THF and the molecular weights were determined based on polystyrene calibration.

**Table IV-11: Viscosity Molecular Weights, Mark-Houwink Constants
and Calculated Intrinsic Viscosities**

Polymer	$M_v \times 10^{-3}$	a	$K \times 10^3$	$[\eta]$ (dl/g)
IV-6	10.1	0.312	8.974	0.16
IV-7	9.95	0.659	2.483	1.07
IV-8	11.0	0.494	1.982	0.20
IV-9	13.0	0.712	0.2564	0.22
IV-10	10.3	0.792	0.1361	0.21
IV-11	15.1	0.578	1.334	0.36

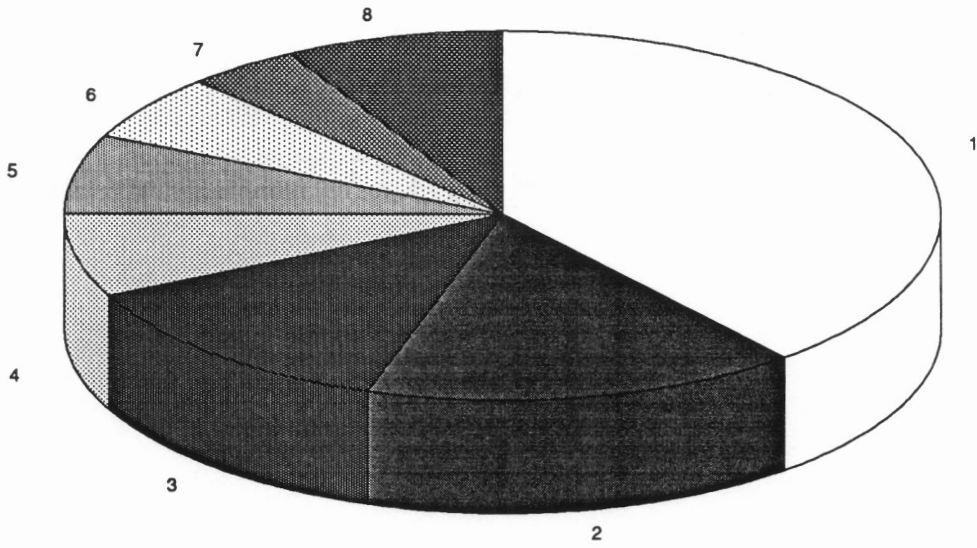
* Data were obtained from GPC-Viscometry Analyses.

Table IV-12: The Melting Points of Crown Ethers: in Pure Solid State versus in Polyrotaxane Systems

Crown Ether	m.p. (°C) (in Pure Solid State) ^a	m.p. (°C) (in Polyrotaxane) ^b
36C12	37.0 - 37.5	not observed
42C14	53.6 - 54.4	not observed
48C16	49.6 - 50.8	39.5 (in IV-8)
60C20	52.2 - 53.9	46.2 (in IV-9)
60C20	52.2 - 53.9	40.0 (in IV-10)

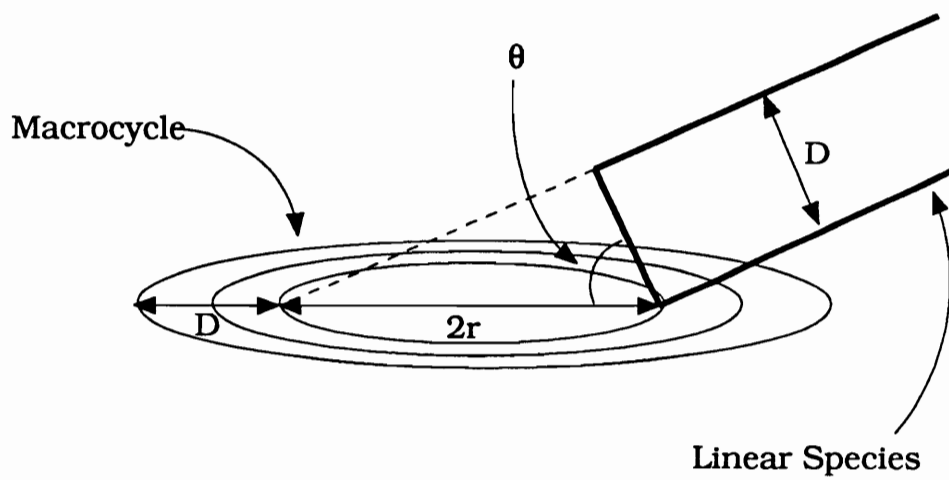
a. Measured on a HAAKE BUCHLER Capillary Melting Point Apparatus.

b. From DCS Analyses at 10°C/min.



1: Furniture, Bedding, 2: Automotive, 3: Construction, 4: Refrigerators and Freezers, 5: Coating, 6: Textile Industry and Carpet Backing, 7: Shoe Soles, 8: Miscellaneous.

Figure IV-1: Polyurethane Applications.⁵



$$\cos\theta = D/2r$$

Figure IV-2: Illustration of Threading Angles.

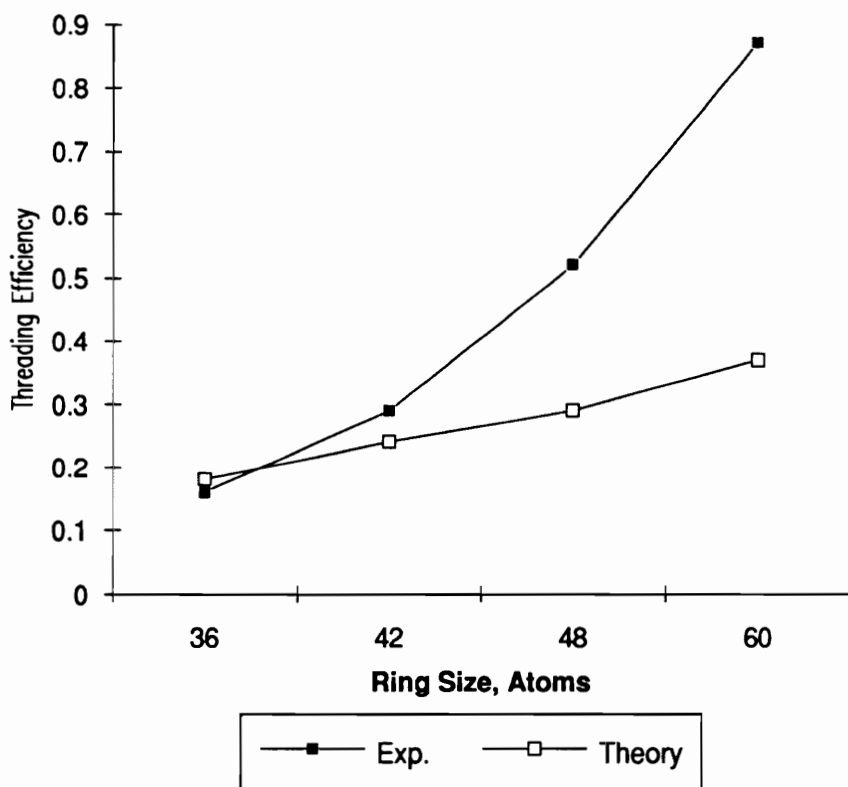


Figure IV-3: Plot of Threading Efficiency Versus Ring Size of Crown Ether Represented by Skeletal Atoms. Neat Reactions, Monomer Feed Molar Ratio: Crown/Glycol = 1.5.

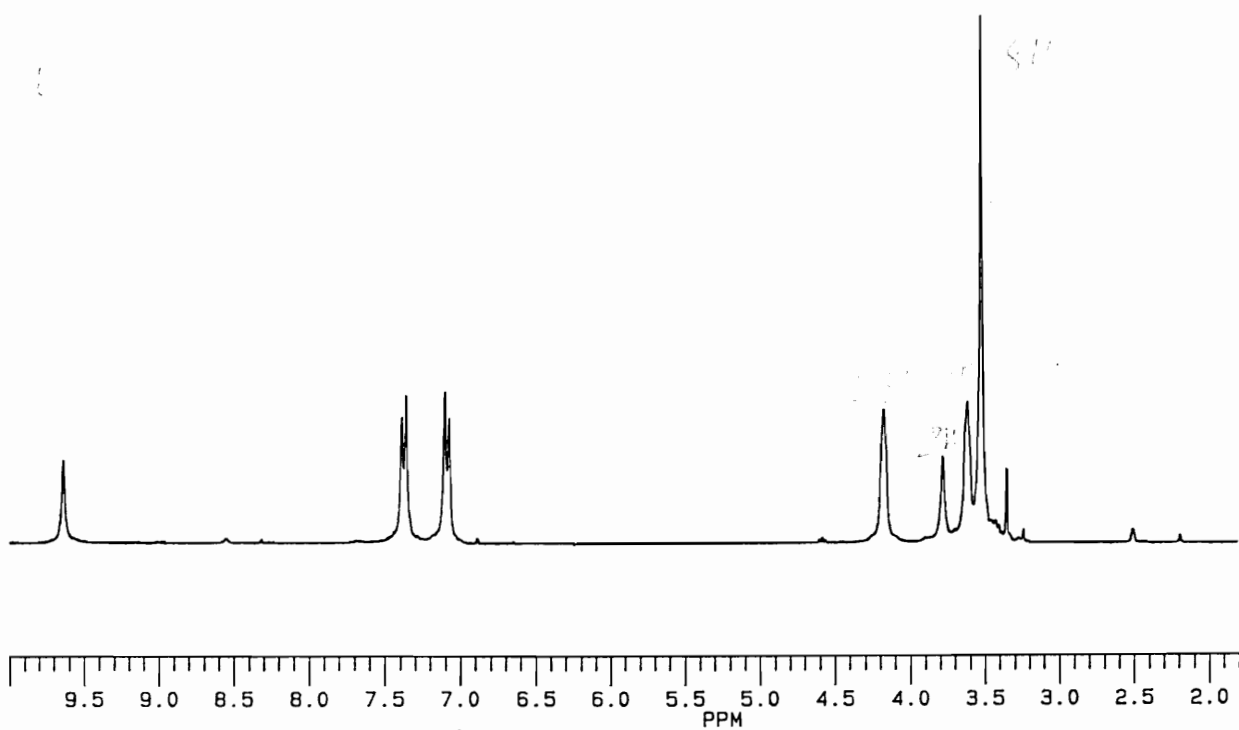
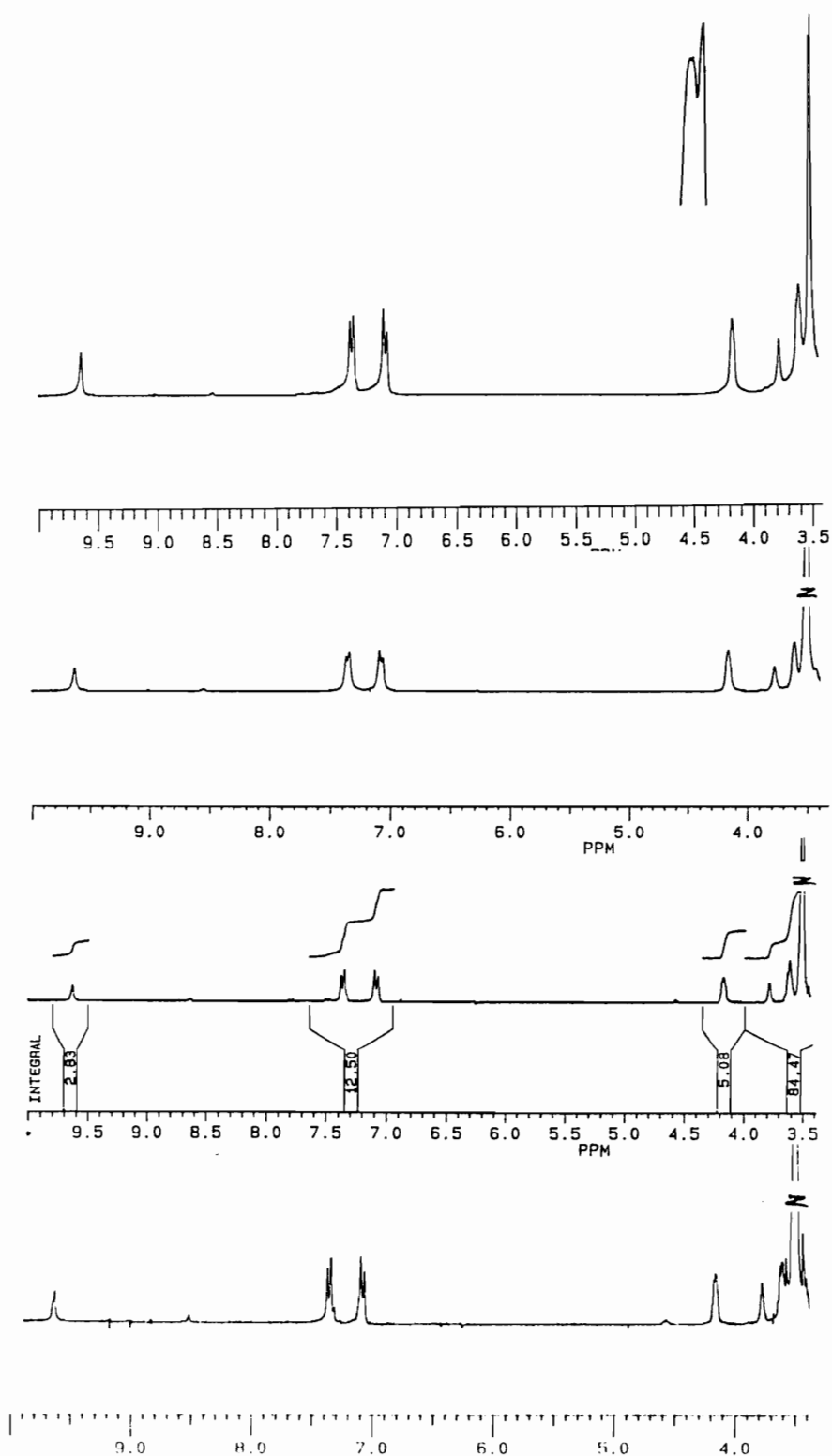


Figure IV-4: $^1\text{H-NMR}$ Spectra of the Model Polyurethane (IV-11).



**Figure IV-5: $^1\text{H-NMR}$ Spectra of Polyurethane-Based Polyrotaxanes:
 (a) IV-6, (b) IV-7, (c) IV-8 and (d) IV-9.**

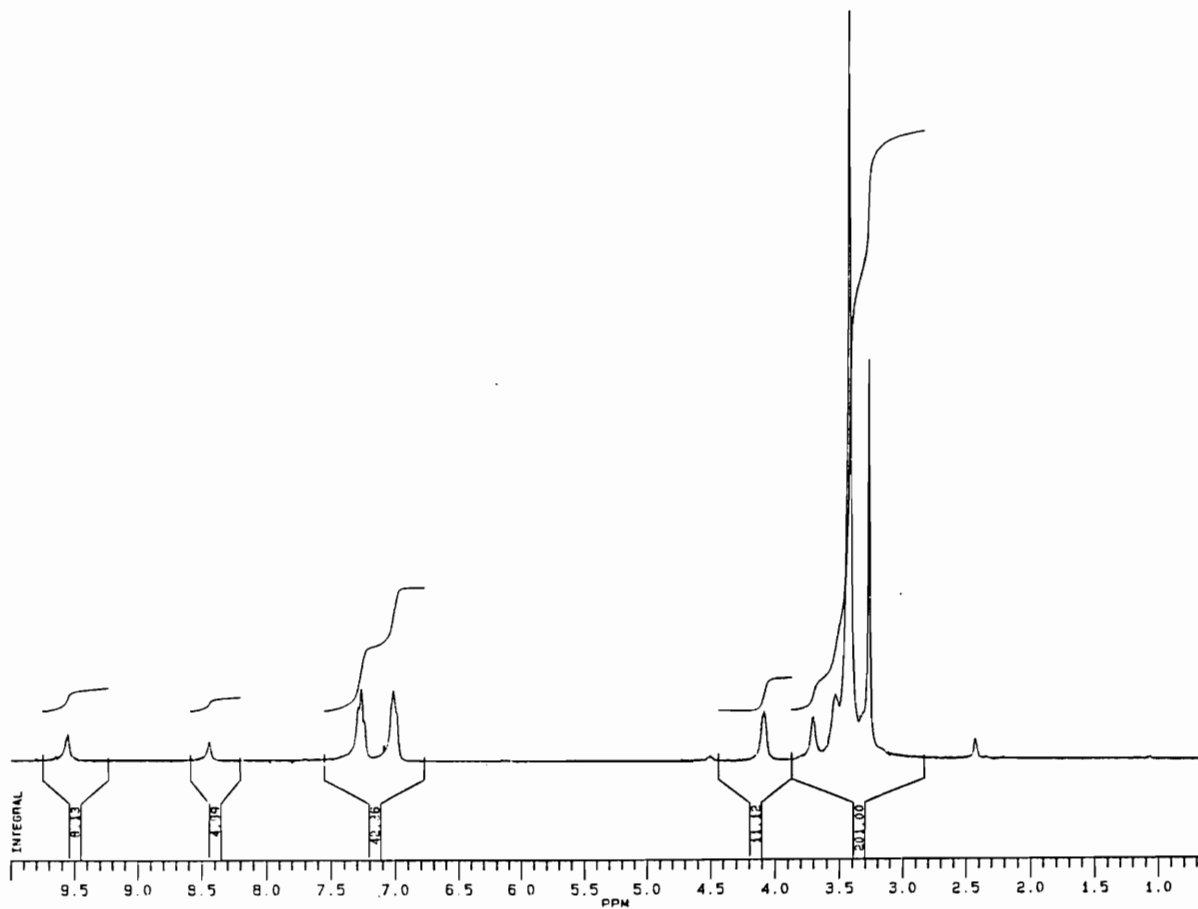


Figure IV-6: $^1\text{H-NMR}$ Spectra of Polyurethane-urea-Based Polyrotaxane (IV-10).

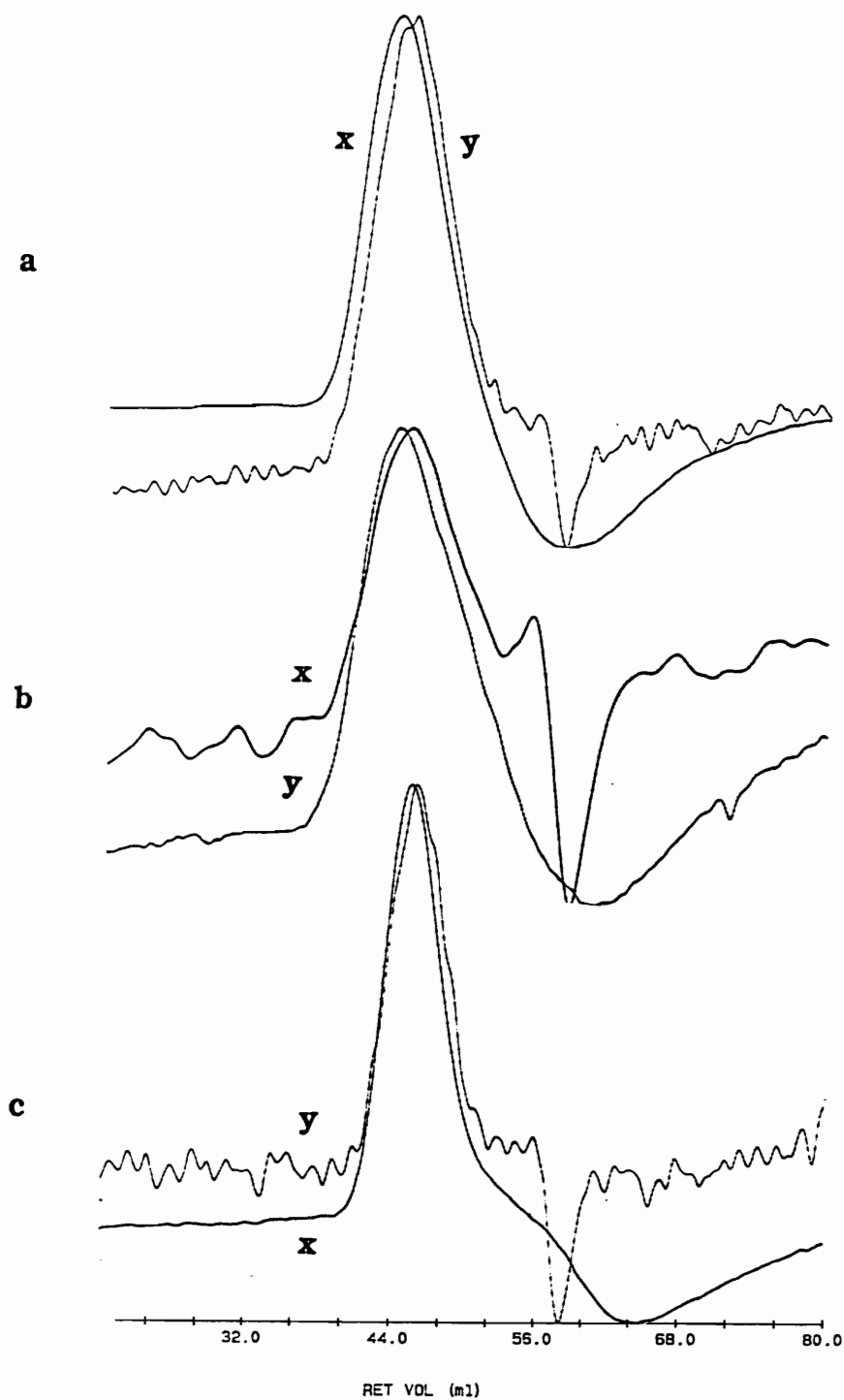


Figure IV-7: GPC Traces of (a) Model Polyurethane (IV-11), (b) Blend of IV-11 with 50 wt% of 60C20 and (c) Polyrotaxane (IV-9). Solvent was NPM + LiBr (0.006 M). x: Traces Recorded by Viscosity Detector; y: Traces Recorded by RI Detector.

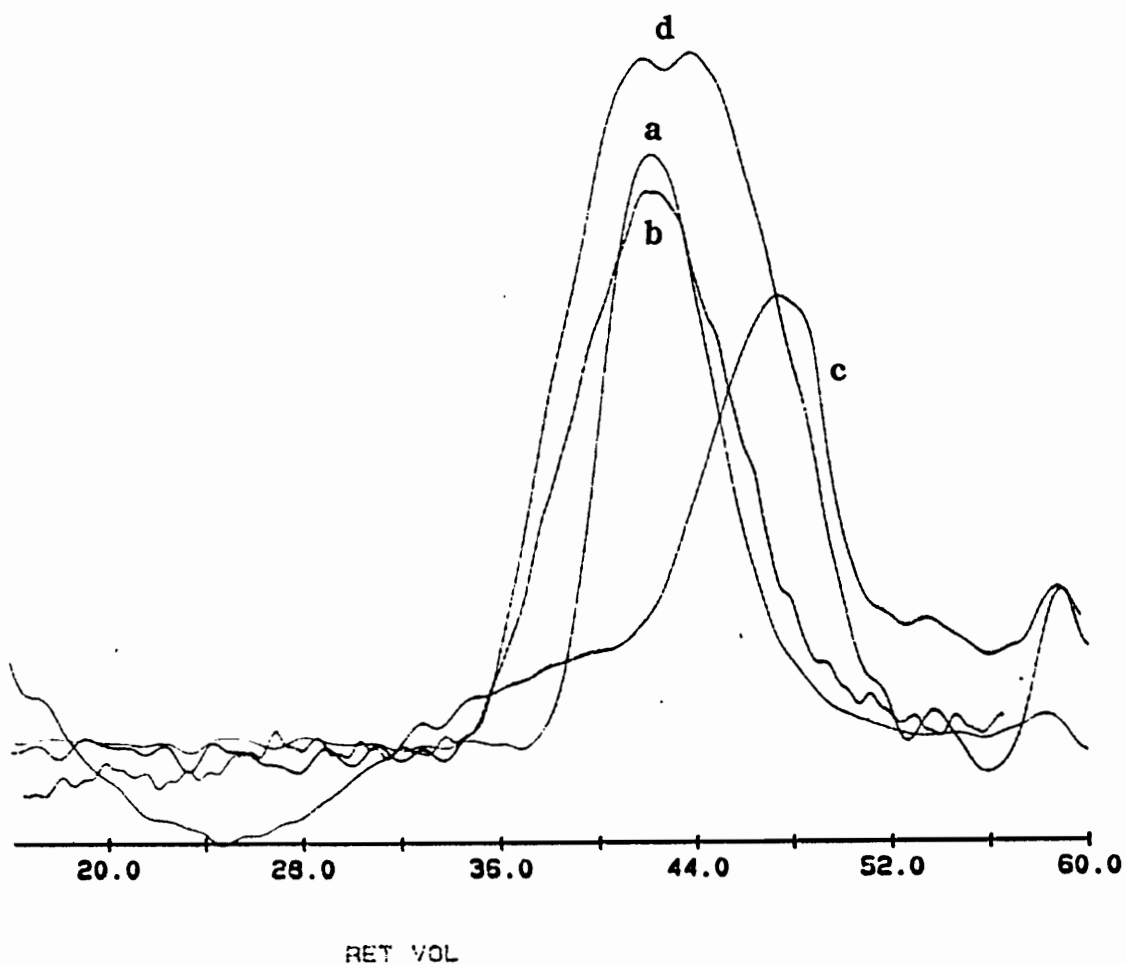


Figure IV-8: GPC Traces of (a) Polyurethane-rotaxa-60C20 (IV-9), (b) Model Polyurethane (IV-11), (c) 60C20 and (d) a Blend Containing IV-11 and 47 wt% of 60C20. Solvent: THF.

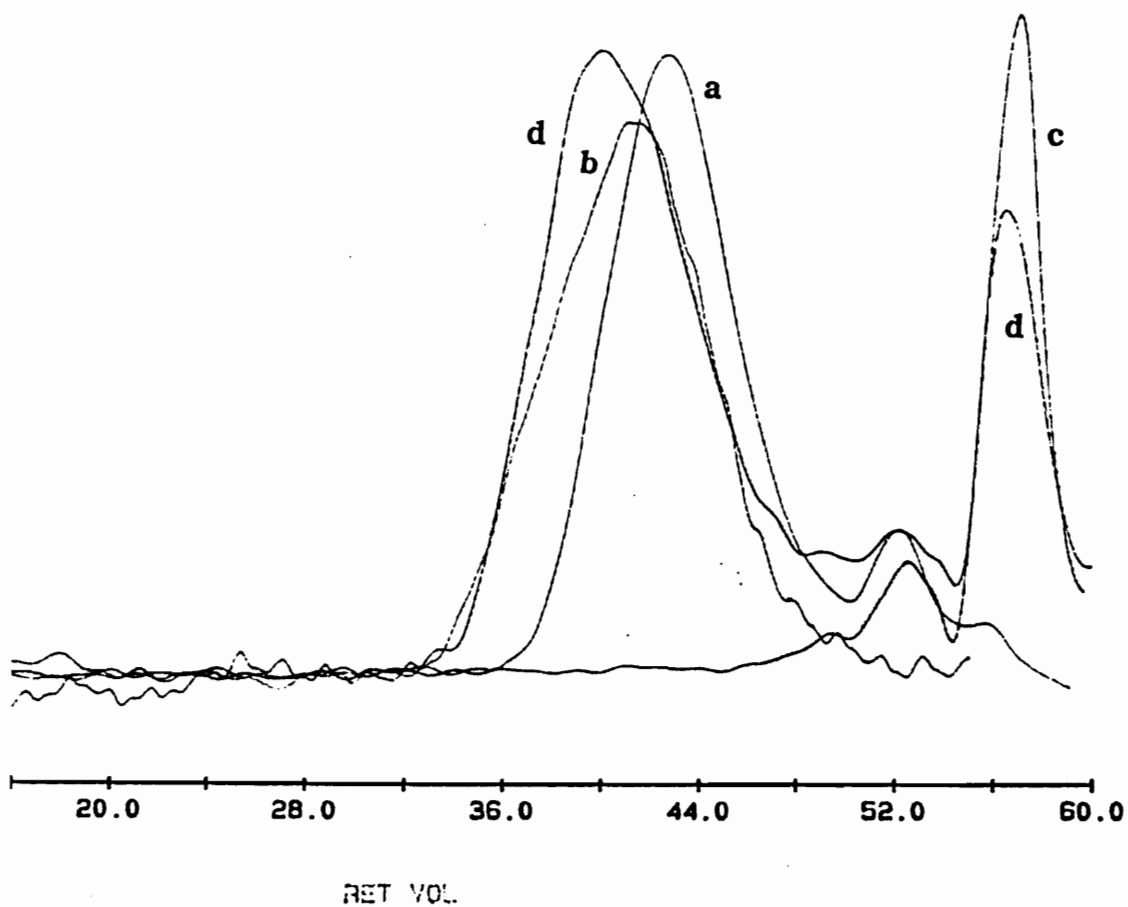


Figure IV-9: GPC Traces of (a) Polyurethane-rotaxa-36C12 (IV-6), (b) Model Polyurethane (IV-11), (c) 36C12 and (d) a Blend Containing IV-11 and 25 wt% of 36C12. Solvent: THF.

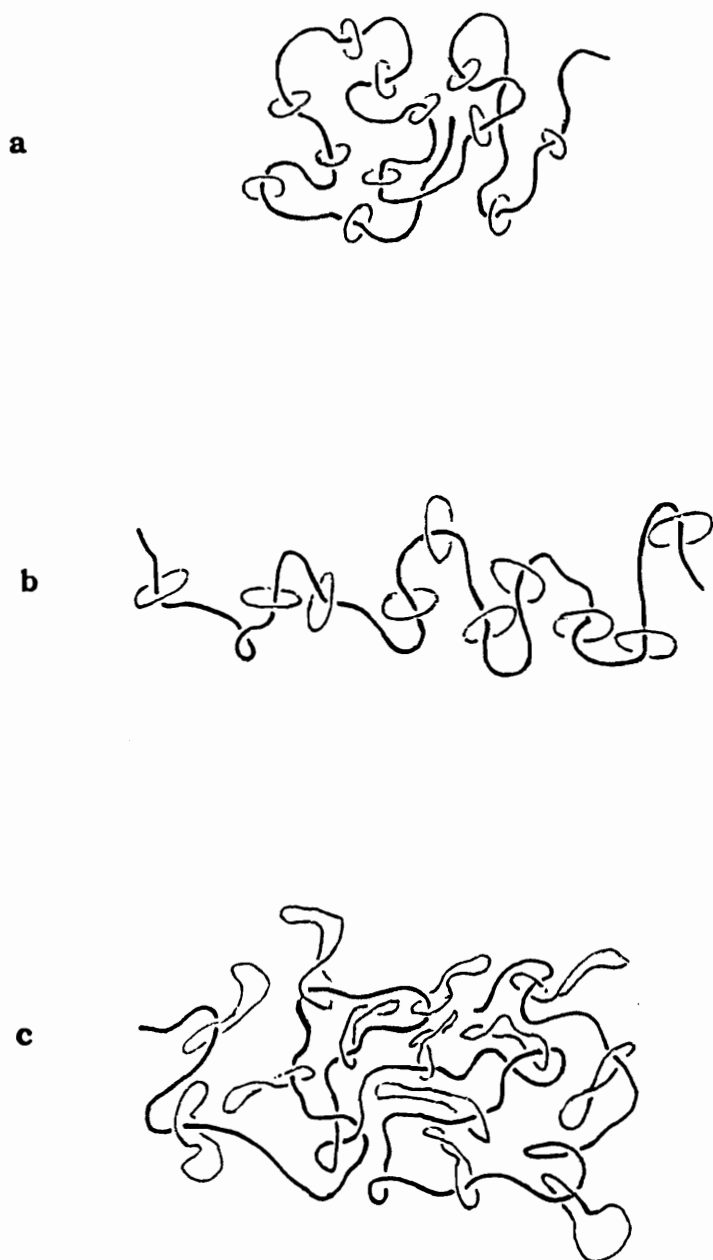


Figure IV-10: Illustration of Possible Effect of Ring Size on the Random Coils of Polyrotaxanes. (a) Small Rings, (b) Medium Sized Rings, (c) Large Rings.

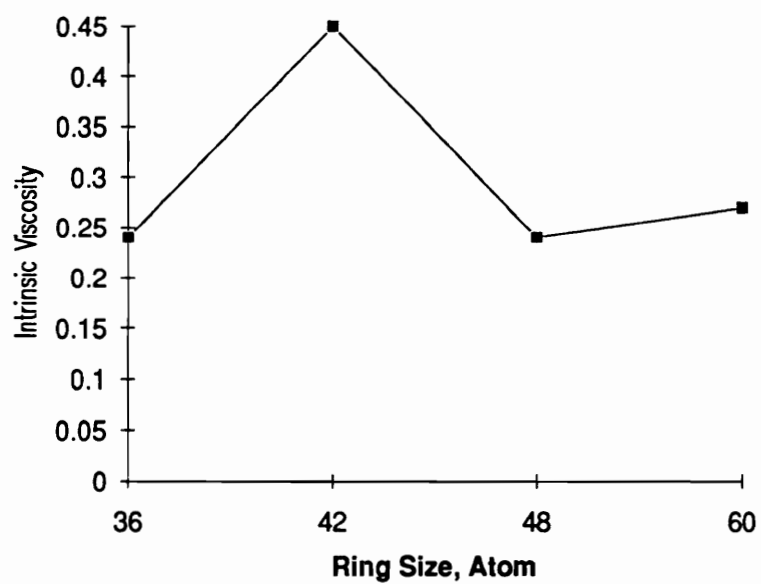


Figure IV-11: Plot of Intrinsic Viscosity versus Ring Size of Crown Ethers for Polyurethane-Based Polyrotaxanes.

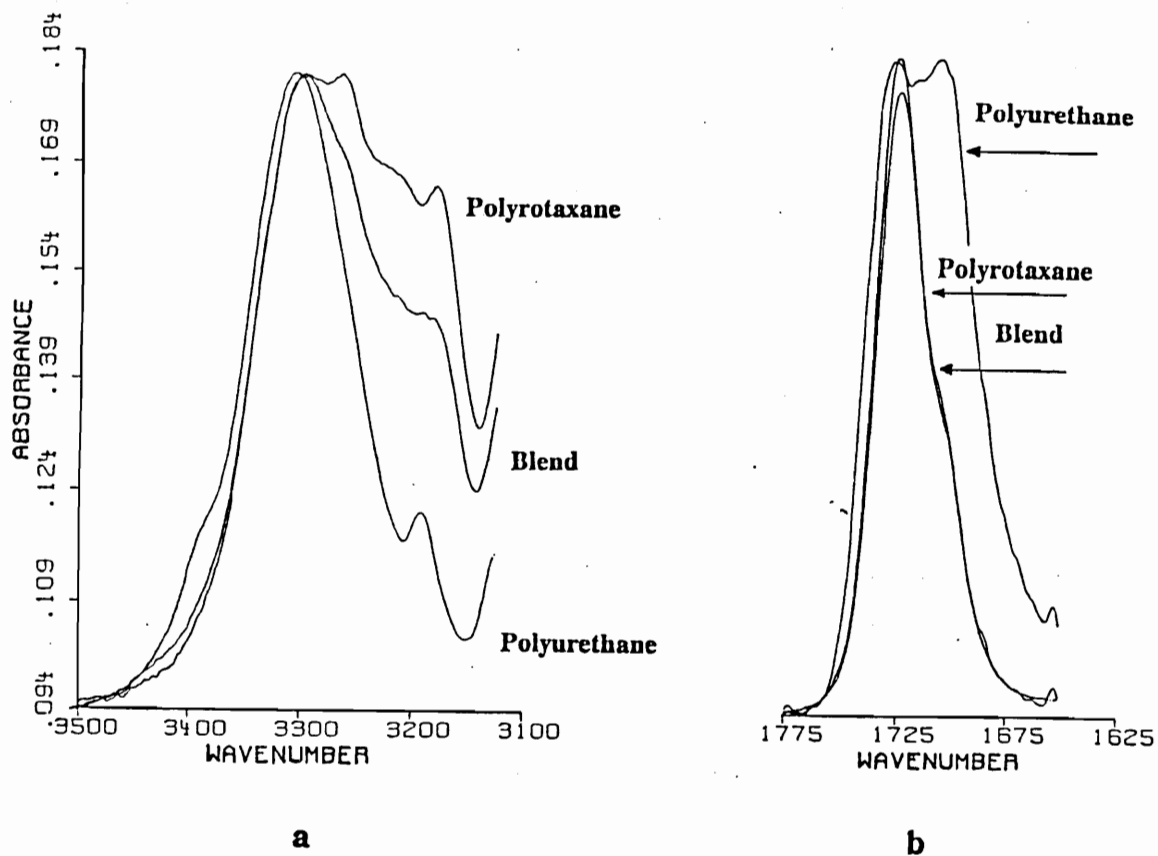


Figure IV-12: FTIR Spectra of Thin Films of Polyurethane-rotaxa-60C20 (IV-9), Model Polyurethane (IV-11) and a Blend Containing IV-11 and 60C20 in the Same Weight Percent of that in the IV-9: (a) N-H Stretch and (b) Carbonyl Stretch.

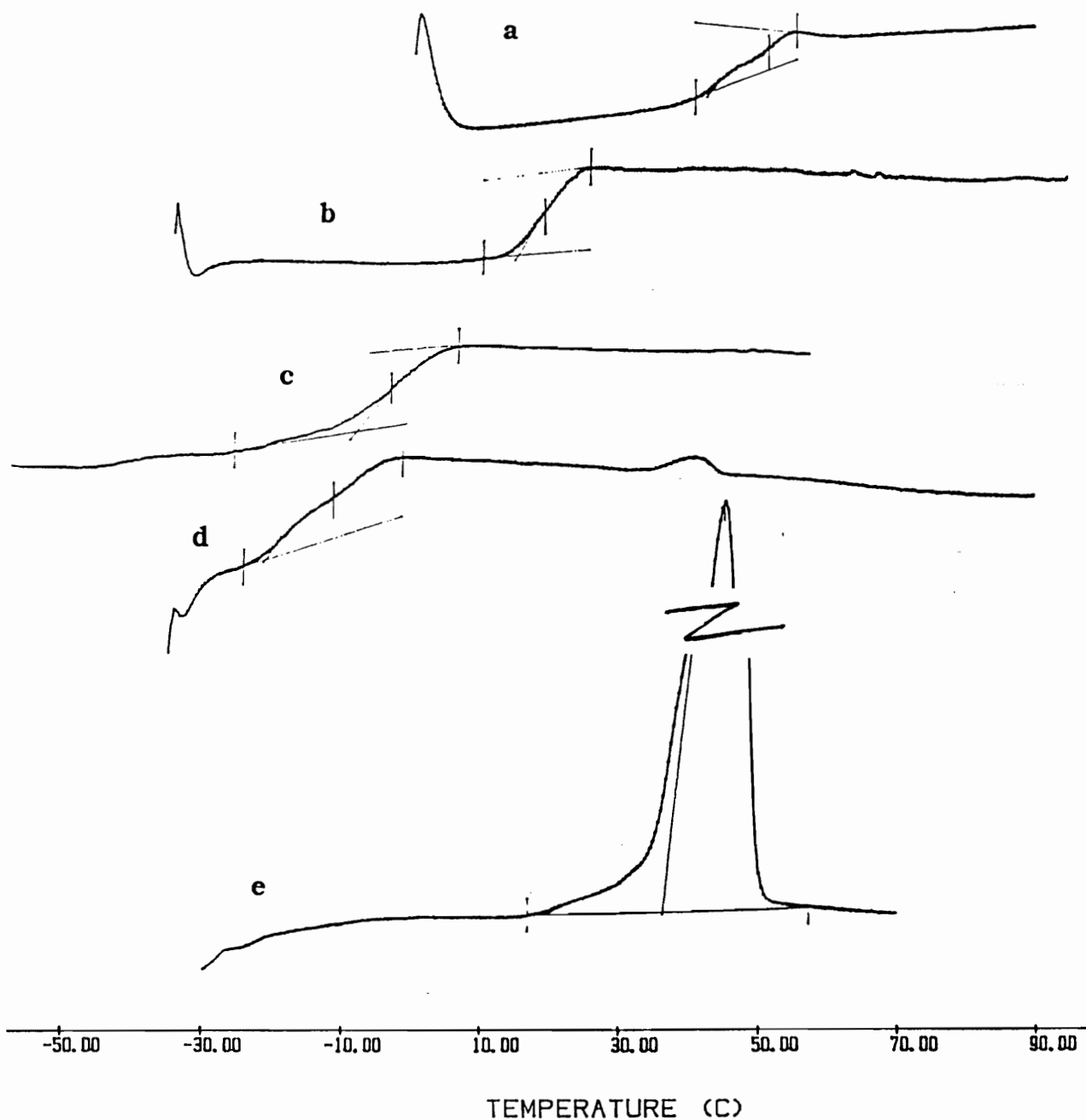


Figure IV-13: DSC Traces of (a) the Model Polyurethane (IV-11), (b) Polyurethane-rotaxa-36C12 (IV-6), (c) Polyurethane-rotaxa-42C14 (IV-7), (d) Polyurethane-rotaxa-48C16 (IV-8) and (e) Polyurethane-rotaxa-60C20 (IV-9).

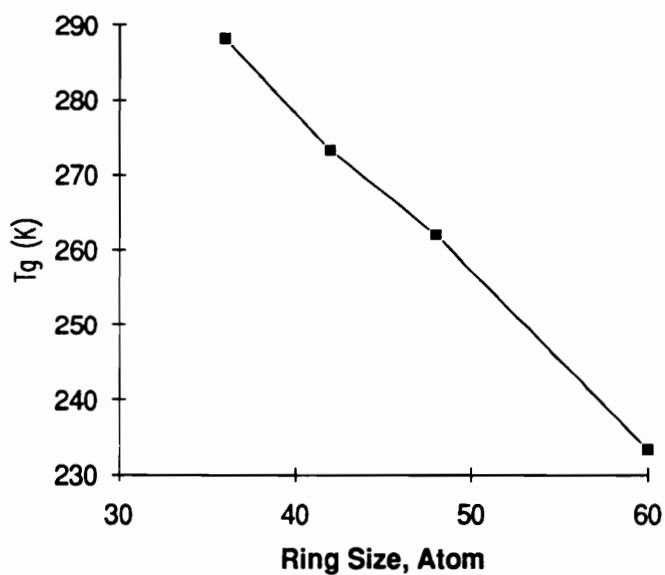


Figure IV-14: Plot of Glass Transition Temperature of Polyurethane-Based Polyrotaxane versus Ring Size of Crown Ether Incorporated.

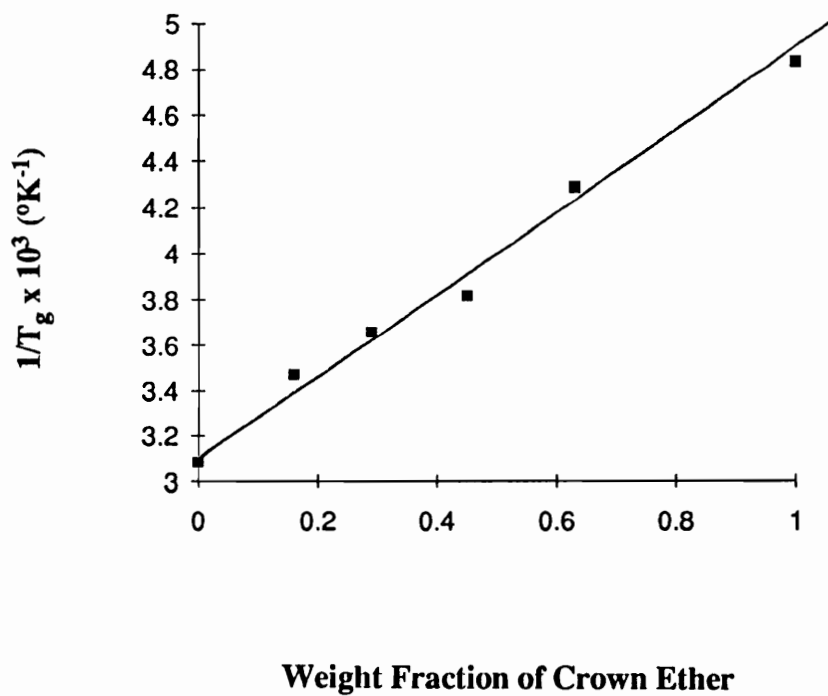


Figure IV-15: Application of Fox Equation to the Polyrotaxane Systems.

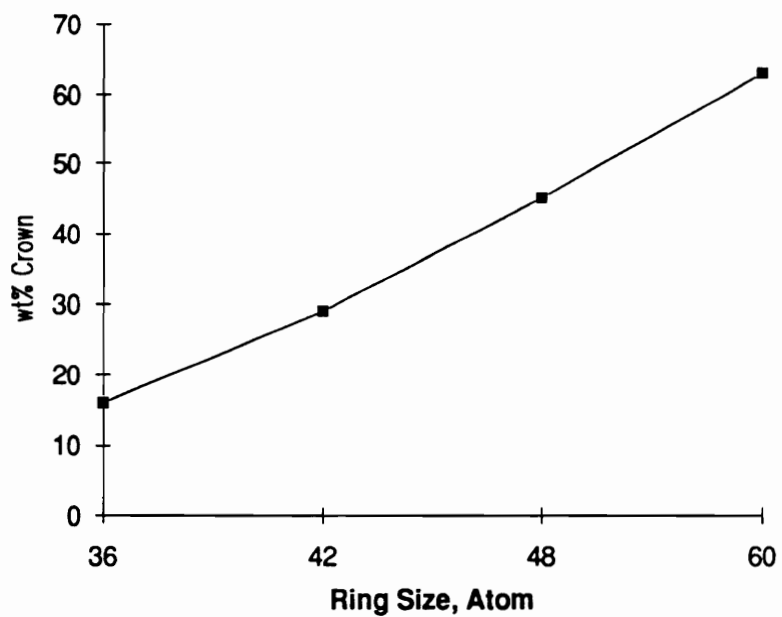
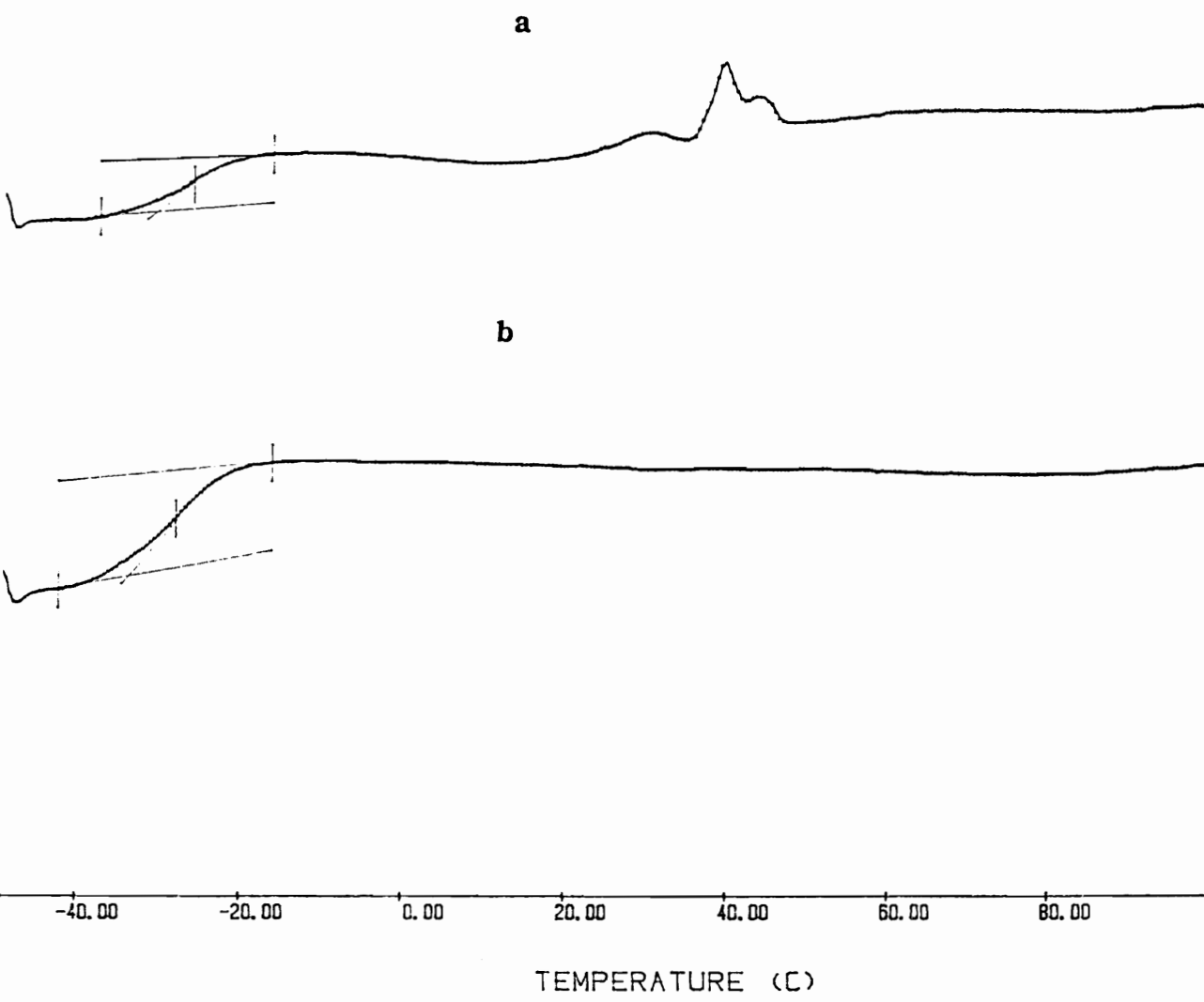


Figure IV-16: Plot of Weight Percentage of Crown Ethers versus Ring Size in Polyrotaxanes.



**Figure IV-17: DSC Traces of Polyurethane-urea-rotaxa-60C20 (IV-10):
(a) First Run after the Sample Was Aged for Six Months
at Room Temperature and (b) Second Run after
Naturally Cooling.**

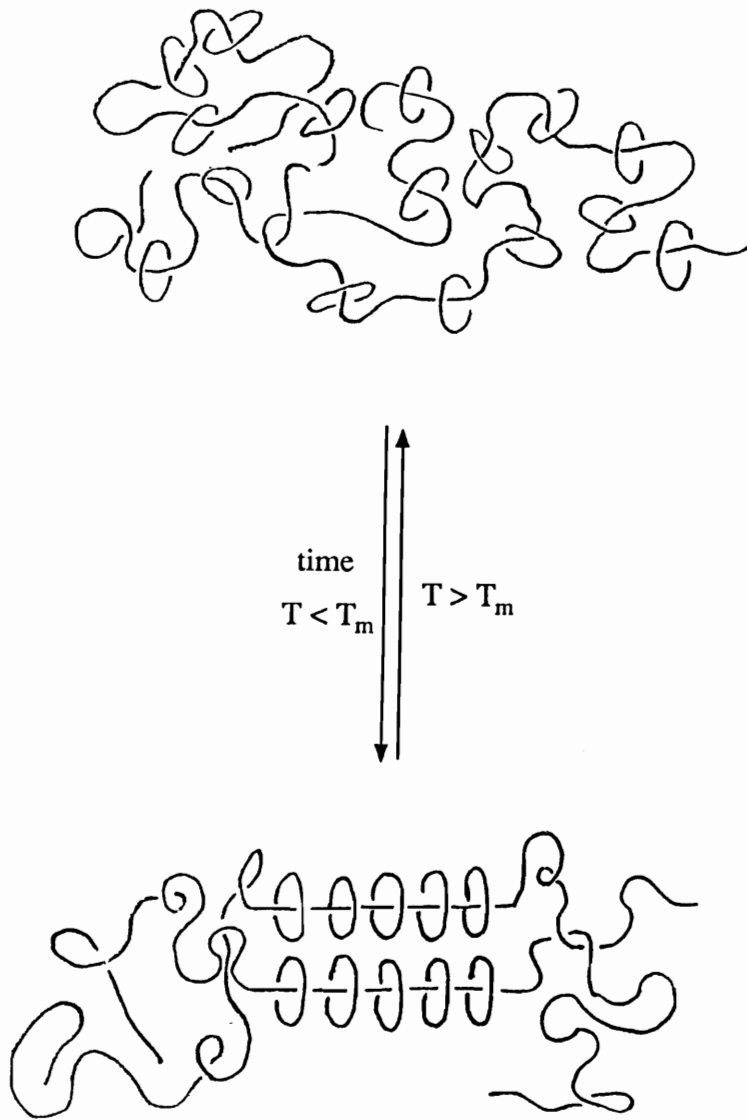


Figure IV-18: Illustration of Macrocycle Recrystallization Process in a Polyrotaxane System.

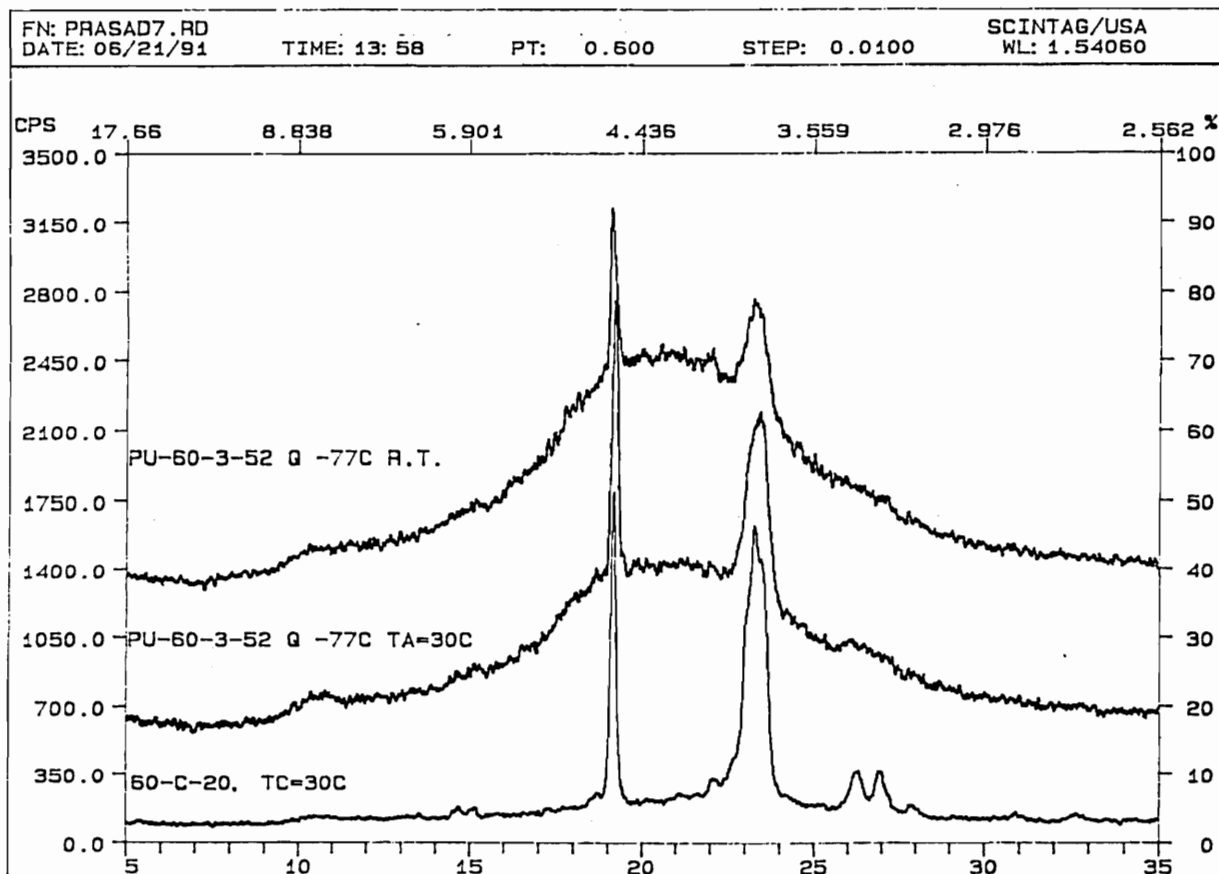


Figure IV-19: Wide Angle X-Ray Diffraction Patterns of 60C20 at 30°C (a), Polyurethane-rotaxa-60C20 (IV-9) at 30°C (b) and at Room Temperature (c).

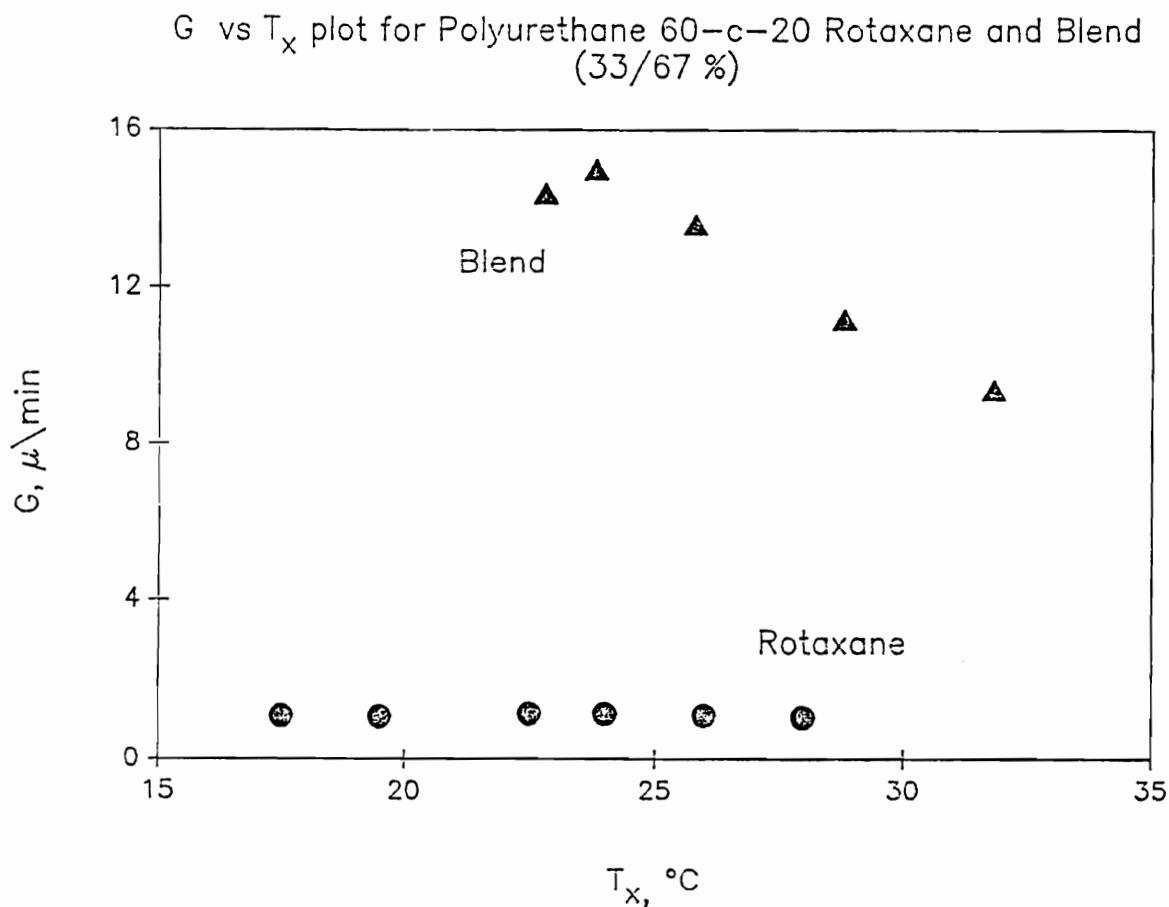


Figure IV-20: Plot of Spherulite Growth Rate (G) versus Crystallization Temperature (T_x) for Polyurethane-rotaxa-60C20 (IV-9) and a Physical Blend Containing Model Polyurethane (IV-11) and 60C20 in the Same Composition as IV-9.

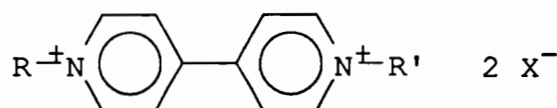
CHAPTER V:
HOST-GUEST COMPLEXATION OF
PARAQUAT DICATION DERIVATIVES
AND BPP34C10.
PART 1: ROTAXANE MODEL STUDIES

In chapter IV, I used the statistical threading method for polyrotaxane syntheses. The threading efficiency, however, is limited by many variables such as ring size, chain length, ring and chain rigidity, concentration, etc., since this method is predominantly entropy driven. To increase the threading efficiency, on the other hand, one could introduce negative enthalpy changes to the threading process. This could be achieved by using the template effect. In that case, the enthalpy change, generally much larger than the entropy change, serves as a dominant driving force for the threading. The threading efficiency obtained by this method could be as high as quantitative ($x/n = 1.0$). As discussed in Chapter I, there are several different types of template syntheses of interlocking molecules including rotaxanes and catenanes. In the following two chapters, I will report the template syntheses of monomeric and polymeric rotaxanes via the host-guest complexation of paraquat dication derivatives and BPP34C10. This is a bimolecular self-

assembling process without the addition of any foreign species. In other words, the paraquat dication derivatives (linear species) and BPP34C10 (cyclic species) serve as templates for each other.

V-1: PARAQUAT DICATION DERIVATIVES¹

Paraquat dication derivatives, also called viologens, have the structure shown as IV-1. The basic unit of this class of compounds is the diquaternary salt of 4,4'-bipyridyl. Generally R and R' groups are -CH₃, -CH₂CH₃, -Ph, -CH₂Ph, -CH₂CH₂OH, -CH₂CH₂COOH, -CH₂CH₂COOCH₃, etc. and X is Cl, Br, I, PF₆, CH₃SO₄, SCN, etc.



IV-1

V-1-1: SYNTHESIS

The classical and still commonly used method to synthesize paraquat dication derivatives is based on Menschutkin reaction, the reaction of 4,4'-dipyridyl and an alkyl halide or other alkylating agent; the latter are generally used in excess amount. The reactions are performed in a solvent and the product, in most of cases, precipitates out of the reaction medium in over 90% yield. The direct reaction of 4,4'-dipyridyl and an excess amount of an alkylating agent produces a

paraquat dication with $R = R'$. If the stoichiometry is one to one, a monocation is obtained and if this monocation salt is further treated with another alkylating agent, a paraquat dication salt with R different from R' results. The first paraquat dication derivatives were synthesized by this method. Anderson synthesized a paraquat salt with $R = R' = -CH_2CH_3$ and $X = I$ in 1870.² However, the structure was authenticated by Weidel *et al.* in 1882 and then they also synthesized the paraquat salt $R = R' = -CH_3$ and $X = I$.³ Since the paraquat dication derivatives are herbicidally active compounds, especially paraquat ($R = R' = -CH_3$), these compounds are industrially manufactured. This method plays the major role even though there are some other methods under investigation as possible manufacturing routes.

Some examples of paraquat dication derivatives are given in Table V-1 along with the reference sources.

V-1-2: GENERAL PROPERTIES

V-1-2-1: Physical Properties

The counter-ion of paraquat dication derivatives determines the color of the compounds. For example, the diiodide salts are usually red; the dibromides are yellow and the dichlorides and hexafluorophosphates are colorless. All paraquat dication derivatives are high melting. Most of them have melting points above 250°C (Table V-1). Some of them decompose before melting. The decomposed products are monoquaternary salts and 4,4'-dipyridyl.²² The melting points are

significantly effected by R and R' groups and counter-ions. When R = R' = Me and X = I, the compound melted above 330°C¹¹, however, if the R and R' were replaced by CH₂CH₂OEt (with X = I), the melting point dropped to 218 - 220°C;¹⁵ if the I's were replaced by PO(O)(SMe)(SEt) (with R = R' = Me), the melting point dropped to as low as 118°C.⁹

The compounds are more likely to be soluble in polar solvents such as DMSO, acetonitrile, water, methanol, etc. Similar to the melting points, the solubilities are effected by R and R' groups and counter-ions. For example, the halide salts are generally soluble in water if R and R' are not bulky hydrophobic groups;^{3,23} however, hexafluorophosphates are more like organic compounds and have good solubilities in organic solvents.²⁴⁻²⁶

The X-ray crystal structures of some paraquat dication derivatives have been obtained.²⁷⁻³⁰ As a general result, the the two pyridine rings of paraquat dication with R and R' groups are on the same plane. The bond lengths and angles for R = R' = Me are listed in Table V-2.

V-1-2-2: Chemical Properties

Paraquat dication derivatives are stable in acidic solutions but unstable in alkaline solutions^{31,32} and the decomposition mechanism in the alkaline condition is quite complicated.³³⁻³⁵

Paraquat dication derivatives can be reduced by many reducing agents. The reduction follows a multi-step mechanism and the final product is determined by the reducing agent. Generally they undergo

one-electron reduction with mild reducing agents such as zinc dust, sodium amalgam, nitric oxide in solution to gave a deep blue-violet color.³⁶⁻⁴ This two-step one-electron reduction process is illustrated in Scheme V-1. The first electron transfer step results in a deep colored radical cation **V-2** which further accepts one more electron to form a neutral compound **V-3**. The compound **V-3** is a strong reducing agent which is readily oxidized back to the paraquat dication.⁴¹

More complete reduction can be done by using stronger reducing agents or under extreme conditions. For examples, paraquat dication derivatives can be fully reduced to totally aliphatic biperidine derivatives by hydrogenation catalyzed by PtO₂.^{11,42} When NaBH₄ is used, the product is an octahydro-4,4'-bipyridine derivative.^{10,43}

Paraquat dication derivatives are electron poor systems and they act as electron acceptors in complexations with electron donor molecules. They can form complexes with metal salts such as silver(I) iodide, copper(I) chloride, mercury(II) iodide, lead(II) iodide, zinc nitrate etc.;^{44,45} with neutral organic molecules such as amines, phenols, acetic acid, urea, polycyclic hydrocarbon, etc.;⁴⁶⁻⁴⁸ even with their own associated counter-ions.⁴⁹ The complexation of paraquat dication with 7,7,8,8-tetracyanoquinodimethane (TCNQ) forms an electrically conducting material.⁵⁰ The TCNQ first forms an anion radical (TCNQ^{•-}) and the radical complexes with the paraquat dication. Different from normal charge transfer complexes, in the TCNQ salts, an unpaired electron is delocalized over the stacking domain of the TCNQ rings

leading to a relatively high electrical conductivity. The most interesting class of complexes, recently studied by Stoddart *et al.*, are the host-guest complexes of paraquat dication derivatives with bis(para-phenylene)-based crown ethers. This host-guest complexation is the basis of the viologen-containing rotaxane and polyrotaxane syntheses reported in this and next chapters. Detailed discussions of this complexation will appear in the next section.

V-2: HOST-GUEST COMPLEXATION OF BPP34C10 AND PARAQUAT DICATION DERIVATIVES

A research group in England headed by Prof. J. F. Stoddart has extensively studied the host-guest complexation of paraquat dication derivatives and BPP34C10 and successfully applied this complexation to catenane and rotaxane chemistry in the last decade. In this section, some of their important works will be reviewed.

V-2-1: X-RAY STRUCTURES AND CAVITY SIZE OF BPP34C10

The synthesis of BPP34C10 was reported in Chapter II. The X-ray crystal structures of this macrocycle have been obtained by Stoddart *et al.*⁵¹ The crystal data are reported as: C₂₈H₄₀O₁₀, M = 536.7, monoclinic, space group P2₁/c, a = 10.890(2), b = 21.450(6), c = 12.361(4) Å, β = 106.31(2)°, U = 2771 Å³, Z = 4 (2 independent

centrosymmetric molecules in the asymmetric unit), $D_c = 1.29 \text{ g cm}^{-3}$, $R = 0.052$, $R_w = 0.060$ for 2638 independent observed reflections [$\theta \leq 50^\circ$, $|F_o| > 3\sigma(|F_o|)$].

In the crystalline solid state, BPP34C10 exists in two crystallographically independent conformations as shown in Figure V-1. Both possess a crystallographic center of symmetry and display unusually open conformations. In both conformations, the aromatic rings are parallel. The distances between their main planes are 7.1 Å in conformation (a) (Figure V-1a) and 7.3 Å in conformation (b) (Figure V-1b). The space-filling structure of the conformation with the more open cavity [conformation (b)] is represented by Figure V-2. The effective cavity (free pathway) is 10.6 x 4.7 Å which is sufficiently large for receiving a paraquat dication as a guest molecule to form an interlocking complex.

V-2-2: THE HOST-GUEST COMPLEXATION

The host-guest complexation involving paraquat or diquat dication units as electron receptors and electron rich aromatic rings as electron donors and its applications in catenane and rotaxane chemistry have been studied in great detail by Stoddart *et al.*^{24-26,30,51-61} For the sake of this work, let us focus our discussion on a specific system: N,N'-dimethylparaquat hexafluorophosphate and BPP34C10.^{25,26} These two compounds form a deep red colored complex in some polar solvents such as acetone, methanol, acetonitrile, etc. It is a one to one host-guest complex and the formation is mainly driven by charge transfer since the

paraquat dication is an electron deficient system and the hydroquinone moiety is an electron rich system. This bimolecular self-assembling results in the paraquat dication set inside the cavity of BPP34C10 to achieve a maximum π - π interaction.

The X-ray single crystal studies gave a clear structural picture of the complex. The crystal data of the complex with two acetone molecules reported by Stoddart *et al.* are: $C_{12}H_{14}N_2 \cdot C_{28}H_{40}O_{10} \cdot P_2F_{12} \cdot C_6H_{12}O_2$, $M = 1129$, triclinic, space group P1, $a = 10.204(2)$, $b = 11.562(2)$, $c = 13.835(5)$ Å, $\alpha = 105.59(2)$, $\beta = 98.70(2)$, $\gamma = 115.47(1)^\circ$, $U = 1350$ Å³, $Z = 1$ (the complex possesses a crystallographic centre of symmetry), $D_c = 1.39$ g cm⁻³, $R = 0.080$, $R_w = 0.095$ for 2369 independent observed reflections [$\theta \leq 50^\circ$, $|F_o| > 3\sigma(|F_o|)$].

The X-ray solid state structure is shown in Figure V-3 and the space filling representations and side-on view of the structure are shown in Figure V-4. As a matter of fact, there is not much change in conformation upon the formation of the complex. In other words, the conformations of paraquat dication and BPP34C10 in the complex are similar to those in pure crystalline solid states as discussed in section V-1-2-1 (for the paraquat dication) and section V-2-1 [for BPP34C10 in the conformation (b)]. The only slight torsional changes are 21° and 10° , respectively about the O(1)-C(14') and C(5)-C(6) bonds of BPP34C10 and the distance between the two parallel benzo rings in the BPP34C10 is 7.4 Å, while it is 7.3 Å when the macrocycle is in the pure state. This complex also possesses a crystallographic center of symmetry as does

pure BPP34C10, but here it is coincident for the macrocycle and the paraquat dication which is also planar. As expected, the three aromatic domain planes are parallel for the maximum π - π interaction. It can be clearly seen from the figures, especially the side-on view (Figure V-4b), that the two end groups (Me) of the linear paraquat dication stretch out from the both faces of the macrocycle; this is significant in the design of rotaxanes and polyrotaxanes. Actually, the complex is a rotaxane without blocking groups.

Stoddart *et al.* have also reported the stability constant (K_a) of the complex as $730 \text{ dm}^3 \text{ mol}^{-1}$ which corresponds to a free energy of complexation (ΔG^0) of $-3.90 \text{ kcal mol}^{-1}$. It can be seen that the threading is strongly driven by the formation of the stable complex.

V-3: RESULTS AND DISCUSSION

V-3-1: SYNTHESSES OF DIFUNCTIONALIZED PARAQUAT DICATION DERIVATIVES

The difunctionalized paraquat dication derivatives which are capable of forming host-guest complexes with BPP34C10 have been synthesized with various functional group available. These compounds were synthesized from the Menshutkin reaction of 4,4'-dipyridyl and functionalized alkyl halides; the later was used in large excess. The

products, N,N'-dialkylparaquat halide salts, precipitated out from the reaction media. These halide salts were further subjected to anion conversion to hexafluorophosphate salts by treatment with NH_4PF_6 in aqueous solution. The recrystallizations of the precipitates from the NH_4PF_6 aqueous solutions gave pure difunctionalized N,N'-dialkylparaquat hexafluorophosphate salts. The conversion of counter anion from iodide to hexafluorophosphate is done to enhance the solubility in organic solvents which are common solvents for polymerizations.

N,N'-bis(carbomethoxyethyl)-4,4'-bipyridinium hexafluorophosphate (**V-5**) and N,N'-bis(carboxyethyl)-4,4'-bipyridinium hexafluorophosphate (**V-6**) were synthesized using the corresponding functionalized alkyl bromides as the alkylation agents in DMSO and acetonitrile, respectively. Even though the alkyl bromides were used in large excess, some mono-quaternary salt always existed as a by-product. Since this by-product is difficult to remove from the diquarternary salts, it is desired to obtain a quantitative yield of the diquarternary salt. This can be achieved by increasing the reactivity of functionalized alkyl halides toward 4,4'-dipyridyl. Thus, for the N,N'-bis(2-hydroxyethyl)-4,4'-bipyridinium hexafluorophosphate (**V-4**), I used 2-iodoethanol-1 instead of 2-bromoethanol-1 as the reaction solvent as well as the alkylation agent; the unreacted alkyl iodides were recovered after the reaction. The synthetic route is illustrated in Scheme V-2. The alkyl iodides were prepared from corresponding alkyl chlorides which are relatively cheap materials. This functional group conversion was done with an excess

amount of sodium iodide in refluxing acetone and the reaction yielded quantitatively.

Attempts were made with R as polyethylene oxide chains and longer hydrocarbon chains than ethylene such as $(\text{CH}_2)_4$ and $(\text{CH}_2)_{10}$. Unfortunately they were unsuccessful due to some difficulties in the work-up processes. For examples, when $\text{R} = \text{CH}_2\text{CH}_2\text{OCH}_2\text{CH}_2$, the paraquat iodide salts were unable to be converted to the hexafluorophosphate salts by treating with NH_4PF_6 aqueous solution since both salts are water soluble; when $\text{R} = (\text{CH}_2)_4$ or $(\text{CH}_2)_{10}$, we could not carry out any filtration or extraction since the compounds formed emulsions in the aqueous solutions because the molecules possesses hydrophilic (paraquat unit) and hydrophobic (long hydrocarbon chain) parts.

The compounds were characterized by $^1\text{H-NMR}$, melting point measurements and elemental analyses. The $^1\text{H-NMR}$ spectra (in DMSO-d_6) of three compounds (**V-4**, **V-5** and **V-6**) are shown in Figure V-5. Due to solvent effects, NMR chemical shifts were found to be different in different solvents. The chemical shifts determined in acetone- d_6 and DMSO-d_6 are listed in Table V-3. Generally, chemical shifts of all protons are more upfield in DMSO-d_6 than their corresponding ones in acetone- d_6 . It is known that paraquat dications, when they form charge transfer complexes with electron donors, undergo changes in chemical shifts of their protons upfield; this can be taken as evidence of charge transfer complexation.^{24,26} Thus, it is obvious that charge transfer

complexation occurred between the paraquat dication derivatives and the solvent DMSO. Besides the chemical shift changes, I also observed that an orange color developed when the paraquat dication derivatives were dissolved in DMSO. This again indicated charge transfer complex formation.

All three compounds formed white fine, mica-like crystals with very close melting points: 213 - 214°C (**V-4**), 211.3 - 212.5°C (**V-5**) and 199 - 201°C (**V-6**); these are lower than N,N'-dimethylparaquat dications because of the presence of flexible R groups.

V-3-2: COMPLEXATION OF DIFUNCTIONALIZED PARAQUAT DICATION DERIVATIVES AND BPP34C10: PSEUDOROTAXANES

V-3-2-1: Solution Complexation and Preparation of Complex Crystals

Just as the other paraquat dication salts discussed in section V-1 and V-2, difunctionalized paraquat dication derivatives **V-4**, **V-5** and **V-6** are capable of forming host-guest complexes with BPP34C10. The complexation and the formation of the complex crystals are shown in Scheme V-3. Mixing the colorless salts with the colorless BPP34C10 in acetone or acetonitrile afforded deep red solutions, indicating that charge transfer complexes had been formed. If the solvent was removed slowly by natural evaporation, deep red colored crystals grew on the wall of the vial. These crystals were suitable for X-ray structure determination. Generally the melting points of the complexes were lower than those of

the paraquat salts but much higher than that of BPP34C10. The melting ranges were broader than those of normal compounds; indicating that non-covalent bonding exists in these molecules.

The $^1\text{H-NMR}$ analysis and X-ray crystal structure study of the complexation will be discussed in the following sections (section V-4-2 and V-3-2-3).

V-3-2-2: $^1\text{H-NMR}$ Study of Solution Complexation

We have discussed that host-guest complexation takes place between difunctionalized paraquat dication derivatives and BPP34C10 in solution to form pseudorotaxanes. This bimolecular self-assembly process is driven by charge transfer between the donor (electron-rich hydroquinone moieties) and acceptor (electron-poor bipyridinium rings), which is not only evidenced by the appearance of intense red color, but also changes in NMR chemical shifts of some protons. I have studied this complexation by solution $^1\text{H-NMR}$ analysis.

As discussed in section V-3-1, the paraquat dication derivatives were not found to form charge transfer complexes with acetone. Therefore, I chose acetone- d_6 as the solvent for our $^1\text{H-NMR}$ analyses, excluding interferences from solvent complexation. $^1\text{H-NMR}$ spectra of host-guest complexes **V-7**, **V-8** and **V-9** are shown in Figure V-6, Figure V-7 and Figure V-8, respectively, in comparison with the spectra of their corresponding starting materials, BPP34C10 and the paraquat dication derivatives. It is common that most of protons either on the paraquat

dications or on BPP34C10 have chemical shifts moved upfield through the complexation. The differences in chemical shift ($\Delta\delta$) determined for each proton are listed in Table V-4 and Table V-5 for the paraquat dication derivatives and BPP34C10, respectively, where $\Delta\delta = \delta$ of a proton in the complex - δ of the proton in free uncomplexed molecule. It is seen from Table V-4 that the chemical shifts of aliphatic protons of the paraquat dication derivatives generally shifted downfield a little and those of aromatic protons shifted upfield on a relatively larger scale, especially that of A_1 protons, upon the formation of complexes. It was similar for BPP34C10; aromatic protons moved upfield more than α and β aliphatic protons (γ and δ had downfield movement). These results indicate that bipyridinium rings and hydroquinone moieties play an important role in the formation and stabilization of complexes.

As proposed by Reddington, a graduate student of Professor Stoddart, the bipyridinium and bisphenylene rings in inclusion complexes may exist as three orientations as shown in Figure V-9.⁶² Even though the orientation **V-10a** ($\theta = 0^\circ$) has the maximum π - π overlap and $[N^+\cdots OAr]$ electrostatic interactions, it is obvious that this orientation is difficult to achieve because of unfavorable steric interaction between the polyether chains of BPP34C10 and the bipyridinium nitrogen atom substituents. The steric hindrance becomes minimal when the axis of the bipyridinium molecule is perpendicular to the plane of BPP34C10 (orientation **V-10c**, $\theta = 90^\circ$); but, on the other hand, this orientation also has minimum π - π overlap and $[N^+\cdots OAr]$ electrostatic interactions. Consequently, the most probable orientation which

balances these two opposite effects is orientation **V-10b** ($0^\circ < \theta < 90^\circ$). The molecules may exist in this orientation as the lowest energy conformation or undergo rapid oscillation of the substrate in the cavity between different angles of the molecular axis of the substrate to the plane of BPP34C10. X-ray crystal analysis has proven that **V-10b** is the orientation of the molecule in the crystalline state (see next section).

Either conformation **V-10a** or **V-10b** would result in chemical shift changes ($\Delta\delta$) of related protons. Since **V-10a** has the maximum π - π overlap and $[N^+\cdots OAc]$ electrostatic interactions, it should give the largest $\Delta\delta$ values. As the matter of fact, the largest $\Delta\delta$ values were observed by Reddington for bishydrobipyridinium hexafluorophosphate, a bipyridinium salt with the smallest nitrogen atom substituent, a hydrogen atom, indicating that the hydrogen atom is smaller enough to have the dication fit into the cavity of BPP34C10 with $\theta = 0^\circ$ (orientation **V-10a**).⁶⁴ According to this result, we could assume that the magnitudes of changes in $^1\text{H-NMR}$ chemical shifts of related protons reflect the orientation angle. In other words, $\Delta\delta$ increases with decreasing θ . Even though the paraquat dication derivatives **V-4**, **V-5** and **V-6** have bipyridinium nitrogen substituents of similar sizes and the differences in $\Delta\delta$ values for each proton are small, still we are able to distinguish the slight difference in their complex orientations. By examining data listed in Table V-4 and V-5, it seems that the largest $\Delta\delta$ values are observed with paraquat diacid-BPP34C10 system and the smallest values are observed for paraquat diester-BPP34C10 system. From this point of view, we could conclude that the all three complexes

V-7, **V-8** and **V-9** have similar orientations described by **V-10b**; but, **V-8** has the largest θ angle due to the large size of COOCH₃ group; **V-9** has the smallest θ angle, which is probably caused by hydrogen bonding between the acid group and polyether chains of BPP34C10. These interactions are weaker in system **V-7**.

V-3-2-3: X-Ray Crystal Analysis

Recently, Stoddart *at al.* have reported the X-ray crystal structure of **V-7**.⁶³ I have determined the structure of **V-8**; unfortunately, the attempt with **V-9** was unsuccessful.

The X-ray crystal structure of **V-7** along with the data obtained by Stoddart *at al.* is shown in Figure V-10. In Figure V-11, Figure V-12 and Table V-13, the crystal structure of complex **V-8** from side view, the space-filling representing of the structure and crystal packing data are shown, respectively. Also the detailed crystal data of this complex are given in Appendix V-1.

Figures V-10 to V-12 give clear pictures of the structural chemistry of the host-guest complexes of difunctionalized paraquat dication derivatives and BPP34C10. There are several important features that need to be emphasized:

(1) Conformations of BPP34C10 and paraquat dication remain as in their free states, e.g. BPP34C10 is roughly planar and the two phenylene rings are parallel to each other but perpendicular to the molecule plane and also the bipyridinium rings are coplanar.

(2) Paraquat dication derivatives are threaded through the cavity center of BPP34C10.

(3) All aromatic rings are arrayed parallel to each other and perpendicular to the molecular plane of BPP34C10 so that a maximum π - π overlap and $[N^+\cdots OAr]$ electrostatic interaction can be achieved.

(4) Functionalized groups are stretched out from both faces of BPP34C10 with a certain angle (θ) of paraquat dication molecular axis to BPP34C10 molecular plane, making them accessible for polymerizations.

(5) The orientation angle (θ) of **V-8** is 57° ; however, **V-7** has a θ value of 26° .⁶² This is consistent with the conclusion from $^1\text{H-NMR}$ solution complexation studies that **V-8** has a larger orientation angle (θ) than that of **V-7** due to larger volume of COOCH_3 group relative to the hydroxyl group; also the latter is hydrogen bonded to O7 and O7' of BPP34C10.⁶⁴

The packing diagram (overall structure) for the complex **V-8** is shown in Figure V-13. It seems that the complexes form a continuous regular arrangement, creating long channels in the crystallographic a direction. The channels are expanded by threaded paraquat dication derivatives. Thus, the hexafluorophosphate counter anions, in spite of large volumes, stack into the channels, making the crystals perfect.

Finally, it is obvious why this class of complexes called pseudorotaxanes is so important in rotaxane chemistry. Only one further step is required to produce either rotaxanes (via reactions with

monofunctionalized blocking groups) or polyrotaxanes (via polymerizations).

V-4: EXPERIMENTAL

4,4'-Dipyridyl (98%), 2-chloroethanol (99%), 3-bromopropionic acid (99%), sodium iodide (98%) and ammonium hexafluorophosphate (99%) were purchased from Aldrich Chemical Co. and used without further purification.

Melting Points were determined on a HAAKE BUCHLER capillary melting point apparatus and are corrected. The $^1\text{H-NMR}$ spectra were recorded on a Bruker WP 270 MHz instrument using TMS as the internal standard. Elemental analyses were done by Atlantic Microlab, Inc., Norcross, Georgia.

The X-ray crystal analysis was done on Siemens SHELXTL PLUS (VMS) with Siemens R3m/V diffractometer and $\text{MoK}\alpha$ radiation ($\lambda = 0.71073 \text{ \AA}$). The structure was solved by direct methods and refined by the full-matrix least-square procedure to $R = 0.0522$ and 0.0729 for reflections with $F > 3\sigma$ (for more information on the solution, refinement and data collection, please see Appendix V-1).

**V-4-1: N,N'-BIS(2-HYDROXYETHYL)-4,4'-BIPYRIDINIUM
HEXAFLUOROPHOSPHATE (V-4)**

V-4-1-1: Preparation of 2-Iodoethanol-1

2-Chloroethanol-1 (30.0 g, 0.370 mol) was dissolved in acetone (350 mL) in a 500-mL 1-necked flask. Sodium iodide (149 g, 1.00 mol) was added. The mixture was refluxed under magnetic stirring for 3 days.

The system was cooled down to room temperature. Solid precipitate was filtered and the filtrate was rotary evaporated down to a brown oil. The product was extracted 3 times with ethyl ether (3 x 200 mL). The combined organic phase was washed 3 times with water (3 x 300 mL) and dried with MgSO₄. A slightly brown oil (60.0 g) was obtained after the removal of the solvent by rotary evaporation. This compound was characterized by ¹H-NMR analysis; no other analysis was done. Since it would be used as a solvent in the next step of reaction, it was unnecessary to carry out further purification.

Yield: 94%; ¹H-NMR (chloroform-d/TMS, ppm): 3.31 (t, 2 H, ICH₂CH₂OH), 3.85 (t, 2 H, ICH₂CH₂OH), the OH peak was broad due to hydrogen bonding.

V-4-1-2: The Menshutkin Reaction

To 2-iodoethanol-1 (58.0 g, 0.337 mol) in a 250-mL 1-necked flask, 4,4'-dipyridyl (5.65 g, 0.0361 mol) was added. The flask was immersed

in an oil-bath with temperature 80°C. The mixture was magnetically stirred under nitrogen for 40 hours.

Solid precipitate was filtered and the filtrate (unreacted 2-iodoethanol-1) was recovered. The solid was dissolved in water (100 mL) (some water insoluble impurities were filtered and discarded) in a 300-mL beaker. NH_4PF_6 (15.0 g, 0.0920 mol) dissolved in water (100 mL) was added into the solution. White precipitate was observed immediately. The mixture was stirred for 30 minutes and the white precipitate was filtered. This precipitate was subjected to recrystallization 3 times in water. Fine white mica-like crystals (16.5 g) were obtained.

Yield: 85%; m.p. 213 - 214°C; $^1\text{H-NMR}$ (ppm): 4.22 (m, in acetone- d_6/TMS) and 3.95 (m, in $\text{DMSO-d}_6/\text{TMS}$) (4 H, $\underline{\text{CH}_2\text{OH}}$), 5.03 (t, in acetone- d_6/TMS) and 4.78 (t, in $\text{DMSO-d}_6/\text{TMS}$) (4 H, CH_2N^+), 4.61 (t, in acetone- d_6/TMS) and 5.34 (t, in $\text{DMSO-d}_6/\text{TMS}$) (2 H, OH), 8.84 (d, in acetone- d_6/TMS) and 8.78 (d, in $\text{DMSO-d}_6/\text{TMS}$) (4 H, aromatic), 9.36 (d, in acetone- d_6/TMS) and 9.30 (d, in $\text{DMSO-d}_6/\text{TMS}$) (4 H, aromatic); the DMSO spectrum is shown in Figure V-5a. Elemental analysis (%): calculated for $\text{C}_{14}\text{H}_{20}\text{N}_2\text{O}_2\text{P}_2\text{F}_{12}$, C: 31.35, H: 3.76, N: 5.23, O: 5.97, P: 11.55, F: 42.52; found: C: 31.36, H: 3.35, N: 5.28.

**V-4-2: N,N'-BIS(CARBOMETHOXYETHYL)-4,4'-BIPYRIDINIUM
HEXAFLUOROPHOSPHATE (V-5)**

V-4-2-1: Preparation of Methyl 3-Bromopropionate

3-Bromopropionic acid (9.70 g, 0.0634 mol) was placed in a 250-mL 1-necked flask with methanol (50 mL) and concentrated H₂SO₄ (1.00 mL). The solution was magnetically stirred overnight at reflux.

The solution was cooled down to room temperature. Most of the unreacted methanol was rotary evaporated. The product was extracted 2 times with ethyl ether (2 x 100 mL). The combined organic phase was washed 3 times with water (3 x 200 mL) and dried with MgSO₄. A slightly brown oil (8.50 g) was obtained after removal of the solvent by rotary evaporation. This compound was characterized by ¹H-NMR analysis and used in the next reaction with further purification.

Yield: 80%; ¹H-NMR (chloroform-d/TMS, ppm): 2.93 (t, 2 H, BrCH₂), 3.59 (t, 2 H, CH₂COOCH₃), 3.73 (s, 3 H, COOCH₃).

V-3-2-2: The Menschutkin Reaction

4,4'-dipyridyl (2.00 g, 0.0128 mol) and methyl 3-bromopropionate (8.00 g, 0.0479 mol) were mixed with DMSO (20 mL) in a 100-mL 1-necked flask. The flask was immersed in an oil-bath with temperature 65°C. The mixture was magnetically stirred overnight under nitrogen.

The mixture was poured into acetone (50 mL). A slightly yellow precipitate was observed. The precipitate was filtered and dissolved in

water (50 mL) in a 100-mL beaker. NH_4PF_6 (6.00 g, 0.0368 mol) dissolved in water (50 mL) was added to the solution. A white precipitate was observed immediately. The mixture was magnetically stirred for 30 minutes. The precipitate was filtered and subjected to recrystallization 3 times from a mixture of water and acetone (9:1/v:v). Fine white mica-like crystals (6.10 g) were obtained.

Yield: 77%; m.p. 211.3 - 212.5°C; $^1\text{H-NMR}$ (ppm): 3.39 (t, in acetone- d_6 /TMS) and 3.16 (t, in DMSO- d_6 /TMS) (4 H, $\text{CH}_2\text{COOCH}_3$), 3.66 (s, in acetone- d_6 /TMS) and 3.57 (s, in DMSO- d_6 /TMS) (6 H, COOCH_3), 5.23 (t, in acetone- d_6 /TMS) and 4.83 (t, in DMSO- d_6 /TMS) (4 H, CH_2N^+), 8.82 (d, in acetone- d_6 /TMS) and 8.69 (d, in DMSO- d_6 /TMS) (4 H, aromatic), 9.48 (d, in acetone- d_6 /TMS) and 9.30 (d, in DMSO- d_6 /TMS) (4 H, aromatic); The DMSO spectrum is presented in Figure V-5b. Elemental analysis (%): calculated for $\text{C}_{18}\text{H}_{22}\text{O}_4\text{N}_2\text{P}_2\text{F}_{12}$, C: 34.85, H: 3.57, N: 4.52, O: 10.32, P: 9.99, F: 36.75; found: C: 34.76, H: 3.56, N: 4.49.

**V-4-3: N,N'-BIS(CARBOXYETHYL)-4,4'-BIPYRIDINIUM
HEXAFLUOROPHOSPHATE (V-6)**

4,4'-dipyridyl (2.00 g, 0.0128 mol) and 3-bromopropionic acid (7.80 g, 0.0512 mol) were mixed with acetonitrile (30 mL) in a 100-mL 1-necked flask. The flask was immersed in an oil-bath with temperature high enough to reflux. The mixture was magnetically stirred for 48 hours at reflux under nitrogen. A slightly yellow precipitate was observed.

The mixture was cooled down to room temperature. The precipitate was filtered and dissolved in water (30 mL) in a 100-mL beaker. NH_4PF_6 (8.00 g, 0.0491 mol) dissolved in water (30 mL) was added to the solution. A white precipitate was observed immediately. This precipitate was filtered and subjected to recrystallization 3 times from water. Fine white mica-like crystals (6.98 g) were obtained.

Yield: 96%; m.p. 199 - 201°C; $^1\text{H-NMR}$ (ppm): 3.39 (t, in acetone- d_6/TMS) and 3.15 (t, in $\text{DMSO-d}_6/\text{TMS}$) (4 H, CH_2COOH), 3.43 (broad s, in $\text{DMSO-d}_6/\text{TMS}$ but not seen in acetone- d_6/TMS) (2 H, COOH), 5.20 (t, in acetone- d_6/TMS) and 4.88 (t, in $\text{DMSO-d}_6/\text{TMS}$) (4 H, CH_2N^+), 8.82 (d, in acetone- d_6/TMS) and 8.78 (d, in $\text{DMSO-d}_6/\text{TMS}$) (4 H, aromatic), 9.47 (d, in acetone- d_6/TMS) and 9.37 (d, in $\text{DMSO-d}_6/\text{TMS}$) (4 H, aromatic). The DMSO spectrum is shown in Figure V-5c.

V-4-4: A TYPICAL PROCEDURE FOR V-7, V-8 AND V-9

In a dry 10-mL snap-cap vial, a mixture of N,N'-bis(carbomethoxyethyl)-4,4'-bipyridinium hexafluorophosphate (0.500 g, 9.32×10^{-4} mol) and BPP34C10 (0.500 g, 9.32×10^{-4} mol) were dissolved in a mixture of methanol and acetone (6.00 mL, 1:1/v:v). A deep red color was observed immediately. This solution was allowed to evaporate naturally through a small hole in the cap. Deep red crystals were observed growing on the wall of the vial. The crystals (0.96 g) were separated after 3 days and most of the solvent had gone.

Yield: 96% - 100%; m.p. 195 - 198°C (**V-7**), 197 - 201°C (**V-8**), 178 - 183°C (**V-9**); ¹H-NMR of **V-7** (Figure V-6c, acetone-d₆/TMS, ppm): 3.74 [s, 16 H, arom.-O(CH₂)₂O(CH₂)₂O], 3.76 (m, 8 H, arom.-OCH₂CH₂O), 3.79 (m, 8 H, arom.-OCH₂CH₂O), 4.28 (m, 4 H, CH₂OH), 4.66 (t, 2 H, OH), 5.05 (t, 4 H, CH₂N⁺), 6.47 (s, 8 H, aromatic of BPP34C10), 8.48 (d, 4 H, aromatic of paraquat), 9.23 (d, 4 H, aromatic of paraquat); ¹H-NMR of **V-8** (Figure V-7c, acetone-d₆/TMS, ppm): 3.48 (t, 4 H, CH₂COOCH₃), 3.72 (s, 6 H, COOCH₃), 3.75 (s, 16 H, arom.-O(CH₂)₂O(CH₂)₂O), 3.78 (m, 8 H, arom.-OCH₂CH₂O), 3.79 (m, 8 H, arom.-OCH₂CH₂O), 5.21 (t, 4 H, CH₂N⁺), 6.46 (s, 8 H, aromatic of BPP34C10), 8.53 (d, 4 H, aromatic of paraquat), 9.33 (d, 4 H, aromatic of paraquat); ¹H-NMR of **V-9** (Figure V-8c, acetone-d₆/TMS, ppm): 3.47 (t, 4 H, CH₂COOH), 3.74 (m, 16 H, arom.-OCH₂CH₂O), 3.79 [s, 16 H, arom.-O(CH₂)₂O(CH₂)₂O], 5.18 (t, 4 H, CH₂N⁺), 6.37 (s, 8 H, aromatic of BPP34C10), 8.42 (d, 4 H, aromatic of paraquat), 9.28 (d, 4 H, aromatic of paraquat).

REFERENCE

1. Summers, L. A. "The Bipyridinium Herbicides", Academic Press, N. Y. **1980**.
2. Anderson, T. *Liebigs Ann. Chem.* **1870**, 154, 270.
3. Weidel, H.; Russo, M. *Monatsh. Chem.* **1882**, 3, 850.
4. Slade, P. *Weed. Res.* **1966**, 6, 158.
5. Emmert, B.; Stawitz, J. *Ber.* **1923**, 56B, 83.
6. Beyerman, H. C.; Bontekoe, J. S. *Rec. Trav. Chim.* **1955**, 74, 1395.
7. Hünig, S.; Ruider, G. *Tetrahedron Lett.* **1968**, 773.
8. Bonczos, J.; Szarvas, P.; Gyori, E.; Gyori, B.; Emri, J.; Arany, S.; Punkosty, K.; Nagy, Z. *German Patent* **1969**, 1926535 [*Chem. Abstr.* **1970**, 72, 55271].
9. Khaskin, B. A.; Mel'nikov, N. N.; Sablina, I. V. *Zh. Obshch. Khim.* **1968**, 38, 1561.
10. Draffan, G. H.; Clare, R. A.; Davies, D. L.; Hawksworth, G.; Murray, S.; Davies, D. S. *J. Chromatogr.* **1977**, 139, 311.
11. Phillips, A. P.; Mentha, J. *J. Am. Chem. Soc.* **1955**, 6393.

12. Shapiro, B. I.; Minin, V. V.; Srykin, Y. K. *Zh. Strukt. Khim.* **1973**, *14*, 642.
13. Muzychenko, V. A.; Miskidzh'yan, S. P. *Strukt. Mekh. Deistviya Fiziol. Aktiv. Veshchestv.* **1972**, 86.
14. Kazarinova, N. F.; Solomko, K. A.; Kotelenets, M. N. *Metody Poluch. Khim. Reaktivov Prep.* **1966**, No. 14, 22.
15. Brian, R. C.; Driver, G. W.; Homer, R. F.; Jones, R. L. *British Patent* **1959**, 813532 [*Chem. Abstr.* **1961**, *55*, 4541].
16. LeBerre, A.; Delacroix, A. *Bull. Soc. Chim. France* 1973, 2404.
17. Leberre, A.; Delacroix, A. *Bull. Soc. Chim. France* **1973**, 640.
18. Müller, E.; Bruhn, K. A. *Chem. Ber.* **1953**, *86*, 1122.
19. Weitz, E.; König, T.; Wistinghausen, L. V. *Ber.* **1924**, *57B*, 153.
20. Imperial Chemical Industries Ltd. *French Addn. Patent* **1965**, 84655 [*Chem. Abstr.* **1966**, *64*, 712].
21. Braunheltz, J. T. *Belgian Patent* **1963**, 626303 [*Chem. Abstr.* **1964**, *60*, 8001].
22. Mel'nikov, N. N.; Khaskin, B. A.; Voronkova, V. V.; Yakimenko, E. F.; Sablina, I. V. *Khim. Sredstva Zashch. Rast.* **1972**, *2*, 306.
23. Michaelis, L.; Hill, E. S. *J. Gen. Physiol.* **1933**, *16*, 859.

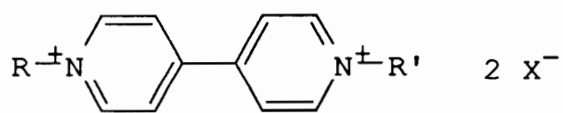
24. Allwood, B. L.; Shahriari-Zavareh, H.; Stoddart, J. F.; Williams, D. J. *J. Chem. Soc., Chem. Commun.* **1987**, 1058.
25. Allwood, B. L.; Spencer, N.; Shahriari-Zavareh, H.; Stoddart, J. F.; Williams, D. J. *J. Chem. Soc., Chem. Commun.* **1987**, 1064.
26. Ashton, P. R.; Slawin, A. M. Z.; Spencer, N.; Stoddart, J. F.; Williams, D. J. *J. Chem. Soc., Chem. Commun.* **1987**, 1066.
27. Russell, J. H.; Wallwork, S. C. *Acta Crystallogr. Sect. B* **1972**, 28, 1527.
28. Russell, J. H.; Wallwork, S. C. *Acta Crystallogr. Sect. B* **1969**, 25, 1691.
29. Murray-Rust, P. *Acta Crystallogr. Sect. B* **1975**, 31, 1771.
30. Allwood, B. L.; Colquhoun, H. M.; Doughty, S. M.; Kohnke, F. H.; Slawin, A. M. Z.; Stoddart, J. F.; Williams, D. J.; Zarzycki, R. J. *J. Chem. Soc., Chem. Commun.* **1987**, 1054.
31. Verhoeven, J. W.; Verhoeven-Schoff, A. M. A.; Masson, A.; Schwyzer, R. *Helv. Chim. Acta* **1974**, 57, 2503.
32. Fielden, R.; Summers, L. A. *Experientia* **1974**, 30, 843.
33. Corwin, A. H.; Arellano, R. R.; Chivvis, A. B. *Biochim. Biophys. Acta* **1968**, 162, 533.

34. Farrington, J. A.; Ledwith, A.; Stam, M. F. *Chem. Commun.* **1969**, 259.
35. Calderbank, A.; Charlton, D. F.; Farrington, J. A.; James, R. J. *Chem. Soc., Perkin Trans. I* **1972**, 138.
36. Weitz, E.; Ludwig, R. *Ber.* **1922**, 55B, 395.
37. Weitz, E.; Konig, T. *Ber.* **1922**, 55B, 2864.
38. Emmert, B.; Varenkamp, O. *Ber.* **1923**, 56B, 491.
39. Müller, E.; Bruhn, K. A. *Chem. Ber.* 1953, 86, 1122.
40. Weitz, E. *Angew. Chem.* **1954**, 66, 658.
41. Carey, J. G.; Cairns, J. F.; Colchester, J. E. *Chem. Commun.* **1969**, 1280.
42. Ukai, S.; Hirose, K.; Kawase, S. *Eisei Kagaku* **1977**, 23, 32.
43. Ukai, S.; Hirose, K.; Kawase, S. *Eisei Kagaku* **1973**, 19, 281.
44. Emmert, B.; Lauritzen, H. *Ber.* **1938**, 71B, 240.
45. Novakovskii, M. S.; Voinova, V. N.; Pivnenko, N. S.; Kozarinova, N. F. *Zh. Nerogan. Khim.* **1966**, 11, 1738.
46. Ledwith, A.; Woods, H. J. *J. Chem. Soc. (C)* **1970**, 1422.
47. Mel'nikov, N. N.; Khaskin, B. A.; Sablina, I. V.; Supin, G. S. *Zh. Obshch. Khim.* **1974**, 44, 93.

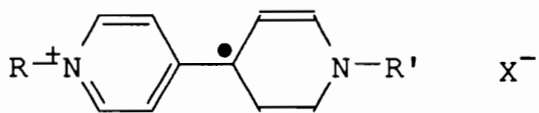
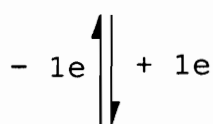
48. White, B. G. *Trans. Faraday Soc.* **1969**, 65, 2000.
49. Nakahara, A.; Wang, J. H. *J. Phys. Chem.* **1963**, 67, 496.
50. Ashwell, G. J.; Eley, D. D.; Willis, M. R.; Woodward, J. *J. Chem. Soc., Faraday Trans. II* **1975**, 71, 1785.
51. Allwood, B. L.; Spencer, N.; Shachriari-Zavareh, H.; Stoddart, J. F.; Williams, D. J. *J. Chem. Soc., Chem. Commun.* **1987**, 1061.
52. Odell, B.; Reddington, M. V.; Slawin, A. M. Z.; Spencer, N.; Stoddart, J. F.; Williams, D. J. *Angew. Chem. Int. Ed. Engl.* **1988**, 27, 1547.
53. Ashton, P. R.; Odell, B.; Reddington, M. V.; Slawin, A. M. Z.; Stoddart, J. F.; Williams, D. J. *Angew. Chem. Int. Ed. Engl.* **1988**, 27, 1550.
54. Ortholand, J-Y.; Slawin, A. M. Z.; Spencer, N.; Stoddart, J. F.; Williams, D. J. *Angew. Chem. Int. Ed. Engl.* **1989**, 28, 1394.
55. Stoddart, J. F. "Frontiers in Supramolecular Organic Chemistry and Photochemistry", Edited by Schneider, H-J.; Durr, H., VCH Verlagsgesellschaft mbH, Weinheim, **1991**, p 251-263.
56. Stoddart, J. F. "**1991** Host-guest Molecular Interactions: From Chemistry to Biology", Wiley, Chichester (Ciba Foundation Symposium 158) p 5-22.

57. Reddington, M. V.; Spencer, N.; Stoddart, J. F. "Inclusion Phenomena and Molecular Recognition", Edited by Atwood, J., Plenum, New York, **1990**, p 41-48.
58. Ashton, P. R.; Groguz, M.; Slawin, A. M. Z.; Stoddart, J. F.; Williams, D. J. *Tetrahedron Lett.* **1991**, *32*, 6235; *J. A. Chem. Soc.* **1991**, *113*, 5131.
59. Anelli, P. L.; Ashton, P. R.; Spencer, N.; Slawin, A. M. Z.; Stoddart, J. F.; Williams, D. J. *Angew. Chem. Int. Ed. Engl.* **1991**, *30*, 1036.
60. Ashton, P. R.; Brown, C. L.; Chrystal, E. J. T.; Goodnow, T. T.; Kaifer, A. E.; Parry, K. P.; Slawin, A. M. Z.; Spencer, N.; Stoddart, J. F.; Williams, D. J. *Angew. Chem. Int. Ed. Engl.* **1991**, *30*, 1039.
61. Ashton, P. R.; Brown, C. L.; Chrystal, E. J. T.; Parry, K. P.; Pietraszkiewicz, M.; Spencer, N.; Stoddart, J. F. *Angew. Chem. Int. Ed. Engl.* **1991**, *30*, 1042.
62. Reddington, M. V. "PhD. Dissertation", **1989**, University of Sheffield, England.
63. Ashton, P. R.; Philp, D.; Reddington, M. V.; Slawin, A. M. Z.; Spencer, N.; Stoddart, J. F.; Williams, D. J. *J. Chem. Soc., Chem. Commun.* **1991**, 1680.

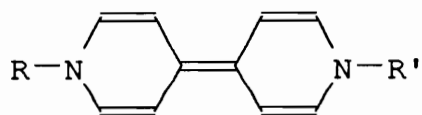
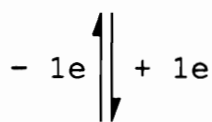
**Scheme V-1: One-Electron Reduction of Paraquat
Dication Derivatives**



V-1

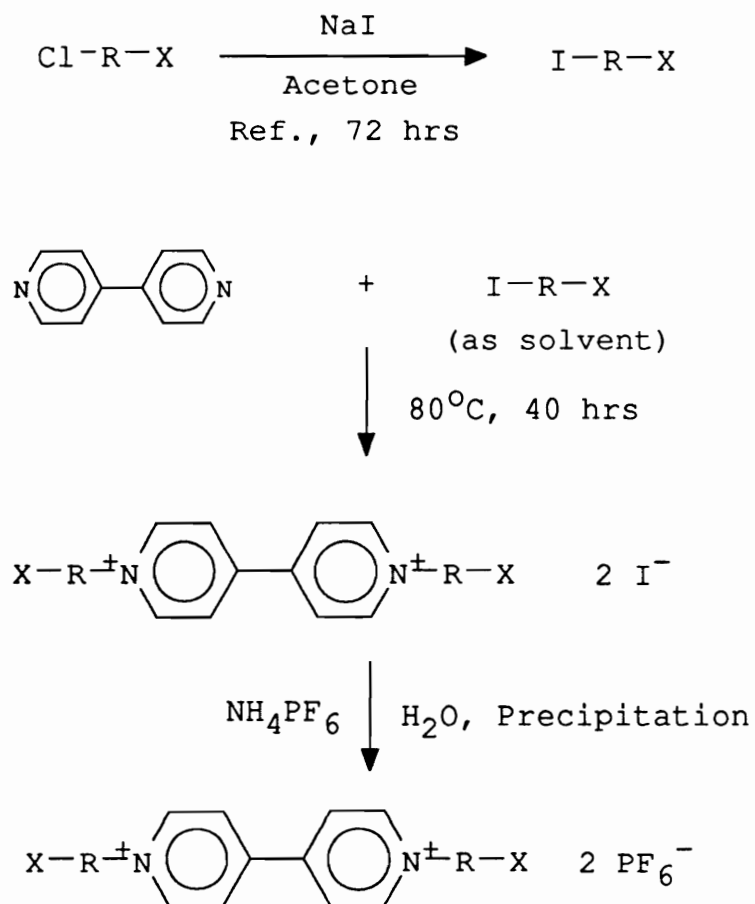


V-2



V-3

**Scheme V-2: Syntheses of Difunctionalized Paraquat
Dication Derivatives**

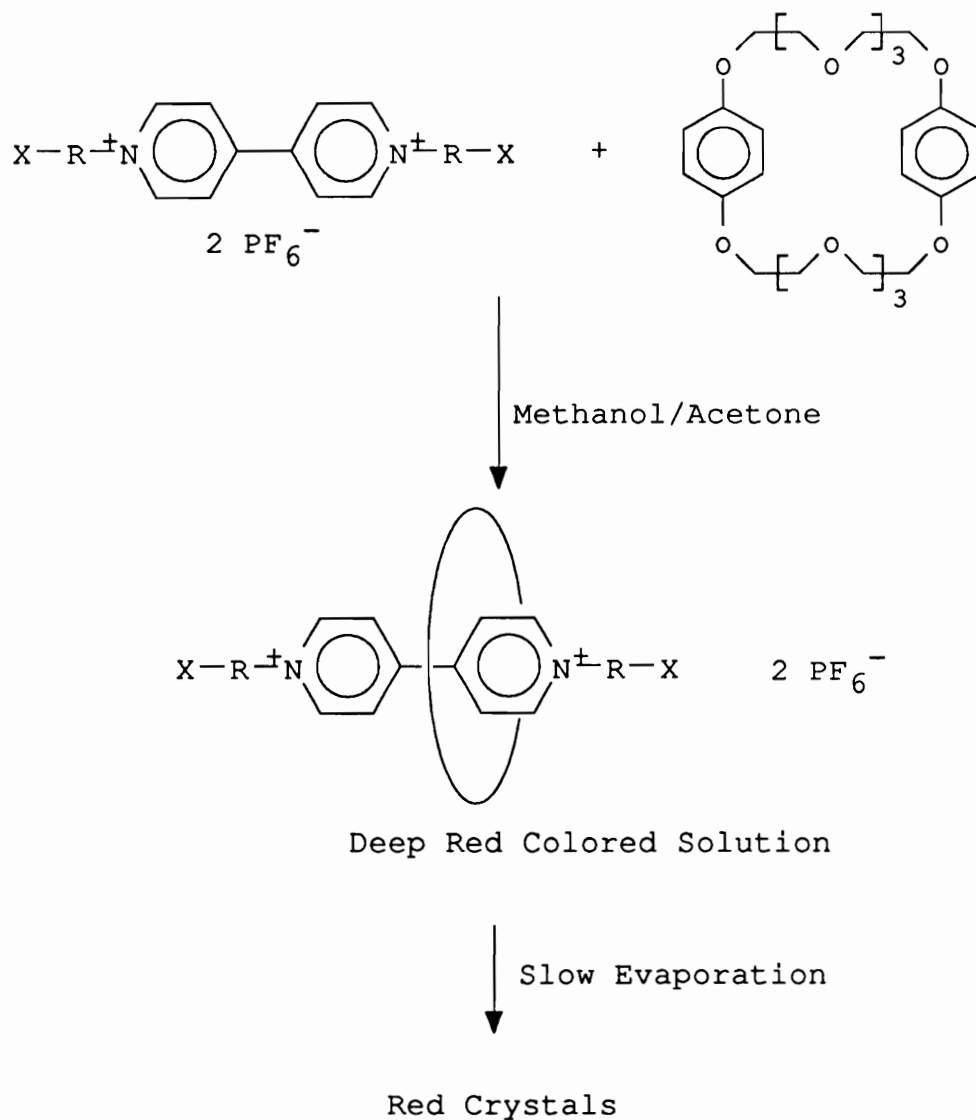


V-4. R = CH₂CH₂, X = OH

V-5. R = CH₂CH₂, X = COOCH₃

V-6. R = CH₂CH₂, X = COOH

Scheme V-3: The Formation of Host-Guest Complexes between Difunctionalized Paraquat Dication Derivatives and BPP34C10

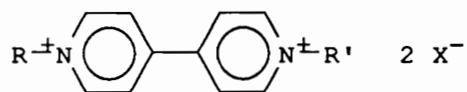


V-7. R = CH₂CH₂, X = OH

V-8. R = CH₂CH₂, X = COOCH₃

V-9. R = CH₂CH₂, X = COOH

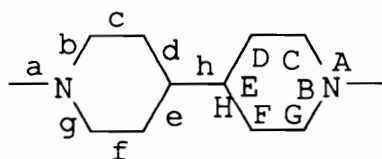
Table V-1: Some Examples of Paraquat Dication Derivatives¹



R	R'	X	m.p. (°C)	Ref.
Me	Me	Cl	> 250	4
Me	Me	Br	-	5
Me	Me	I	300	6
Me	Me	BF ₄	263	7
Me	Me	MeSO ₄	-	8
Me	Me	PO(O)SMe ₂	138	9
Et	Et	Cl	-	10
Et	Et	I	273 -274	11
iso-Bu	iso-Bu	Br	-	12
CH ₂ CH=CH ₂	CH ₂ CH=CH ₂	SCN	-	13
CH ₂ COOH	CH ₂ COOH	Cl	> 300	14

CH ₂ CH ₂ OH	CH ₂ CH ₂ OH	Cl	>300	14
CH ₂ CH ₂ OEt	CH ₂ CH ₂ OEt	I	218-220	15
CH ₂ OCOEt	CH ₂ OCOEt	Cl	-	15
(CH ₂) ₂ COOH	(CH ₂) ₂ COOH	Cl	314-315	15, 16
CH ₂ CH ₂ Cl	CH ₂ CH ₂ Cl	Br	>350	15
(CH ₂) ₂ CONH ₂	(CH ₂) ₂ CONH ₂	Br	325-330	17
(CH ₂) ₃ COOEt	(CH ₂) ₃ COOEt	Br	216-218	15
Benzyl	Benzyl	I	231	18
Phenyl	Phenyl	I	360	19
Me	Et	I	291	20
Me	Bu	Br	256	20
Me	CH ₂ CH ₂ OH	Cl	256	21
CH ₂ CH ₂ OH	CH ₂ OCOEt	Cl	189-190	21
CH ₂ CH ₂ OH	CH ₂ CONEt ₂	Cl	242-244	21
CH ₂ OCCH ₃	Benzyl	Cl	141-143	21
CH ₂ CONEt ₂	CH ₂ COOH	Cl	274	21

**Table V-2: Mean Bond Lengths and Angles in the
1,1'-Dimethyl-4,4'-bipyridinium Dication¹**



Bond Lengths

Bond	a	b	c	d	e	f	g	h
X=Cl	0.141	0.134	0.141	0.138	0.137	0.135	0.134	0.146
X=Br	0.147	0.135	0.136	0.141	0.139	0.138	0.134	0.145
X=I	0.145	0.135	0.137	0.139	0.140	0.139	0.134	0.148

Bond Angles

Angle (°)	A	B	C	D	E	F	G	H
X=Cl	120.6	120.1	122.0	121.1	116.5	121.9	118.2	122.9
X=Br	119.1	119.9	120.8	120.6	116.6	120.5	121.5	122.1
X=I	120.1	120.9	121.2	118.6	118.8	119.9	120.6	119.3

* Data were obtained by Russell *et al.*^{27,28}

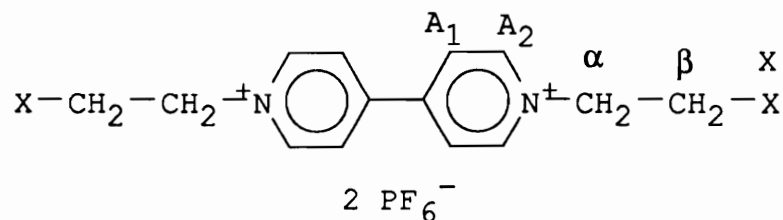
Table V-3: $^1\text{H-NMR}$ Chemical Shifts (ppm) of Difunctionalized Paraquat Dication Derivatives

Compound	V-4		V-5		V-6	
	A	B	A	B	A	B
-OH	4.61	5.34				
-COOCH ₃			3.66	3.57		
-COOH					-	3.43
-CH ₂ -X	4.22	3.95	3.39	3.16	3.39	3.15
-CH ₂ -N ⁺	5.03	4.78	5.23	4.83	5.20	4.88
Aromatic	8.84	8.78,	8.82	8.69,	8.82	8.78,
	9.36	9.30	9.48	9.30	9.47	9.37

Solvent A: Acetone-d₆.

Solvent B: DMSO-d.

Table V-4: Changes in $^1\text{H-NMR}$ Chemical Shift ($\Delta\delta^*$) of Protons on the Difunctionalized Paraquat Dication Derivatives in the Formation of Host-Guest Complexes with BPP34C10

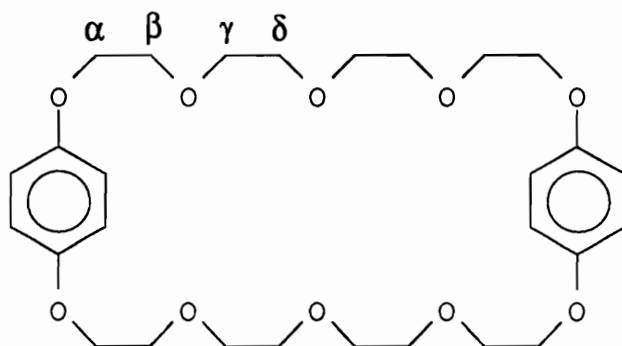


V-4: X = OH, **V-5:** X = COOCH₃, **V-6:** X = COOH

Proton	X	α	β	A ₁	A ₂
V-4	0.05	0.06	0.02	-0.36	-0.13
V-5	0.06	0.09	-0.02	-0.29	-0.15
V-6		0.08	-0.02	-0.40	-0.19

* $\Delta\delta = \delta(\text{complex}) - \delta(\text{free})$.

Table V-5: Changes in $^1\text{H-NMR}$ Chemical Shift ($\Delta\delta^*$) of Protons on BPP34C10 in the Formation of Host-Guest Complexes with the Difunctionalized Paraquat Dication Derivatives

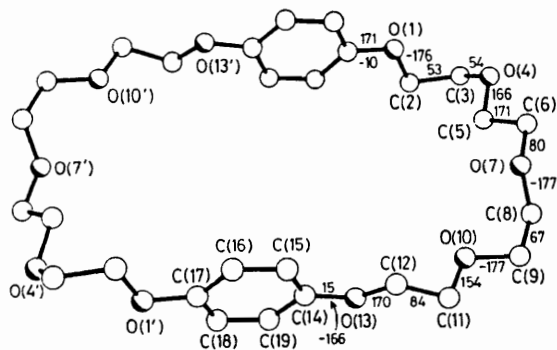


Proton	α	β	$\gamma + \delta$	Aromatic
V-7	-0.20	-0.04	0.10	-0.32
V-8	-0.20	-0.02	0.11	-0.33
V-9	-0.25	-0.06	0.15	-0.42

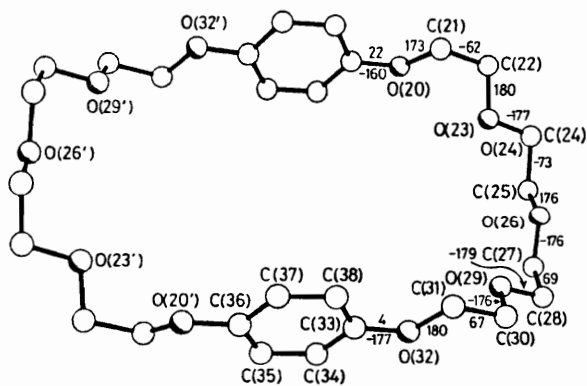
* $\Delta\delta = \delta(\text{complex}) - \delta(\text{free})$.

Table V-6: X-Ray Crystal Data of Complex V-8

Empirical Formula	$C_{46} H_{62} F_{12} N_2 O_{14} P_2$
Color; Habit	Red rectangular prism
Crystal Size (mm)	0.6 x 0.8 x 0.8
Crystal System	Monoclinic
Space Group	C2/c
Unit Cell Dimensions	$\underline{a} = 28.137(6) \text{ \AA}$ $\underline{b} = 11.677(3) \text{ \AA}$ $\underline{c} = 18.465(4) \text{ \AA}$ $\beta = 117.34(2)^\circ$
Volume	$5389(2) \text{ \AA}^3$
Z	4
Formula weight	1156.9
Density(calc.)	1.426 Mg/m^3
Absorption Coefficient	0.178 mm^{-1}
F(000)	2408



(a)



(b)

Figure V-1: The X-Ray Solid State Structures of the Two Crystallographically Independent Conformations of BPP34C10. The Bond Lengths and Angles are Shown on the Structures. Printed from Stoddart et. al.⁵¹

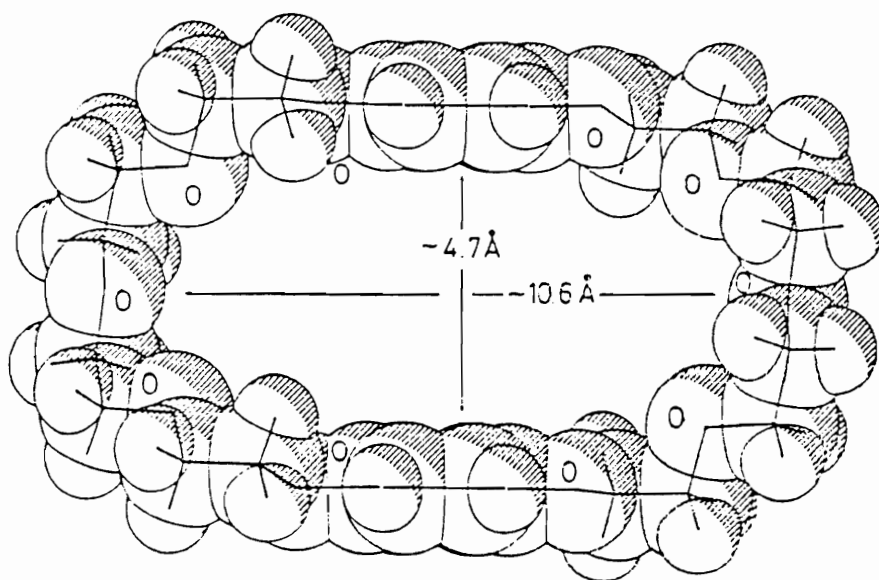
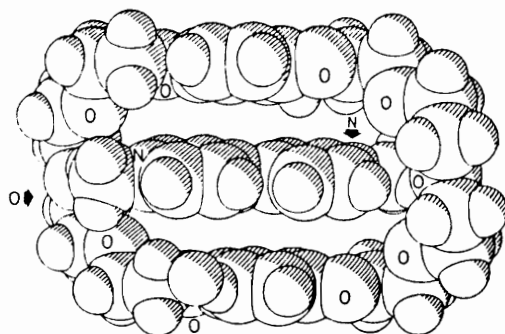
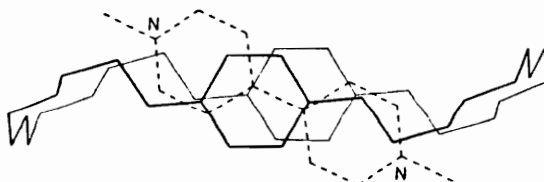


Figure V-2: Space Filling Representation of Conformation (b) of BPP34C10. Printed from Stoddart et al.⁵¹



(a)



(b)

Figure V-4: Space-Filling (a) and Side-on View of the Skeletal (b) Representations of the Complex Formed from N,N'-Dimethylparaquat Hexafluorophosphate and BPP34C10. Printed from Stoddart et al.²⁵

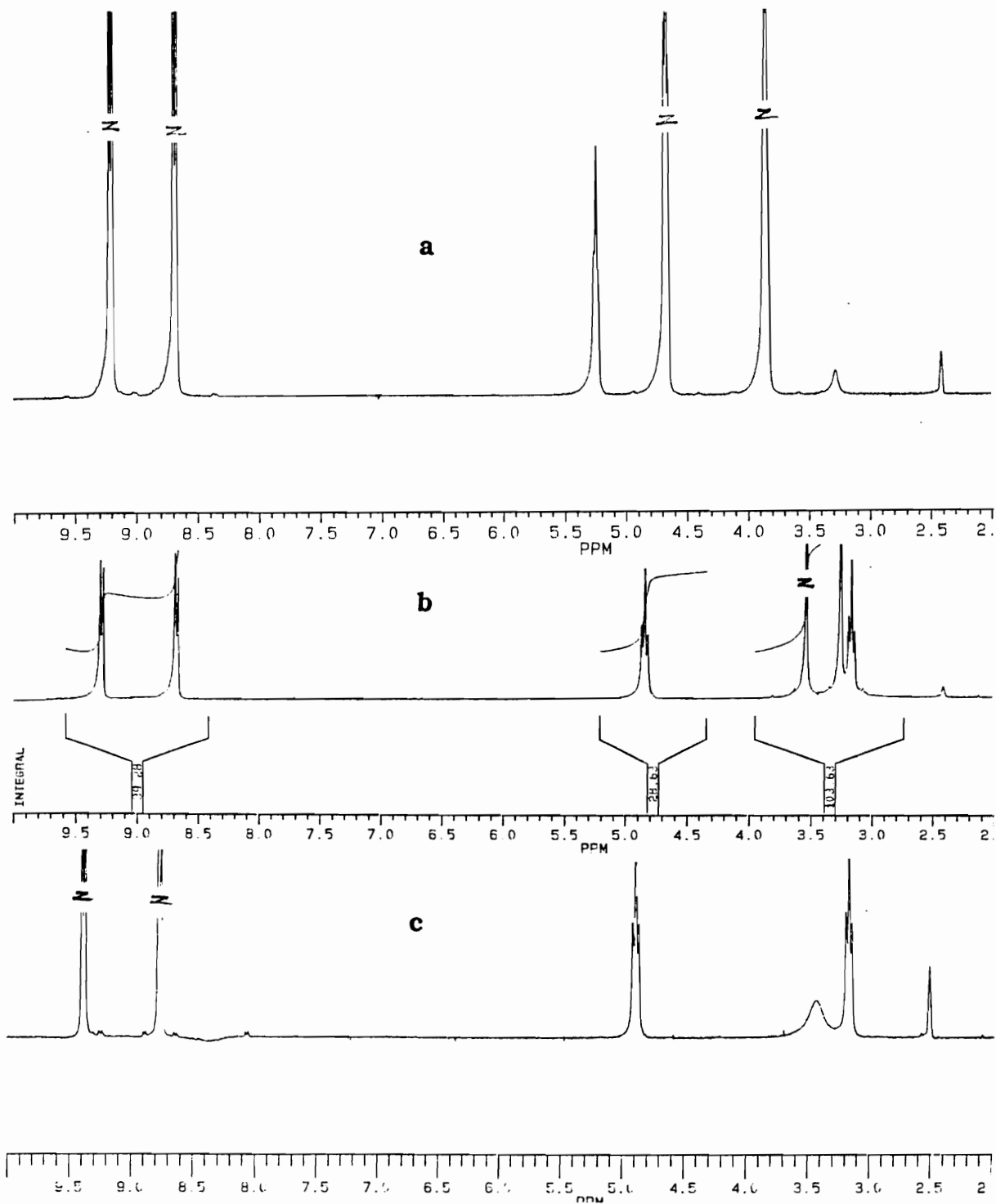


Figure V-5: ¹H-NMR Spectra of (a) Paraquat Diol (V-4), (b) Paraquat Diester (V-5) and (c) Paraquat Diacid (V-6). Solvent: DMSO-d₆.

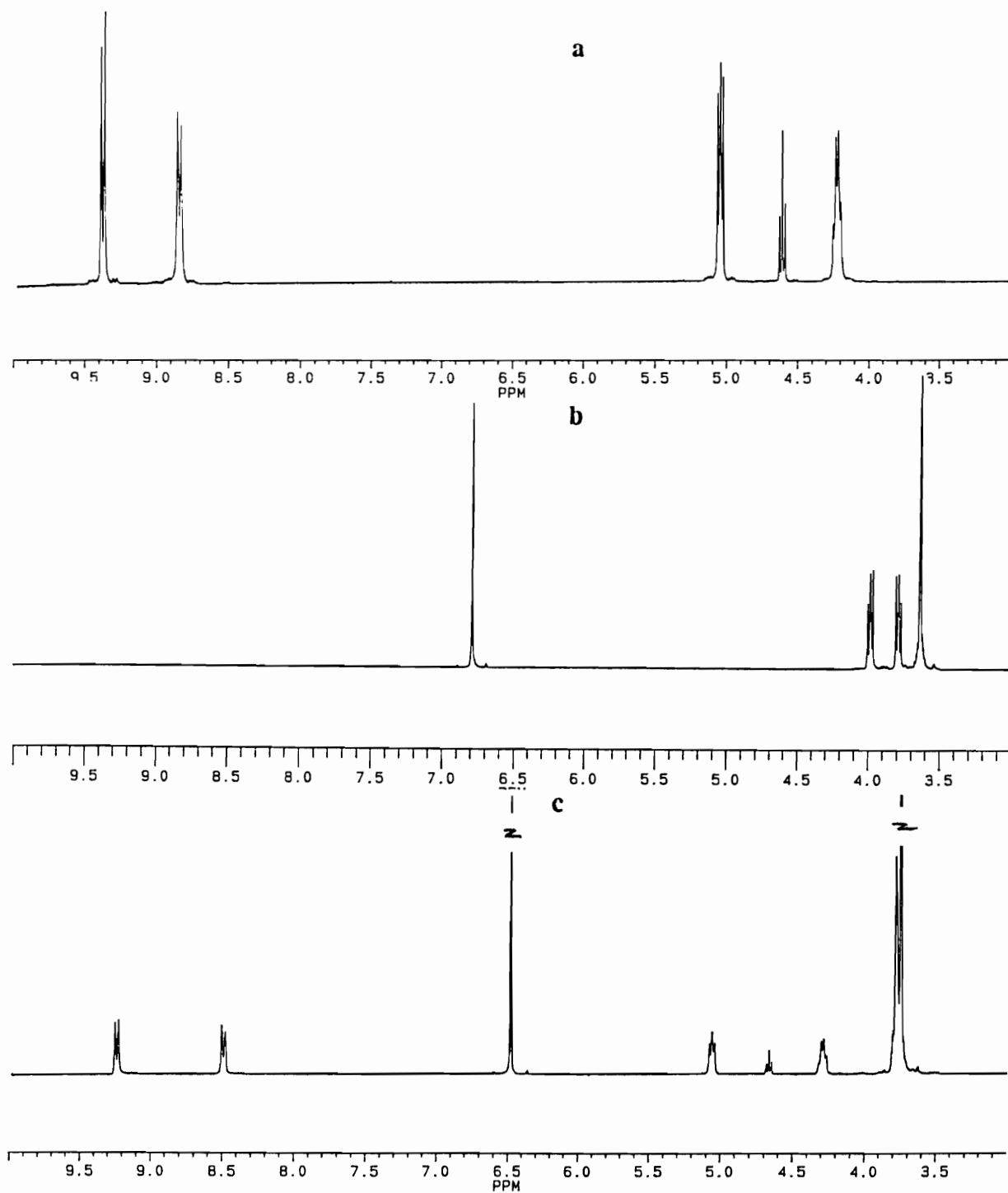


Figure V-6: $^1\text{H-NMR}$ Spectra of (a) BPP34C10, (b) Paraquat Diol (V-4) and (c) Complex (V-7) formed from V-4 and BPP34C10. Solvent: $\text{Acetone-}d_6$.

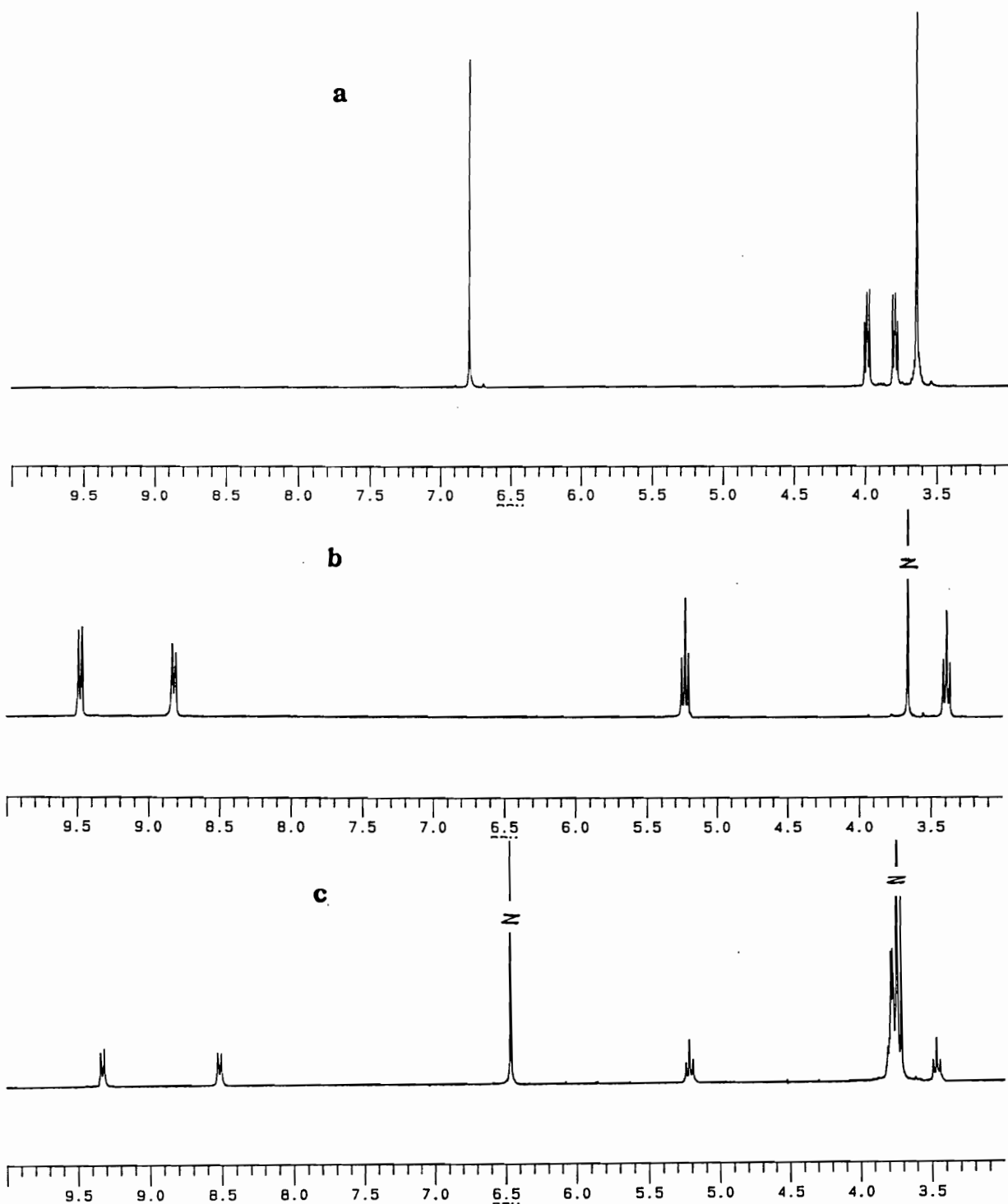


Figure V-7: $^1\text{H-NMR}$ Spectra of (a) BPP34C10, (b) Paraquat Diester (V-5) and (c) Complex (V-8) formed from V-5 and BPP34C10. Solvent: $\text{Acetone-}d_6$.

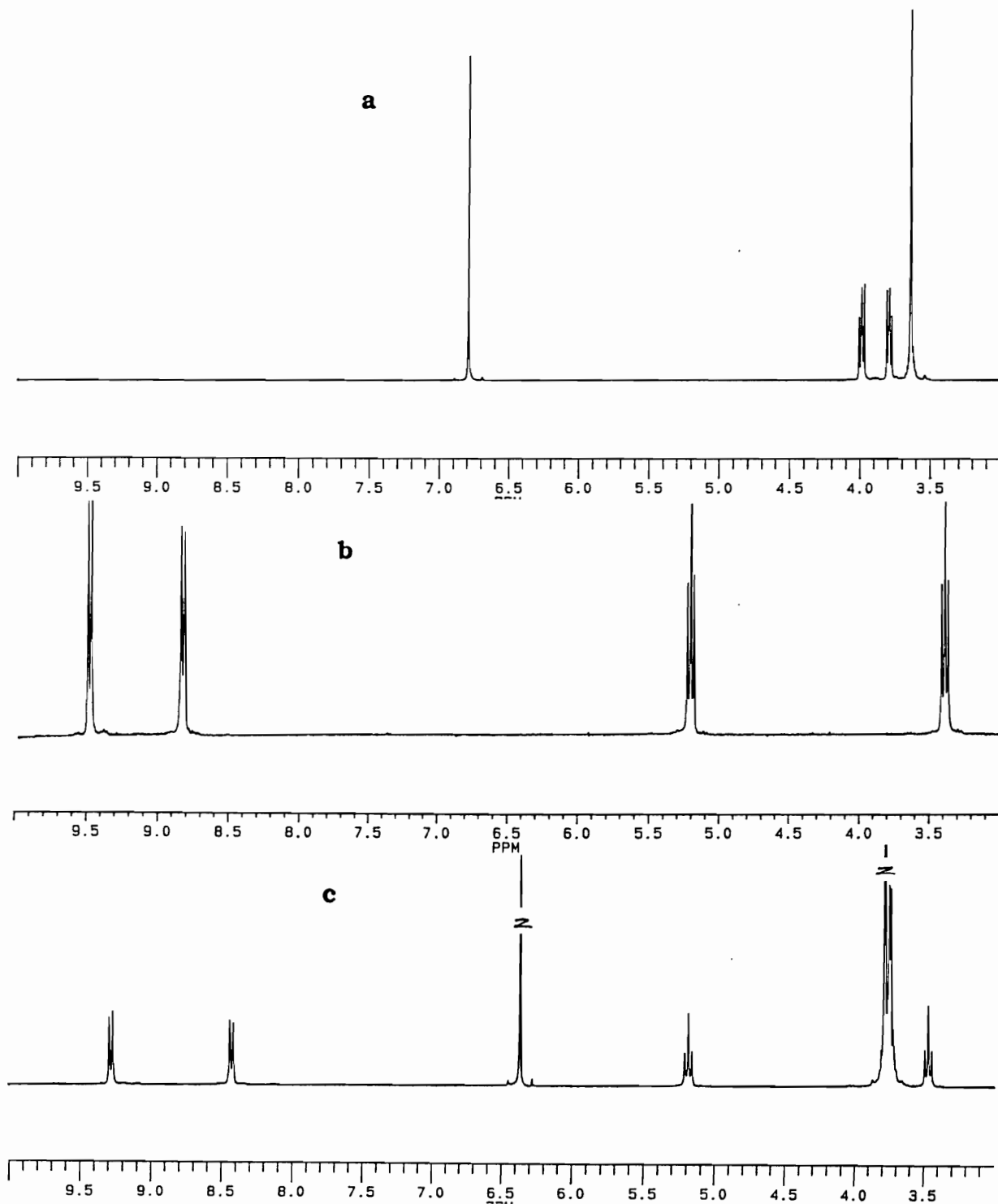
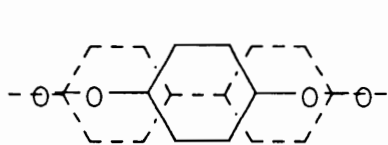
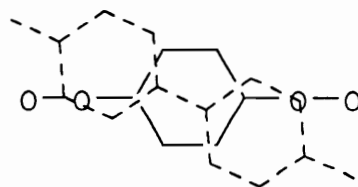


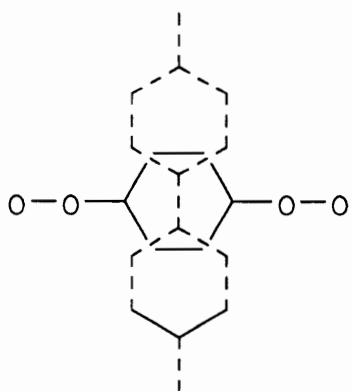
Figure V-8: $^1\text{H-NMR}$ Spectra of (a) BPP34C10, (b) Paraquat Diacid (V-6) and (c) Complex (V-9) formed from V-6 and BPP34C10. Solvent: Acetone- d_6 .



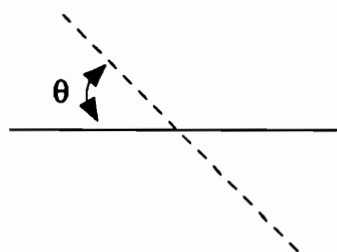
V-10a



V-10b

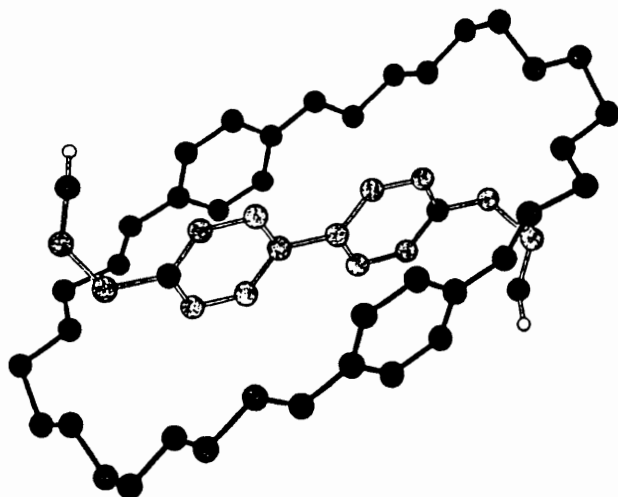


V-10c



General Representation

Figure V-9: Proposed Orientations of the Bipyridinium Rings Inside the Cavity of BPP34C10.



Crystal Data: $C_{45}H_{64}F_{12}N_2O_{13}P_2$, $M = 1130.9$, monoclinic, space group $I2/c$ (body-centred cell chosen because C-face-centred cell had $\beta = 139^\circ$), $a = 18.723(4)$, $b = 11.827(2)$, $c = 24.880(7)$ Å, $\beta = 101.61(2)^\circ$, $U = 5397$ Å³, $Z = 4$ (the complex is disposed about a centre of symmetry and the Me_2CO molecule about a two-fold axis), $D_c = 1.39$ g,cm⁻³, $\mu = 16$ cm⁻¹.

Figure V-10: X-Ray Crystal Structure and Crystal Data of Complex V-7 Obtained by Stoddart *at al.*

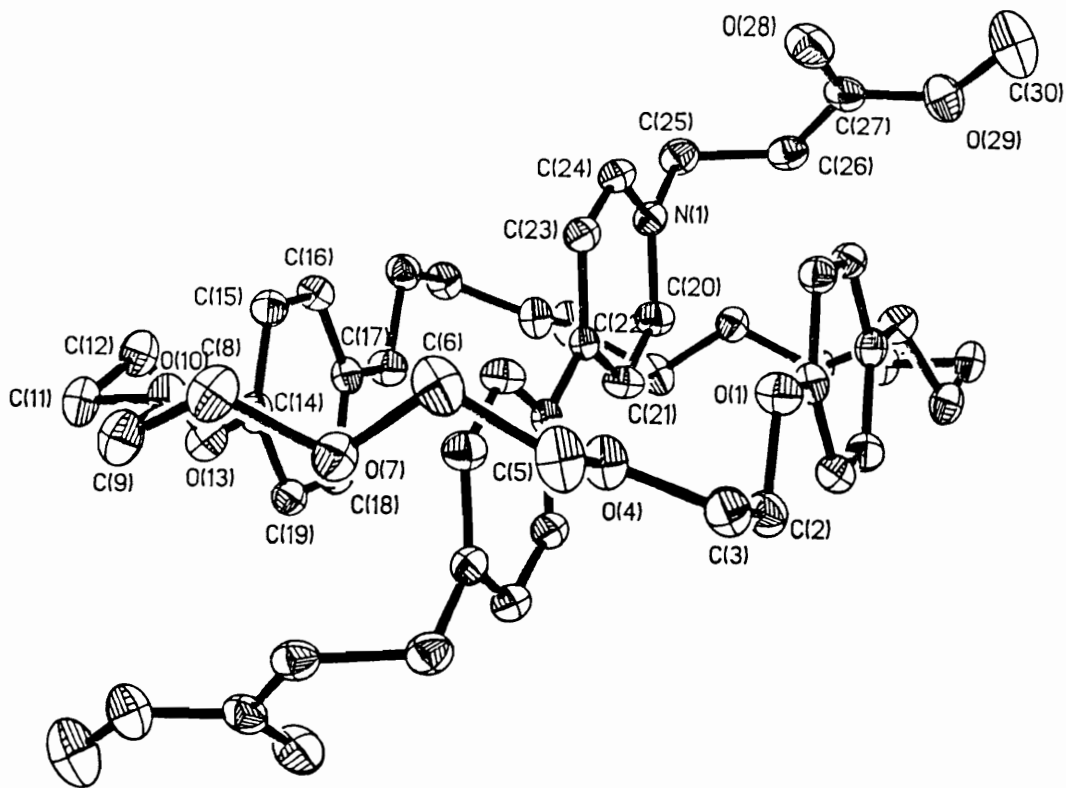


Figure V-11: X-Ray Crystal Structure of Complex V-8 (Side View).

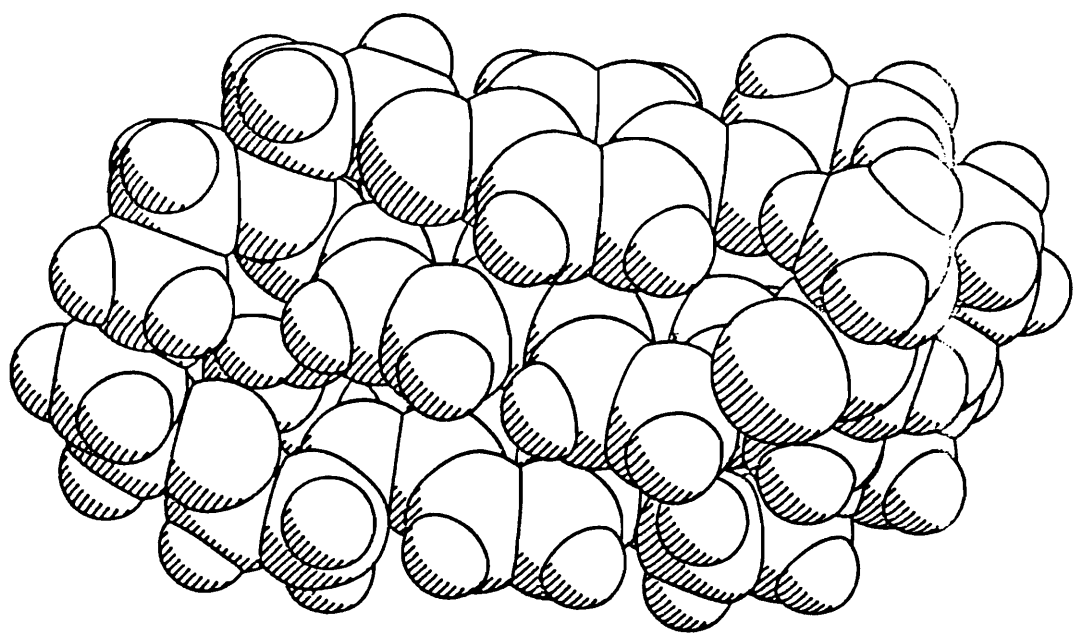


Figure V-12: X-Ray Crystal Structure of Complex V-8 (Space-Filling Representation).

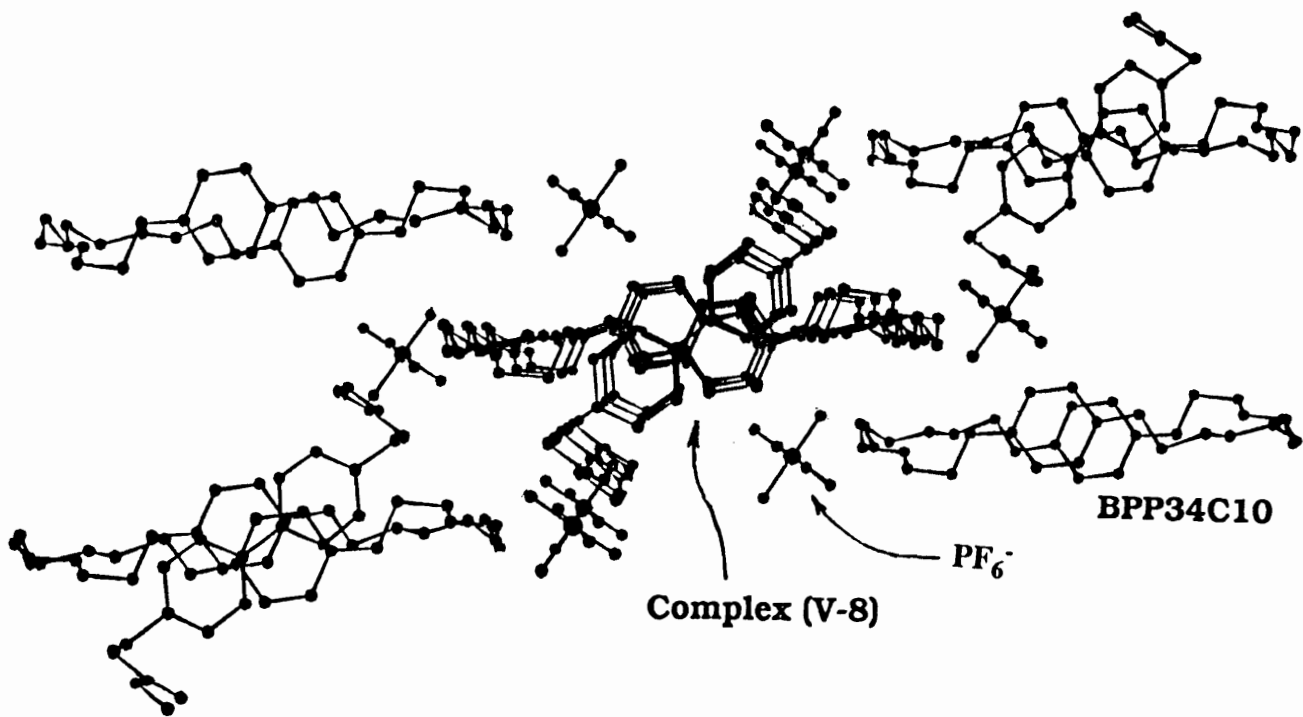
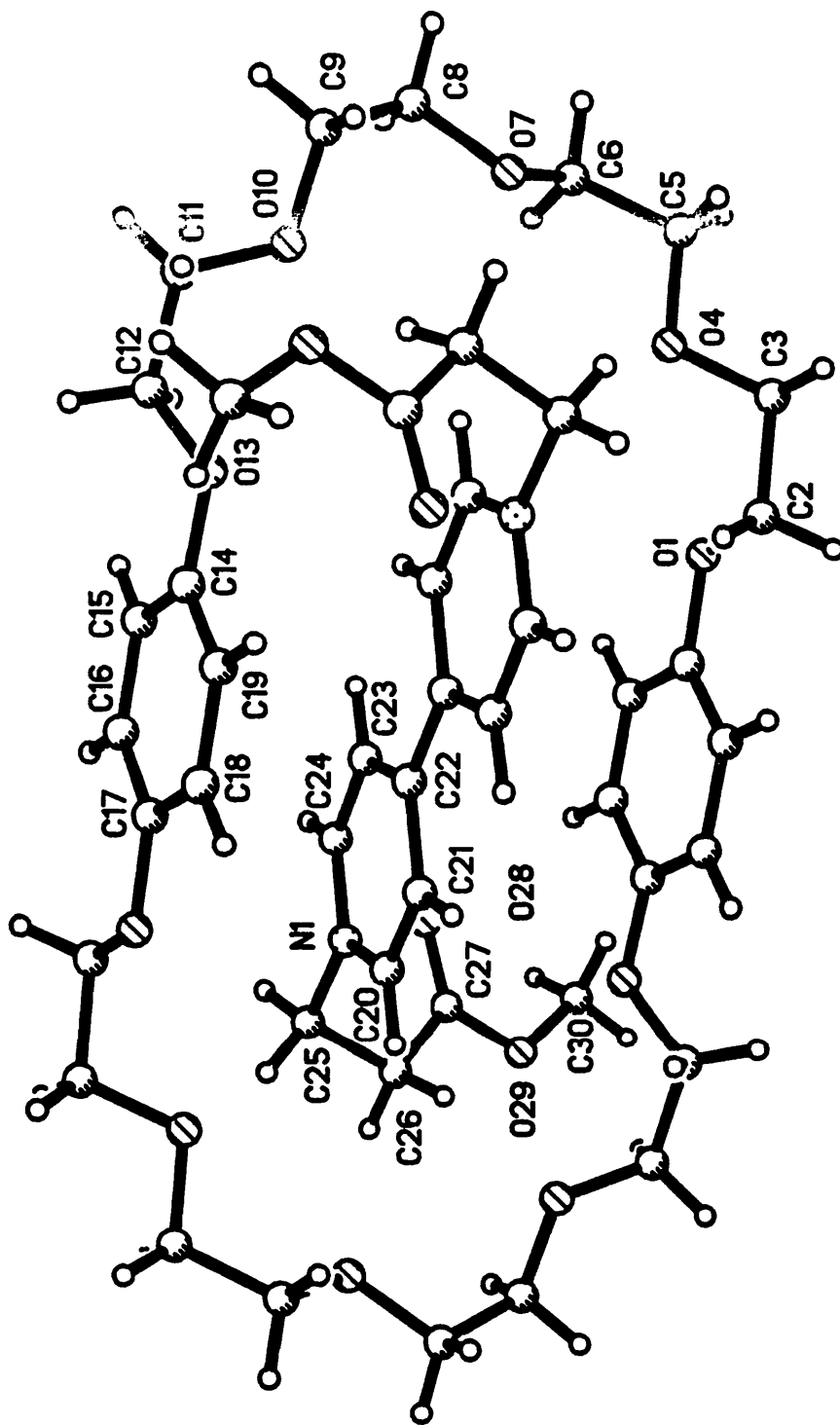
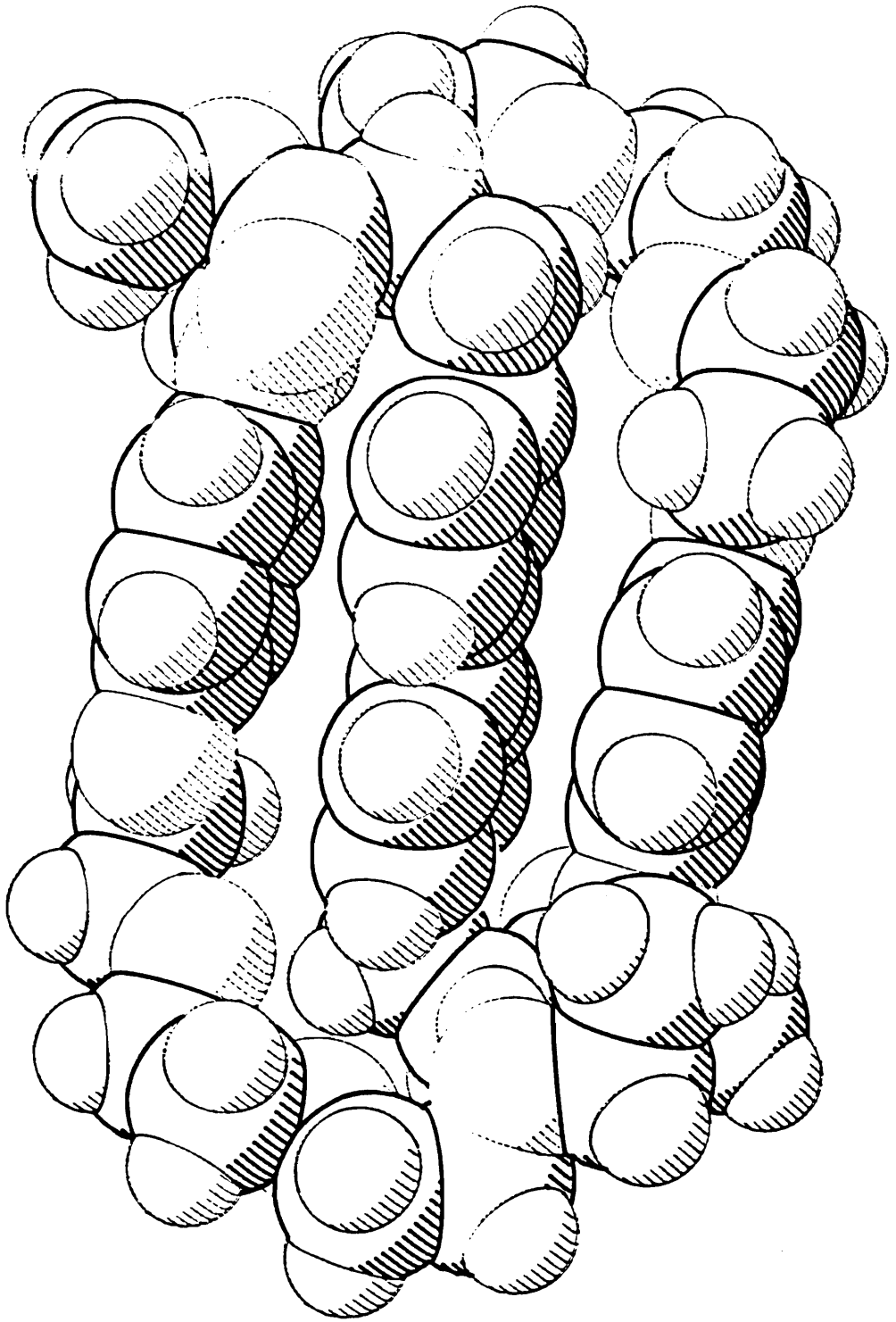


Figure V-13: Crystal Packing Diagram for Complex V-8.

APPENDIX V-1:

X-RAY CRYSTAL DATA OF HOST-GUEST COMPLEX (V-8)





Data Collection

Diffractometer Used	Siemens R3m/V
Radiation	MoK α ($\lambda = 0.71073 \text{ \AA}$)
Temperature (K)	298
Monochromator	Highly oriented graphite crystal
2 θ Range	3.5 to 45.0 $^{\circ}$
Scan Type	ω
Scan Speed	Variable; 3.00 to 14.65 $^{\circ}$ /min. in ω
Scan Range (ω)	0.60 $^{\circ}$
Background Measurement	Stationary crystal and stationary counter at beginning and end of scan, each for 25.0% of total scan time
Standard Reflections	3 measured every 300 reflections
Index Ranges	$0 \leq h \leq 30$, $0 \leq k \leq 12$ $-19 \leq l \leq 17$
Reflections Collected	3815
Independent Reflections	3517 ($R_{\text{int}} = 4.35\%$)
Observed Reflections	2982 ($F > 3.0\sigma(F)$)
Absorption Correction	N/A

Solution and Refinement

System Used	Siemens SHELXTL PLUS (VMS)
Solution	Direct Methods
Refinement Method	Full-Matrix Least-Squares
Quantity Minimized	$\sum w(F_o - F_c)^2$
Absolute Structure	N/A
Extinction Correction	$\chi = 0.0044(3)$, where $F^* = F [1 + 0.002\chi F^2 / \sin(2\theta)]^{-1/4}$
Hydrogen Atoms	Riding model, fixed isotropic U
Weighting Scheme	$w^{-1} = \sigma^2(F) + 0.0010F^2$
Number of Parameters refined	344
Final R indices (obs. data)	R = 5.22 %, wR = 7.29 %
R Indices (all data)	R = 6.00 %, wR = 7.86 %
Goodness-of-Fit	1.86
Largest and Mean Δ/σ	0.049, 0.004
Data-to-Parameter Ratio	8.7:1
Largest Difference Peak	0.31 eÅ ⁻³
Largest Difference Hole	-0.23 eÅ ⁻³

Atomic coordinates ($\times 10^4$) and equivalent isotropic displacement coefficients ($\text{\AA}^2 \times 10^3$)

	x	y	z	U(eq)
O(1)	-1433(1)	2074(2)	4028(1)	59(1)
C(2)	-1645(1)	1941(3)	4593(2)	59(1)
C(3)	-2205(1)	1509(3)	4149(2)	63(2)
O(4)	-2220(1)	377(2)	3865(1)	61(1)
C(5)	-2750(1)	-33(3)	3447(3)	74(2)
C(6)	-2777(1)	-1123(3)	3038(2)	71(2)
O(7)	-2567(1)	-2048(2)	3593(1)	57(1)
C(8)	-2679(1)	-3119(3)	3170(2)	68(2)
C(9)	-2319(1)	-4033(3)	3693(2)	63(2)
O(10)	-1791(1)	-3759(2)	3854(1)	57(1)
C(11)	-1429(1)	-4688(3)	4145(2)	57(1)
C(12)	-901(1)	-4293(3)	4225(2)	57(1)
O(13)	-629(1)	-3663(2)	4967(1)	56(1)
C(14)	-121(1)	-3278(2)	5162(2)	49(1)
C(15)	81(1)	-3191(3)	4610(2)	52(1)
C(16)	600(1)	-2788(3)	4860(2)	53(1)
C(17)	915(1)	-2472(2)	5662(2)	48(1)
C(18)	708(1)	-2547(3)	6213(2)	50(1)
C(19)	194(1)	-2957(2)	5964(2)	49(1)
N(1)	1035(1)	920(2)	4582(2)	53(1)
C(20)	1094(1)	991(3)	5342(2)	61(1)
C(21)	697(1)	638(3)	5518(2)	59(1)
C(22)	217(1)	194(2)	4908(2)	47(1)
C(23)	171(1)	139(3)	4130(2)	57(2)
C(24)	581(1)	515(3)	3983(2)	62(2)
C(25)	1486(1)	1267(3)	4412(2)	64(2)
C(26)	1542(1)	2552(3)	4404(2)	60(1)
C(27)	1102(1)	3119(3)	3692(2)	61(2)
O(28)	734(1)	2650(3)	3142(2)	89(1)
O(29)	1164(1)	4249(2)	3748(2)	81(1)
C(30)	756(2)	4911(5)	3121(3)	126(3)
P(1)	1298(1)	1564(1)	7921(1)	63(1)
F(1)	1492(1)	2795(2)	8260(2)	128(2)
F(2)	1639(1)	1559(3)	7458(2)	148(2)
F(3)	1091(1)	312(2)	7590(2)	118(2)
F(4)	951(1)	1549(3)	8393(2)	121(2)
F(5)	1780(1)	1038(2)	8697(2)	125(1)
F(6)	808(1)	2055(2)	7147(2)	116(1)

* Equivalent isotropic U defined as one third of the trace of the orthogonalized U_{ij} tensor

Bond lengths (Å)

O(1)-C(2)	1.428 (5)	O(1)-C(17A)	1.379 (3)
C(2)-C(3)	1.492 (4)	C(3)-O(4)	1.415 (4)
O(4)-C(5)	1.412 (4)	C(5)-C(6)	1.464 (5)
C(6)-O(7)	1.418 (4)	O(7)-C(8)	1.431 (4)
C(8)-C(9)	1.482 (4)	C(9)-O(10)	1.412 (4)
O(10)-C(11)	1.414 (3)	C(11)-C(12)	1.497 (5)
C(12)-O(13)	1.428 (4)	O(13)-C(14)	1.380 (4)
C(14)-C(15)	1.379 (6)	C(14)-C(19)	1.384 (4)
C(15)-C(16)	1.396 (4)	C(16)-C(17)	1.381 (4)
C(17)-C(18)	1.388 (5)	C(17)-O(1A)	1.379 (3)
C(18)-C(19)	1.386 (4)	N(1)-C(20)	1.339 (5)
N(1)-C(24)	1.334 (4)	N(1)-C(25)	1.497 (5)
C(20)-C(21)	1.363 (6)	C(21)-C(22)	1.401 (4)
C(22)-C(23)	1.383 (5)	C(22)-C(22A)	1.483 (7)
C(23)-C(24)	1.372 (6)	C(25)-C(26)	1.510 (5)
C(26)-C(27)	1.485 (4)	C(27)-O(28)	1.199 (4)
C(27)-O(29)	1.328 (4)	O(29)-C(30)	1.427 (5)
P(1)-F(1)	1.563 (3)	P(1)-F(2)	1.551 (5)
P(1)-F(3)	1.588 (3)	P(1)-F(4)	1.579 (4)
P(1)-F(5)	1.576 (2)	P(1)-F(6)	1.569 (2)

Bond angles (°)

C(2)-O(1)-C(17A)	116.7(2)	O(1)-C(2)-C(3)	109.0(3)
C(2)-C(3)-O(4)	111.2(3)	C(3)-O(4)-C(5)	111.3(3)
O(4)-C(5)-C(6)	111.6(3)	C(5)-C(6)-O(7)	112.6(3)
C(6)-O(7)-C(8)	111.0(2)	O(7)-C(8)-C(9)	111.2(2)
C(8)-C(9)-O(10)	108.2(3)	C(9)-O(10)-C(11)	114.2(2)
O(10)-C(11)-C(12)	108.1(3)	C(11)-C(12)-O(13)	108.8(3)
C(12)-O(13)-C(14)	116.9(3)	O(13)-C(14)-C(15)	124.1(2)
O(13)-C(14)-C(19)	116.5(3)	C(15)-C(14)-C(19)	119.5(3)
C(14)-C(15)-C(16)	120.3(3)	C(15)-C(16)-C(17)	120.3(4)
C(16)-C(17)-C(18)	119.3(3)	C(16)-C(17)-O(1A)	124.9(3)
C(18)-C(17)-O(1A)	115.9(2)	C(17)-C(18)-C(19)	120.3(3)
C(14)-C(19)-C(18)	120.4(3)	C(20)-N(1)-C(24)	120.1(3)
C(20)-N(1)-C(25)	119.6(2)	C(24)-N(1)-C(25)	120.3(3)
N(1)-C(20)-C(21)	120.7(3)	C(20)-C(21)-C(22)	120.8(3)
C(21)-C(22)-C(23)	116.7(3)	C(21)-C(22)-C(22A)	121.3(4)
C(23)-C(22)-C(22A)	122.0(3)	C(22)-C(23)-C(24)	120.3(3)
N(1)-C(24)-C(23)	121.4(3)	N(1)-C(25)-C(26)	111.9(3)
C(25)-C(26)-C(27)	113.9(2)	C(26)-C(27)-O(28)	126.2(3)
C(26)-C(27)-O(29)	110.4(3)	O(28)-C(27)-O(29)	123.4(3)
C(27)-O(29)-C(30)	116.6(3)	F(1)-P(1)-F(2)	91.9(2)
F(1)-P(1)-F(3)	178.4(2)	F(2)-P(1)-F(3)	89.7(2)
F(1)-P(1)-F(4)	88.9(2)	F(2)-P(1)-F(4)	179.1(2)
F(3)-P(1)-F(4)	89.5(2)	F(1)-P(1)-F(5)	89.9(1)
F(2)-P(1)-F(5)	90.5(2)	F(3)-P(1)-F(5)	90.0(1)
F(4)-P(1)-F(5)	89.2(2)	F(1)-P(1)-F(6)	91.6(1)
F(2)-P(1)-F(6)	90.4(2)	F(3)-P(1)-F(6)	88.4(1)
F(4)-P(1)-F(6)	89.9(2)	F(5)-P(1)-F(6)	178.2(2)

Anisotropic displacement coefficients ($\text{\AA}^2 \times 10^3$)

	U_{11}	U_{22}	U_{33}	U_{12}	U_{13}	U_{23}
O(1)	49(1)	72(1)	56(1)	-12(1)	23(1)	-3(1)
C(2)	59(2)	57(2)	67(2)	-4(2)	33(2)	2(2)
C(3)	56(2)	63(2)	75(2)	4(2)	35(2)	6(2)
O(4)	45(1)	56(1)	81(2)	-2(1)	26(1)	3(1)
C(5)	45(2)	63(2)	101(3)	0(2)	22(2)	9(2)
C(6)	52(2)	73(2)	70(2)	-4(2)	13(2)	13(2)
O(7)	53(1)	56(1)	57(1)	4(1)	21(1)	-1(1)
C(8)	50(2)	72(2)	69(2)	0(2)	17(2)	-13(2)
C(9)	47(2)	60(2)	76(2)	-8(2)	23(2)	-12(2)
C(10)	45(1)	50(1)	73(1)	1(1)	25(1)	0(1)
C(11)	54(2)	42(2)	66(2)	0(1)	21(2)	-6(1)
C(12)	47(2)	51(2)	65(2)	5(1)	20(2)	-5(2)
O(13)	44(1)	63(1)	61(1)	-5(1)	24(1)	-10(1)
C(14)	43(2)	42(2)	58(2)	7(1)	21(1)	2(1)
C(15)	50(2)	54(2)	47(2)	0(1)	16(1)	0(1)
C(16)	53(2)	55(2)	52(2)	1(1)	25(2)	5(1)
C(17)	45(2)	42(2)	52(2)	0(1)	18(1)	5(1)
C(18)	51(2)	50(2)	47(2)	1(1)	20(1)	-1(1)
C(19)	48(2)	48(2)	50(2)	2(1)	23(1)	1(1)
N(1)	59(2)	49(2)	59(2)	5(1)	33(1)	-1(1)
C(20)	61(2)	71(2)	48(2)	4(2)	23(2)	1(2)
C(21)	63(2)	73(2)	46(2)	3(2)	28(2)	4(2)
C(22)	62(2)	34(2)	46(2)	7(1)	26(2)	4(1)
C(23)	71(2)	52(2)	54(2)	-9(2)	35(2)	-7(1)
C(24)	80(2)	58(2)	54(2)	-6(2)	37(2)	-9(2)
C(25)	62(2)	73(2)	70(2)	3(2)	40(2)	-3(2)
C(26)	53(2)	77(2)	58(2)	-8(2)	31(2)	-7(2)
C(27)	58(2)	71(2)	61(2)	-12(2)	35(2)	1(2)
O(28)	86(2)	96(2)	63(2)	-24(2)	15(1)	4(1)
O(29)	71(2)	71(2)	96(2)	-8(1)	35(1)	11(1)
C(30)	103(4)	98(4)	164(5)	3(3)	49(4)	39(4)
P(1)	71(1)	60(1)	56(1)	-7(1)	27(1)	4(1)
F(1)	114(2)	67(2)	176(3)	-21(1)	44(2)	-20(2)
F(2)	155(3)	181(3)	170(3)	12(2)	127(3)	25(2)
F(3)	170(3)	75(2)	87(2)	-27(2)	40(2)	-12(1)
F(4)	128(2)	164(3)	98(2)	-30(2)	74(2)	-16(2)
F(5)	117(2)	118(2)	89(2)	24(2)	4(2)	6(2)
F(6)	112(2)	125(2)	80(2)	24(2)	18(1)	30(1)

The anisotropic displacement exponent takes the form:

$$-2\pi^2(h^2a^2U_{11} + \dots + 2hka*b*U_{12})$$

H-Atom coordinates ($\times 10^4$) and isotropic displacement coefficients ($\text{\AA}^2 \times 10^3$)

	x	y	z	U
H(2A)	-1430	1410	5013	80
H(2B)	-1640	2664	4844	80
H(3A)	-2368	1526	4506	80
H(3B)	-2408	2002	3694	80
H(5A)	-2967	524	3050	80
H(5B)	-2891	-133	3828	80
H(6A)	-3144	-1283	2663	80
H(6B)	-2582	-1056	2730	80
H(7A)	-2834	-3040	2883	80
H(8B)	-3044	-3330	3006	80
H(9A)	-2343	-4084	4194	80
H(9B)	-2421	-4759	3420	80
H(11A)	-1560	-5318	3770	80
H(11B)	-1390	-4938	4664	80
H(12A)	-689	-4942	4231	80
H(12B)	-955	-3817	3770	80
H(15A)	-137	-3407	4052	80
H(16A)	738	-2732	4474	80
H(18A)	922	-2314	6768	80
H(19A)	56	-3020	6351	80
H(20A)	1420	1293	5768	80
H(21A)	746	694	6067	80
H(23B)	-149	-163	3692	80
H(24A)	540	486	3438	80
H(25B)	1426	962	3894	80
H(25A)	1814	946	4822	80
H(26B)	1875	2730	4405	80
H(26A)	1555	2861	4894	80
H(30C)	840	5710	3222	80
H(30B)	734	4705	2603	80
H(30A)	418	4762	3115	80

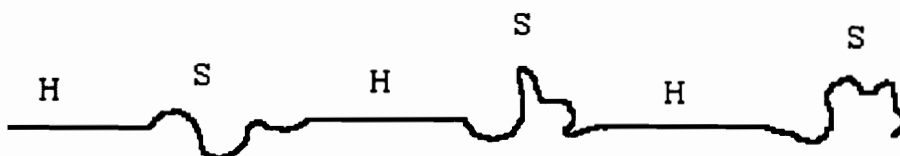
CHAPTER VI:
HOST-GUEST COMPLEXATION OF
PARAQUAT DICATION DERIVATIVES
AND BPP34C10.

PART 2: SYNTHESIS OF VILOGEN-
CONTAINING POLYURETHANE
ELASTOMERIC ROTAXANES

The formation of host-guest complexes (pseudorotaxanes) between difunctionalized paraquat dication derivatives and BPP34C10 has been extensively studied (Chapter V). However, this complexation has not yet been used in polyrotaxane synthesis, even though it has been known that it could offer a high threading efficiency. In this chapter, I will report the use of this complexation in synthesis of viologen-containing elastomeric polyurethane rotaxanes. Thus, this interesting host-guest chemistry is introduced to polyrotaxane synthesis.

VI-1: LINEAR THERMOPLASTIC POLYURETHANE ELASTOMERS

Polyurethane chemistry has been reviewed in Chapter IV. I will briefly discuss an important class of polyurethane materials, thermoplastic polyurethane elastomers. This class of materials fall into the category of $(AB)_n$ type of segmented copolymers.



VI-1

VI-1-1: THERMOPLASTIC ELASTOMERS¹⁻⁴

Let us first discuss thermoplastic elastomers in general. From a molecular point of view, the macromolecules composed of "hard" and "soft" segments as shown by schematic structure **VI-1**, where H and S represent the "hard" and "soft" segments, respectively. The "soft" segment is an amorphous polymer above its glass transition temperature (T_g). The "hard" segment is a crystalline or high T_g polymer below its T_m or T_g . Thus, the "soft" segment is generally a flexible polyether, polyester, polyalkyl, or polydimethylsiloxane, and so on. The "hard" segment is generally rigid containing rigid moieties such as aromatic

rings or has high structural regularity such as polystyrene or contains highly polar groups such as urethane or urea. It is able to undergo thermally reversible intermolecular association.

From a morphological point of view, the polymer is not homogeneous. Instead it is microphase separated. More specifically, the "hard" and the "soft" segments are not uniformly mixed but segregate to form domains. Figure VI-1 shows the morphological model of thermoplastic elastomers. Since the "hard" segment is below its T_m or T_g , the domain is crystalline or glassy. It forms solid microparticles distributed in the matrix. On the other hand, the "soft" segment is an amorphous polymer above its T_g ; it is rubbery and undergoes viscous flow, which is essential for the matrix. The interface is chemically bonded. Thus, we can envision that many, many solid microparticles ("hard" segment domain) are fastened together by many, many flexible chains ("soft" segment domain). The two domains offer intermediate overall polymer thermal and mechanical properties on a mutual improvement basis. The "hard" segment domains reinforce the "soft" segment matrix by acting as both tie down points and filler particles and the "soft" segment domains dilute the "hard" segment domain to increase the material flexibility and toughness.

Most important of all, this unique morphology causes the material to behave as a rubber. This is because the "hard" segment domain, which is analogous to cross-linking points in rubbers, provides dimensional stability and recovery after mechanical deflection. However,

this pseudocrosslinking points can be thermally untied and retied due to the nature of secondary bonding.

It is well known that properties, especially the thermal and mechanical properties, of a thermoplastic elastomer depend on the degree of phase separation and molecular ordering within each domain; both are essentially determined by the nature of the two segments, such as rigidity of "hard" segment and flexibility of "soft" segment, lengths of the segments, stereoregularity, intermolecular interactions, etc. and also the thermal history. Generally, the longer sequence length (it is required that sequences are above a critical length for the phase separation to occur) and bigger the difference in the nature of the two segments, the higher the degree of phase separation.

VI-1-2: SYNTHESIS OF THERMOPLASTIC POLYURETHANE ELASTOMERS⁵

Three basic starting materials are required for the synthesis of thermoplastic polyurethane elastomers: polyol, diisocyanate and chain extender. The chain extender is generally a low molecular weight diol or diamine. The polyol is relatively flexible and high molecular weight (above critical molecular weight) and used to build up the "soft" block, while the "hard" block is made up of urethane derived from the diisocyanate and chain extender as well as the hydroxyl end group of the polyol or urethane-urea if a diamine is used as the chain extender. Since the chain extender is a low molecular weight species, the "hard" segment

domain contains a high concentration of urethane or urethane and urea groups, making it high T_g and/or crystallizable.

There are two synthetic strategies leading to the formation of thermoplastic polyurethane elastomers: one-shot process and two-step process.

The one-shot process is straightforward. Three starting materials, a polyol, a diisocyanate and a chain extender are mixed simultaneously with a catalyst (in most of cases). It could be a neat reaction or in the presence of a polar solvent. The reaction is carried out at a temperature below 110°C to avoid side reactions as discussed in Chapter IV. The polymer is obtained with random distribution of "hard" and "soft" segments. However, the polymer structure may not be well defined.

A two-step process which produces a well defined polymer structure is widely used. As shown in Scheme VI-1, a large excess of diisocyanate first reacts with a polyol, resulting in a low molecular weight intermediate polymer called "prepolymer" which is terminated with isocyanate groups. In fact, this "prepolymer" is a macrodiisocyanate which can further react with a diol or a diamine. Thus, in the second step, a chain extender which is a low molecular weight diol or diamine is added. The chain extender molecules function as "adapters" to connect the "prepolymer" molecules together, resulting in a high molecular weight segmented copolymer in which the "soft" segment is introduced from the polyol and the "hard" segment is from the diisocyanate and chain extender and the functional groups formed during the polymerization.

The diol and diamine chain extenders lead to the formation of polyurethane elastomers and polyurethane-urea elastomers, respectively.

It is obvious that properties of the polymer depend on the building blocks, that is, molecular weight and type of the "soft" and the "hard" segment, their interactions and crystallinity. Therefore, it is possible to obtain a polymer having desired properties by proper design of "hard" and "soft" segments through the choice of polyol, diisocyanate and chain extender and polymerization conditions.

VI-1-3: STARTING MATERIALS

Polyols used for polyurethane elastomer synthesis are usually polyethers, polyesters, polydimethylsiloxanes, etc. having molecular weight ranging from 500 to 3000. Table VI-1 lists some examples of common used polyols. Most of polyurethane elastomers have been produced with polyester and polyether as "soft" segment. Polyester based elastomers offers better material properties than the polyether based ones. However, poor water resistance was found with polyester based materials since ester bonds can be hydrolytically cleaved.^{19,20} Concerning materials properties, polypropylene oxide (PPO) and polytetramethylene oxide (PTMO) may be good choices as the polyols.

PTMO based polyurethane elastomers display excellent physical properties such as hydrolytic stability, thermal stability, low temperature flexibility, high fungus resistance, etc.²¹ The PTMO's with molecular weights 650, 1000 and 2000 are the most commonly used. This

molecular weight range (650 - 2000) of PTMO covers the variation range of the most useful properties of PTMO based polyurethane elastomers and offers a general view on relationship between elastomer properties and PTMO soft segment molecular weight.

The diisocyanates used for polyurethane elastomers could be aromatic, such as methylene-di-phenylene diisocyanate (MDI) or tolylene diisocyanate (TDI), or aliphatic, such as methane-di-cyclohexyl diisocyanate (H-MDI) and hexamethylene diisocyanate (HDI). Some examples of commonly used diisocyanates were given in Chapter IV (see Table IV-1). Since diisocyanate is incorporated in the hard segment with the chain extender, the nature of the diisocyanate such as rigidity and intermolecular interactions along with nature of the chain extender determine properties of the hard segment domain. For example, polymers derived from aromatic diisocyanates such as TDI and MDI possess higher softening temperature than their aliphatic counterparts.

Chain extenders are low molecular weight diols or diamines; the latter give tougher materials since urea is a more polar group than urethane. Commonly used chain extenders are given in Table VI-2. Diphenols such as hydroquinone and bis-phenol-A are not widely used due to their lack of reactivity toward prepolymer. However, aromatic chain extenders yield harder materials than aliphatic ones.

High molecular weight polyurethane elastomers are prepared from a 1:1 molar ratio of isocyanate group to the total hydroxyl group if diol is used as chain extender or total hydroxyl and amine groups if diamine is

used as chain extender. Molecular weight control is possible by variation of this ratio or use of a monofunctional chain terminator. On the other hand, polymer properties depend on the molar ratio of polyol to chain extender, which determines the weight percentage of hard segment of the polymer. Of course, softer materials are obtained with higher molar ratio polyol to chain extender.

VI-1-4: MORPHOLOGY WITHIN THE HARD SEGMENT DOMAIN²²

It would be interesting to look at how molecules array within the hard segment domain; this would be helpful for us to understand the effect of rings on the morphology of the hard segment domain in polyrotaxane systems. Morphology within the hard segment domain is determined by the primary structure (chemical nature and length of the segment) and secondary structure (three dimensional organized proximity zones formed through parallel spacing in a direction diagonal to the chain). The secondary structure results from intermolecular hydrogen bonding and π - π interaction between adjacent aromatic rings of symmetric isocyanate if an aromatic diisocyanate is used. It is obvious that the secondary structure formation depends not only on the nature of hard segment but also thermal environments and history of the sample. Due to the hard segment length difference (non-ideal situation) and incomplete segregation, the domain may be ragged.^{23,24} However, the hard segment domain could be predominantly paracrystalline in most cases. Blackwell *et al.* have obtained an X-ray single crystal structure of a model diurethane formed from MDI and butanediol as shown in Figure

VI-2. It is a clear picture showing the molecular ordering within the hard segment, forming beautiful molecular "sheets" stacked to a three dimensional architecture.

VI-2: VIOLOGEN-CONTAINING POLYMERS

Due to the redox property of viologen, viologen-containing polymers are widely used as photo- and electrochromic redox polymers.^{26,27} They are also used as electrodes and electron-transfer catalysts in oxidation-reduction systems.²⁸ Furthermore, they could be used as optical recorders,²⁹ liquid crystalline polymers³⁰ and thermoplastic elastomers.³¹⁻³³

VI-2-1: Conventional Viologen-Containing Polymers

Viologen-containing polymers have appeared for several decades.³⁴⁻³⁸ However, it seems that the polymers with good film-forming properties were reported by Simon *et al.*²⁷ They synthesized viologen-containing polyamides by interfacial condensation of N,N'-bis(aminoalkyl)-4,4'-dipyridinium salts with di-, tri-, or tetrafunctional acid chlorides. They have also studied photochromic redox properties of the polymers.

There are two synthetic methods to incorporate viologen units into a polymer chain. First, direct polymerization of 4,4'-dipyridyl and

dihalogen monomers such as dibromides or diiodides;²⁶ dichlorides are not used because of lack of reactivity toward 4,4'-dipyridyl. This method is shown in Scheme VI-2. It is a common method for polyviologen preparation. Most polyviologens prepared from this method are derived from dibenzylic halides such as dibromoxylene because of their high reactivity toward 4,4'-dipyridyl. Of course, other types of leaving groups instead of halogens can also be applied. For example, a poly(ethylene glycol) ditosylate was employed as the comonomer to produce viologen-containing polymers with 4,4'-dipyridyl by Endo *et al.*²⁸

The second method for the preparation of viologen-containing polymers involves two-steps as illustrated in Figure VI-3: (1) preparation of difunctionalized viologen derivatives and (2) polymerization of the difunctionalized viologen derivatives and another monomer to form a high molecular weight polymer. For example, Simon *et al.* have prepared numbers of viologen-containing polymers by condensation polymerizations involving N,N'-bis(γ -aminopropyl)-4,4'-dipyridinium bromide.²⁷ This method may be better for designing a more complicated polymer structure since the nitrogen substituents could be chosen from a range of types. However, the substituents may not be long chains or the viologen derivatives would be difficult to purify. Another advantage of this method is that viologen-containing polymers may be prepared via any type of polymerization by proper choice of f and g groups.

VI-2-2: VILOGEN-CONTAINING THERMOPLASTIC ELASTOMERS

It has been known that viologens are highly crystalline compounds because of positive charges on the bipyridinium rings. Thus, viologen units have been incorporated into the hard segment of thermoplastic elastomers.³¹⁻³³ Kohjiya *et al.* have synthesized viologen-containing elastomers using poly(tetrahydrofuran) chains as the soft segments.³² The polymerization process is illustrated in Scheme VI-4. The polymer having poly(tetrahydrofuran) as the soft segment and the viologen unit as the hard segment was obtained by the polymerization of living dicationic poly(tetrahydrofuran) macromonomer and 4,4'-dipyridyl. The polymer exhibited excellent mechanical and elastomeric properties.³³ Kohjiya *et al.* have also observed that the tensile stress of the elastomer was effected by light. The stress decreased with time when the material was subjected to photo-illumination. Their result indicates that the accelerated stress relaxation is induced by photo-induced transformation of the viologen dication to a viologen cation-radical, resulting in decrease in electrostatic interactions among the molecules.

VI-3: RESULTS AND DISCUSSION

VI-3-1: SYNTHESSES OF LINEAR THERMOPLASTIC POLY(URETHANE-VIOLOGEN-PTMO)-ROTA-BPP34C10 AND THEIR CORRESPONDING MODEL POLYMERS

I have previously reported the formation and X-ray solid state structures of host-guest complexes formed from difunctionalized paraquat dication derivatives and BPP34C10 (Chapter V). One of these threaded complexes (**V-7**, dihydroxyl functionalized) was used as one of the monomers leading to ionic polyrotaxanes.

VI-3-1-1: Polymerizations

The synthetic approach to poly(urethane-viologen-PTMO) and BPP34C10 based polyrotaxanes and their corresponding model polymers is shown in Scheme VI-5. A typical two-step technique leading to the formation of segmented polyurethanes was used.

In the first step, a so-called prepolymer was prepared *in situ* from MDI and PTMO. When MDI was used in large excess (molar ratio: MDI/PTMO > 2/1), the prepolymer, a trimer having monomer sequence MDI-PTMO-MDI, was terminated with isocyanate groups and hence, retained reactivity toward diols. The reaction was performed very carefully under nitrogen to prevent hydrolysis of MDI and in refluxing acetonitrile, that was at 85°C, a temperature which provided a reasonable reaction rate without side reactions. After 1.5 hours of

reaction, the prepolymer had formed and the solution became a slightly yellow viscous oil.

In the second step, generally referred to as the chain extension step, N,N'-bis(2-hydroxyethyl)paraquat hexafluorophosphate (**V-4**) or its BPP34C10 host-guest complex (**V-7**) was used a chain extender which interconnects prepolymers to produce a high molecular weight segmented copolymer; the former produced a model polymer and the latter produced a polyrotaxane. The soft segment of the copolymer was derived from PTMO and the hard segment included MDI and paraquat linkages. In the polyrotaxane system, BPP34C10 tends to stay in the hard segment due to its strong charge transfer interaction with paraquat dication. A total 1:1 stoichiometry of isocyanate group to hydroxyl group (from both PTMO and chain extender) was used to achieve a high molecular weight polymer. Our chain extender **V-4**, especially its BPP34C10 host-guest complex (**V-7**) is less reactive with diisocyanate compared to common aliphatic diols such as ethylene glycol and butanediol because the hydroxyl group was deactivated by the electron withdrawing positively-charged nitrogen atom on the β -carbon and furthermore, the steric hindrance from the encircled BPP34C10 for **V-7**. Therefore, the second-step reaction was allowed 36 hours which is much longer than a normal chain extension step. Viscosity was observed to increase during this step.

Three different molecular weight PTMOs, MW = 650 (PTMO-650); 1000 (PTMO-1000); 2000 (PTMO-2000), were used in order to observe

variation of properties with the soft segment length at a constant hard segment. Thus, a total six of polymers (three polyrotaxanes with three corresponding model polymers) have been synthesized: PTMO-650 model (VI-2); PTMO-650 polyrotaxane (VI-3); PTMO-1000 model (VI-4); PTMO-1000 polyrotaxane (VI-5); PTMO-2000 model (VI-6) and PTMO-2000 polyrotaxane (VI-7).

The solvents used for the polymerizations were a mixture of acetonitrile and diglyme. It is known that acetonitrile provides a good medium for the formation of the host-guest complex. Diglyme, an open chain analog of crown ethers, was used to increase the solubility of PTMO in the reaction medium. However, the solubility of PTMOs are different due to differences in their molecular weight. Thus, the ratio of acetonitrile to diglyme has to be different for each case: 2.5 for PTMO-650 systems, 1.3 for PTMO-1000 systems and 0.8 for PTMO-2000 systems.

VI-3-1-2: Purifications

In the case of the statistical threading approach reported in Chapter IV, the polymers were purified by multiple reprecipitations. Polymers were first dissolved in small volumes of acetone, and then reprecipitated into large volumes of methanol in which BPP34C10 is very soluble but the polymers are not. The reprecipitations were continued until a constant composition of the polymer was reached based on NMR analysis, and therefore, we expect no free (unthreaded) BPP34C10 in the systems.

VI-3-1-3: ^1H -NMR Analysis and Polymer Compositions

^1H -NMR analyses were done after each reprecipitation. All three model polymers (**VI-2**, **VI-4** and **VI-6**) have the same spectra except for signal integration differences because of different molecular weight PTMO used. Again, all three polyrotaxanes (**VI-3**, **VI-5** and **VI-7**) have the same spectra but with different signal integrations. The ^1H -NMR spectra of two examples from the polymers containing PTMO-2000, one model polymer (**VI-6**) and one polyrotaxane (**VI-7**), are shown in Figure VI-3. They were taken in acetone- d_6 . By comparison of these two spectra along with the spectrum of BPP34C10 (Figure V-6a), it is obvious that (1) the spectra of the polyrotaxane (Figure VI-3b) shows signals of BPP34C10 and (2) chemical shift changes similar to those reported in Chapter V for the probe protons on paraquat dication and BPP34C10 upon the formation of host-guest complex were observed, i.e., upfield shifts of aromatic paraquat and BPP34C10 protons and collapse of aliphatic protons of BPP34C10 into a broad singlet. These chemical shift changes indicate the inclusion of paraquat dication unit in the cavity of BPP34C10 in the polyrotaxane systems, i.e., the formation of polyrotaxanes. The integration ratio of BPP34C10 aromatic protons to paraquat aromatic protons near nitrogen atoms in the polymer backbone enables us to determine the number of rings incorporated per paraquat unit (x/y values). Also the integration ratio of PTMO protons to the paraphenylene protons in the polymer backbone enables us to determine the relative content of soft and hard segment (a/y values).

Rings per paraquat unit (x/y values) for polyrotaxanes after each reprecipitation determined by the NMR analysis are listed in Table VI-3. A constant value was obtained for each polymer after two reprecipitations. Thus, there was no free BPP34C10 remaining in the polyrotaxanes systems. The molar ratio of BPP34C10 to **V-4** monomer feed (to form **V-7** *in situ*) for all three polyrotaxanes was 1.15; the final x/y values are close to 1 (0.98, 0.98 1.00), indicating that the threading efficiencies for all three cases are nearly quantitative. The total polymer compositions are summarized in Table VI-4. It is seen that, with the same molar ratios of monomer feed, the weight percentage of hard segment decreases with increase in PTMO molecular weight and so does the weight percentage of BPP34C10 incorporated. However, for each polymer, the ratio of PTMO unit to MDI unit to paraquat unit (a/R/y value) determined is close to the ratio of its monomer feed, indicating that all monomers were converted into polymer.

VI-3-1-4: Viscosity Measurements

The viscosity measurements were first done in acetone at 31°C. The results are reported as plots of reduced viscosities (η_{red}) versus concentration and shown in Figure VI-4. Nonlinear relationships were obtained; the polyelectrolyte effect on viscosity of dilute solutions can be clearly seen for all samples. In the high dilution region (concentration < 0.5 g/dl), the reduced viscosities increase dramatically with decrease in concentration. This phenomenon generally reflects the polyelectrolyte effect. The presence of cationic charged nitrogen atoms along the

polymer chain causes intra- as well as inter-molecular repulsions and an extended conformation results. This effect is more pronounced at high dilutions. Therefore, a rapid increase of viscosity with concentration in the high dilution region was observed and I was unable to obtain intrinsic viscosities.

Fortunately I found that this polyelectrolyte effect can be minimized in NMP with the addition of LiBr (5 g/L). As illustrated in Figure VI-5, the added salt causes a contraction of the polyelectrolyte conformation by a so-called screening of the electrostatic repulsions and hence, the polyelectrolytes behave as normal polymers that form random coils. Because the added LiBr causes the polyelectrolyte molecule to coil up, and resemble the "classical" behavior of a polymer in the solution, I was able to obtain meaningful intrinsic viscosity values, and hence the average molecular weight estimate.

Again, the reduced viscosities of the polymers obtained in NMP with the addition of LiBr are plotted against concentration and shown in Figure VI-6. It can be seen that a linear relationship is maintained generally for all polymers. Also, as shown in Table VI-5, intrinsic viscosity increases with increasing in molecular weight of the PTMO (soft segment) incorporated in the polymers. However, the intrinsic viscosities of all polyrotaxanes are close to their corresponding model polymers. Thus, we could estimate that the polyrotaxanes possess molecular weights comparable to their corresponding model polymers.

Attempts have also been made to determine molecular weights of polymers by equilibrium light scattering measurements. Unfortunately, it was unsuccessful due some difficulties such as the polyelectrolyte effect, low solubilities of polymers in many solvents, low light scattering signal difference between solvents and polymer solutions, etc.

VI-3-1-5: Counter Anion Exchanges

The counter anion of the polymers, hexafluorophosphate (PF_6^-), was changed to bromide (Br^-) in order to observe the effect of counter anion on polymer properties. The exchanges were done by reprecipitations of the polymers initially having PF_6^- counter anions from small amounts of acetone or THF into a relatively large amounts of concentrated NaBr aqueous solutions. After the treatments, the polymers (with Br^- as counter anion) showed some significant differences in properties. For example, the polymers seem harder and lighter in color; also the polymers were insoluble in acetone and less soluble in THF, while the the polymers with PF_6^- counter anion were very soluble in these two solvents.

VI-3-1-6: Polymer Films

All polymers form very nice transparent elastomeric films behaving as rubbers. They can be either cast from acetone or THF. Films of model polymers are slightly yellow and those of polyrotaxanes are deep red. Flexibility of the films increases with increasing PTMO molecular

weight. On the other hand, it seems that the polyrotaxanes are more flexible than their corresponding model polymers.

Tensile tests showed different stress-strain behaviors between polyrotaxanes and the corresponding model polymers. The stress-strain behavior of poly(urethane-viologen-PTMO-650) (**VI-2**) and poly(urethane-viologen-PTMO-650)-rotaxa-BPP34C10 (**VI-3**) is shown in Figure VI-7. It can be seen that the model polymer (**VI-2**) displays a normal stress-strain behavior as a elastomer. However, a plastic yielding signal was observed for the polyrotaxane (**VI-3**), indicating that the threaded macrocycle acts as a plasticizer which increases the free volume in the "hard" segment domain. Interestingly, the polyrotaxane does not lose strength, instead it is stronger and tougher than the model polymer. This is probably due to the strong electronic interactions between BPP34C10 and viologen moieties, not only intra-annular interaction but also inter-molecular interaction. Thus, the presence of BPP34C10 in the hard segment domain increases free volumes, but may not decrease the intermolecular association.

The more extensive study on the structure-property relationships of this class of polymers is currently being carried out by Prof. G. L. Wilkes and Don Loveday in the Chemical Engineering Department at Virginia Polytechnic Institute and State University and the results will be reported in Loveday's Ph. D. dissertation (Virginia Polytechnic Institute and State University, Blacksburg, Virginia)

VI-4: EXPERIMENTAL

BPP34C10 was prepared from hydroquinone and tetra(ethylene glycol) ditosylate via one-pot reaction in refluxing mixture of 1-butanol and 1,4-dioxane and purified by recrystallization three times in a mixture of toluene and n-hexane (see Chapter II). N,N'-Bis(2-hydroxyethyl)paraquat hexafluorophosphate (**V-4**) was prepared from the Menschutkin reaction of 4,4-dipyridyl and 2-iodoethanol used as the reaction solvent as well and then anion exchanged with NH_4PF_6 in water. It was also purified by recrystallization three times in water (see Chapter V). MDI was purchased from Aldrich Chemical Co. and further purified by vacuum distillation two times (0.10 torr, 188°C, collected only middle fraction). PTMOs were purchased from Monomers-Polymers Co. and used without further purification. NaBr (99%) was purchased from Aldrich Chemical Co. and used without further purification. Solvents acetonitrile and diglyme were also purchased from Aldrich Chemical Co. as anhydrous reagents and used directly.

The FT-NMR (proton) spectra were recorded on a Bruker WP270 MHz instrument using tetramethylsilane as the internal standard. The viscosity measurements were done using a Cannon-Ubbelohde semi-micro dilution solution viscometer with 50 centipoise inner diameter capillary when acetone was used as solvent and 100 centipoise inner diameter capillary when NMP + LiBr (0.006 M) was used as solvent. The temperature (31°C) was controlled by a constant temperature water

bath. The viscosities at various concentrations were taken and calculated reduced viscosities were plotted against concentration and intrinsic viscosities were obtained by extensions of straight lines to zero concentration.

Uniaxial stress-strain experiments were performed on dog-bone specimens using an Instron Tensile Tester (Model 1122) at room temperature.

VI-4-1: SYNTHESIS OF POLY(URETHANE-VIOLOGEN-PTMO-650)

(VI-2)

To an oven-dried 15-mL 1-necked flask, MDI (0.81370 g, 0.0032514 mol) was added with dry acetonitrile (5.00 mL) and dry diglyme (2.00 mL). The flask was immersed in an oil-bath with temperature 90°C - 100°C and magnetically stirred under nitrogen until MDI was totally dissolved and then PTMO-650 (1.0692 g, 0.0016449 mol) was added and the mixture was stirred for 1.5 hours at reflux under nitrogen. N,N'-Bis(2-hydroxyethyl)paraquat hexafluorophosphate (**V-4**) (0.86148 g, 0.0016065 mol) was added and the reaction solution turned to light yellow in 10 min. The reaction was continued for 3 days under the same conditions.

VI-4-2: SYNTHESIS OF POLY(URETHANE-VIOLOGEN-PTMO-650)-

ROTAXA-BPP34C10 (VI-3)

To an oven-dried 15-mL 1-necked flask, MDI (0.82790 g, 0.0033082 mol) was added with dry acetonitrile (5.00 mL) and dry

diglyme (1.00 mL). The flask was immersed in an oil-bath with temperature 90°C - 100°C and magnetically stirred under nitrogen until MDI was totally dissolved and then PTMO-650 (1.0794 g, 0.0016606 mol) was added and the mixture was stirred for 1.5 hours at reflux under nitrogen. N,N'-Bis(2-hydroxyethyl)paraquat hexafluorophosphate (**V-4**) (0.88352 g, 0.0016476 mol) was added 10 min. after the addition of BPP34C10 (1.0200 g, 0.0019050 mol). Deep red color developed immediately upon the addition of **V-4**. The reaction was continued for 3 days under the same conditions.

VI-4-3: SYNTHESIS OF POLY(URETHANE-VIOLOGEN-PTMO-1000)

(VI-4)

To an oven-dried 15-mL 1-necked flask, MDI (0.78580 g, 0.0031399 mol) was added with dry acetonitrile (4.00 mL) and dry diglyme (2.00 mL). The flask was immersed in an oil-bath with temperature 90°C - 100°C and magnetically stirred under nitrogen until MDI was totally dissolved and then PTMO-1000 (1.7305 g, 0.0017305 mol) was added and the mixture was stirred for 1.5 hours at reflux under nitrogen. N,N'-Bis(2-hydroxyethyl)paraquat hexafluorophosphate (**V-4**) (0.75578 g, 0.0014094 mol) was added and the reaction solution turned to light yellow in 10 min. After one hour, the solution became cloudy and hence more diglyme (2.00 mL) was added to re-dissolve the precipitate. The reaction was continued for 3 days under the same conditions.

**VI-4-4: SYNTHESIS OF POLY(URETHANE-VIOLOGEN-PTMO-1000)-
ROTAXA-BPP34C10 (VI-5)**

To an oven-dried 15-mL 1-necked flask, MDI (0.80140 g, 0.0030492 mol) was added with dry acetonitrile (4.00 mL) and dry diglyme (2.00 mL). The flask was immersed in an oil-bath with temperature 90°C - 100°C and magnetically stirred under nitrogen until MDI was totally dissolved and then PTMO-1000 (1.8133 g, 0.0018133 mol) was added and the mixture was stirred for 1.5 hours at reflux under nitrogen. N,N'-Bis(2-hydroxyethyl)paraquat hexafluorophosphate (**V-4**) (0.66275 g, 0.0012359 mol) was added 10 min. after the addition of BPP34C10 (0.8000 g, 0.0014925 mol). Deep red color developed immediately upon the addition of **V-4**. After 2 hours, the solution became cloudy and hence more diglyme (1.00 mL) was added to re-dissolve the precipitate. The reaction was continued for 3 days under the same conditions.

**VI-4-5: SYNTHESIS OF POLY(URETHANE-VIOLOGEN-PTMO-2000)
(VI-6)**

To an oven-dried 15-mL 1-necked flask, MDI (0.60620 g, 0.0024223 mol) was added with dry acetonitrile (4.00 mL) and dry diglyme (5.00 mL). The flask was immersed in an oil-bath with temperature 90°C - 100°C and magnetically stirred under nitrogen until MDI was totally dissolved and then PTMO-2000 (2.4171 g, 0.0012086 mol) was added and the mixture was stirred for 1.5 hours at reflux under nitrogen. N,N'-Bis(2-hydroxyethyl)paraquat hexafluorophosphate (**V-4**)

(0.65086 g, 0.0012137 mol) was added and the reaction solution turned to light yellow in 10 min. After one hour, the solution became cloudy and hence more diglyme (1.00 mL) was added to re-dissolve the precipitate. The reaction was continued for 3 days under the same conditions.

VI-4-6: SYNTHESIS OF POLY(URETHANE-VIOLOGEN-PTMO-2000)- ROTAXA-BPP34C10 (VI-7)

To an oven-dried 15-mL 1-necked flask, MDI (0.60460 g, 0.0024159 mol) was added with dry acetonitrile (5.00 mL) and dry diglyme (4.00 mL). The flask was immersed in an oil-bath with temperature 90°C - 100°C and magnetically stirred under nitrogen until MDI was totally dissolved and then PTMO-2000 (2.4188 g, 0.0012094 mol) was added and the mixture was stirred for 1.5 hours at reflux under nitrogen. N,N'-Bis(2-hydroxyethyl)paraquat hexafluorophosphate (**V-4**) (0.64697 g, 0.0012065 mol) was added 10 min. after the addition of BPP34C10 (0.8000 g, 0.0014925 mol). Deep red color developed immediately upon the addition of **V-4**. The reaction was continued for 3 days under the same conditions.

VI-4-7: ISOLATION

When the reaction system had cooled down to room temperature, the solution was added dropwise into methanol (400 mL) with stirring and the precipitated polymer was collected. All polymers were isolated with this method.

VI-4-8: PURIFICATION

The polymer was dissolved in acetone (15 mL) and added dropwise into methanol (400 mL) with stirring and the precipitated polymer was collected. The same procedure was repeated three times (1H-NMR analysis was done on polyrotaxane samples after each reprecipitations). All polymers were purified by these multiple reprecipitations.

VI-4-9: FILM CASTING

The polymer was dissolved in acetone (10 mL) and the solution was poured into a Teflon dish. The film was peeled off after it had air dried for 2 days and vacuum dried overnight at room temperature. The same procedures were repeated for all polymers.

REFERENCES

1. Noshay, A.; McGrath, J. E. "*Block Copolymers: Overview and Critical Survey*", Academic Press, New York, **1977**.
2. Allport, D. C.; James, W. H. (Eds) "*Block Copolymers*", Wiley, New York, **1973**.
3. Burke, J. J.; Weiss, V. (Eds) "*Block and Graft Copolymers*", Syracuse University Press, New York, **1973**.
4. Goodman, I. (Eds) "*Development in Block Copolymers*", Vol.1, Applied Science Publishing, Essex, UK, **1982**.
5. Hepburn, C. "*Polyurethane Elastomers*", Applied Science Publishing, New York, **1982**.
6. Ishihara, H.; Kimura, I.; Yoshibara, N. *J. Macromol. Sci., Phys. Ed.* **1983**, B22(5), 713.
7. Hu, C. B.; Ward, R. S.; Schneider, N. S. *J. Appl. Polym. Sci.* **1982**, 27, 2167.
8. Yoon, S. C.; Ratner, B. D. *Macromolecules* **1986**, 19, 1068.
9. Chen, C. T.; Eaton, R. F.; Chang, Y. J.; Tobolsky, A. V. *J. Appl. Polym. Sci.* **1972**, 16, 2105.
10. Koberstein, J. T.; Russell, T. P. *Macromolecules* **1986**, 19, 714.

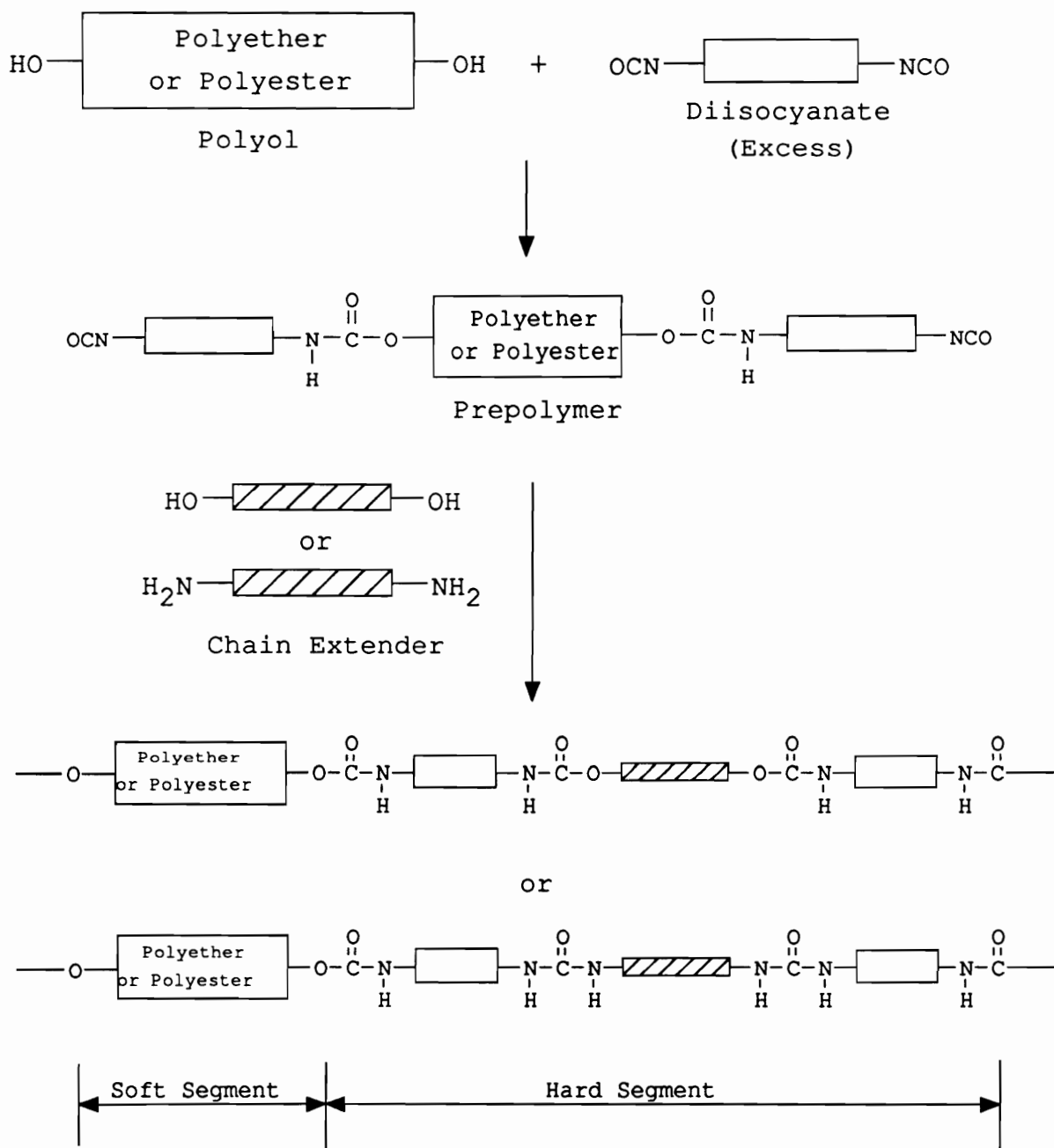
11. Watanabe, M.; Sanui, K.; Ogata, N. *Macromolecules* **1986**, *19*, 815.
12. Pascault, J. P.; Camberlin, Y. *Polym. Commun.* **1986**, *27*, 230.
13. Camberlin, Y.; Pascault, J. P. *J. Polym. Sci., Polym., Phys. Ed.* **1984**, *22*, 1835.
14. Tyagi, D.; Wilkes, G. L.; Yilgor, I.; McGrath, J. E. *Polym. Bull.* **1982**, *8*, 543.
15. Seymour, R. W.; Allegrezza, A. E.; Cooper, S. L. *Macromolecules* **1973**, *6(6)*, 896.
16. Seymour, R. W.; Estes, G. M.; Cooper, S. L. *Macromolecules* **1970**, *3(5)*, 579.
17. Speckhard, T. A.; Cooper, S. L.; Chang, V. S. C.; Kennedy, J. P. *Polymer* **1984**, *25*, 55.
18. Speckhard, T. A.; Cooper, S. L.; Chang, V. S. C.; Kennedy, J. P. *Polymer* **1985**, *26*, 55.
19. Wright, P.; Cumming, A. P. C. "*Solid Polyurethane Elastomers*", Gordon and Breach, New York, **1969**.
20. Brown, D. W.; Lowry, R. E.; Smith, L. E. *Macromolecules* **1980**, *13*, 248.
21. Dreyfuss, P. "*Poly(tetrahydrofuran)*", Gordon and Breach Science Publishers, New York, **1982**.

22. Oerdel, G. "*Polyurethane Handbook*" Hanser Publishers, N. Y., **1985**.
23. Hespe, H. *et al. Colloid. Polym. Sci.* **1972**, 250, 797.
24. Goyert, W.; Hespe, H. *Kunststoffe* **1978**, 68, 819.
25. Blackwell, I.; Gardner, K. H. *Polymer* **1979**, 20, 13.
26. Factor, A.; Heinsohn, G. E. *Polym. lett.* **1971**, 9, 289.
27. Simon, M. S.; Moore, P. T. *J. Polym. Sci., Polym. Chem.* **1975**, 13, 1.
28. Endo, T.; Kameyama, A.; Manbu, Y.; Kashi, Y.; Okawara, M. *J. Polym. Sci., Polym. Chem.* **1990**, 28, 2509.
29. Nagamara, T.; Isoda, Y. *J. Chem. Soc., Chem. Commun.* **1991**, 72.
30. Yousif, Y. Z.; Jenkins, A. D.; Walton, D. R. N.; Al-Rawi, J. M. A. *Eur. Polym. J.* **1990**, 26, 901.
31. Hashimoto, T.; Kohjiya, S.; Yamashita, S.; Irie, M. *J. Polym. Sci., Polym. Chem.* **1991**, 29, 651.
32. Kohjiya, S.; Hashimoto, T.; Yamashita, S. *Makromol. Chem., Rapid Commun.* **1989**, 10, 9.
33. Kohjiya, S.; Hashimoto, T.; Yamashita, S.; Irie, M. *Chem. lett.* **1985**, 1497.
34. Berlin, A. A.; Zhrebtsova, L. V.; Razvobovskii, Ye. F. *Polymer Sci., (USSR)* **1964**, 6, 67.

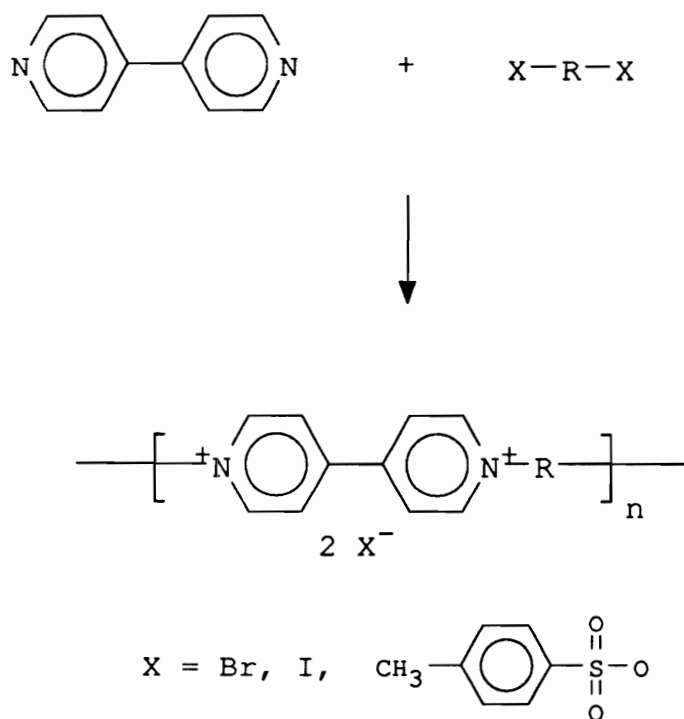
35. Simon, M. S. (to Polaroid Corp.), *US Patent* 3641034, **1972**.
36. Andrews, T. D.; Short, G. D.; Thomas, I. (to I. C. I.) *US Patent* 3671250, **1972**.
37. Factor, A.; Heinsohn, G. E. (to G. E.) *US Patent* 3694384, **1972**.
38. Factor, A.; Heinsohn, G. E. *J. Polym. Sci. B* **1971**, 9, 289.

Scheme VI-1: Two-Step Synthesis of Thermoplastic Polyurethane

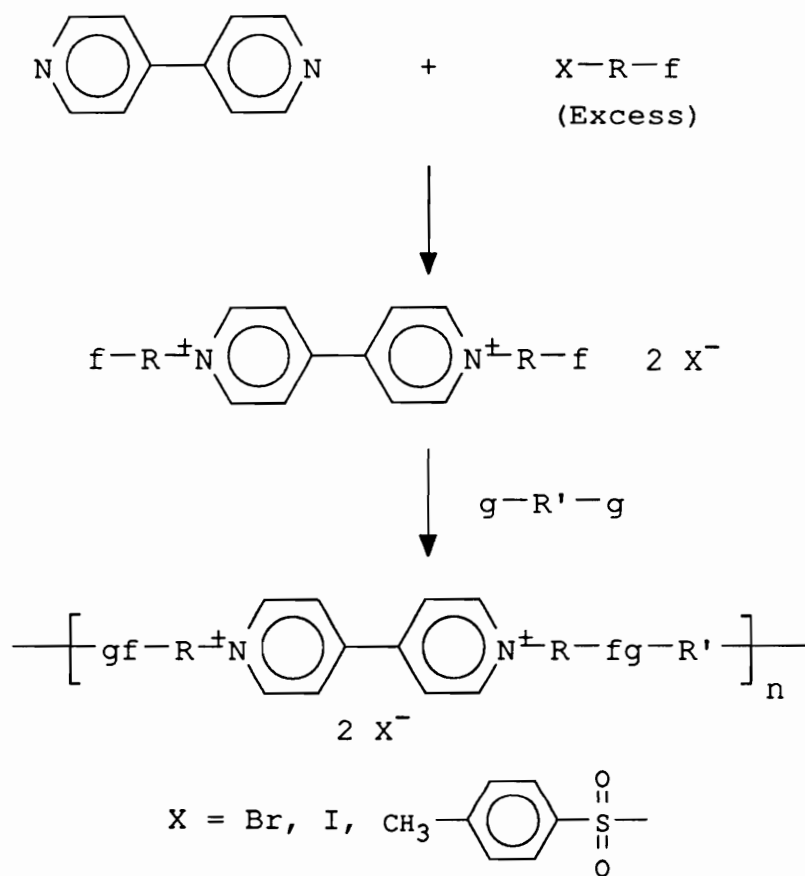
Elastomers



**Scheme VI-2: Synthesis of Viologen-Containing Polymers directly
from 4,4'-Dipyridyl**



**Scheme VI-3: Synthesis of Viologen-Containing Polymers from
Difunctionalized Viologen Derivatives**



f and g are functional groups
f is reactive toward g

Scheme VI-4: Synthesized of Linear Elastomeric Viologen-Containing Poly(tetrahydrofuran)

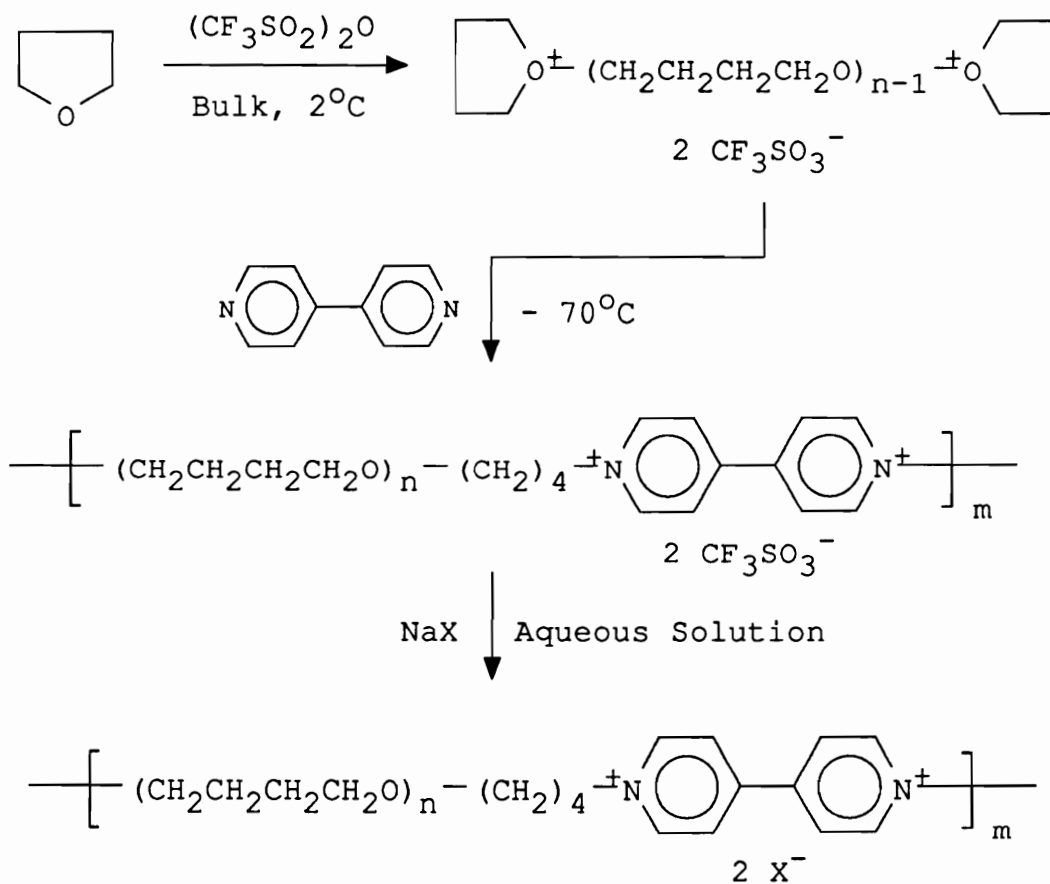


Table VI-1: Some Examples of Polyols for Polyurethane Elastomer Synthesis

Name	Abb.	Structure	Ref.
Polytetramethylene Oxide	PTMO	$\text{HO}(\text{CH}_2\text{CH}_2\text{CH}_2\text{CH}_2\text{O})_n\text{H}$	6-8
Polyethylene Oxide	PEO	$\text{HO}(\text{CH}_2\text{CH}_2\text{O})_n\text{H}$	9
Polypropylene Oxide	PPO	$\text{HO}(\text{CH}_2-\underset{\text{CH}_3}{\text{CH}}-\text{O})_n\text{H}$	10,11
Polydimethylsiloxane	PDMS	$\text{HO}(\text{CH}_2)_4(\underset{\text{CH}_3}{\text{SiO}})_n(\underset{\text{CH}_3}{\text{Si}})(\text{CH}_2)_4\text{OH}$	12-14
Polyethylene Adipate	PEA	$\text{HO}[(\text{CH}_2)_4\overset{\text{O}}{\parallel}{\text{C}}(\text{CH}_2)_4\overset{\text{O}}{\parallel}{\text{C}}\text{O}]_n\text{H}$	15,16
Polyisobutylene	PIB	$\text{HO}(\underset{\text{CH}_3}{\text{C}}\text{CH}_2)_n\text{OH}$	17,18

**Table VI-2: Common Used Chain Extenders in the Synthesis of
Polyurethane Elastomers**

Name	Structure	b.p. (°C)
Ethylene Glycol	$\text{HO}(\text{CH}_2)_2\text{OH}$	196 - 198
Propylene Glycol	$\begin{array}{c} \text{HO}-\text{CH}-\text{CH}_2\text{OH} \\ \\ \text{CH}_3 \end{array}$	187 /765 mm
1,4-Butanediol	$\text{HO}(\text{CH}_2)_4\text{OH}$	230
1,6-Hexanediol	$\text{HO}(\text{CH}_2)_6\text{OH}$	250
Ethylenediamine	$\text{H}_2\text{N}(\text{CH}_2)_2\text{NH}_2$	118
Butanediamine	$\text{H}_2\text{N}(\text{CH}_2)_4\text{NH}_2$	158 - 160
Hexanediamine	$\text{H}_2\text{N}(\text{CH}_2)_6\text{NH}_2$	204 - 205

Table VI-3: Rings Per Paraquat Unit (x/y^a) for Polyrotaxanes after Each Reprecipitations

Polymer	1st Reprecip.	2nd Reprecip.	3rd Reprecip.	4th Reprecip.
VI-3	1.04	0.98	0.95	0.98
VI-5	1.02	0.99	0.98	0.98
VI-7	1.04	0.99	0.99	1.00

a. x/y values were obtained from ¹H-NMR analysis.

Table VI-4: Summary of Polymer Compositions^a

Polym.	Soft Seg.	Hard Seg. ^b	x/y Value ^c	a/R/y Value ^d	WT% HSE ^e	WT% BPP
VI-2	PTMO-650	MDI/PQ	0.00	1.02/2.02 /1.00	61.04	0.00
VI-3	PTMO-650	MDI/PQ /BPP	0.98	1.01/2.01 /1.00	61.32	24.04
VI-4	PTMO-1000	MDI/PQ	0.00	1.22/2.22 /1.00	47.11	0.00
VI-5	PTMO-1000	MDI/PQ /BPP	0.98	1.46/2.46 /1.00	44.67	16.82
VI-6	PTMO-2000	MDI/PQ	0.00	1.00/2.00 /1.00	34.21	0.00
VI-7	PTMO-2000	MDI/PQ /BPP	1.00	1.00/2.00 /1.00	34.10	14.97

a. Values were determined by ¹H-NMR analysis;

b. PQ: paraquat linkage, BPP: BPP34C10;

c. Rings per paraquat unit;

d. Ratio of PTMO unit to MDI unit to paraquat unit;

e. HS: Hard segment (BPP34C10 is not included).

Table VI-5: Intrinsic Viscosities of the Polymers Measured in NMP + LiBr (0.006 M) at 31°C.

Polymer	$[\eta]$ (dl/g)
VI-2	0.26
VI-3	0.23
VI-4	0.35
VI-5	0.43
VI-6	0.41
VI-7	0.40

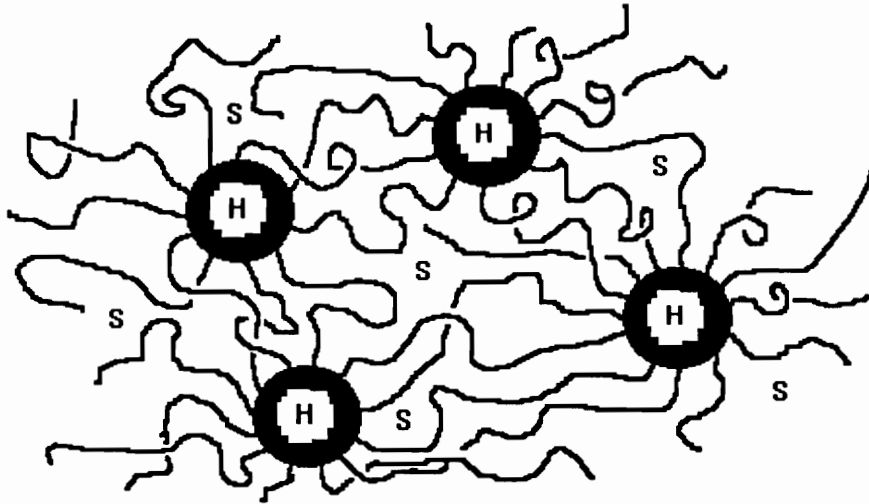


Figure VI-1: Morphological Model of a Thermoplastic Elastomer. H: Hard Segment Domain; S: Soft Segment Domain.

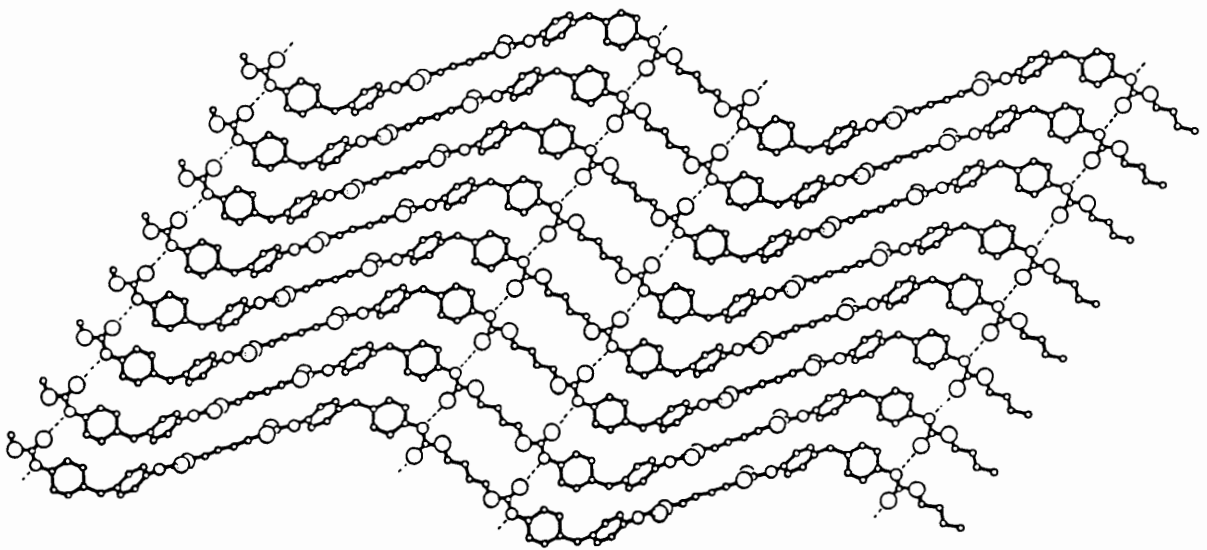


Figure VI-2: X-Ray Crystal Structure within the Hard Segment Domain. Printed from Blackwell et al.²²

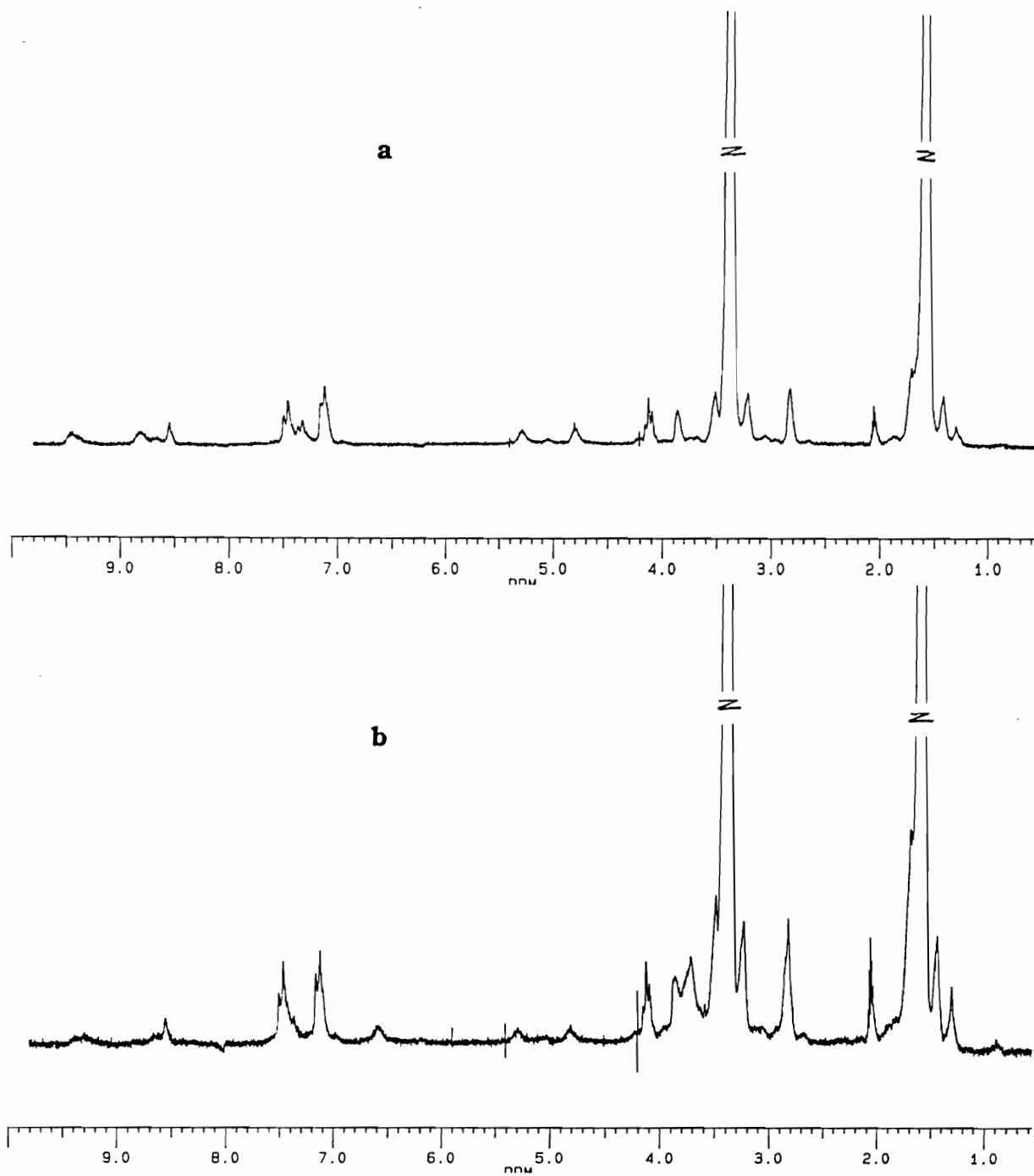


Figure VI-3: $^1\text{H-NMR}$ Spectra of (a) Model Poly(urethane-viologen-PTMO-650) (VI-2) and (b) Poly(urethane-viologen-PTMO-650)-rotaxa-BPP34C10 (VI-3).

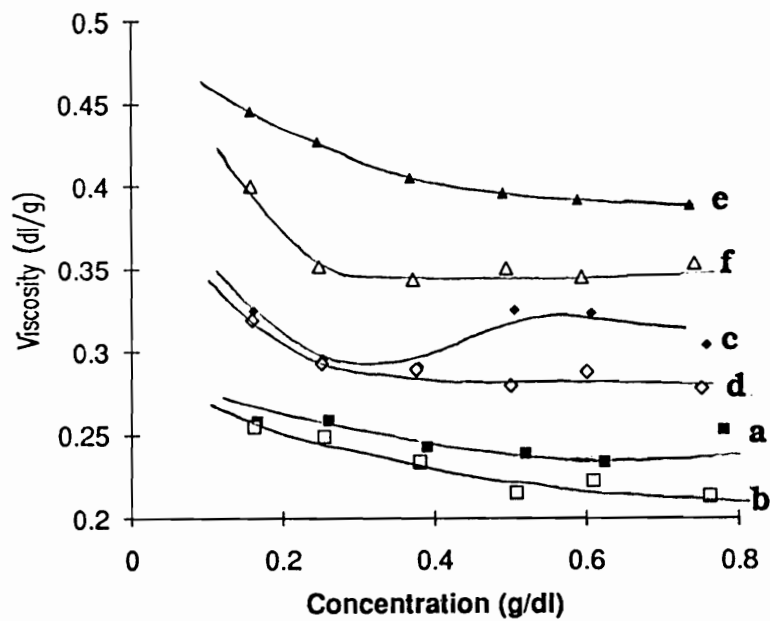


Figure VI-4: Plots of Reduced Viscosity versus Concentration in Acetone at 31°C. (a) VI-2, (b) VI-3, (c) VI-4, (d) VI-5, (e) VI-6 and (f) VI-7.

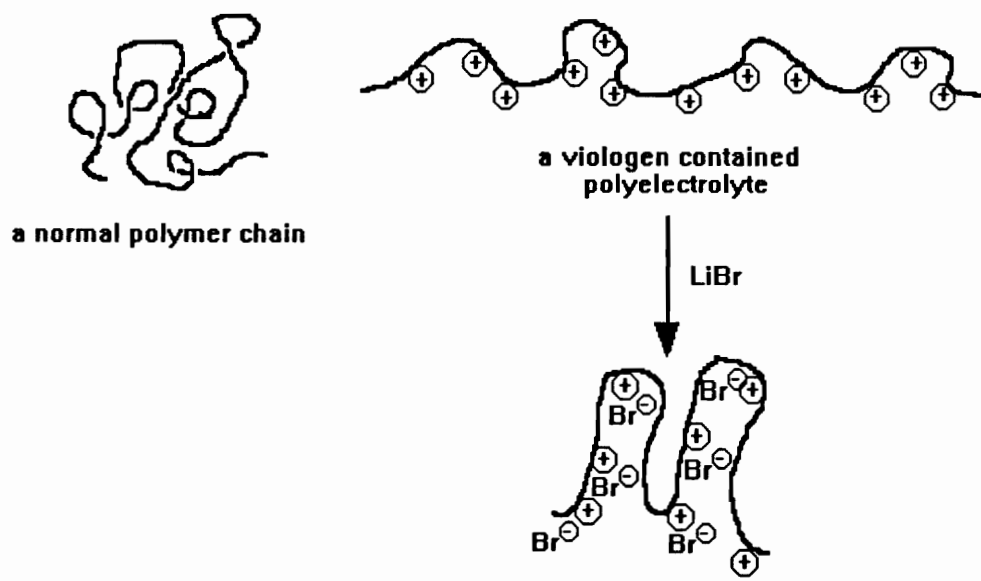


Figure VI-5: Illustration of Salt Effect on the Conformation of Polyelectrolyte.

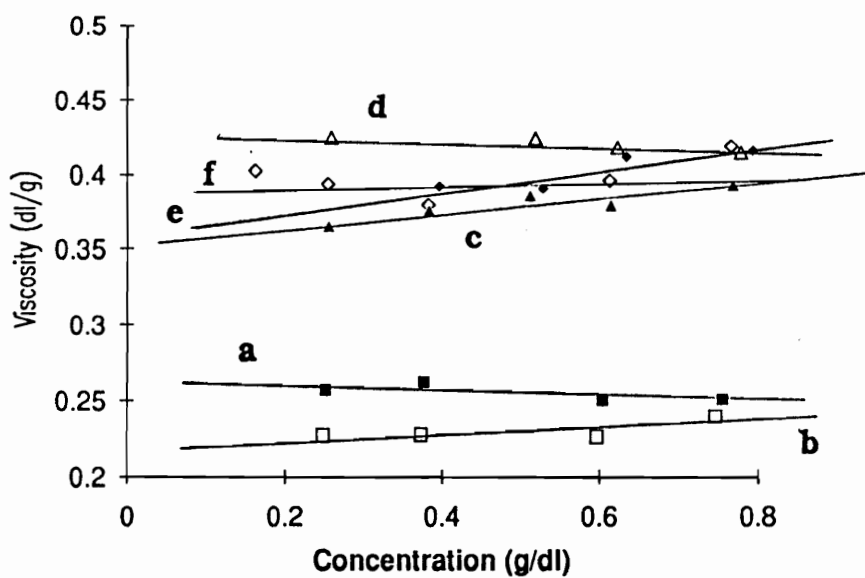


Figure VI-6: Plots of Reduced Viscosity versus Concentration in NMP + LiBr (0.006 M) at 31°C. (a) VI-2, (b) VI-3, (c) VI-4, (d) VI-5, (e) VI-6 and (f) VI-7.

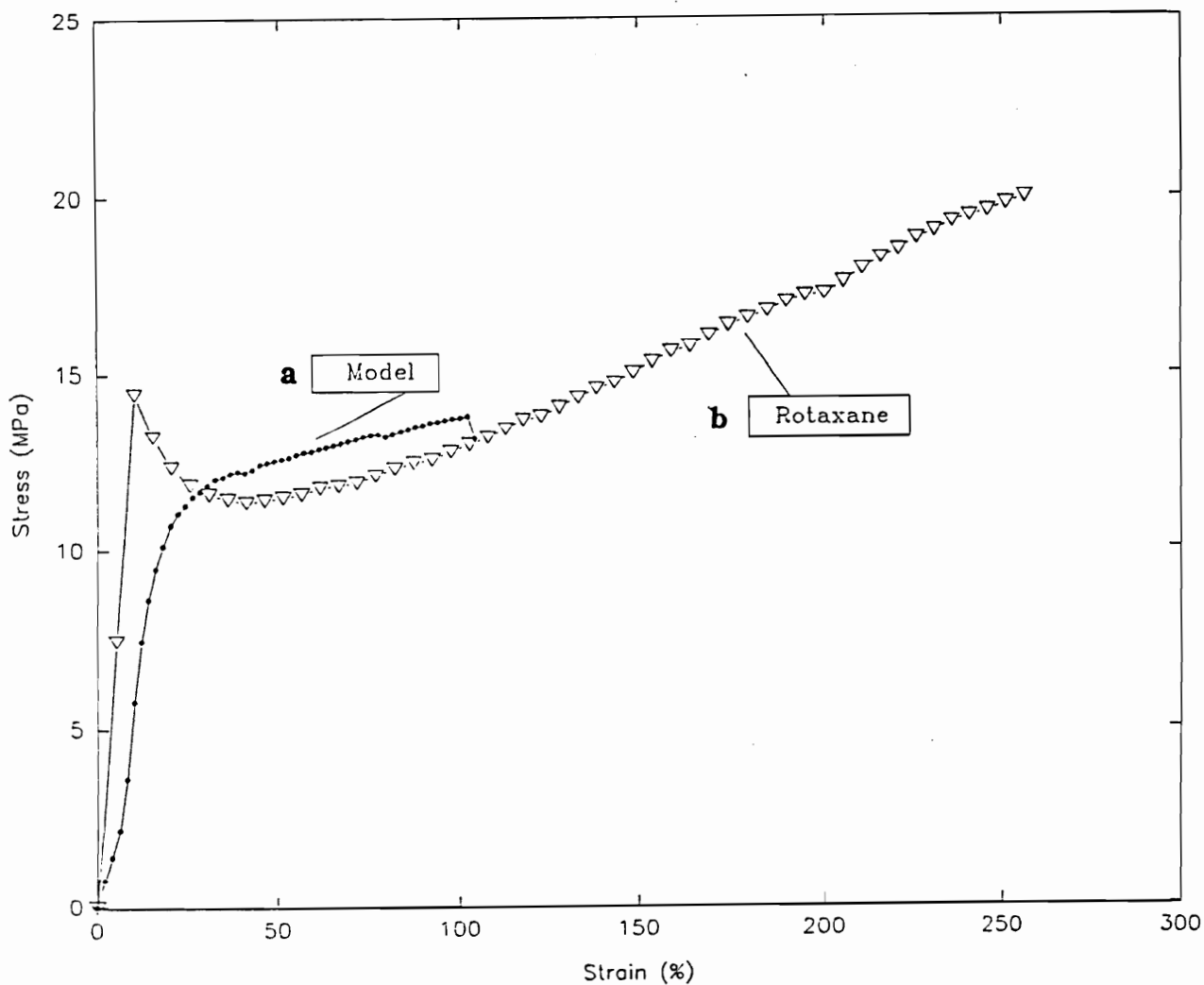


Figure VI-7: Stress-Strain Behavior of (a) Poly(urethane-viologen-PTMO-650) (VI-2) and (b) Poly(urethane-viologen-PTMO-650)-rotaxa-BPP34C10 (VI-3).

CHAPTER VII:

SUMMARIZATION, GENERAL CONCLUSIONS, POLYROTAXANE POTENTIAL APPLICATIONS AND SUGGESTIONS FOR FUTURE WORK

VII-1: SUMMARIZATION AND GENERAL CONCLUSIONS

VII-1-1: MACROCYCLES

The macrocycles I have synthesized, characterized and used in my polyrotaxane syntheses are two types of crown ethers: poly(ethylene oxide) crown ethers and bis(p-phenylene) based crown ethers.

Poly(ethylene oxide) crown ethers include 30C10, 36C12, 42C14, 48C16 and 60C20. They were systematically synthesized starting from commercially available low molecular weight oligo(ethylene glycol)s such as ethylene glycol, di-, tri- and tetra(ethylene glycol) and oligo(ethylene glycol) ditosylates which were obtained by tosylations of corresponding glycols. Each reaction produced two crown ethers: one formed by "two piece combination" and the other formed by "four piece combination"; the later has twice the ring size of the former one. The overall yield of crown ethers ranged from 30 - 50%. The higher dilution the system, the higher overall yield of crown ethers. However, the relative yield of each crown

ether depends on reaction dynamics such as ring sizes of crown ethers, reaction temperature, concentration and template used. It seems that in order to be reactive toward the ditosylate, the glycol chain has to be long enough (> 10 skeleton atoms).

I have also synthesized two bis(*p*-phenylene) based crown ethers: BPP34C10 and BPP32C4; the later was synthesized via a one-pot reaction of hydroquinone and 1,10-dibromodecane. However, BPP34C10 was synthesized via four different methods in order to find out the most efficient and economic method since I had need of this macrocycle in large quantity.

The four methods studied for the synthesis of BPP34C10 were summarized as the follows:

- (1) One-pot reaction of hydroquinone and tetra(ethylene glycol) ditosylate without template. Yield: 10.5%.
- (2) One-pot reaction of hydroquinone and tetra(ethylene glycol) ditosylate with Cs⁺ as template. Yield: 12.5%.
- (3) Two-step route: step a: reaction of excess amount of hydroquinone with tetra(ethylene glycol) to produce a trimer with phenol as end groups; step 2: cyclization of the trimer (diphenol) with tetra(ethylene glycol) ditosylate. Yield: 14.2%.
- (4) Four-step route: step 1: monoprotection of hydroquinone with benzyl group; (2) reaction of tetra(ethylene glycol) ditosylate with excess

amount of the monoprotected hydroquinone to produce a trimer (a benzyl diprotected diphenol); (3) deprotection by catalytic hydrogenation to yield a diphenol (the same diphenol as that produced in the step 1 of the two-step route); (4) cyclization of the diphenol with tetra(ethylene glycol) ditosylate. Yield: 11.3%.

By considering cost, time consumption and overall yield of BPP34C10, it can be concluded that the one-pot reaction of hydroquinone and tetra(ethylene glycol) ditosylate without template is the most efficient and economic method to synthesize BPP34C10.

VII-1-2: BLOCKING GROUPS

Even though the use of blocking groups are not reported in this dissertation, blocking group chemistry has been studied for the benefit of the overall polyrotaxane project.

A series of monofunctionalized blocking groups based on bulky triarylmethanes has been synthesized and characterized. They were functionalized with hydroxyl, chloride, iodide, phenol, amine, etc. The triarylmethane basic units were built up by Grignard reaction of 4-t-butylbromobenzene Grignard reagent with methyl p-substituted benzoate. Then modifications were done to functionalize the blocking groups and relocate the functional group so that it is remote from the steric hindrance region.

There were two methods employed to do the modifications starting from triarylmethanol derivatives:

- (1) Reduction of triarylmethanol derivatives to the triarylmethane derivatives (> 90% yield) which were reacted via their carbanions with THP-protected linear chloroalcohols (about 40% yield) followed by the deprotection (100% yield) to produce hydroxyl terminated blocking groups which underwent further functional group conversions to halides.
- (2) Reaction of triarylmethanol derivatives with phenol via trityl type carbocations to produce phenol terminated blocking groups (> 85% yield) which further were reacted with linear bromoalcohols (> 95% yield) resulting in hydroxyl terminated blocking groups.

It is obvious that the modification method (2) is simpler and higher yielding than the method (1).

VII-1-3: POLYROTAXANES VIA STATISTICAL THREADING METHODS

The linear polymer backbone was polyurethane derived from MDI and tetra(ethylene glycol). Four polyrotaxanes with this backbone and respectively 36C12, 42C14, 48C16 and 60C20 have been synthesized along with the model polyurethane. Also a polyrotaxane comprised of 60C20 and polyurethane-urea backbone derived from MDI, tetra(ethylene glycol) and moisture had been synthesized.

The statistical threading approach was performed by carrying out the polycondensation using a melted crown ether as solvent. The model polyurethane was prepared under the same condition except diglyme was used as solvent instead of a crown ether. Threadings were efficient and

the threading efficiency defined as rings threaded per repeat unit increased as the ring size of crown ether increased and followed the same profile as a theoretical prediction.

The polyrotaxane structures were proven by multiple reprecipitations, $^1\text{H-NMR}$ and GPC analyses. I expected no free crown ethers after the multiple reprecipitations; however, $^1\text{H-NMR}$ detected the existence of crown ethers, but they were not detectable by GPC. Significant dethreading has not been observed even though no blocking group was used.

FTIR studies indicated that hydrogen bonding between the polyurethane backbone and crown ethers existed and it seems that hydrogen bonding is more efficient in polyrotaxane systems than that in physical blend systems.

Rotaxane formation enhances the solubilities of polymers in common solvents generally due to the strong interaction between crown ethers and solvents and also by reducing the backbone intermolecular interactions. When polyrotaxanes are comprised of large crown ethers such as 48C16 and 60C20 in relatively high contents, the polymers become water soluble.

Glass transition temperatures of polyrotaxanes are lower than that of the model polymer and decrease with increase in ring size and content of crown ether. Also the change in T_g follows the Fox equation.

Evidenced by DSC and wide angle X-ray analyses, crystallization of crown ether occurs without dethreading. The crystallization kinetics was also studied. This crystallization process is kinetically "retarded". It is time and temperature dependent and reversible. It can only be observed for polyrotaxanes with large rings and high ring contents, which provide high mobilities of rings along the polymer chain and also wide $T_m - T_g$ windows.

In summary, properties of polyrotaxanes, especially thermal and solid state properties, kinetics crystallization are influenced by the type, size and proportion of rings on the chain.

VII-1-4: POLYROTAXANES VIA HOST-GUEST COMPLEXATION

A number of difunctionalized paraquat dication derivatives have been prepared. These paraquat dications are able to form 1:1 host-guest complexes (pseudorotaxanes) with BPP34C10. The complexes were formed in polar solvents such as acetone, methanol, acetonitrile, etc. in quantitative yields; however, they can not form in DMSO since DMSO also complexes with paraquat dications, thus preventing the formation of the inclusion systems. The driving force for the complexation is electrostatic interactions and charge transfer interaction where the paraquat dication serves as electron acceptor and BPP34C10 serves as electron donor.

The formation of the host-guest complexes was proven by $^1\text{H-NMR}$ studies and X-ray single crystal structure determination. The $^1\text{H-NMR}$

chemical shift changes for probe protons indicate the formation of inclusion complexes. The sign and magnitude of chemical shift changes reveal the geometric conformation of the complexes. X-ray structures clearly showed the nature of a host-guest complex: paraquat dication threaded through the cavity center of BPP34C10; parallel array of aromatic rings to achieve a maximum π - π interaction; functional groups extended outside of BPP34C10 providing the accessibility required for polymerization.

One of the complexes, N,N'-bis(2-hydroxyethyl)paraquat hexafluorophosphate-rota-BPP34C10, was used in the synthesis of poly(urethane-viologen-PTMO) and BPP34C10 based elastomeric polyrotaxanes. The viologen-containing polyurethane thermoplastic elastomers were synthesized via a two-step process: preparation of prepolymers and chain extension. The host-guest complex formed *in situ* was used as chain extender. PTMOs with three different molecular weights, 650, 1000 and 2000, were used. Thus, three polyrotaxanes with their corresponding model polymers have been synthesized. The threading efficiencies are nearly quantitative and all polymers are able to form nice elastomeric films. The properties of these polymers are currently under study.

VII-2: POTENTIAL APPLICATIONS OF POLYROTAXANES

Polyrotaxanes may possibly be applied to the following areas:

- (1) **Blend compatibilization:** Incompatible polymers may become compatible through rotaxane formation since the macrocycle could reduce inter-backbone interactions.
- (2) **Adhesion and controlled release:** Rotaxane type physical interfacial bonding can form and bonds may be released by chemical cleavage of rings.
- (3) **Novel tough physical crosslinked systems:** Two polymer chains may be able to thread through one ring if the ring is sufficiently large. Also a linear polymer chain can thread through a macrocycle which is chemically bonded to another polymer chain. This could produce soft but tough materials, "springy" type of materials.
- (4) **Energy or electron transfer materials:** Energy or electrons may be transferred through the "ring bridge" or carried by rings.
- (5) **Increased processibility:** The processibilities of polymers may be increased through the rotaxane formation which enhances polymer solubilities and decreases glass transition temperatures.

- (6) **Controlled processing:** Processing and molecular ordering can be achieved simultaneously through phase separation, dethreading or chemical cleavage of macrocycles.

VII-3: SUGGESTIONS FOR FUTURE WORK

As a new class of materials, the study in this area has just begun. There is a tremendous amount of work to do in the future. For examples, synthesis and characterization of polyrotaxanes with different types of polymer backbone and macrocycles, especially those ring/chain incompatible systems, are necessary; developing cheaper, more thermal and oxidatively stable and nontoxic macrocycles is very important, especially for the industrial and commercial applications of polyrotaxanes in the future; computer simulations of rotaxane chemistry such as the threading process, molecular mechanics calculations, prediction of rotaxane and polyrotaxane conformation and properties. The following are some specific topics suggested for these polyurethane systems.

VII-3-1: DIFUNCTIONAL BLOCKING GROUPS AND POLYROTAXANES WITH BULKY SPACERS

It is necessary to investigate polyrotaxanes with bulky spacers along the chain. I have found that polyrotaxanes without bulky spacers

along the chain show interesting crystallization behavior. This phenomenon could be suppressed and the polymers could be totally amorphous. This type of polymers may show some unexpected properties such as large free volume, more solubility increases and T_g decreases (due to more extended but uncrystallizable chains), etc.

In the syntheses of monofunctional blocking groups, I have clearly demonstrated that triarylmethanol can be reacted with phenol in the presence of a catalytic amount of HCl resulting in phenol type functionalized blocking group in over 85% yield. On the other hand, difunctionalized blocking groups can also be synthesized with a similar approach. The proposed synthetic route is shown in Scheme VII-1.

The diols **VII-1** with various R groups can be synthesized via Grignard reaction of 4-t-butylbromobenzene Grignard reagent with a diester. The reactions of **VII-1** with phenol or aniline give **VII-2** or **VII-3**, respectively. Compound **VII-3** can be directly used as a comonomer in polyurethane-urea-rotaxane syntheses to produce desired polyrotaxane architecture. Compound **VII-2** can be further chain extended to **VII-4** which can be directly used in the polyurethane-rotaxane, polyester-rotaxane and some other type polyrotaxane syntheses. The diol **VII-4** can also be further converted to diiodide which can be subjected to viologen-containing polyrotaxane syntheses. The solubility and crystallizability of **VII-4** may be adjusted by proper choice of the value of n.

VII-3-2: POLYMERIC "MOLECULAR SHUTTLES"

The host-guest complexation between paraquat tetracationic macrocycle and a linear backbone containing hydroquinone moiety has led to an interesting rotaxane containing two hydroquinone moieties on the linear backbone and one paraquat tetracationic macrocycle prepared by Stoddart *et al.*¹ Since an electronic force exists between the macrocycle and hydroquinone unit, the macrocycle was observed switching between the two hydroquinone units like a "shuttle" shifting between two "stations". A potential application of this property is in computer information processor area, as stated by Stoddart *et al.*

It is necessary to investigate this property in polyrotaxane systems since polymers offer more advantages over small molecules in terms of "materials" such as formulation, processing, etc. This property may be more complicated but controllable in the polymer system since stations on the backbone can be varied. Therefore, the energy barriers among stations can be controlled, as well as the distribution of macrocycle molecules along the backbone. Furthermore, difunctionalized blocking groups may be used as spacers to stop this transformation in some certain range.

As proposed in Scheme VII-2, "shuttle"-like polymeric rotaxanes may be synthesized via the host-guest complexation of BPP34C10 and paraquat dication containing monomers when the ratio of BPP34C10 to the paraquat monomer is less than one (for example, 0.5). In that case, there are some free "stations" for the "shuttle" to relocate. The distance

between two "stations" is controlled by the choice of spacer. Also, the "railway" between two "stations" could be "smooth" or "rough" depending on the type of spacer. Of course, the energy barrier will depend on the distance and "road" roughness between two "stations".

VII-3-3: SLIP-LINKED POLYMERS

Slip-linked polymers are expected to show interesting properties due to the fact that segments can slip without disconnecting. This type of architecture can be constructed only if the threading efficiency is quantitative. Therefore, one to one host-guest complexation of paraquat dication and bisparaphenylene-based macrocycle could be the best choice from the synthetic point of view. Scheme VII-3 shows the synthetic approach to a slip-linked polymer.

The monofunctionalized dibenzo-32-crown-10 can be prepared via a four-step route. First, hydroquinone reacts with THP-protected tetraethylene glycol monochloride and a diol is obtained after deprotection. The diols then reacted with monofunctionalized catechol to give monofunctionalized dibenzo-32-crown-10. This type of four-step route has been studied in our group. The reaction conditions have been well-established.

The synthesis of viologen-containing monofunctionalized blocking group (**VII-8**) is illustrated in Scheme VII-4. I have already prepared the phenol type blocking group **III-3h** (see Chapter III). The paraquat monocation **VII-13** can be prepared from 1,4-dipyridyl and a dichloride.

This reaction produces only dimer (monocation) because of the low reactivity of dichloride compounds toward 1,4-dipyridyl. The reaction of **III-3h** and **VII-12** is carried out in KOH/butanol system. Finally, **VII-13** reacts with 2-bromoethanol to produce the desired blocking group **VII-8**. Of course, the solubility of **VII-8** can be adjusted by proper choice of R group on **VII-12**,

The complex **VII-9** is prepared *in-situ* and self-polymerization of the complex results in a slip-linked polymer **VII-10** under proper conditions. The R group on **VII-8** should be a linear with length long enough that the host-guest complex is not effected by the bulky triaryl group. On the other hand, the hydroxyl group should not be too remote from the viologen unit; otherwise it will prevent the threading.

VII-3-4: POLYROTAXANES BASED ON REDOX-SWITCHED CROWN ETHERS

Redox-switched crown ethers have been studied for some time.²⁻⁷ This cyclic-acyclic interconversion by reversible bond formation and bond scission has preliminarily found applications in ion binding, selecting and membrane transport. A specific example is a crown ether as redox-switch by inter-conversion of thiol and disulfide bonds studied by Shinkai *et al.*⁷ The structures of the redox pair are shown in Scheme VII-5. The oxidation process is remarkably effected by the template cation. The cyclic formation increased drastically in the presence of a template cation.

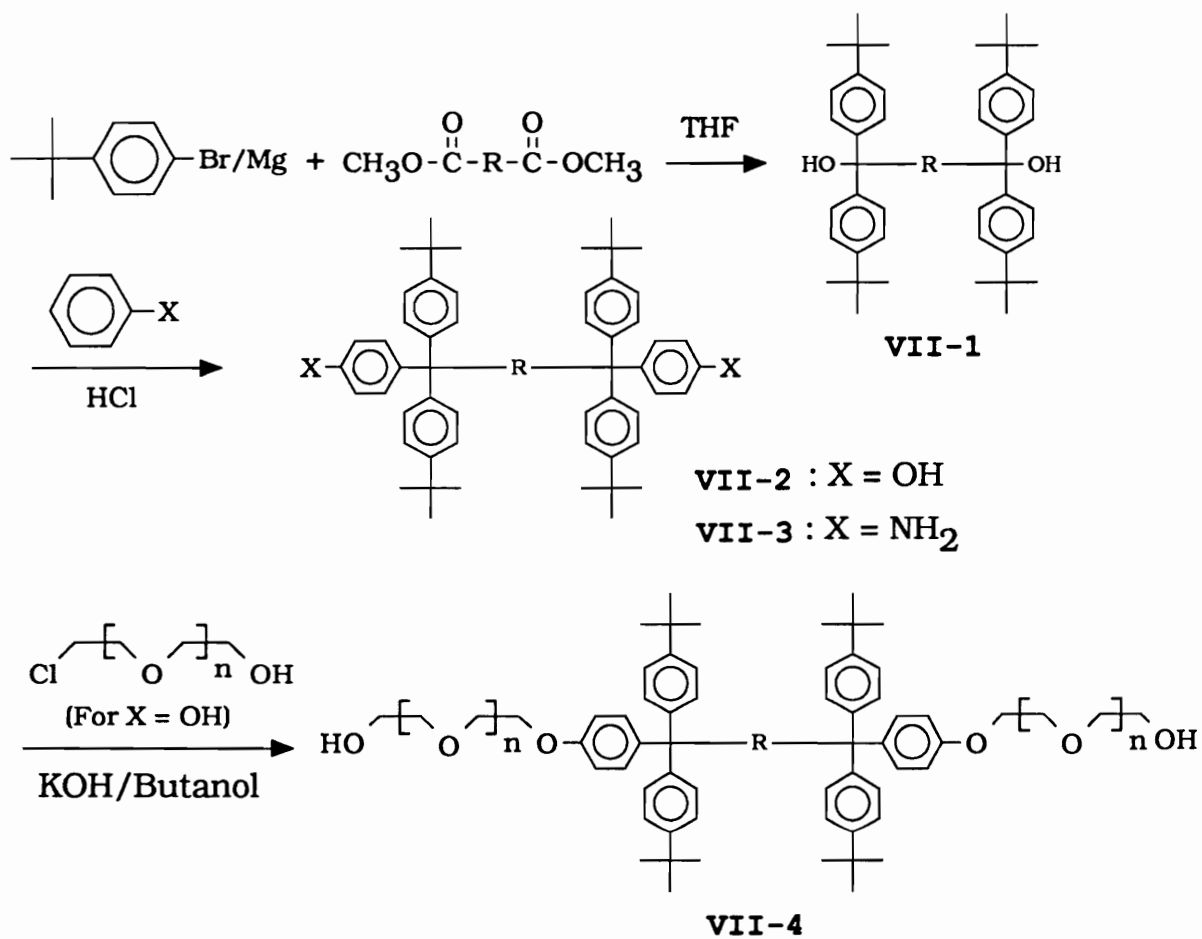
We could use this type of macrocycle in two ways: (1) cyclization (oxidation) in the presence of a polymer template and (2) acyclization (reduction) of threaded macrocycles.

Polyrotaxanes can be synthesized by cyclization in the presence of a polymer template, the polymer with cation incorporated into its chain. This synthetic method offers the advantage that the polyrotaxane backbone has exactly the same molecular weight as the model polymer which, indeed, is one of the starting materials. On the other hand, through rotaxane formation, an insoluble and a high T_g polymer can be a soluble and low T_g one for processing. Simultaneously with the processing or after the processing, the crown ether can be released by reduction (ring opening) and the same polymer backbone retained.

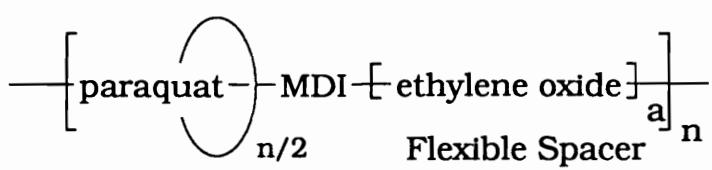
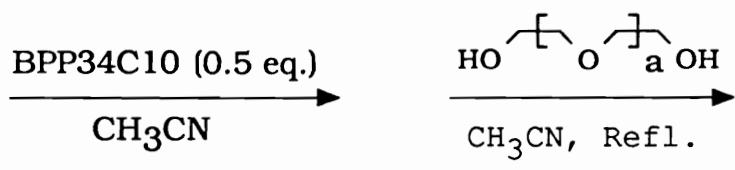
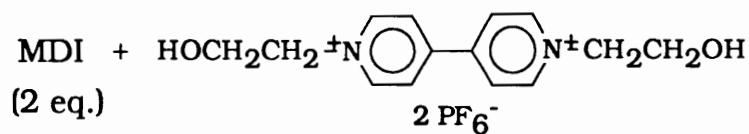
REFERENCES

1. Ashton, P. R.; Groguz, M.; Slawin, A. M. Z.; Stoddart, J. F.; Williams, D. J. *Tetrahedron Lett.* **1991**, *32*, 6235; *J. Am. Chem. Soc.* **1991**, *113*, 5131.
2. Shinkai, S.; Inuzuka, K.; Miyazaki, O.; Manabe, O. *J. Org. Chem.* **1984**, *49*, 3440.
3. Minami, T.; Shinkai, S.; Manabe, O. *Tetrahedron Lett.* **1982**, *23*, 5167.
4. Shinkai, S.; Inuzuka, K.; Manabe, O. *Chem. Lett.* **1983**, 747.
5. Shinkai, S.; Inuzuka, K.; Hara, K.; Sone, T.; Manabe, O. *Bull. Chem. Soc. Japan.* **1984**, *57*, 2150.
6. Raban, M.; Greenblatt, J. Kandil, F. *J. Chem. Soc., Chem. Commun.* **1983**, 1409.
7. Shinkai, S.; Inuzuka, K.; Miyazaki, O.; Manabe, O. *J. Am. Chem. Soc.* **1985**, *107*, 3950.

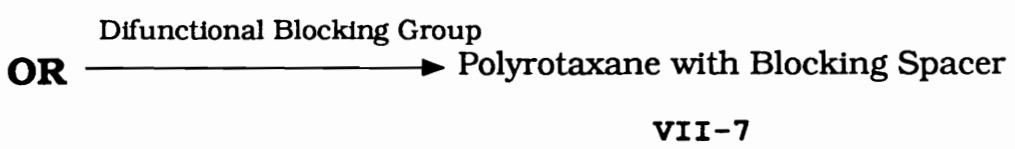
Scheme VII-1: Synthesis of Difunctionalized Blocking Groups



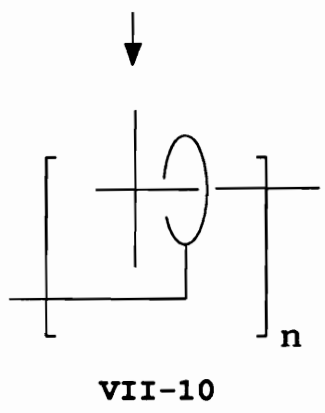
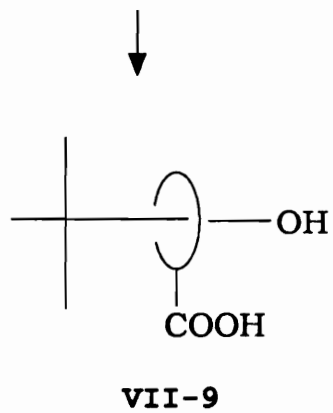
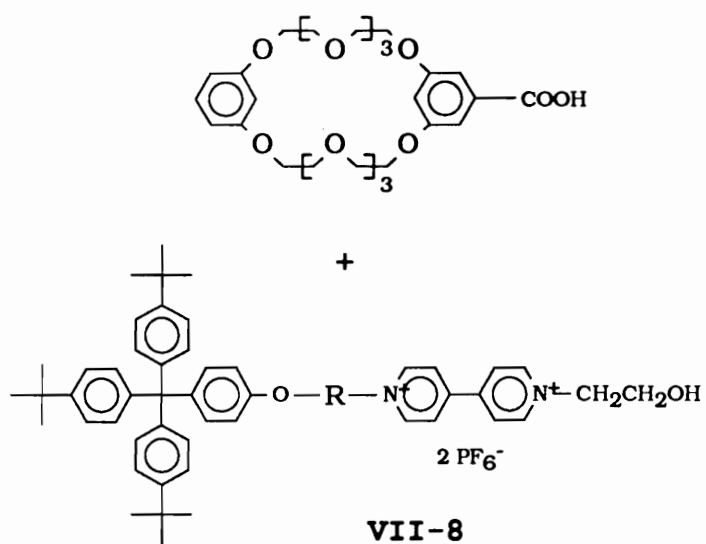
Scheme VII-2: Syntheses of Polymeric "Molecular Shuttles"



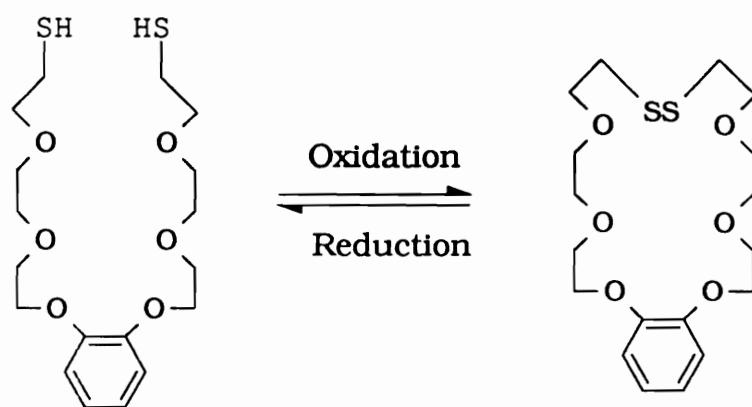
VII-5



Scheme VII-3: Synthesis of a "Slip-Linked" Polymer



Scheme VII-5: An Example of Redox Switched Crown Ethers



VITA

Ya Xi Shen was born in May 4, 1958 in Yingshan, Hubei, China and spent his childhood in a little town in Huangme, Hubei, China.

Upon graduation from Huazhong Normal University, Wuhan, China with B.S. in Chemistry in 1979, he was employed by the university as a Physical Chemistry instructor. After five years teaching at Huazhong Normal University, he came to the USA and joined the graduate school at East Tennessee State University, Johnson City, Tennessee and obtained a M.S. degree in Physical Chemistry in 1987. Immediately, he entered graduate school at Virginia Polytechnic Institute and State University and joined Dr. Harry W. Gibson's research group.

A handwritten signature in black ink, appearing to read 'Ya Xi Shen', with a stylized flourish at the end.